

# THE HIGH LUMINOSITY CHALLENGE: POTENTIAL AND LIMITATIONS OF HIGH INTENSITY HIGH BRIGHTNESS BEAMS IN THE LHC AND ITS INJECTORS\*

R. De Maria, G. Arduini, D. Banfi, J. Barranco, H. Bartosik, E. Benedetto, R. Bruce, O. Brüning, R. Calaga, F. Cerutti, H. Damerau, L. Esposito, S. Fartoukh, M. Fitterer, R. Garoby, S. Gilardoni, M. Giovannozzi, B. Goddard, B. Gorini, K. Hanke, G. Iadarola, M. Lamont, M. Meddahi, E. Métral, B. Mikulec, N. Mounet, Y. Papaphilippou, T. Pieloni, S. Redaelli, L. Rossi, G. Rumolo, E. Shaposhnikova, G. Sterbini, E. Todesco, R. Tomás, F. Zimmermann (CERN, Geneva), A. Valishev (Fermilab, Batavia, Illinois)

## Abstract

High-intensity and high-brightness beams are key ingredients to maximize the LHC integrated luminosity and to exploit its full potential. This contribution describes the optimization of beam and machine parameters to maximize the integrated luminosity as seen by the LHC experiments, by taking into account the expected intensity and brightness reach of LHC itself and its injector chain as well as the capabilities of the detectors for next run and foreseen upgrade scenarios.

## INTRODUCTION

The LHC proton-proton programme aims at steadily increasing the luminosity production rate in the next two decades, in order to reach the target of  $3000 \text{ fb}^{-1}$  with the High-Luminosity LHC project (HL-LHC) [1, 2]. High intensity, high brightness beams are key ingredients to reach these goals. Several interventions associated to long shutdowns (LS), will address and overcome several limitations. Notably the LHC injector upgrade project (LIU) [3, 4], scheduled for implementation during LS2, aims at providing the most intense and bright beams that LHC can store, accelerate, and collide with high efficiency and reliability. In the following we discuss the intensity and brightness limitations in LHC and injectors, together with their potential in terms of expected integrated luminosity for ATLAS and CMS experiments.

## LHC LIMITATIONS

The LHC has been designed to store and collide 2808 25 ns spaced bunches populated by  $1.1 \cdot 10^{11}$  protons in two counter-rotating beams. Magnet apertures have been specified to allow a normalized emittance of  $3.75 \mu\text{rad}$  to be used operationally [5]. Together with  $\beta^* = 55 \text{ cm}$ , the beam parameters allow reaching the so-called nominal luminosity of  $1 \cdot 10^{34} \text{ cm}^{-2}\text{s}^{-1}$ . During Run I the LHC operated at 50 ns and with up to  $1.7 \cdot 10^{11}$  protons per bunch (ppb) in 1380 bunches, which represented the best parameters to maximize the integrated luminosity in the presence of strong e-cloud effects observed and anticipated for 25 ns beams [6]. However, 50 ns beams saturate quickly the reconstruction capabilities of the detectors due to the large pile up of events per crossing. Therefore, Run II will be devoted to establish 25 ns bunch

spacing beams to aim at doubling the integrated luminosity for about the same pile up, thanks to the higher-than-nominal bunch intensities that may be obtained from the injectors' chain after mitigation measures addressed during LS1, and an aggressive plan of scrubbing with special beams [7].

On a longer time scales, it is expected to be possible to bring in collision  $2.2 \cdot 10^{11}$  ppb for a total of about 1 A of circulating beam current, provided that: a) e-cloud issues are solved by increasing the cooling capacity of the standalone quadrupoles (possibly including also coating of the upgraded ones), and by efficient scrubbing of the arcs; b) coupled-bunch instabilities are stabilized by the transverse damper; c) single-bunch instabilities can be stabilized by means of Landau octupoles or by the head-on beam-beam tune spread in a collide-and-squeeze operation mode (see Ref. [8] and references therein). It is expected that 5% of the total intensity is lost during the whole cycle, but keeping an average lifetime below 22 h and in any case never lower than 0.2 h.

Large bunch intensities associated with small emittance result also in large emittance blow-up due to intra-beam scattering (IBS), which has to be added to that generated by unknown noise sources (about 10 % from injection to stable beam and more in the vertical plane). Figure 1 shows the expected horizontal emittance blow-up as predicted by an IBS model through an injection, ramp and squeeze cycle [9], to which a 10 % should be added to account for observed and unknown sources of emittance growth. High brightness beams, in particular those that can be obtained with small emittance, may surpass the damage limit of the injection protection devices in case of failure scenarios, because of the energy density. A programme to replace these devices with more robust material is foreseen for after LS2 [10]. Nonetheless, it is worth noting that small emittances, even if not completely exploitable due to, e.g., IBS effects, provide a natural safety margin against growth effects. For large emittance, the very good alignment of the LHC magnets resulted in ample margins to fit comfortably nominal emittance beams with the typical injection oscillations.

\* The research leading to these results is partly funded by the European Commission within the Framework Programme 7 Capacities Specific Programme, Grant Agreement 284404. The HiLumi LHC Design Study is included in the High Luminosity LHC project

# LESSONS FROM 1-MW PROTON RCS BEAM TUNING

Hideaki Hotchi<sup>#</sup> for the J-PARC RCS beam commissioning group  
J-PARC center, Japan Atomic Energy Agency, Tokai, Naka, Ibaraki, 319-1195 Japan

## Abstract

Via a series of the injector linac upgrades in 2013 and 2014, the J-PARC 3-GeV RCS got all the hardware parameters required for the 1-MW design beam operation. This paper presents the recent high intensity beam experimental results in the RCS including the first 1-MW trial, mainly focusing on our approaches to beam loss issues that appeared on the process of the beam power ramp-up.

## INTRODUCTION

The J-PARC 3-GeV Rapid Cycling Synchrotron (RCS) is the world's highest class of high-power pulsed proton driver aiming at the output beam power of 1 MW [1]. The injector linac delivers a 400-MeV  $H^-$  beam to the RCS injection point, where it is multi-turn charge-exchange injected through a 300- $\mu\text{g}/\text{cm}^2$ -thick carbon stripping foil over a period of 0.5 ms. RCS accelerates the injected protons up to 3 GeV with a repetition rate of 25 Hz, alternately providing the 3-GeV proton beam to the Material and Life Science Experimental Facility (MLF) and to the following 50-GeV Main Ring Synchrotron (MR) by switching the beam destination pulse by pulse.

In the last summer shutdown in 2013, the ACS linac section was installed [2], by which the injection beam energy from the linac was upgraded from 181 MeV to the design value of 400 MeV. In addition, in this summer shutdown in 2014, the front-end system (IS and RFQ) of the linac was replaced [3], by which the maximum peak current of the injection beam was increased from 30 mA to the design value of 50 mA. Via these series of the injector linac upgrades, the RCS has got all the design parameters. Thus the RCS is now in the final beam commissioning phase aiming for the 1-MW design output beam power.

Fig. 1 shows the history of the RCS beam operation. Since the start-up of the user program in December, 2008, the output beam power from the RCS has been steadily increasing as per progressions in beam tuning and hardware improvements [4,5]. The output beam power for the routine user program has been increased to 300 kW as planned to date. In addition to such a routine user operation, the RCS have intermittently been continuing the high intensity beam tests toward the design output beam power of 1 MW. As shown in Fig. 1, the RCS successfully achieved high intensity beam accelerations of up to 539-573 kW for both injection energies of 181 MeV and 400 MeV before and after the installation of the ACS. Besides, the RCS has very recently conducted the first 1-MW trial right after the replacement of the front-end system. The most important issues in increasing the

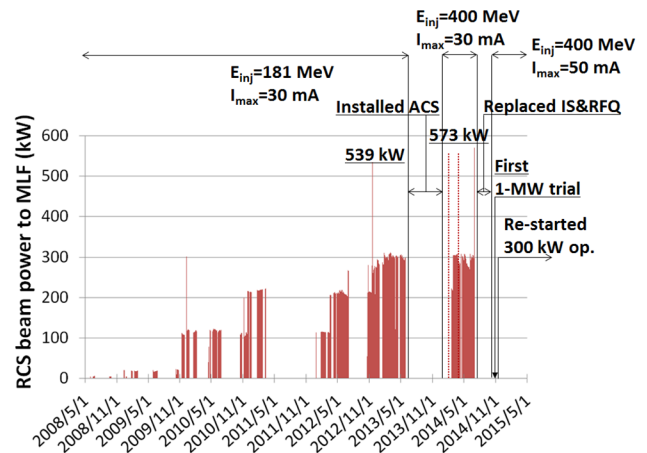


Figure 1: History of the RCS output beam power.

output beam power are control and minimization of beam loss to keep the machine activation within the permissible level. This paper presents the experimental results of these series of recent high intensity beam tests in the RCS mainly focusing on our approaches to beam loss issues that appeared on the process of the beam power ramp-up.

## HIGH INTENSITY BEAM TESTS OF UP TO 553-573 kW

In April (Run#54) and June (Run#56), 2014 after installing the ACS, the RCS conducted high intensity beam tests of up to 553 (Run#54)-573 (Run#56) kW with the upgraded injection energy of 400 MeV, using a 0.5 ms-long injection pulse with a peak current of 24.6 (Run#54)-25.5 (Run#56) mA and a chopper beam-on duty factor of 60%. In these beam tests, the operating point was set at (6.45, 6.42), where the systematic beam loss measurements were performed with various injection painting parameters and beam intensities.

### *Painting parameter dependence of beam loss (Run#54)*

In order to minimize space-charge induced beam loss at the low energy, the RCS employs injection painting both for the transverse and longitudinal phase spaces [6]. On the transverse plane, correlated painting with a painting emittance of  $100\pi$  mm mrad ( $\epsilon_{ip}$ ) was applied. On the other hand, for longitudinal painting [7,8], the momentum offset injection of 0.0, -0.1 and -0.2% ( $\Delta p/p$ ) was tested in combination with superposing a 2nd harmonic rf with an amplitude of 80% ( $V_2/V_1$ ) of the fundamental rf. As an additional control in longitudinal painting, the phase sweep of the 2nd harmonic rf was also employed during injection from -100 to 0 degrees ( $\phi_2$ ) relatively to that of the fundamental rf.

<sup>#</sup>hotchi.hideaki@jaea.go.jp

# ACCELERATOR CHALLENGES OF HIGH INTENSITY LINACS AND THE FACILITY FOR RARE ISOTOPE BEAMS\*

J. Wei<sup>#1</sup>, N. Bultman<sup>1</sup>, F. Casagrande<sup>1</sup>, C. Compton<sup>1</sup>, K. Davidson<sup>1</sup>, B. Drewyor<sup>1</sup>, K. Dixon<sup>2</sup>, A. Facco<sup>1,4</sup>, F. Feyzi<sup>1</sup>, V. Ganni<sup>2</sup>, P. Gibson<sup>1</sup>, T. Glasmacher<sup>1</sup>, L. Hoff<sup>1</sup>, K. Holland<sup>1</sup>, M. Ikegami<sup>1</sup>, M. Johnson<sup>1</sup>, S. Jones<sup>1</sup>, M. Kelly<sup>3</sup>, R.E. Laxdal<sup>5</sup>, S. Lidia<sup>1</sup>, G. Machicoane<sup>1</sup>, F. Marti<sup>1</sup>, S. Miller<sup>1</sup>, D. Morris<sup>1</sup>, P. Ostroumov<sup>3</sup>, J. Nolen<sup>1,3</sup>, S. Peng<sup>1</sup>, J. Popielarski<sup>1</sup>, L. Popielarski<sup>1</sup>, E. Pozdeyev<sup>1</sup>, T. Russo<sup>1</sup>, K. Saito<sup>1</sup>, T. Xu<sup>1</sup>, Y. Yamazaki<sup>1</sup>

<sup>1</sup> Facility for Rare Isotope Beams, Michigan State University, East Lansing, MI 48824 USA

<sup>2</sup> Thomas Jefferson National Accelerator Facility, Newport News, VA 23606, USA

<sup>3</sup> Argonne National Laboratory, Argonne, IL 60439, USA

<sup>4</sup> INFN - Laboratori Nazionali di Legnaro, Legnaro (Padova), Italy

<sup>5</sup> TRIUMF, Vancouver, Canada

## Abstract

This paper surveys the key technologies and design challenges that form a basis for the next generation of high intensity hadron accelerators, including projects operating, under construction, and under design for science and applications at MW beam power level. Emphasis is made on high intensity linacs like the Facility for Rare Isotope Beams (FRIB).

## INTRODUCTION

During the past decades, accelerator-based neutron-generating facilities like SNS [1], J-PARC [2], PSI [3] and LANSCE [4] advanced the frontier of proton beam power to 1 MW level, as shown in Fig. 1 with the beam-on-target power as the product of the average beam current and the beam kinetic energy [5]. For heavy ion, the power frontier will be advanced by more than two-order-of-magnitudes to 400 kW with the construction of the Facility for Rare Isotope Beams currently underway at Michigan State University [6].

Cutting edge technologies continuously developed for accelerator systems have sustained continuous growth in beam intensity and power. High-power operations have been made possible by various types of accelerators: linac, cyclotron, synchrotron and accumulator. During the past decade, superconducting RF related technology has become indispensable for next generation machines.

High power hadron accelerators [5] can be categorized by their goals for high-energy physics (AGS [7], SPS [8], MI [9], J-PARC/MR [2], PIP-II [10] for neutrino, Kaon and Muon physics), nuclear physics (RIKEN [11], SPIRAL2 [12], FAIR [13], FRIB for rare isotope physics; FAIR for antiproton physics; LANSCE), basic energy science and applications (LANSCE, PSI, SNS, J-PARC/RCS [2], ISIS [14], SARAF [15], SPIRAL2, CSNS [16], ESS [17] for neutron sources; KOMAC [18] for proton applications), radioisotope production (SARAF), material neutron irradiation (IFMIF and its validation prototype LIPAc [19]), and accelerator driven subcritical systems (CADS [20] and MYRRHA [21] for

nuclear waste transmutation and power generation). Other operating or proposed projects include LEDA [22], PSR [23], HIAF [24], RAON [25], CPHS [26] and those proposed at CERN (SPL, LAGUNA-LBNO, SHIP) [27] and RAL [28].

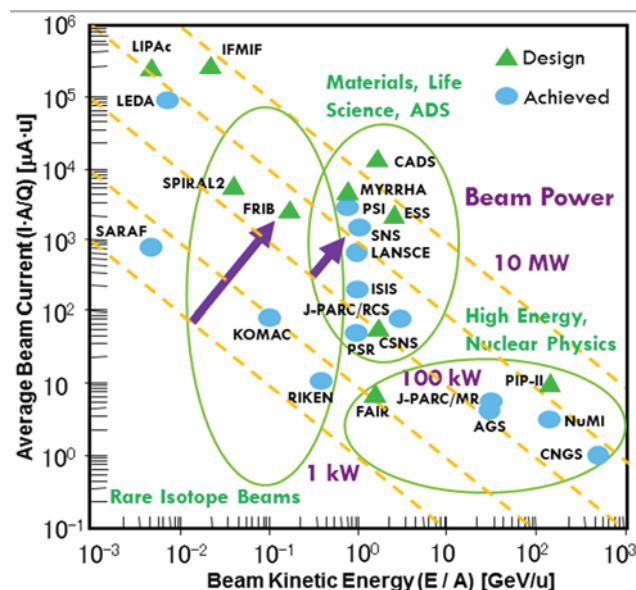


Figure 1: Hadron accelerator power frontier at design, construction, and operation stages.

The figure of merit of these accelerator facilities is the amount of useful secondary beams produced from the target. It is proportional to the target yield and the primary beam intensity. As the optimum energy range is often determined by the target yield, high beam intensity corresponds to a high beam-on-target power.

The beam structure on target largely determines the accelerator type. Synchrotrons (AGS, SPS, MI, J-PARC, ISIS, FAIR, CSNS, PIP-II) and accumulators (PSR, SNS) are used downstream of the injector accelerators to

\*Work supported by the U.S. Department of Energy Office of Science under Cooperative Agreement DE-SC0000661

#wei@frib.msu.edu

# HEAVY-ION CYCLOTRON GYMNASTICS AND ASSOCIATED BEAM DYNAMICS ISSUES

N. Fukunishi, Nishina Center for Accelerator-Based Science, RIKEN, Wako, Japan

## Abstract

After a brief introduction to heavy-ion cyclotrons, their beam dynamics are outlined, with an emphasis on the space-charge effect, and important achievements in both proton and heavy-ion cyclotrons are described.

## INTRODUCTION

The first heavy-ion acceleration using a cyclotron was a 50-MeV  $^{12}\text{C}$  beam accelerated by the 37-inch Berkeley cyclotron in 1940 [1]. The beam intensity was only 8 particles/s. To illustrate the subsequent development of heavy-ion cyclotrons, data compiled by Livingston [1] (up to 1969) and data taken from the “List of Cyclotrons” published in 2004 [2] are combined in Fig. 1. Each cyclotron is classified according to its type and first-beam date (or the date of acceleration of the heavy-ion beam as listed in Livingston’s tables). Although Fig. 1 is an incomplete historical review, we can observe a remarkable increase in energy. Beam intensity seems to stay relatively constant, but that is because the beam intensity of very light ions was high even in the very early stages of cyclotron history. However, beam intensities for heavier ions, such as  $^{48}\text{Ca}$  and  $^{238}\text{U}$ , have greatly increased thanks to advances in ion sources. Because recent low-energy nuclear physics experiments pursue very rare events, beam intensity has become a crucial issue.

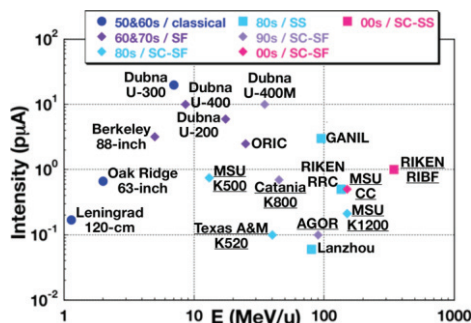


Figure 1: Historical development of heavy-ion cyclotrons.

Nuclear physics is one of the most important applications of heavy-ion cyclotrons: unstable nuclei far from the  $\beta$ -stability line are being extensively studied and many new superheavy elements have been synthesized at JINR FLNR [3]. Heavy-ion beams are also widely used for material modification and analysis (PIXE, RBS, etc.) [4]. The high biological effectiveness of energetic heavy ions has also enabled applications in medical science, biology, agriculture and so on. A compact superconducting cyclotron capable of delivering a 400 MeV/amu carbon beam for cancer therapy has been designed by an IBA-JINR collaboration [5]. Also, wide variety of plant mutations have been induced by energetic

light ions [6] accelerated in the RIKEN Ring Cyclotron (RRC) [7]. The reviews of Onishchenko [8] and Goto [9] provide more detail.

## BASIC FEATURES OF CYCLOTRONS

### Types of Cyclotron

The classical cyclotron invented by Lawrence [10] employed an azimuthally uniform and radially decreasing magnetic field to produce approximate isochronism and vertical stability of particle motion. However, as Bethe pointed out [11], the relativistic mass increase of ions requires a radially increasing field, which impairs vertical stability. The inventions of synchrocyclotrons [12-14] and Thomas cyclotrons solved this conflict. Thomas proposed the use of an azimuthally varying field [15] (AVF) for an isochronous magnetic field. In this case, an ion’s orbit is non-circular and ions can experience edge focusing in the vertical direction. The Thomas cyclotron, also called the isochronous or sector focusing cyclotron, was first demonstrated by Richardson but this fact was classified until 1956 [16]. A further modification of the isochronous magnetic field by using spirally ridged magnet poles was proposed by Kerst et al. [17], which is effective to increase vertical focusing. Cyclotrons with spirally ridged poles are widely used, especially for high-energy cyclotrons.

To realize meson factories, a separate sector or ring cyclotron was proposed [18,19]. A single magnet producing an isochronous magnetic field is divided into sector magnets which are arranged in a ring with spaces between them. This configuration loses one virtue of cyclotrons, compactness, but gains stronger vertical focusing and higher acceleration voltages because azimuthal modulation of the isochronous magnetic field is much stronger than in AVF cyclotrons and high-voltage resonators can be installed in the spaces between the sector magnets. Thus, separate sector cyclotrons are used to produce high-intensity beams. A separated orbit cyclotron (SOC), proposed by Russell [20] and Martin [21], and demonstrated by Trinks [22], is another important variation, but there are no SOCs routinely serving heavy-ion beams to users. For more details of cyclotron development, many review articles are available: for example, the review by Craddock [16].

Among the currently working heavy-ion cyclotrons, GANIL, IMP-Lanzhou, RCNP and RIBF use separate sector cyclotrons, U-400 and U-400m of JINR FLNR are normal conducting AVF cyclotrons, and K500 and K1200 (MSU/NSCL), K500 (TAM), K800 (Catania) and AGOR (K600) are very compact superconducting AVF-type cyclotrons. A coupled cyclotron system at MSU/NSCL accelerates heavy ions up to 160 MeV/amu, though their

# PROGRESS IN THE UPGRADE OF THE CERN PS BOOSTER RECOMBINATION

J. L. Abelleira, W. Bartmann, J. Borburgh, E. Bravin, U. Raich, , CERN, Geneva, Switzerland

## Abstract

The CERN PS Booster recombination lines (BT) will be upgraded following the extraction energy increase foreseen for the long shutdown 2 (LS2) and meant to reduce the direct space-charge tune shift in the PS injection for the future HL-LHC beams. Henceforth the main line elements, recombination septa, quadrupoles and dipoles must be scaled up to this energy. An increase in the beam rigidity by a factor 1.3 requires the same factor in the field integral of the septa,  $\int Bdl$ , in order to bend the same angle and preserve the present recombination geometry, which is one of the main upgrade constraints. This paper describes the new optics, in particular in the new and longer septa. In addition we consider the upgrade of the so called BTM line that brings the beam to the external dump and where emittance measurements are taken thanks to three pairs of grids. The new proposed optics has also the advantage to simplify the design of the new dipoles. Here we study this new optics and the issues related to the emittance measurement at the new higher energy.

## INTRODUCTION TO THE RECOMBINATION LINES

The four transfer lines that extract protons from each ring of the PSB to the PS (BT1, BT2, BT3, BT4) are recombined in the BT line (Fig. 1).

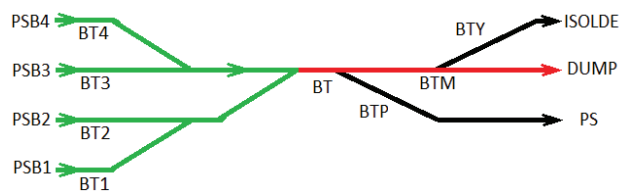


Figure 1: Scheme of the PSB ejection lines, not to scale

From the BT line, the beam can go to three different locations: to the PS (BTP line), to the ISOLDE facility (BTY) or to a dump (BTM). BT.BHZ10 is the switch magnet to the BTP line and BTY.BVT101 is the switch magnet to BTY (off when sending to the dump). Figure 2 represents the scheme of the BT-BTM magnets. A set of three couples of SEM grids lo-cated in the BTM line is used for the emittance measurement in the two planes. In this paper we describe the works on the recombination part (in green in Fig. 1) and the BT-BTM line (in red).

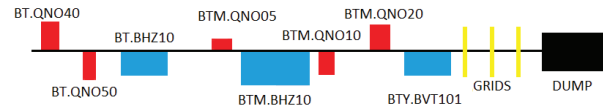


Figure 2: Scheme of the BT-BTM line. Quadrupoles are shown in red and dipoles in blue. It corresponds to the red line in Fig. 1.

## UPGRADING

The LHC Injectors Upgrade (LIU) project [1] aims to an injection energy in the PS of 2 GeV, so that the present lines must work at that energy. In addition, the upgrade of the recombination lines must not hinder a possible upgrade of the ISOLDE facility from 1.4 to 2.0 GeV. In particular, the energy upgrade translates into a 30% increase in beam rigidity, so that the same increase have to followed by the field integral  $\int Bdl$  in all the bending elements: dipoles, septa and kickers. At the same time, a working energy of 1.4 GeV must be allowed in terms of element acceptances. The present 1.0-GeV working energy will be discarded after long shutdown 2 (LS2).

## OPTICS

In order to deal with the different users of the extracted beams from the PSB, four different optics configurations for the BT-BTM line exist [2]:

1. Dump optics
2.  $\epsilon_x$  (Horizontal emittance) measurement: large  $D_x$
3.  $\epsilon_x$  measurement: small  $D_x$
4.  $\epsilon_y$  (Vertical emittance) measurement

The first one is a common configuration to dump the beam and to send it to the ISOLDE facility, while the optics 2, 3 and 4 are used to measure the beam emittances. The reason for having two configurations for the  $\epsilon_x$ -measurement is the large variety of beams that the PSB is supposed to deal with, which are summarized in Table 1.

Table 1: Expected Normalized rms Emittances and Momentum Spreads of the Different Beam Types in the PS Complex, after LS2

Beam	$\epsilon_{N,x} [\mu\text{m}]$	$\epsilon_{N,y} [\mu\text{m}]$	$\sigma_\delta$
LHC (BCMS)	1.2	1.2	$1.1 \times 10^{-3}$
LHC	1.6	1.6	$1.5 \times 10^{-3}$
Fixed target	10	5	$1.35 \times 10^{-3}$
ISOLDE	15	9	$1.35 \times 10^{-3}$

# AN OVERVIEW OF THE PREPARATION AND CHARACTERISTICS OF THE ISIS STRIPPING FOIL

H.V. Smith, B. Jones, ISIS, STFC, Rutherford Appleton Laboratory, UK

## Abstract

The ISIS facility at the Rutherford Appleton Laboratory is a pulsed neutron and muon source, for materials and life science research.  $H^-$  ions are injected into an 800 MeV, 50 Hz rapid cycling synchrotron from a 70 MeV linear accelerator, over  $\sim 130$  turns by charge exchange injection. Up to  $3 \times 10^{13}$  protons per pulse can be accelerated, with the beam current of 240  $\mu A$  split between the two spallation neutron targets.

The  $40 \times 120$  mm aluminium oxide stripping foils used for injection are manufactured on-site. This paper gives an overview of the preparation and characteristics of the ISIS foils, including measurements of foil thickness and elemental composition. Consideration is also given to the beam footprint on the foil and how this could be optimised.

## THE ISIS INJECTION SYSTEM

Injection into the synchrotron occurs via 70 MeV  $H^-$  charge exchange injection over 200  $\mu s$  ( $\sim 130$  turns) beginning 400  $\mu s$  before field minimum of the 50 Hz sinusoidal main dipole field. The foil is mounted in the middle of four dipole magnets which create a 65 mm symmetrical horizontal orbit bump and remove any unstripped beam, Fig. 1. The bump collapses immediately after injection, in 100  $\mu s$ , limiting re-circulations to  $\sim 30$ .

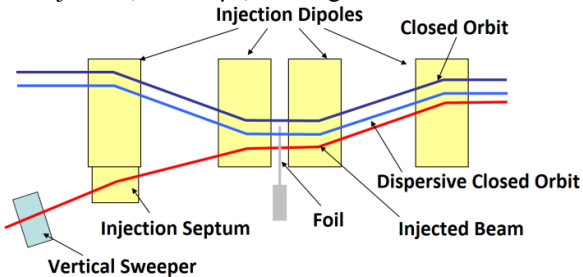


Figure 1: Schematic of the bump and injection magnets overlaid with the trajectories of the incoming  $H^-$  beam, and circulating protons.

Throughout the injection process the beam is painted transversely to reduce the effect of space charge forces, Fig. 2. The injected beam spot is fixed horizontally but painting is realised in this plane by the 20 mm movement of the dispersive closed orbit generated by the energy mismatch between the constant injection energy and changing synchronous energy of the ring. Vertical painting is achieved with a programmable dipole located upstream of the foil. The dipole current is swept such that the beam is moved 12 mm on the foil. The flexible positioning and painting system allows beam to be injected even when some areas of the foil are damaged, this can extend the useful foil life and avoid a foil change.

Operational experience shows that foil lifetimes are often in excess of 200,000  $\mu A$  hrs, with an average of  $\sim 80,000$   $\mu A$  hrs, limited primarily by mechanical factors. A new foil is posted in preparation for each ISIS user cycle in order to avoid a foil change during the cycle which would require access to the synchrotron hall and result in  $\sim 4$  hrs without beam.

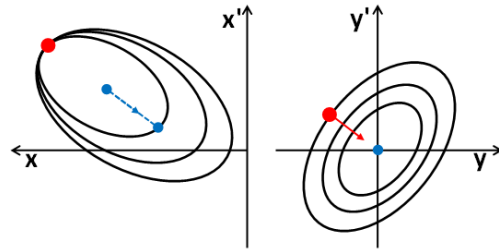


Figure 2: Phase space painting (schematic) on the foil in the horizontal and vertical planes. The injection spot is marked in red, with the closed orbit marked in blue.

## MOTIVATIONS

It is important to understand the properties of the stripping foil to optimise machine operations and design future upgrades.

Previous papers and reports [1, 2] give conflicting statements about the thickness and composition of the stripping foil. Most state that the foil is aluminium oxide (alumina) and that the thickness is 0.25  $\mu m$  or 50  $\mu g cm^{-2}$ . Using the accepted density of aluminium oxide, 3.95  $g cm^{-3}$ , the quoted areal density and thickness of the foil are inconsistent. These discrepancies prompted a fresh study of the foil production mechanism and measurements of the resulting foil properties.

## FOIL PREPARATION

The stripping foils used in ISIS operations are manufactured on site. Production requires numerous complex, non-automated stages and the skill, experience and judgement of staff is heavily relied upon to create usable foils. In total it takes around 20 hours to produce a single foil via the following eight stages, Fig. 3:

1. A 0.15 mm thick sheet of 99% pure aluminium is cut to  $70 \times 130$  mm, two mounting holes are punched through and two wedges clipped out of the edges of the sheet in preparation for final installation.
2. One long edge of the aluminium sheet is then bent in a custom jig to strengthen it. The top short edge of the sheet is slid into a slot in a pre-prepared custom made mounting pin that is used to hold the foil in the mounting mechanism in the synchrotron.

# GLOBAL LINEAR OPTICS CORRECTION FOR LOW ENERGY RHIC RUN\*

C. Liu<sup>†</sup>, K.A. Drees, A. Marusic, M. Minty, C. Montag, BNL, Upton, NY 11973, USA

## Abstract

There has been increasing interest in low energy runs in RHIC, in order to probe the phase diagram at the low energy end. The optics is one of the critical pieces for a successful low energy run since it affects the beam lifetime and thus the achievable luminosity. While acquiring optics measurement data remains difficult, progress has been made in recent years in the analysis of such data and in correcting global optics errors. The analysis technique and the results of optics correction for low energy runs are presented in this report.

## INTRODUCTION

Collisions in the low energy range are motivated by one of the key questions of quantum chromodynamics (QCD) about the existence and location of a critical point on the QCD phase diagram [1]. The beam energy range for low energy runs is between 2.5 and 20 GeV/nucleon. Within this range an energy scan will be conducted over 7 different energies. The luminosity of low energy collisions is expected to improve substantially with the help of low energy electron cooling of the colliding beams [2].

The dynamic aperture of the low energy beam has been improved over the years by fixing the machine non-linearity [3]. On the other hand, it was not possible to systematically measure the optical functions due to the low beam intensity and its short lifetime. During the 2013 and 2014 runs, we managed to measure the linear optics using injection oscillations recorded by turn-by-turn beam position monitors (BPMs), which avoided exciting coherent betatron oscillation. Furthermore, optics corrections were implemented which reduced the global relative errors of beta functions (beta-beat) and corrected the beta functions at the collision points. The analysis technique applied to the turn-by-turn BPM data is presented in the following together with the measured and successfully corrected linear optics during the low energy runs.

## OPTICS MEASUREMENTS DURING LOW ENERGY TEST IN 2013

RHIC was operated for a dedicated test with proton beams at  $\sim 6$  GeV in 2013. One horizontal injection oscillation BPM data is shown in Fig. 1. Two irregularities can be seen in this data set. One is the beam positions reported around turn 200, which looks like pure noise and is present in data recorded by all BPMs. The other one is the sudden

increase of the coherent oscillation amplitude around turn 800. Both remain not understood due to time limitations during the test.

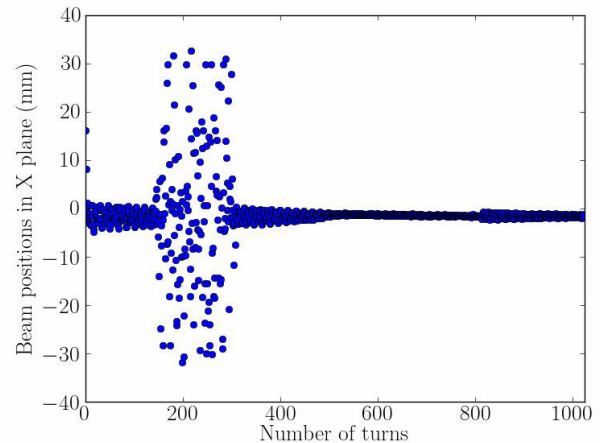


Figure 1: The horizontal injection oscillation BPM data in the Yellow ring during the low energy test in 2013.

The acquired injection oscillation data imposed difficulties on the analysis, which is based on a frequency domain Fourier transform. The Fast Fourier Transform (FFT) produced a spectrum shown in Fig. 2, which is dominated by noise. Therefore, one can neither extract useful tune information nor any other optical functions.

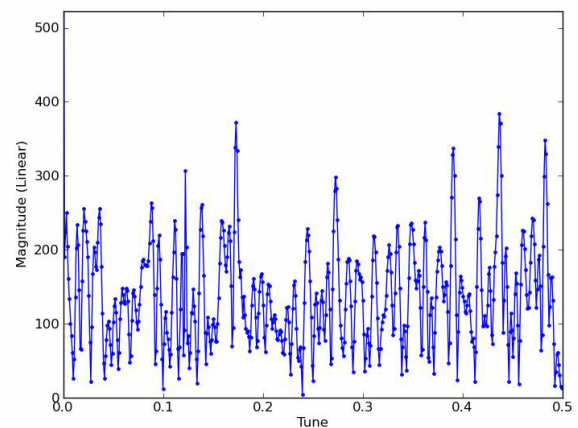


Figure 2: The raw spectrum of the injection oscillation obtained using the FFT technique.

The noise problem was solved later by applying a window (or filter in frequency domain) on the turn-by-turn

\* The work was performed under Contract No. DE-AC02-98CH10886 with the U.S. Department of Energy.

<sup>†</sup> cliu1@bnl.gov

# LONGITUDINAL DYNAMICS SIMULATION AT TRANSITION CROSSING IN RHIC WITH NEW LANDAU CAVITY\*

C. Liu<sup>†</sup>, M. Blaskiewicz, J.M. Brennan, K. Mernick, M. Minty, C. Montag, K. Smith  
BNL, Upton, NY 11973, USA

## Abstract

At the Relativistic Heavy Ion Collider (RHIC), heavy ion beams cross transition energy during acceleration to energies required by the physics programs. In the past, to battle longitudinal instabilities, a Landau cavity was turned on just after acceleration through transition energy. The Landau cavity with modified frequency will be implemented before beam crosses transition in Run-14. Longitudinal dynamics with this new configuration have been simulated to optimize the phase and amplitude of the Landau cavity. We will present simulation results in the report.

## INTRODUCTION

At RHIC, heavy ion beams cross transition energy during acceleration to full energies. For example, Au beam is injected into RHIC with  $\gamma = 10.5$ . It crosses the transition energy ( $\gamma = 23$ ) at  $\sim 85$  s after the start of the acceleration. The heavy ion beams are accelerated by the 28 MHz cavities, whose harmonic number is 360. In the past, the Landau cavity ( $\sim 197$  MHz) was turned on after transition. For Run-14, it was proposed by J.M. Brennan to turn on the Landau cavity before transition crossing for better beam transmission efficiency. In addition, the frequency of the Landau cavity was slightly modified (harmonic number from 2640 to 2580) to better control coupled bunch instability [1]. There were several questions associated with the mentioned changes: what is the impact on the beam emittance if we turn on the Landau cavity before transition? what to do with the phase of the Landau cavity at transition? and what is the optimal configuration for the voltage of the Landau cavity? The simulations will be presented in this report were carried out to answer these questions.

The simulation was performed with a tracking program, ESME [2], which calculates the evolution of a distribution of particles in energy and azimuth as it is acted upon by the radio frequency system of a synchrotron or storage ring. The basis of the program is the pair of single particle difference equations

$$\begin{aligned} \vartheta_{i,n} &= \left[ \frac{\tau_{s,n-1}}{\tau_{s,n}} \vartheta_{i,n-1} + 2\pi \left( \frac{\tau_{i,n}}{\tau_{s,n}} - 1 \right) \right] \text{mod}(\pi) \\ E_{i,n} &= E_{i,n-1} + eV(\phi_{s,n} + h\vartheta_{i,n}) - eV(\phi_{s,n}) \end{aligned} \quad (1)$$

where  $\vartheta$  is the particle azimuth, in the range of  $(-\pi, \pi)$ .  $E_{i,n}$  is the beam energy of the  $i$ th particle at the  $n$ th turn, relative to that of the synchronous particle.  $\tau_{i,n}$  is the revolution period of the  $i$ th particle at the  $n$ th turn.  $\phi_{i,n}$  is the synchronous phase at the  $n$ th turn.

\* The work was performed under Contract No. DE-AC02-98CH10886 with the U.S. Department of Energy.

<sup>†</sup> cliu1@bnl.gov

As one of the inputs to the program, the revolution period is correlated with the machine lattice design. According to Ref. [3], the revolution period is expanded as follows

$$\frac{\tau}{\tau_0} = 1 + \left(\alpha_0 - \frac{1}{\gamma_0^2}\right)\delta + \left(\alpha_0\alpha_1 - \frac{\alpha_0}{\gamma_0^2} + \frac{3}{2\gamma_0^2} - \frac{1}{2\gamma_0^4}\right)\delta^2 + O(\delta^3) \quad (2)$$

where the  $\gamma_0$  is the Lorentz factor of the beam.  $\delta$  is the beam energy spread. The first and second order compaction factors,  $\alpha_0$  and  $\alpha_1$ , can be obtained from the optics model or measurement. It was showed in Ref. [3] that the agreement between measured and the model  $\alpha_1$  was within 10%. The measurement ( $\alpha_1 = -1.15$ ) was used in the simulation.

## HEAVY ION BEAM ACCELERATION AT RHIC

The  $\gamma_t$  jump scheme [4], changing the  $\gamma_t$  by quickly switching the polarity of a group of designated quadrupoles, has been implemented at transition crossing for the heavy ion beams. It takes 35 ms to change the  $\gamma_t$  by 1 unit at RHIC.

The voltage of the 28 MHz cavity during acceleration is shown in Fig. 1. The initial RF voltage was set to the maximum value to reduce intra-beam scattering contribution to longitudinal emittance by sacrificing momentum spread. The voltage is halved around transition to reduce the bucket height.

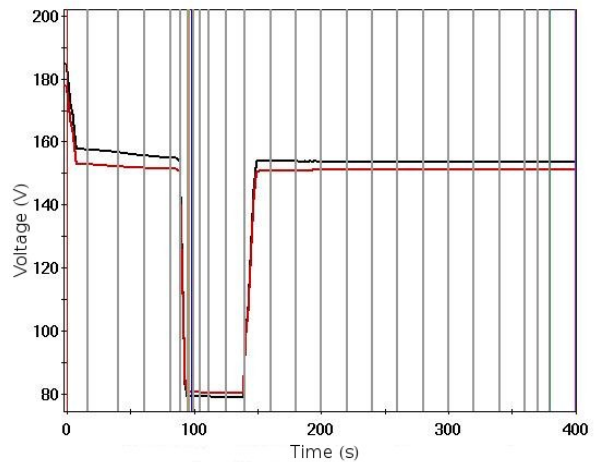


Figure 1: The voltage of the two 28 MHz cavities during acceleration in 2011 Au-Au physics program.

The synchronous phase is determined by the voltage evolution and the beam energy on the ramp. The beam rigidity and its derivatives are shown in Fig. 2.

# BEAM-BASED PERFORMANCE OF THE CERN PS TRANSVERSE FEEDBACK

G. Sterbini, A. Blas, S. Gilardoni, CERN, Geneva, Switzerland

## Abstract

The CERN PS transverse damper is a flexible wideband system to damp injection coherent oscillations, inter and intra-bunch transverse instabilities at different energies along the cycle, to perform controlled emittance blow-up and to serve as abort cleaning device. In this paper we summarise some beam-based observations of the CERN PS transverse feedback performance and compare them with the expected results.

## INTRODUCTION

The CERN PS has to cope with several beam dynamic challenges to produce the present and the future high brightness and high intensity beams [1]. The PS Transverse Feedback (TFB) will be used mainly to address three aspects of the PS beam dynamics to reach the required performance:

- *The injection misteering* due to an injection error. This is expected to be an important source of the emittance growth [2] which drove the specifications of the TFB system. The system has been designed to damp a  $3 \text{ mm}_p$  oscillation with a time constant  $< 50$  turns at injection energy ( $E_k=1.4 \text{ GeV}$ ) while its bandwidth should cover from the first betatron line at  $Q=6.1$  (40 kHz) up to 23 MHz corresponding to the ripple observed on the injection kicker bending field. Given the TFB kicker design, this translates into the power specifications for the present driving amplifiers of 3 kW per kicker plate. Considering a  $E_k=2 \text{ GeV}$  injection and maintaining the same requirements of the 1.4 GeV case, the amplifier power should be increased to 5 kW. The new amplifiers are presently under construction and will be commissioned during the 2015 in the framework of the LHC Injectors Upgrade project [3].
- *The head-tail instability*. This effect is due to the interplay between the machine transverse impedance, its chromaticity and the bunch longitudinal motion [4–6]. It can have a detrimental effect of the beam characteristics up to prevent the beam transmission or to degrade the beam emittance to unacceptable level. The TFB proved to be a valuable tool against this issue.
- *The transverse coupled instability at extraction*. In specific, not yet operational, conditions it has been observed a coupled bunch instabilities at the PS extraction flattop with the 25 ns bunch train. Investigations are ongoing to understand if a similar instabilities will be present with the production LIU beams. Measurements demonstrate that the PS TFB can delay by 10 ms the the instability rise [7]. This result may indicate that an increase of the loop gain should cure the instability.

In addition to that, the TFB can perform controlled emittance blow-up, serve as abort cleaning device, excite the beam for tune measurement and machine development studies.

## THE SYSTEM AND ITS PERFORMANCE

A description of the present system is provided in the following, highlighting its performance and limits. A more detailed description can be found in [8–10]. The envisaged upgrade for 2015 will also be discussed. A simplified block diagram of the present system from the pick-up to the kicker is shown in Fig. 1 (only the horizontal plane is depicted). The transverse pick-up [9, 11], PU, feeding the TFB is positioned in section 98. The PU signal is amplified to match the input dynamic of the digital card (DSPU). The output of the digital card is amplified, combined with the Q-meter signal and splitted on the input of the two power amplifiers that drives the two horizontal plates of the kicker. The matching between the output impedance of the power amplifier ( $50 \Omega$ ) and the kicker impedance ( $100 \Omega$ ) is performed with a transformer. The transverse kicker is positioned in section 97. The TFB is composed of the subsystems described in the following sections.

### The Pick-up Pre-amplifier

The PU preamplifier is a critical subsystem for the TFB since it is used to set the feedback loop gain and to adjust the  $\Delta H$  and  $\Delta V$  signals to the  $1 V_p$  input dynamics of the DSPU ADC. It is a low-noise pre-amplifier with a gain range of  $-60$  to  $+40$  dB (down to  $-60$  dB provided by an attenuator in 3 steps of  $-20$  dB and up to  $+40$  dB provided by an amplifier in 255 steps of  $\approx 0.155$  dB) that allows to adjust it to the different PS beam flavours [9]. The pre-amplifier has a global attenuation block shared by all three channels ( $\Sigma$ ,  $\Delta H$  and  $\Delta V$ ) together with an analog gain separately adjustable on each single channel. Attenuation and gain can vary from cycle to cycle but not within a cycle. This implies that if the TFB has to address different problems within one cycle (e.g. damping injection oscillation, head-tail instability, coupled bunches instabilities at extraction) the loop gain cannot be adjusted and optimised for each physical process. The  $-10$  dB bandwidth of the PU amplifier is 60 MHz with less than 10 degrees of non-linear phase error on the entire amplification and attenuation range. Presently the transverse signals are not normalised therefore the gain of the feedback loop varies along the bunch for not uniform longitudinal distributions.

### The Digital Signal Processing Unit

There is one digital signal processing unit (DSPU) for each plane, clocked with harmonic 200 of the beam revolution

# TRANSVERSE DECOHERENCE OF ION BUNCHES WITH SPACE CHARGE AND FEEDBACK SYSTEM

I. Karpov<sup>1</sup>, V. Kornilov<sup>2</sup>, O. Boine-Frankenheim<sup>1,2</sup>

<sup>1</sup>TEMF, TU Darmstadt, Schloßgartenstraße 8, 64289 Darmstadt, Germany

<sup>2</sup>GSI, Planckstr. 1, 64291 Darmstadt, Germany

## Abstract

The transverse decoherence of the bunch signal after an initial bunch displacement is an important process in synchrotrons and storage rings. It can be useful, for the diagnostic purposes, or undesirable. Collective bunch oscillations can appear after the bunch-to-bucket transfer between synchrotrons and can lead to the emittance blow-up. In order to preserve the beam quality and to control the emittance blow-up, transverse feedback system (TFS) are used. In heavy ion and proton beams, like in SIS18 and SIS100 synchrotrons of the FAIR project, transverse space charge strongly modify decoherence. The resulting bunch decoherence and beam blow-up is due to a combination of the lattice settings (like chromaticity), nonlinearities (residual or imposed by octupole magnets), strong space-charge, and the TFS. We study these effects using particle tracking simulations with the objective of correct combinations for a controlled beam blow-up.

## DECOHERENCE DUE TO TRANSVERSE NONLINEARITY AND CHROMATICITY

A beam after an initial transverse displacement performs betatron oscillations. In the absence of collective effects, the evolution of the beam centroid has been described in [1, 2]. Calculations are performed for the case of transverse nonlinearity in one plane, the initial Gaussian distribution (GS) in  $(x, x')$ , the linear synchrotron motion and the Gaussian energy distribution. Extension to 2-D, including  $x-y$  coupling in the tune dependence from amplitudes, is addressed in [3]. Here we present the 1D results for the KV (Kapchinsky-Vladimirsky) distribution in the transverse plane in the case of uncoupled transverse oscillations and compare with the results for the GS distribution and with particle tracking simulations.

We use the constant focusing for derivations and for simulations. In this case it is convenient to use the normalized coordinates,

$$q = \frac{x}{\sigma_{x0}} \text{ and } p = \frac{Rx'}{Q_0\sigma_{x0}}, \quad (1)$$

where  $R$  is the ring radius,  $Q_0$  is the bare tune,  $\sigma_{x0} = \sqrt{R\epsilon_{\text{rms}0}/Q_0}$  is the initial rms beam size,  $\epsilon_{\text{rms}0}$  is the initial rms emittance. We normalize the initial beam offset in  $x$  plane by defining  $Z = \Delta x/\sigma_{x0}$ . The amplitude  $a$  and the phase  $\phi$  of single particle oscillations are defined by relations  $q = a \cos(\phi)$  and  $p = -a \sin(\phi)$ , where  $a = \sqrt{q^2 + p^2}$ .

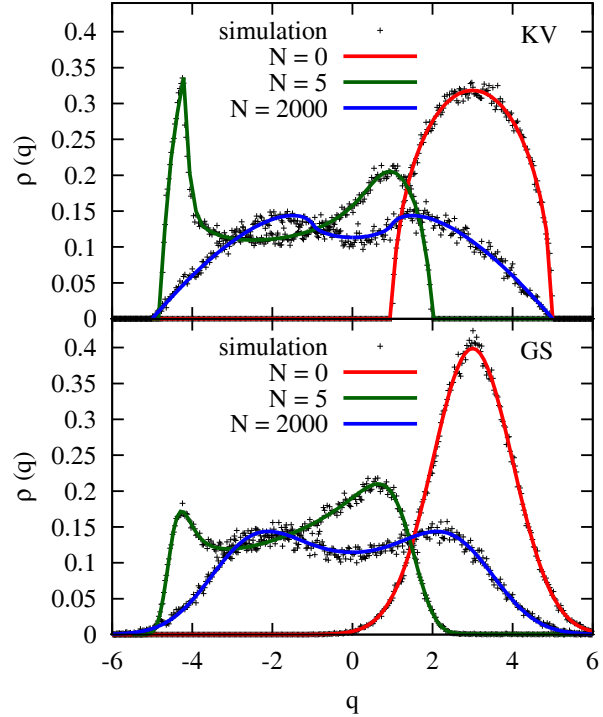


Figure 1: Beam profiles at different turn numbers for the KV (top plot) and for the GS (bottom plot) distributions. Crosses are simulation results. Solid lines are obtained by the numerical integration of Eq. (7).  $Z = 3$ ,  $Q_0 = 4.18$ ,  $q_{\text{nl}} = 0.3$ .

The initial beam distribution at turn  $N = 0$  is

$$\rho_0(a, \phi_0) = \frac{a}{4\pi} H \left[ 1 - \frac{1}{4} (a^2 + Z^2 - 2aZ \cos(\phi_0)) \right], \quad (2)$$

where  $H$  is the Heaviside function and  $\phi_0$  is the initial betatron phase of the particle. External nonlinearities induce amplitude-dependent incoherent tune shifts. We assume that a transverse nonlinearity is produced by the cubic component of the octupole magnetic field,

$$B_x = -K_3 \frac{B\rho}{6} y^3, \quad B_y = K_3 \frac{B\rho}{6} x^3, \quad (3)$$

with  $K_3 = \frac{1}{B\rho} \frac{d^3 B_y}{dx^3}$ .

The resulting tune shift in  $x$  plane is given by

$$\Delta Q_{\text{nl}}(a) = -\frac{K_3 R^3}{16 Q_0^2} \epsilon_{\text{rms}0} a^2 = -\mu a^2, \quad (4)$$

# SLIP-STACKING DYNAMICS AND THE 20 Hz BOOSTER

J. Eldred, Department of Physics, Indiana University, Bloomington, IN 47405, USA  
R. Zwaska, FNAL, Batavia, IL 60510, USA

## Abstract

Slip-stacking is an accumulation technique used at Fermilab since 2004 which nearly doubles the proton intensity. The Proton Improvement Plan II intensity upgrades require a reduction in slip-stacking losses by approximately a factor of 2. We introduce universal area factors to calculate the available phase space area for any set of beam parameters without individual simulation. We show the particle loss as a function of time and slip-stacking resonances. We calculate the injection efficiency as a function of longitudinal emittance and aspect-ratio. We demonstrate that the losses from RF single particle dynamics can be reduced by a factor of 4-10 (depending on beam parameters) by upgrading the Fermilab Booster from a 15-Hz cycle-rate to a 20-Hz cycle-rate. We recommend a change in injection scheme to eliminate the need for a greater momentum aperture in the Fermilab Recycler.

## INTRODUCTION

Slip-stacking is integral to high-intensity operation at Fermilab and will play a central role in upgrades to the accelerator complex [1–3]. The Fermilab Proton Improvement Plan-II [1] calls for an improvement in beam power from 700 kW (with slip-stacking) to 1.2 MW with an eye towards multi-MW improvements. The increase in proton intensity requires a commensurate decrease in the slip-stacking loss-rate to limit activation in the tunnel. Single-particle dynamics associated with slip-stacking contribute directly to the particle losses. Our numerical results completely characterize the stable phase-space boundary and express this information as limits on the Booster beam quality. We show that including a 20-Hz Booster cycle-rate in the PIP-II upgrade relaxes the limits on the Booster beam quality and cuts particle losses due to slip-stacking.

## BACKGROUND

Slip-stacking is a particle accelerator configuration that permits two high-energy particle beams of different momenta to use the same transverse space in a cyclic accelerator. The two beams are longitudinally focused by two sets of rf cavities with a small frequency difference between them. Each frequency is tuned to the momentum of one of the beams.

The two azimuthal beam distributions are manipulated as a consequence of their difference in rf frequency. Figure 1 shows the slip-stacking accumulation process. The two beams injected on separated portions of azimuth with a small frequency difference and overlap gradually, allowing injection [4]. When the cyclic accelerator is filled and the azimuthal distribution of the two beams coincide then the

two beams are accelerated together by RF cavities operating at the average frequency. The potential beam intensity of a synchrotron is doubled through the application of this technique.

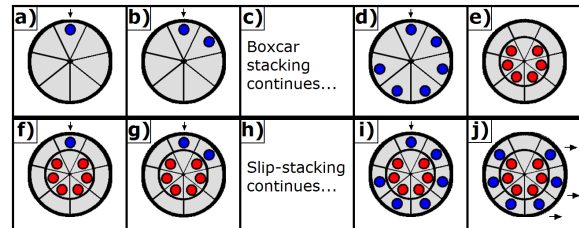


Figure 1: The Booster batch is represented by the circles and the Recycler (or Main Injector) is represented by the seven-sector wheel. **a)** The first batch is injected into the ring. **b)** One Booster cycle later the second batch is injected in the azimuthal space immediately behind the first batch. This is known as boxcar stacking. **c, d)** Boxcar stacking injections continue until six Booster batches are stored in the ring. **e)** The RF frequency is adiabatically lowered in between the sixth and seventh batch injection. **f)** The seventh batch is injected in the gap left by the previous six batches. Both cavities are operating at different frequency (slip-stacking). The first RF cavity matches the first six batches and the second RF cavity matches the next set of batches. **g)** One Booster cycle later the eighth batch is boxcar stacked with respect to the seventh batch but the frequency difference allows the injection to occur in the gap left by the first six batches. **h, i)** Slip-stacking injections continue until twelve Booster batches are stored in the ring. **j)** One Booster cycle later the kicker gaps of the first six and last six batches are aligned. At that time the batches are extracted to the Main Injector (if needed) and both beams are accelerated as one.

A preliminary study explored the beam dynamics in a 2-rf system [5]. The slipping of bunched beams was first demonstrated at the CERN SPS [6] but the emittance growth led to unacceptable particle losses. Fermilab has subsequently implemented slip-stacking operationally since 2004 [4, 7, 8]. Initially, the higher beam intensity was used to increase antiproton production for proton-antiproton collider experiments [9]. Subsequently, slip-stacking was applied to neutrino production for Neutrinos at Main Injector (NuMI) experiments [10–12].

Beam-loading effects can impact the effectiveness of slip-stacking and were addressed in the Main Injector by the development of a beam-loading compensation system with -14dB feedback and -20dB feedforward [13–15]. The beam-loading effects on slip-stacking in the Recycler will be an order of magnitude weaker than in the Main Injector and

# RMS EMITTANCE MEASURES FOR SOLENOID TRANSPORT AND FACILITY FOR RARE ISOTOPE BEAMS FRONT-END SIMULATIONS\*

Steven M Lund<sup>†</sup>, Eduard Pozdeyev, Haitao Ren, and Qiang Zhao

Facility for Rare Isotope Beams, Michigan State University, East Lansing, MI, USA 48824

## Abstract

Measurement of beam phase-space area via rms emittances in solenoid focusing channels with  $x$ - $y$  coupling is complicated relative to transport channels with decoupled plane focusing. This stems from correlated azimuthal flow of the beam induced by the coupled focusing influencing how the thermal component of the flow should be measured. This is exacerbated when the beam has net canonical angular momentum — as is the case for beams born in a magnetic field within ECR-type sources. In this study, a systematic analysis is carried out to derive a multi-species beam envelope equation and motivate measures of rms emittance and phase-space area for use in solenoid transport for beams with canonical angular momentum. These results are applied in Warp PIC simulations of the near-source region of the front-end of the Facility for Rare Isotope Beams (FRIB) linac. In these simulations, a multi-species heavy-ion DC beam emerging from an ECR source are simulated in transverse slice mode using a realistic lattice description. Emittance growth due to nonlinear applied fields and space-charge is analyzed including the influence of net canonical angular momentum. It is found that emittance growth in the near source region of FRIB front-end should in most cases be minimal and that the beam size can be readily controlled over a wide range of parameter uncertainties.

## INTRODUCTION

The Facility for Rare Isotope Beams (FRIB) is a high continuous-wave power (CW) linear accelerator now under construction at Michigan State University to enable state-of-the-art nuclear physics experiments [1]. It will simultaneously accelerate multiple charge states of heavy ions to kinetic energies above 200 MeV/u with 400 kW power on target delivered within a compact spot. Although the FRIB linac has high CW power, space-charge intensity is modest in most of the machine. However, near the electron cyclotron resonance (ECR) sources in the front end (see Fig. 1), space-charge can be an issue [2]. Here, kinetic energy is low ( $\sim 35$  kV ECR extraction bias followed by a grating dc gap typically biased to  $\sim 50$  kV to achieve 12 kV/u in target species) and the ECRs produce numerous charge states and ions resulting in relatively high DC current until extra species are removed downstream beginning with the first bending dipole. Uranium and Oxygen species, (unneutralized) particle currents, and particle rigidities (at

extractor bias) expected for Uranium ECR operation are given in Table 1. It is anticipated that space-charge of the DC beam will be  $\sim 75\%$  electron neutralized outside of the grating gap (strong sweep and guarded downstream by a negatively biased suppressor electrode). Typically only two target species will be transported downstream of the front-end. A compact beam phase-space (low emittance and halo suppressed) in the target species must be preserved in transport near the source in the presence of the parasitic species to insure reliable machine operation with minimal potential losses. In the transport immediately downstream of the ECR two solenoids are employed to transversely focus the multi-species beam. Solenoids are short with poor aspect ratio (39.5 cm length and 7.75 cm radius aperture) and the extended fringe fields overlap with the solenoid field from the ECR source and the grating gap. Ions are born relatively cold (expect  $\sim 1$ – $3$  eV thermal temperature expected) with a compact radius ( $R \approx 4$  mm) but are strongly magnetized in the high magnetic fields within the ECR sources resulting in significant canonical angular momentum contributions to the transverse beam size.

Table 1: (Color) Species from FRIB Venus-like ECR source for U operation. Color coding shown for species identification in simulations.  $U^{+33}$  and  $U^{+34}$  are target species.

Ion	$I$ (pA)	$Q/A$	$[B\rho]$ (Telsa-m)
$U^{+25}$	0.035	0.105	0.0831
$U^{+26}$	0.051	0.109	0.0815
$U^{+27}$	0.068	0.113	0.0800
$U^{+28}$	0.088	0.118	0.0785
$U^{+29}$	0.115	0.122	0.0772
$U^{+30}$	0.150	0.126	0.0759
$U^{+31}$	0.175	0.130	0.0746
$U^{+32}$	0.192	0.134	0.0735
$U^{+33}$	0.210	0.139	0.0723
$U^{+34}$	0.205	0.143	0.0713
$U^{+35}$	0.178	0.147	0.0702
$U^{+36}$	0.142	0.151	0.0693
$U^{+37}$	0.11	0.155	0.0683
$U^{+38}$	0.072	0.160	0.0674
$U^{+39}$	0.043	0.163	0.0665
$U^{+40}$	0.031	0.168	0.0657
$O^{+1}$	0.3	0.063	0.1077
$O^{+2}$	0.3	0.125	0.0762
$O^{+3}$	0.3	0.188	0.0622
$O^{+4}$	0.2	0.250	0.0539

In this study we employ theory to develop an envelope model (Sec. Envelope Model) and report preliminary particle-in-cell simulations with the Warp code [3] (Sec. Simulations). The envelope model is employed to better understand how to measure effective beam phase-space area for the multi-species beam with canonical angular momentum and solenoid focusing which both induce coherent azimuthal flow in the beam components. The simulations

\* Work supported by the U.S. Department of Energy Office of Science under Cooperative Agreement DE-SC0000661 and the National Science Foundation under Grant No. PHY-1102511.

<sup>†</sup> lund@frib.msu.edu

# AN ESS LINAC COLLIMATION STUDY

R. Miyamoto\*, ESS, Lund, Sweden

## Abstract

The European Spallation Source is planned in Lund, Sweden, and will be a neutron source based on a proton linac with an unprecedented 5 MW beam power. Mitigation of beam losses is the most crucial challenge in beam physics for such a high power proton linac and collimation systems are planned in sections of the medium and high energy beam transport (MEBT and HEBT). A preliminary study of the collimation systems was presented in the previous time of this workshop but the linac design went through a significant revise since then. The system to expand the beam for the target, located in the HEBT, was changed from one based on nonlinear magnets to a raster system and this change particularly had a significant impact on the demand on the collimation systems. This paper presents an updated beam dynamics study of the collimation systems for the present layout of the ESS Linac.

## INTRODUCTION

The European Spallation Source (ESS) will be a neutron source in Lund, Sweden, based on a proton linac with an unprecedented 5 MW beam power [1]. Figure 1 shows a layout of the ESS Linac and Table 1 summarizes its high level parameters. The linac consists of normal conducting accelerating structures, sections of superconducting cavities, and low, medium, and high energy beam transports (LEBT, MEBT, and HEBT). The normal conducting accelerating structures include an ion source (IS), radio frequency quadrupole (RFQ), and drift tube linac (DTL). The ESS Linac uses three types of superconducting cavities: spoke, medium- $\beta$  elliptical, and high- $\beta$  elliptical cavities. The sections of the superconducting cavities are also referred to as the Superconducting (SC) Linac as a whole.

For a high power machine such as the ESS Linac, minimization of beam losses is crucial to allow hands-on maintenance as well as to protect machine components and imposes difficult challenges on the design and machine tuning. Based on the experience of SNS [2], a system of beam scrapers is planned for the MEBT to improve beam quality in an early stage of the linac and thus to lower the risk of the beam losses as possible. Beam dynamics simulations indicated its use for the ESS Linac too [3–5] but its effect throughout the entire linac, taking into account various errors, has not been thoroughly studied yet. Collimation systems have been also considered for the HEBT where the beam power is the highest 5 MW [3, 6]. However, since the design revision in 2013 [7], the system to expand the beam for the target has been switched from one based on nonlinear magnets [8] to the other using raster magnet [9] and the present system is much less sensitive to the transverse beam halo. This



Figure 1: Layout of the ESS Linac. Blue color indicates a section of superconducting cavities.

Table 1: High Level Parameters of the ESS Linac

Parameter	Unit	Value
Average beam power	MW	5
Maximum beam energy	GeV	2
Peak beam current	mA	62.5
Beam pulse length	ms	2.86
Beam pulse repetition rate	Hz	14
Duty cycle	%	4
RF frequency	MHz	352.21/704.42

led present reconsideration of the collimation systems in the HEBT. An input to make the decision is quality of the beam entering the HEBT. Thus, on this occasion, impact of the MEBT scrapers on the beam quality and losses throughout the entire linac, especially the later part of the linac, is studied in detail in this paper

## CONDITIONS FOR SIMULATIONS

This section discusses conditions of the simulations in the following sections. Throughout the paper, the lattice in [1] is used. All the simulations are done by tracking the pre-calculated RFQ output beam from the MEBT entrance with the TraceWin code [10]. Space-charge force is calculated with the 3D PICNIC routine [11] with a step size of 15 per [(relativistic- $\beta$ )  $\times$  (wavelength)] and a mesh of  $10 \times 10 \times 10$ .

### RFQ Output

The output beam from the RFQ is simulated with the Tou-tatis code [12] by assuming 2D Gaussian distribution with a normalized emittance of  $0.25 \pi$  mm mrad at its entrance. The number of macro-particles is either  $1 \times 10^5$ ,  $1 \times 10^6$ , or  $1 \times 10^7$ , depending on a type of a study. Table 2 summarizes the parameters of the simulated output beam.

Table 2: RMS Normalized Emittances ( $\epsilon$ ) and Courant-Snyder Parameters ( $\beta$  and  $\alpha$ ) of the RFQ Output Beam

Plane	$\epsilon$ [ $\pi$ mm mrad]	$\beta$ [m]	$\alpha$
$x$	0.253	0.210	-0.052
$y$	0.252	0.371	-0.310
$z$	0.361	0.926	-0.481

\* ryoichi.miyamoto@ess.se

# SPACE-CHARGE COMPENSATION OF INTENSE ION BEAMS BY NONNEUTRAL PLASMA COLUMNS\*

K. Schulte<sup>†</sup>, M. Droba, S. Klaproth, O. Meusel, D. Noll, U. Ratzinger, K. Zerbe  
 Institute for Applied Physics, Goethe University Frankfurt a.M., Germany  
 O. Kester, GSI, Darmstadt, Germany

## Abstract

Gabor lenses were conceived to focus a passing ion beam using the electrical field of a confined nonneutral plasma column. Beside its application as focusing device, in Gabor lenses space-charge effects can be studied in detail.

The influence of the electron distribution on emittance and space-charge dominated ion beams was investigated in beam transport experiments [1]. In this contribution we want to emphasize one result of these experiments. The measurements indicated a strong contribution of secondary electrons on beam dynamics. Secondary electrons are produced within the transport channel, particularly by interaction of the beam with the surface of the slit-grid emittance scanner. This effect might lead to an increase of the filling degree and to an improved focusing performance of the lens.

Assuming that the loss and production rates within the lens volume and the transport channel determine the equilibrium state of the nonneutral plasma column, the electron cloud was characterized as a function of the external fields and the residual gas pressure in small-scale table top experiments.

In this contribution experimental results will be presented in comparison with numerical simulations.

## BEAM TRANSPORT EXPERIMENTS

A number of diagnostic as well as beam transport experiments were performed in order to investigate how the nonneutral plasma properties are mapped onto the ion beam. At first, the electron density distribution and the plasma parameters were determined in diagnostic experiments without beam. Afterwards the lens was used as focusing device for the transport of an emittance dominated helium and a space charge dominated argon beam to study its performance with respect to image quality and space charge compensation.

### Electron Density Distribution

Figure 1 represents the results of the emittance dominated beam transport experiments.

One important result is that the electron density distribution determines the phase space distribution of the beam. In case of a hollow electron distribution, passing beam ions experience a strong force at the edge of the column and none in the center. For a homogeneous electron density distribution the focusing is linear and therefore the beam is transported without aberrations if the radius of the column is larger than the beam radius. Still, it was found that for given lens parameters the measured electron densities and the electron

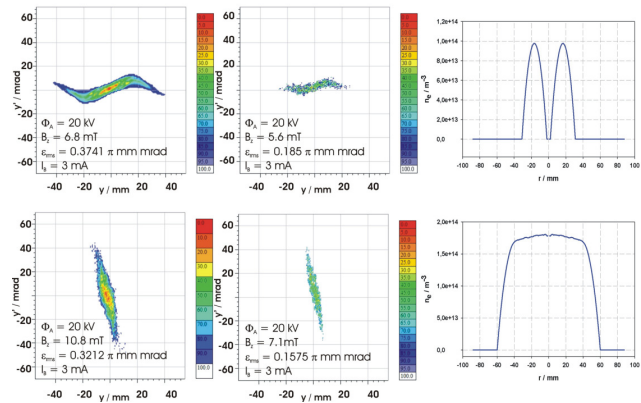


Figure 1: Comparison of measurement (left) and simulation of the transported He<sup>+</sup> beam (center) as well as simulated electron density distribution (right) [2].

density distribution in the diagnostic experiments differed from the results of the beam transport experiments.

An example of the space-charge dominated beam experiments is depicted in Fig. 2.

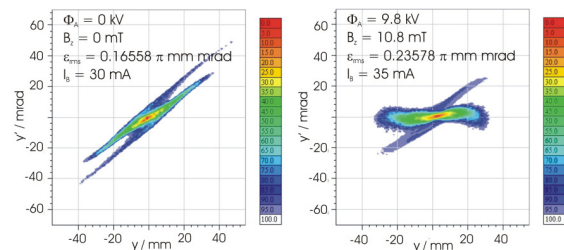


Figure 2: Phase space distribution of the drifted beam when the lens was switched off (left) and of the transported Ar<sup>+</sup> beam when the lens was switched on (right) [2].

Indeed, the focusing performance of the Gabor lens looks very promising, but neither the diagnostic measurements nor the performed numerical simulations show comparable results.

### Influence of Beam Intensity on the Focusing Performance

Furthermore, for the same parameter set-up of the Gabor lens it was observed that the focusing strength increases with the beam current which indicates an increased density of the confined electron column. Figure 3 illustrates the phase space distribution of a 2.2 keV/u Ar<sup>+</sup> beam measured behind the lens for different beam currents.

\* Work supported by HIC for FAIR

<sup>†</sup> Schulte@iap.uni-frankfurt.de

# A NOVEL CODE WITH HIGH-ORDER ADAPTIVE DYNAMICS TO SOLVE THE N-BODY PROBLEM

S. Abeyratne<sup>^</sup>, B. Erdelyi<sup>\*^</sup>, H. Schaumburg<sup>^</sup>

<sup>^</sup>Department of Physics, Northern Illinois University, DeKalb, IL 60115

<sup>\*^</sup>Physics Division, Argonne National Laboratory, Argonne, IL 60439

## Abstract

Although there are several publicly available algorithms to model the behavior of natural systems such as the N-body system, limited computing power hinders the attempt to simulate them efficiently. With the improvement of high performance computing, scientists will be able to run simulations at an unprecedented scale in the future. Therefore, it is necessary to develop new algorithms and data structures to harness the power of high performance computing. In this paper we show a newly developed code, particles' high order adaptive dynamics (PHAD), to serve future computing demands. We use Fast Multipole Method (FMM) to calculate the interactions among charged particles. We use the Strang splitting technique to reduce the number of FMM calls and enhance the efficiency. Picard iterations-based novel integrators are employed to achieve very high accuracies. Electron cooling in the proposed Electron Ion Collider (EIC) has been identified as a potential testing environment for PHAD.

## INTRODUCTION

Computer simulations are heavily used in designing particle accelerators and the efficiency and accuracy of them can be improved with ever changing computational power. Clearly, this demands dramatic improvements on existing code for beam dynamics. In this paper we present a new code developed using novel ideas to significantly divert the existing trend and electron cooling will be one of the potential candidates of its application.

The densely packed particles in a beam, which can be considered as our N-body system, experience two types of forces, long range and short range. The long-range forces are the Coulomb forces and the short-range forces are Coulomb collisions. Also, the motion of the particles in the beam should be taken into consideration for precise modeling and simulation of the beam. Therefore, our code enables to calculate Coulomb interactions and study the changes in the particle configuration with time.

## ALGORITHM

In an N-body system each object continuously interacts with every other object in the system. The direct computation or pairwise calculation of such interactions gives the exact results and needs a computational complexity in the order of  $N^2$ . For very large N, this method quickly becomes untenable. Using some approximate methods, such as the basis function methods, particle-mesh methods, and hierarchical subdivision methods, can circumvent this drawback. The challenge is to mitigate the approximation artifacts. The

hierarchical (or recursive) subdivision method has three distinct flavors: tree, cluster and fast multipole method and the algorithm used to develop our code belongs to the hierarchical fast multipole method (FMM). In FMM particles are confined to spatially bound cells and the interaction between cells are computed. Therefore, the force experienced by any particle inside a cell can be approximated to the addition of Taylor expansions calculated from the multipole expansion of the far away cells. Also, FMM can calculate interactions among N- bodies while retaining accuracy because its computational time typically grows linearly with the number of bodies.

Again, FMM has different versions and they vary with the dimensionality and the type of particle distribution. The code described in this paper uses the 3D adaptive FMM; it is well suited for any arbitrary distribution [1,2]. Even though FMM is considered as an approximation to get the solution of the Poisson equation, its accuracy can be set a priori and can be tuned to get even more accurate results than the direct summation method.

In order to study the beam propagation as time progresses, we need to split the total time into smaller steps and examine the beam dynamics after each small time step. A fixed time step size is not a good choice to study the behavior of the beam. For example, to study the close encounters of particles the step size should be adjustable. Hence, we used a variable order Picard iteration-based integrator. It is an integrator with dense output and flexible for automatic adjustment of the optimal order and time step to achieve a prescribed accuracy with a minimum computational cost.

The implementation of the automatic step size and order selection is not yet completed. Therefore, our code is tested only for the variable order with the fixed time step size [3,4].

To further enhance the computational throughput, we use Strang splitting [5]. Strang splitting is a second order accurate operator splitting method. This method splits a complicated problem into a few simpler parts and solves them separately and composes all solutions to get the final solution of the problem. Two types of forces—strong forces that change rapidly and smooth forces that vary slowly, act upon each particle in a beam. When the particles get closer they experience a very strong force and undergo rapid changes. This type of behavior occurs in the nearby region or the neighborhood of an evaluation point. Therefore, small time steps are needed to model the strong forces and it is possible each particle in the close encounter to have its own time step size. The influence caused by the far away particles can be considered as the mean force exerted by them and

# RESONANCE STRUCTURES IN THE IMPEDANCE OF A CERAMIC BREAK AND THE MEASURED RESULTS

Y. Shobuda, T. Toyama, J-PARC Center, JAEA/KEK, Ibaraki, Japan  
Y.H. Chin, K. Takata, KEK, Ibaraki, Japan

## Abstract

Recently, we have developed a new theory to evaluate longitudinal and transverse impedances of any size of ceramic break sandwiched between metal chambers. The theory successfully reproduces the resonance structures in the impedance due to trapped modes inside the ceramic break. The comparisons between the theoretical and the simulation results such as ABCI and CST Studio show excellent agreements, indicating that they can be used as a good benchmark test for accuracy of simulation codes. To demonstrate the existence of such resonances, the transverse impedance of the ceramic break is measured using the wire-method. The measurement results reproduce the simulations well. The theory is particularly useful for the evaluation of the impedance of the ceramic break with titanium nitride coating.

## INTRODUCTION

A short ceramic ring sandwiched by metal chambers is called a ceramic break. Such ceramic breaks are often inserted between the chambers near bending magnets in proton synchrotrons. Their purpose is to mitigate the eddy current effects over the chambers excited by the outside time-varying magnetic fields, and the induced magnetic turbulence is confined in the chamber between the ceramic breaks [1].

On the other hand, capacitors are typically attached on the outer surface of the ceramic breaks as RF shields to prevent the radiation fields to propagate out of the ceramic breaks. The radiated fields may cause malfunctioning of devices along the accelerators.

In the J-PARC main ring (MR), two ceramic breaks have been additionally installed since 2011. At first, they forgot to attach RF shields around them. When the beam with particles more than  $3.75 \times 10^{13}$  was shot into MR, they discovered that the power source of the quadrupole magnets were suddenly tripped, and the noise level in the adjacent monitors were increased intolerably high. The problems were put under control by attaching RF shields around the ceramic breaks. This accident reminded them the importance of the RF shields to the ceramic breaks.

In the rapid cycling synchrotron (RCS) in J-PARC, titanium nitride (TiN) is coated on the inner surface of the ceramic chambers, to suppress the secondary emission of electrons, caused by the collisions between a part of a proton beam and the chamber surface. The TiN coating is supposed to prevent the build-up of the electron cloud from destabilizing the beams [2, 3].

These ceramic breaks become also sources of the beam impedance [4, 5]. The precise estimation of impedance is an important step toward realization of high intensity beams

in proton synchrotrons [6]. Recently, a new theory is developed to understand the characteristic of the ceramic break impedance [7], which enables us to get an insight about the resonance structure caused by the trapped mode inside the ceramic.

Next, let us show an example of the resonance in the ceramic break.

## IMPEDANCES OF CERAMIC BREAK AND THEIR RESONANCE STRUCTURES

Let us assume that the ceramic has the dielectric constant  $\epsilon'$ . The inner and the outer radii and the length of the ceramic are  $a$ ,  $a_2$  and  $g$ , respectively. Applying the formulae (7) and (18) in the reference [7], we obtain the theoretical impedance. The longitudinal and the transverse impedances are shown in Figs. 1 and 2, respectively. For the longitudinal impedance, the real and the imaginary parts of the impedance are shown in the left and the right figures, respectively. For the transverse impedance, the real and imaginary parts of impedances are shown in the same figure by the solid and the dot lines, respectively.

The large resonance at low frequency in the transverse impedance is approximately given by

$$f \sim \frac{c}{2\pi a} \sqrt{\frac{a^2 + 1.5(a_2^2 - a^2)}{a^2 + 1.5\epsilon'(a_2^2 - a^2)}}, \quad (1)$$

which essentially shows the resonance around the circumference ( $2\pi a$ ) of the ceramic break [8]. The frequency is lowered compared to that for the vacuum gap ( $\epsilon' = 1$ ) case due to the wavelength contraction effects of the ceramic.

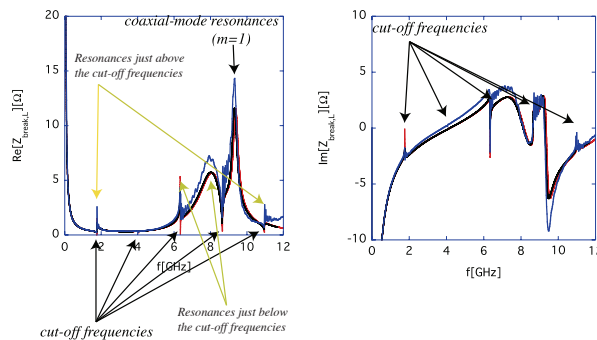


Figure 1: Longitudinal impedances of the ceramic break ( $a = 65$  mm,  $a_2 = 70$  mm,  $g = 10$  mm and  $\epsilon' = 11$ ) calculated by the theory (red), the simulation codes ABCI (black) and CST Studio (blue).

All the calculation results (the theory, ABCI [9] and CST [10]) reproduce the same resonance structures and show

# IDENTIFICATION OF INTRA-BUNCH TRANSVERSE DYNAMICS FOR FEEDBACK CONTROL PURPOSES AT CERN SUPER PROTON SYNCHROTRON\*

O. Turgut<sup>†</sup>, C. Rivetta, and J.D. Fox, SLAC, Menlo Park, CA 94305, USA  
 W. Hofle, CERN, Geneva, Switzerland  
 S.M. Rock<sup>‡</sup>, Stanford University, Stanford, CA, USA

## Abstract

A promising new approach for designing controllers to stabilize intra-bunch transverse instabilities is to use multi-input multi-output (MIMO) feedback design techniques. However, these techniques require a reduced model and estimation of model parameters based on measurements. We present a method to identify a linear reduced order MIMO model for the vertical intra-bunch dynamics. The effort is motivated by the plans to increase currents in the Super Proton Synchrotron as part of the HL-LHC upgrade where feedback control techniques could be applied to stabilize the bunch dynamics, allowing greater freedom in the machine lattice parameters. Identification algorithms use subspace methods to compute a discrete linear MIMO representation of the nonlinear bunch dynamics. Data from macro particle simulation codes (CMAD and HEADTAIL) and SPS machine measurements are used to identify the reduced model for the bunch dynamics. These models capture the essential dynamics of the bunch motion or instability at a particular operating point, and can then be used analytically to design model-based feedback controllers. The robustness of the model parameters against noise and external excitation signals is studied, as is the effect of the MIMO model order on the accuracy of the identification algorithms.

## INTRODUCTION

Electron clouds and machine impedance can cause intra-bunch instabilities at the CERN Super Proton Synchrotron (SPS). The high current operation of the SPS for LHC injection requires mitigation of these problems. Modern control techniques can be used to stabilize the bunch. These techniques are powerful tools allowing us to evaluate and understand the performance and the limits of the system beforehand. Yet, they require reduced order models of intra-bunch dynamics to design optimal or robust controllers for wide-band feedback systems. System identification techniques can be used to get these required reduced order models.

Nanosecond-scale bunch stabilization is more challenging compared to the case of rigid body dipole coupled bunch oscillations. It requires sufficient bandwidth to sense transverse motion at multiple locations along the bunch and apply correction signals to the corresponding parts of the bunch.

Apart from these technological constraints, modeling the intra-bunch dynamics is also more challenging compared to the case of modeling the beam dynamics including bunch to bunch interactions.

The feedback system senses the vertical positions at multiple locations within the nanosecond-scale bunch. Control filters use these measurements to calculate correction signals and apply them back onto the bunch using the kicker as actuator. A 4 Gs/Sec. digital feedback system has been developed to process the motion signals and generate the correction actions [1]. Due to very the fast intrinsic time characteristics of the system, a parallel computation control filter architecture has been developed. A very similar method had been used for bunch by bunch feedback control systems [2].

In this paper, we show the use of system identification techniques to estimate parameters of linear models representing single bunch dynamics. We define the form of the reduced order model. We pose the identification problem in a least squares form [3] for given input-output data set. After a brief discussion of identification constraints, we show results of identification applied to data from SPS measurements and nonlinear macro particle simulation codes.

## MODEL AND IDENTIFICATION

### Reduced Order Model and Identification

Any linear dynamical system can be represented in state space matrix form. A discrete time system sampled at every revolution period  $k$  with  $p$  inputs and  $q$  outputs is represented by

$$\begin{aligned} X_{k+1} &= AX_k + BU_k \\ Y_k &= CX_k \end{aligned} \quad (1)$$

where  $U \in R^p$  is the control variable (external excitation),  $Y \in R^q$  is the vertical displacement measurement,  $A \in R^{n \times n}$  is the system matrix,  $B \in R^{n \times p}$  is the input matrix, and  $C \in R^{q \times n}$  is the output matrix. For a MIMO system, the model order determines the complexity. In this study, we assumed time invariant dynamics which means having constant A, B and C matrices in the state space model. When it comes to the interactions between the bunch with electron clouds or during energy ramping operations, time variant dynamics has to be accounted for tune shifts, changing beam parameters, etc.

System identification techniques require exciting the system with appropriate signals and observing the response.

\* Work supported by the U.S. Department of Energy under contract DE-AC02-76SF00515 and the US LHC Accelerator Research program (LARP).

<sup>†</sup> oturgut@stanford.edu

<sup>‡</sup> Department of Aeronautics and Astronautics

# STUDY OF BEAM DYNAMICS IN LINEAR PAUL TRAPS

D.J. Kelliher, S. Machida, C.R. Prior, S.L. Sheehy  
STFC Rutherford Laboratory, ASTeC, UK.

## Abstract

The Hamiltonian governing the dynamics in a Linear Paul Trap (LPT) is identical in form to that of a beam in a focusing channel. This similarity, together with the LPT's flexibility, compactness and low cost, make it a useful tool for the study of a wide range of accelerator physics topics. Existing work has focused on high intensity collective effects as well as, more recently, the study of integer resonance crossing in the low intensity regime. A natural extension of this work is to investigate space-charge effects of intense beams in more realistic lattices to directly inform accelerator design and development. For this purpose we propose to construct a modified Paul Trap specifically for these studies. Among other features, it is envisaged that this new LPT should be able to model non-linear elements and a wider range of lattice configurations. This work will be undertaken in collaboration with Hiroshimi University.

## INTRODUCTION

In a linear Paul Trap ions are trapped transversely by an oscillating RF field and axially by a static DC field. The use of such a device to study the transverse dynamics in a quadrupole channel was first proposed in ref. [1]. The equivalence between the two cases includes not only the Hamiltonian but also the Vlasov-Poisson equation [2]. It follows that the collective processes and transverse dynamics are identical in the two systems.

A LPT allows the study of beam dynamics in a relatively cheap and compact device. It also allows more flexibility in the choice of parameters (e.g. radio-activation by beam loss does not apply). The time allocated to study accelerator physics on production machines is normally limited - this is not an issue in an ion trap.

A wide range of beam dynamics experiments have already been conducted in LPTs including the study of collective modes [3,4], the crossing of parametric resonances [5], the role of noise in emittance growth and halo production [6,7], the adiabatic compression of a bunch [7] and resonance instability bands in doublet lattices [8].

Experiments to date have been done either on the Paul Trap Simulator Experiment (PTSX) device at Princeton, USA or on the Simulator of Particle Orbit Dynamics (S-POD) series of traps at Hiroshima, Japan. It is proposed to construct a new trap (or series of traps) at Rutherford Appleton Laboratory, UK. This will be done in close collaboration with the Hiroshima group.

While there is certainly much more that could be done using existing traps, it is worth investigating the broader range of experiments that might be made possible with modified designs. Here we consider a multipole trap to allow

non-linear lattices to be studied. In the next section the essential formulae that inform the choice of the principal trap parameters are given. In later sections, collective effects, halo production, detuning and the flexibility in lattice choice are covered.

## LPT DESIGN

In the original "3D" Paul trap, the RF field is zero at just a single point at the centre of the device thus limiting the number of ions that can be cooled. By contrast a "linear" quadrupole field allows a string of ions to be cooled along the axis, hence the development of the linear Paul trap (also called a "linear quadrupole trap"). This device can be generalised to the "linear multipole trap" (henceforth referred to as a multipole trap) in which additional electrodes add non-linear field components [9].

For the case of a linear quadrupole trap, we follow the analysis in ref. [10], which starts with the envelope equation for each transverse plane. Throughout this paper we use  $x$  and  $y$  to refer to the two transverse coordinates and  $z$  for the axial coordinate. In the horizontal case, assuming an rms radius  $a$  and applying the smooth approximation, the equation is

$$\frac{d^2 a}{d\tau^2} + \kappa^2 a - \frac{\epsilon_x^2}{a^3} = \frac{Nr_p}{2a} \quad (1)$$

where  $r_p = q^2/4\pi\epsilon mc^2$  is the classical particle radius,  $N$  is the line density,  $\kappa$  is a focusing constant and  $\tau = ct$  and  $\epsilon_x$  is the horizontal emittance given by

$$\epsilon_x = \frac{1}{mc} \sqrt{\langle x^2 \rangle \langle p_x^2 \rangle - \langle xp_x \rangle^2} \quad (2)$$

A similar equation applies in the vertical plane. The vacuum phase advance per RF oscillation  $\sigma_0$  (equivalent to the phase advance per cell in an accelerator lattice) is defined as

$$\sigma_0 \equiv \kappa c/f = \frac{2\sqrt{2}qgV_0}{\pi^2 m} \left( \frac{1}{fR} \right)^2 \quad (3)$$

where  $f$  is the RF frequency,  $R$  is the radius of the trap,  $V_0$  is the amplitude of the RF waveform applied to the electrodes and  $g$  is a shape function defined in [10]. Note - the transverse oscillation frequency  $\omega_0$ , which will be useful later, is given by  $f\sigma_0$  and the transverse tune  $\nu_0$  is  $2\pi\sigma_0$ . Assuming a stationary plasma ( $\frac{d^2 a}{d\tau^2} = 0$ ) and defining the transverse temperature  $T_\perp$  to be

$$k_B T_\perp = \frac{\langle p_x^2 \rangle}{m} \quad (4)$$

where  $k_B$  is the Boltzmann constant. One obtains

$$N = \frac{2}{r_p} \left[ \sigma_0^2 \left( \frac{af}{c} \right)^2 - \frac{k_B T_\perp}{mc^2} \right] \quad (5)$$

# CHARACTERISATION OF THE KURRI 150 MeV FFAG AND PLANS FOR HIGH INTENSITY EXPERIMENTS

S. L. Sheehy\*, D. Kelliher, S. Machida, C. Rogers, C. R. Prior, ASTeC/STFC/RAL, United Kingdom  
On behalf of the KURRI-FFAG collaboration

## Abstract

Fixed field alternating gradient (FFAG) accelerators hold a lot of promise for high power operation due to their high repetition rate and strong focusing optics. However, to date these machines have not been operated with high intensity beams. Since November 2013 an experimental collaboration has been underway to characterise the 150 MeV proton FFAG at KURRI, Japan. Here we report on the results of characterisation experiments and discuss plans for further experiments in the high intensity regime.

## INTRODUCTION

Fixed field Alternating Gradient (FFAG) accelerators combine strong focusing optics like a synchrotron with a fixed magnetic field like a cyclotron. Unlike a synchrotron, the magnetic field experienced by the particles is designed to vary with radius, rather than time. This naturally leads to the potential to operate at high repetition rates limited only by the available rf system, while strong focusing provides a possibility of maintaining higher intensity beams than in cyclotrons.

A revival in interest since the 1990s has seen a number of FFAGs constructed, including scaling and linear non-scaling variants. However, high bunch charge operation remains to be demonstrated. A collaboration has been formed to use an existing proton FFAG accelerator at Kyoto University Research Reactor Institute (KURRI) in Japan to explore the high intensity regime in FFAG accelerators. Work has so far been aimed at characterising this machine in detail. Later experiments will be aimed at demonstrating high bunch charge operation in an FFAG accelerator and exploring the fundamental intensity limitations of these machines.

### The KURRI 150 MeV ADSR-FFAG

The 11–150 MeV ADSR-FFAG at KURRI [1] (shown in Fig. 1) is a scaling FFAG where the main magnetic field follows a power law with radius,

$$B_z(r) = B_0(r/r_0)^k. \quad (1)$$

The field index,  $k$ , is designed to be 7.6 and other parameters are given in Table 1.

The primary operational goal of the 150 MeV FFAG is to undertake basic studies toward the realisation of Accelerator Driven Systems (ADS) [2]. It is also used for irradiation experiments for industrial use, medical applications such as BNCT as well as radiobiology experiments.



Figure 1: The KURRI 150 MeV FFAG is the larger ring shown here with the pre-2011 injector ring. Injection from the new linac occurs in the top left of the image.

The ring consists of twelve DFD magnet triplets which are an innovative ‘yoke-free’ design [3] which allows the beam to be injected and extracted through the side of the magnets.

Originally injected by a low energy proton booster ring, in 2011 the injector was upgraded to an 11 MeV  $H^-$  linac to increase the beam intensity from roughly  $6 \times 10^8$  ppp to up to  $3.12 \times 10^{12}$  ppp [4]. The beam is now injected using  $H^-$  charge exchange injection on a  $20 \mu\text{g}\cdot\text{cm}^{-2}$  carbon foil. No bump system is used as the beam moves radially away from the foil as it is accelerated.

At present the linac provides 10 nA average current ( $3.12 \times 10^9$  ppp) with a bunch length of 100  $\mu\text{s}$  at injection and 0.1  $\mu\text{s}$  at extraction, operating at a 20 Hz repetition rate. In principle the linac can provide up to 5  $\mu\text{A}$  average current.

Table 1: Parameters of the 150 MeV FFAG

Parameter	Value	
$r_0$	4.54	m
Cell structure	DFD	
$N_{\text{cells}}$	12	
$k$ , field index	7.6	
Injection Energy	11	MeV
Extraction Energy	100 or 150	MeV
$f_{\text{rf}}$	1.6-5.2	MHz
$B_{\text{max}}$	1.6	T

\* suzie.sheehy@stfc.ac.uk

# EFFICIENT 3D POISSON SOLVERS FOR SPACE-CHARGE SIMULATION\*

J. Qiang<sup>†</sup>, LBNL, Berkeley, CA 94720, USA

## Abstract

Three-dimensional Poisson solver plays an important role in the self-consistent space-charge simulation. In this paper, we present several efficient 3D Poisson solvers inside an open rectangular conducting pipe for space-charge simulation. We describe numerical algorithm of each solver, show comparative results for these solvers and discuss the pros and cons associated with each solver.

## INTRODUCTION

Nonlinear space-charge effect in charged particle beam has significant impact to particle beam dynamics in high intensity accelerators. A natural way to include the space-charge effect in the simulation is through self-consistent particle-in-cell (PIC) method [1–4]. In the PIC method, macroparticles are advanced step by step in phase space subject to both the external forces and the space-charge forces. Normally, at each step, the external forces can be quickly computed using the given external fields. The space-charge forces are calculated self-consistently using the charge density distribution at that step by solving the Poisson equation. This involves a large number of numerical operations and is much more computational expensive compared with the external force calculation. An efficient Poisson solver will be of importance in the PIC simulation in order to quickly calculate the space-charge forces and to reduce the total simulation time.

In previous studies, a number of Poisson solvers have been studied subject to different boundary conditions [5–12]. In this paper, we proposed three new Poisson solvers in an open rectangular conducting pipe. Figure 1 shows a schematic plot of charged particle beam inside an open rectangular conducting pipe. Even with the longitudinal open boundary condition, these three Poisson solvers will use a computational domain that longitudinally contains the beam itself. No extra computational domain is needed in the longitudinal direction in order to meet the open boundary conditions on both sides of the beam.

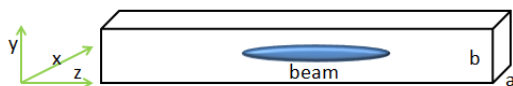


Figure 1: A schematic plot of a charged particle beam inside an open rectangular conducting pipe.

## NUMERICAL METHODS

For a perfect conducting pipe with rectangular cross section, we write the three-dimensional (3D) Poisson equation as:

$$\frac{\partial^2 \phi}{\partial x^2} + \frac{\partial^2 \phi}{\partial y^2} + \frac{\partial^2 \phi}{\partial z^2} = -\frac{\rho}{\epsilon_0} \quad (1)$$

Here,  $\phi$  denotes the electrostatic potential,  $\rho$  the dimensionless charge density function,  $x, y$  and  $z$  denote the horizontal, vertical, and longitudinal coordinates respectively. The boundary conditions for the potential in the open perfect rectangular conducting pipe are:

$$\phi(x=0, y, z) = 0 \quad (2)$$

$$\phi(x=a, y, z) = 0 \quad (3)$$

$$\phi(x, y=0, z) = 0 \quad (4)$$

$$\phi(x, y=b, z) = 0 \quad (5)$$

$$\phi(x, y, z = \pm\infty) = 0 \quad (6)$$

where  $a$  is the horizontal width of the pipe and  $b$  is the vertical width of the pipe. In the following, we propose three efficient numerical methods to solve the Poisson equation subject to above boundary conditions.

### Spectral-Integrated Green Function Method

Given the boundary conditions in Eq. 2-6, the potential  $\phi$  and the source term  $\rho$  can be approximated using two sine functions as:

$$\rho(x, y, z) = \sum_{l=1}^{N_l} \sum_{m=1}^{N_m} \rho^{lm}(z) \sin(\alpha_l x) \sin(\beta_m y) \quad (7)$$

$$\phi(x, y, z) = \sum_{l=1}^{N_l} \sum_{m=1}^{N_m} \phi^{lm}(z) \sin(\alpha_l x) \sin(\beta_m y) \quad (8)$$

where

$$\rho^{lm}(x, y, z) = \frac{4}{ab} \int_0^a \int_0^b \rho(x, y, z) \sin(\alpha_l x) \sin(\beta_m y) dx dy \quad (9)$$

$$\phi^{lm}(x, y, z) = \frac{4}{ab} \int_0^a \int_0^b \phi(x, y, z) \sin(\alpha_l x) \sin(\beta_m y) dx dy \quad (10)$$

where  $\alpha_l = l\pi/a$  and  $\beta_m = m\pi/b$ . Substituting above expansions into the Poisson equation and making use of the orthonormal conditions of the sine functions, we obtain

$$\frac{\partial^2 \phi^{lm}(z)}{\partial z^2} - \gamma_{lm}^2 \phi^{lm}(z) = -\frac{\rho^{lm}}{\epsilon_0} \quad (11)$$

\* Work supported by the U.S. Department of Energy under Contract No. DE-AC02-05CH11231.

<sup>†</sup> jqiang@lbl.gov

# A MULTI-PARTICLE ONLINE BEAM DYNAMICS SIMULATOR FOR HIGH POWER ION LINAC OPERATIONS\*

X. Pang<sup>†</sup>, L.J. Rybarcyk, S.A. Baily  
 Los Alamos National Laboratory, Los Alamos, NM, 87544, USA

## Abstract

A fast multi-particle online beam dynamics simulator has been developed at LANL. It is a marriage of multi-particle beam physics algorithms and graphics processing unit (GPU) technology. It combines the execution efficiency of the C/C++ programming language and a powerful yet flexible user interface via Python scripts. Therefore, it is not only accurate and fast, but also very easy to use. We have used this simulator at LANSCE to guide linac tuning, explore optimal operational settings, and test new ideas.

## INTRODUCTION

### Why Another Simulator?

Accelerator control rooms are usually equipped with on-line beam modeling tools to help guide machine tuning. These tools, which typically have access to machine set points through the control system, can not only help physicists and operators set up the machine faster, but also provide information on the beam properties in areas where no measurements can be made. However, almost all of the existing online modeling tools today are either based on single-particle tracking or on envelope models. While they might perform sufficiently well for nicely formed beams, they cannot predict the nonlinear motions of a real beam or estimate losses, especially in high-power operations when beams can be highly nonlinear and chaotic.

The logical next step to improve the status quo is to use a multi-particle beam dynamics code to provide more realistic predictions. However, most of the existing multi-particle simulation tools need either significant computational time or supercomputer resources. This makes them impractical to use during real world machine operations where fast turn-around is required and where they may be in use for long periods of time. In addition, they are typically not configured to have ready access to online machine specific set points.

One can clearly see the gap that exists between the oversimplified but fast models used in control rooms and the highly sophisticated yet slow multi-particle simulation tools which are usually used during the design process. The goal of our development is to fill this gap by providing a multi-particle simulation tool that is both accurate and fast enough to be used in real world accelerator tuning and operation.

### Why Use a GPU?

The graphics processing unit (GPU) is at the frontier of high performance computing [1]. It powers several of the

world's most powerful supercomputers and it has also democratized super-computing by enabling cluster performance on people's personal desktops. For us, the GPU offers outstanding parallel performance and it is also the most cost effective way to provide 24/7 availability for our online simulator. With around a \$600 USD investment in the GPU hardware, one can get up to 100 times speedup compared to a single threaded CPU. And this GPU workstation can be dedicated to accelerator operations 24/7.

### How to Use It?

This is where the users can freely apply their creativity. We have applied this tool to guide turn-on of the LANSCE linac, to test what-if scenarios, to optimize operational machine settings by combining it with the multi-objective optimization algorithms, and to test a new automatic tuning/control scheme. More details will be covered in later sections.

## THE SIMULATOR

### Code Design

The goal of our code design is to ensure fast execution and ease of use. This led us to adopt a combination of a low-level compiled language, i.e. C++/CUDA and a high-level scripting language, i.e. Python. The number-crunching is efficiently carried out by CUDA and C++, however, the users don't have to deal with the complex syntax and the lengthy compilation processes associated with them, but instead can configure and execute a simulation with a high-level script. Figure 1 shows the code hierarchy. The shallow learning

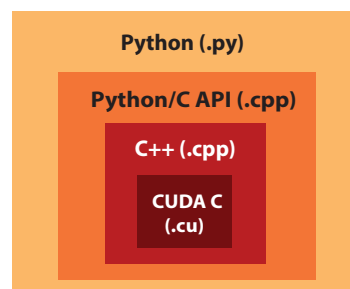


Figure 1: Lower-level CUDA and C++ are wrapped up by Python/C API and compiled into a shared library that can be imported in Python.

curve of Python and the richness of its application libraries allow users with the minimal programming experiences to quickly prototype their ideas.

The major components of the code structure design are shown in Figure 2. The components that are shaded in blue

\* Work supported by U.S. DOE, NNSA under contract DE-AC52-06NA25396. LA-UR-14-28658

<sup>†</sup> xpang@lanl.gov

# SPACE CHARGE MAP EXTRACTION AND ANALYSIS IN A DIFFERENTIAL ALGEBRAIC FRAMEWORK

A. Gee\*, B. Erdelyi†

Physics Dept., Northern Illinois University, DeKalb, IL 60115, USA

## Abstract

Space charge is a leading concern in high-intensity beams, causing effects such as emittance growth, beam halos, etc. As the need for high-intensity beams spreads, the demand for efficient space charge analysis grows. We developed a self consistent space charge simulation method for this purpose [1]. In order to facilitate space charge analysis, we implemented a method that allows space charge map extraction and analysis from any tracking method [1, 2]. We demonstrate the method by calculating the transverse space charge. We compare the method of moments and the fast multipole method as the tracking methods employed in the transfer map extraction process. We show results from analysis of the raw map elements as well as quantities obtained from normal forms.

## INTRODUCTION

Transfer maps are powerful tools in the analysis of beam dynamics. The information even at low order is invaluable in the design and optimization of charged particle beam guidance systems. Now, we may study multi-particle beam dynamics using transfer maps. For the first time, we can extract a self-consistent space charge transfer map from simulation, opening new possibilities in the field of beam physics. Details of the theory and development can be found in [1].

The map extraction method can be employed in conjunction with any tracking method available. The map itself is smooth as it captures the mean-field limit. The tracking methods themselves are based on splitting and composition methods, more precisely Strang splitting. We implemented two tracking methods: the moment method (MoM) and the fast multipole method (FMM). The tracking methods necessarily produce slightly different results due to innate approximations, thus it is prudent to check that the map extraction procedure itself smooths out the differences, resulting in the same transfer maps for all practical purposes. That is the main goal of this paper.

A few points should be mentioned. To efficiently extract the polynomial representation of beamline elements, we employed differential algebra methods. Differential algebra methods (DA) efficiently calculate Taylor expansions to high order with machine precision and no truncation error, providing polynomial representations for any beamline element of interest. We model the space charge kick as one such element with infinitesimal length. We limit ourselves to a single space charge kick at the center of a beamline element with open boundary conditions. Furthermore, to emphasize

\* agee1@niu.edu  
† erdelyi@anl.gov

Table 1: Beam Parameters

Species	Proton
No. of Particles	5000
Energy [MeV]	5
Shape	Ellipse
Initial spatial distribution	Uniform
Initial maximum radius [m]	0.001
Initial angle distribution	Uniform
Initial maximum angle [rad]	0.03
Initial emittance (X,Y) [ $\mu\text{m}$ ]	(7.63, 7.50)

the effects of space charge, we limited the beamline element maps to first order and calculated the space charge kick up to eighth order with the MoM and the FMM. Previous studies suggested results at the same order would be comparable.

## BEAMLINE SIMULATION

We set up a space-charge dominant beam for our simulations. The parameters are shown in Table 1. We used the same beam conditions for all runs. We chose the number of particles,  $N = 5000$ , for speed with acceptable accuracy.

To analyze some simple maps, we simulated two basic examples. We set up a magnetic triplet and adjusted the quadrupole gradients to achieve imaging as our first example. Our second example is a periodic FODO cell, where we adjusted the quadrupole gradients to match an arbitrarily chosen horizontal and vertical tune.

### Imaging Triplet

The triplet we set up consists of an outer drift, quad (Q1), inner drift, quad (Q2), inner drift, quad (Q3), and outer drift. The system parameters are in Table 2 and the first order system map is shown in (1).

$$\begin{pmatrix} -1 & 3.20 \times 10^{-14} & 0 & 0 \\ 5.69 & -1 & 0 & 0 \\ 0 & 0 & -1 & -1.91 \times 10^{-14} \\ 0 & 0 & -4.39 & -1 \end{pmatrix} \quad (1)$$

A ray trace of the system without space charge is also shown in Figure 1. We drew 3 independent rays in both the X-Z and Y-Z planes and generated the trajectory by applying the calculated map. The ray diagram includes an extra end drift of 6.25 cm to show the focal point at  $z = 1.4$  m. This drift was left out of the system map since it would not affect our analysis.

# BEAM DYNAMICS INFLUENCE FROM QUADRUPOLE COMPONENTS IN FRIB QUARTER WAVE RESONATORS\*

Z. He, Y. Zhang, Z. Zheng, Z. Liu, J. Wei, FRIB, Michigan State University, USA

## Abstract

Non-axisymmetric RF cavities, such as quarter-wave resonators (QWRs), can produce axially asymmetric multipole field components that can influence beam dynamics. For example, dipole components can cause beam steering, an effect that has been well known to the community since 2001. However, higher order multipole field components, such as quadrupole components, which have potential influence on beam dynamics, have never received enough attention yet. In this paper, we choose FRIB QWRs as an example and quadrupole components are extracted by multipole expansion. Then, influence of quadrupole components on a single cavity is studied using thin lens model. After that, the influence of quadrupole components on a whole FRIB linac segment one is studied, and effects such as transverse profile ovalization and blow up of beam size are witnessed. Lastly, a possible way of quadrupole components compensation for FRIB driving linac is discussed.

## INTRODUCTION

Non-axisymmetric RF cavities such as quarter-wave resonators (QWRs), half-wave resonators (HWR), spoke cavities and crab cavities, are now widely used in accelerators. Because of their geometry, dipole terms, quadrupole terms and other higher order multipole terms appear and can influence beam dynamics [1–4]. Dating back to 2001, A. Facco first pointed out possible beam steering effect coming from QWR and described the issue thoroughly in a later paper [1]. In the paper, a physics model is built to estimate the beam steering effect, and an easy way to compensate the steering effect using defocusing effect by shifting the beam axis is proposed.

Besides dipole term which causes beam steering, quadrupole term can cause beam shape deformation [2], and higher order terms can introduce non-linear effect and decrease dynamic aperture. By now, these effects haven't received enough attention yet. In this paper, we choose the QWR at FRIB [5] as an example. A scheme is developed to draw out multipole components through Fourier-Taylor multipole expansion. Then, a thin lens model based on transit time factor (TTF) [6, 7] is used to include multipole components into traditional cavity model. After that, the quadrupole effect is closely examined in both single cavity and whole linac segment one (LS1). At last, the possibility of self-cancellation of quadrupole components by fine tuning of solenoid polarity is discussed. The first two section has been discussed more thoroughly in our previous paper [8],

\* The work is supported by the U.S. National Science Foundation under Grant No. PHY-11-02511, and the U.S. Department of Energy Office of Science under Cooperative Agreement DE-SC0000661

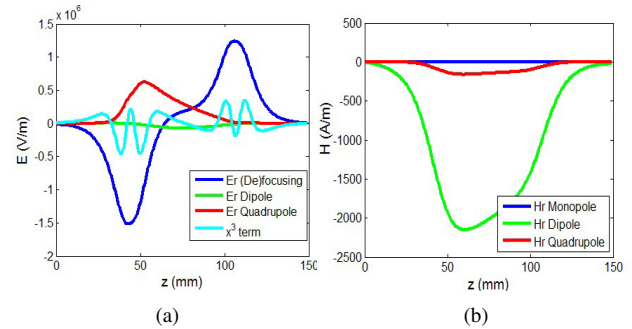


Figure 1: Result of multipole strength curve for radial electric and magnetic field. (a) Radial electric field multipole strength. Blue curve is focusing term, green curve is dipole term, red curve is quadrupole term, and cyan curve is cubic term. (b) Radial magnetic field multipole strength. Blue curve is monopole term, green curve is dipole term, and red curve is quadrupole term.

here, we just list some important results in order to complete the whole story.

## FIELD MULTIPOLE EXPANSION

FRIB QWR 3D field simulated by CST [9] is chosen as the starting point and the numerical approach of Fourier-Taylor multipole expansion is used to draw out the field multipole terms. By expanding radial direction to Taylor series and azimuthal direction to Fourier series in a polar coordinate system, we are able to draw out multipole terms from a certain transverse E&M field to any arbitrary order. The process can be expressed as Eq. 1:

$$\begin{cases} F_{\rho, nm}(\rho, \theta) = F_{max} \sum_{n, m=0}^{\infty} P_n A_{nm} \Theta_m \\ P_n = \rho^n \\ \Theta_m = e^{im\theta} \end{cases} \quad (1)$$

By sampling all transverse plane along the longitudinal direction, we can get a plot indicating multipole strength along longitudinal direction, which is shown in Fig. 1.

## MULTIPOLE THIN LENS MODEL

Assuming small thin lens kick, we can split the kick into electric part and magnetic part of contribution:

$$\begin{aligned} \Delta y' &= \frac{qe\mu_0}{\gamma m_0} \int_{t_1}^{t_2} H_x(x, y, z, t) dt + \frac{qe}{\gamma m_0 \beta c} \int_{t_1}^{t_2} E_y(x, y, z, t) dt \\ &= \Delta y'_{H, y} + \Delta y'_{E, y} \end{aligned} \quad (2)$$

# SIMULATIONS OF THE HEAD-TAIL INSTABILITY ON THE ISIS SYNCHROTRON

R.E. Williamson, D.J. Adams, B. Jones, C.M. Warsop, ISIS, STFC, RAL, UK  
V. Kornilov, GSI, Darmstadt, Germany

## Abstract

ISIS is the pulsed spallation neutron and muon source at the Rutherford Appleton Laboratory in the UK. Operation is centred on a loss limited 50 Hz proton synchrotron which accelerates  $3 \times 10^{13}$  protons per pulse (ppp) from 70 MeV to 800 MeV, delivering a mean beam power of 0.2 MW.

Present studies are focussed on key aspects of high intensity beam dynamics with a view to increasing operational intensity, understanding loss mechanisms and identifying possible upgrade routes. Of particular interest is the head-tail instability observed on ISIS, which is currently a main limitation on beam intensity.

This paper presents initial simulations using HEADTAIL to compare with experimental data taken on the ISIS synchrotron. The details and assumptions of the impedance model and simulations are discussed. Plans for future head-tail measurements, simulations and analysis are outlined.

## INTRODUCTION

The transverse head-tail instability represents a possible intensity limit for bunched beams in many synchrotrons including ISIS and its proposed upgrades. The standard theory of Sacherer [1] does not include space charge and associated incoherent tune spreads. However, recent works [2, 3, 4] have proposed theoretical models to treat head-tail motion in the presence of space charge. In parallel with this, numerical simulations are required to analyse beam behaviour with various collective effects included, as noted in [5].

### ISIS Synchrotron

ISIS operations centre on a rapid cycling synchrotron (RCS) which accelerates  $3 \times 10^{13}$  protons per pulse (ppp) from 70 MeV to 800 MeV on the 10 ms rising edge of a sinusoidal main magnet field. Injection is via charge exchange of a 70 MeV, 25 mA H<sup>+</sup> beam over ~130 turns of the falling main magnet field just prior to field minimum. The unchopped, injected beam is non-adiabatically bunched by the ring dual harmonic RF system (DHRF,  $h = 2$  and 4). Nominal betatron tunes are  $(Q_x, Q_y) = (4.31, 3.83)$ , with peak incoherent tune shifts exceeding ~0.5. The intensity is loss limited with longitudinal trapping, transverse space charge and the head-tail instability being the main driving mechanisms.

Observations on ISIS have shown that the two proton bunches develop coherent vertical growth approximately 2 ms into the acceleration cycle [6]. The growth is suppressed by ramping the vertical tune away from the integer ( $Q_y = 4$ ) during that time. However the growth

rate scales strongly with intensity and lowering the tune further tends to increase loss associated with the half integer resonance [7]. Work is ongoing to develop a beam feedback system [8] to damp the instability. Recent studies have shown that the instability is present both with just the fundamental ( $h = 2$ ) RF system [6] as well as with the DHRF system.

This study presents initial simulations of low intensity head-tail dynamics using HEADTAIL [9] to compare with experimental data using single harmonic RF on the ISIS synchrotron. Calculations of chromatic phase shifts and growth rates from Sacherer theory [1] are compared to HEADTAIL results. Plans for future experimental studies alongside simulation and theory work are outlined.

## SACHERER THEORY

A non-zero value for the chromaticity,  $\xi$ , results in a momentum dependent betatron tune and an accumulated phase shift along the bunch  $\chi = \xi Q \omega_0 \tau / \eta$ , where  $Q$  is the tune,  $\omega_0$  is the angular revolution frequency,  $\tau$  is the bunch length in time and  $\eta = 1/\gamma_c^2 - 1/\gamma^2$ . This chromatic phase shift determines the head-tail mode structure observed through the form factor shown below.

An impedance acting on a beam can introduce a real frequency shift, through its reactive component, as well as instability from its resistive part. The instability growth rate may be calculated for a coasting beam from the equation of motion for a single particle acted on by an impedance. For a bunched beam, the coasting beam growth rate is modified by a sum over the bunch mode spectra. The instability frequency shift [1] is given by

$$\Delta\omega_m = \frac{1}{1 + m} \frac{i}{2Q\omega_0} \frac{e\beta}{\gamma m_0} \frac{I_b}{L_b} \frac{\sum Z_{\perp}(\omega) h_m(\omega - \omega_{\xi})}{\sum h_m(\omega - \omega_{\xi})}, \quad (1)$$

where  $m$  is the oscillation mode number,  $m_0$  is the rest mass,  $I_b$  is the bunch current,  $L_b$  is the bunch length in metres,  $Z_{\perp}(\omega)$  is the transverse impedance as a function of frequency,  $h_m(\omega - \omega_{\xi})$  is the envelope of the bunch line spectrum

$$h_m(\omega) = (m + 1)^2 \frac{\tau^2}{2\pi^4} \frac{1 \pm \cos \omega\tau}{[(\omega\tau/\pi)^2 - (m + 1)^2]^2} \quad (2)$$

where  $\tau$  is the bunch length in seconds. The associated growth rate from equation 1 is  $\tau_m^{-1} = -\text{Im}(\Delta\omega_m)$ .

The resistive wall impedance is thought to be the main driving impedance of the head-tail instability on ISIS. The impedance becomes large for small  $\omega$  predicting large growth rates for the lowest betatron sideband when  $Q$  is just below an integer. It can therefore be approximated by

ISBN 978-3-95450-173-1

# IMAGE FIELDS IN THE RECTANGULAR VACUUM VESSELS OF THE ISIS SYNCHROTRON

B.G. Pine, ISIS, RAL, STFC, UK and JAI, Oxford, UK  
C.M. Warsop, ISIS, RAL, STFC, UK

## Abstract

ISIS is the pulsed spallation neutron source based at Rutherford Appleton Laboratory in the UK. Operation is based on a 50 Hz, 800 MeV proton synchrotron, accelerating up to  $3 \times 10^{13}$  protons per pulse, which provides beam to two target stations. Space charge effects contribute significantly to beam loss. Fields from the intense beam interact strongly with their environment. At ISIS the vacuum vessel is rectangular and profiled to follow the shape of the design beam envelope.

Past studies have suggested that closed orbit induced image fields may contribute to beam loss under certain conditions. Image fields for parallel plate and rectangular geometries are reviewed, in particular their expansion as power series is determined. A simulation tool has been developed for particle tracking with space charge. The code contains both Fast Fourier Transform and Finite Element Analysis based field solvers, which have been used here to test the range of validity for the power series expansions for centred and off-centred beams.

These expansions are then used to determine driving terms for the transverse beam motion. Of particular interest for ISIS is the resonant behaviour of beams with a harmonic closed orbit, which can be compared with the output of beam tracking simulations.

## INTRODUCTION

At the highest intensities it is believed that image forces from off-centred beams can contribute to losses on ISIS [1,2]. These beam losses are difficult to isolate during normal operation of the facility. Therefore a program of analysis and simulation has been established in order to describe the effect of image forces and try to estimate the level of beam loss they could potentially cause. In the future it is hoped that a better understanding of the image forces may allow them to be identified experimentally. Analyses for parallel plate and rectangular geometry including centred and off-centred beams are reviewed. The results are then compared with the output of particle-in-cell (PIC) simulations.

The ISIS rapid cycling synchrotron (RCS) accelerates a high intensity beam at a fast repetition rate of 50 Hz. The synchrotron has a circumference of 163 m. It is composed of 10 super periods, with specialised sections for injection, extraction and collimation. The peak incoherent tune shifts are 0.5 or larger in both planes. Many different loss mechanisms may contribute to beam loss at any particular point in the machine cycle, especially during the time between injection and bunching of the beam, when space charge forces peak. In order to gain insight into the individual loss processes it is

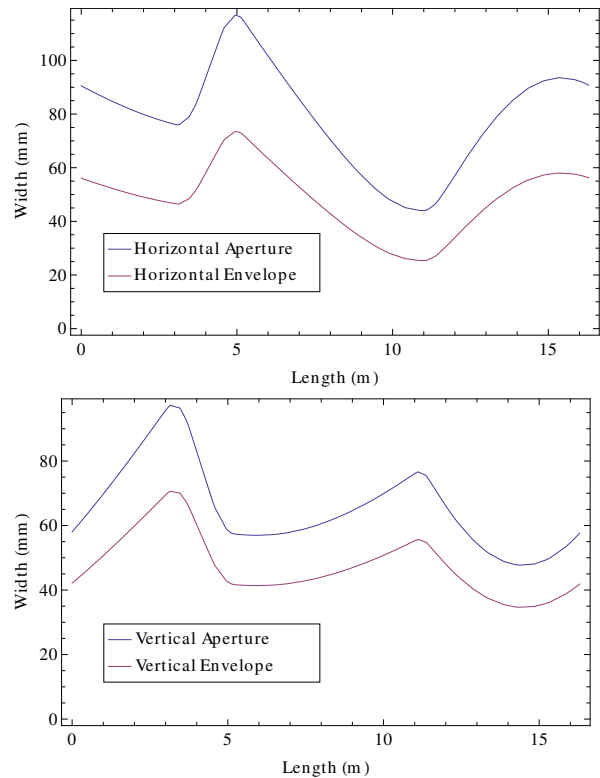


Figure 1: Apertures and envelopes for one super period of the ISIS RCS: (top) horizontal, (bottom) vertical.

helpful to separate out different effects to study. For the purpose of the present paper attention is focused purely on the transverse plane, and in particular a geometrical approach to the image forces.

ISIS has rectangular vacuum vessels and RF shields whose cross section runs parallel to the design beam envelope in both planes (Figure 1). Of particular interest for ISIS are the higher order image terms due to off-centred beams. It has been suggested that these may affect beam loss at the highest intensities [1].

## IMAGE FIELDS IN PARALLEL PLATE AND RECTANGULAR GEOMETRY

### Image Terms due to Laslett

Following Laslett [3], parallel plate geometry is used as an approximation to rectangular. For a beam centred at  $y_1$  between two infinite parallel plates at  $\pm h$  and a field point at  $y$  as shown in Figure 2, there are an infinite series of images above and below the beam. Conformal mapping may be used to transform to a new system where the images are

# STUDIES OF LOSS MECHANISMS ASSOCIATED WITH THE HALF INTEGER LIMIT ON THE ISIS RING

C.M. Warsop, D.J. Adams, B. Jones, B.G. Pine, H.V. Smith, C. Wilcox, R.E. Williamson  
RAL, Oxfordshire, UK

## Abstract

ISIS is the spallation neutron source at the Rutherford Appleton Laboratory in the UK. The facility centres on an 800 MeV rapid cycling proton synchrotron, which provides 0.2 MW of beam power operating at high levels of transverse space charge (peak incoherent tune shift  $\sim 0.5$ ), but with low loss. Half integer resonance is considered to be a main driver for loss that limits the intensity in high power, medium energy proton rings like ISIS. However, the detailed mechanisms causing loss as the half integer limit is approached are not well understood, particularly in the context of a real machine. In this paper we report progress on experiments on the ISIS synchrotron inducing half integer loss, comparing with detailed simulations, and attempts to relate these to simplified theoretical and simulation models. Studies here concentrate on 2D coasting beams, with a view to extending later to the more complicated 3D, bunched beam case of an operational machine.

## INTRODUCTION

### *Motivation and Aims*

Half integer resonance is considered to be a main intensity limitation in medium energy, high intensity proton machines. The existing incoherent and coherent resonance theories give valuable indications of intensity limits, but limited information on the beam behaviour as the half integer limit is approached and particles lost. The aim of this work is to understand more about the detailed mechanisms driving this loss and thus limiting intensity.

The starting point for the study is experimental observations, with the machine configuration optimised as far as possible to allow study of the essential processes. Detailed experimental studies of beam approaching half integer resonance are followed by comparison with (and benchmarking of) simulation codes. It is hoped these results can then be used to guide interpretation in terms of simplified and predictive beam models. This experimental emphasis forces the inclusion of important processes (e.g. approach of resonance) that are simplified in theoretical models, but are important in understanding real loss.

The underlying aim is to understand losses on an operational high intensity machine like ISIS, and requires a treatment of the full 3D dynamics including effects due to longitudinal motion. Presently, the simpler 2D transverse problem is studied with unbunched, coasting beams. In the longer term, experiments and studies will be extended to non-accelerated and accelerated bunched beams.

### *The ISIS Synchrotron*

The ISIS synchrotron accelerates  $3 \times 10^{13}$  protons per pulse (ppp) from 70-800 MeV on the 10 ms ramp of the sinusoidal main magnet field. At the repetition rate of 50 Hz this provides an average beam power of 0.2 MW. Charge exchange injection takes place over 130 turns, with painting in both transverse planes as the high intensity beam is accumulated and contained in the collimated acceptances of  $\sim 300 \pi$  mm mr. The ring has a circumference of 163 m and a revolution time of 1.48  $\mu$ s at injection. Nominal betatron tunes are  $(Q_x, Q_y) = (4.31, 3.83)$ , but these are varied using two families of ten trim quadrupoles. The dual harmonic RF system captures and accelerates the initially unbunched beam, and allows enhanced bunching factors. Peak incoherent tune shifts of  $\Delta Q \sim 0.5$  are reached at about 80 MeV, during bunching. Single turn extraction uses a fast vertical kicker at 800 MeV. Main loss mechanisms are associated with non-adiabatic trapping, transverse space charge and transverse instability. Understanding the action of half integer loss is central to minimising losses on the present machine, as well as guiding optimal designs for future upgrades.

## EXPERIMENTAL OUTLINE

### *Machine and Beam Configuration*

In order to study the essentials of transverse half integer resonance, these experiments make use of unbunched, coasting beams, with the ISIS ring in storage ring mode. The main magnet field is set at a DC level appropriate for the 70 MeV injected beam and RF systems are off. Betatron tunes are controlled with the trim quadrupoles. In these experiments lattice tunes are constant. A small emittance beam of  $\varepsilon_{rms} \sim 20 \pi$  mm mr in both planes is injected: painting amplitudes are constant through the pulse and of small amplitude. These beams ( $\varepsilon_{100\%} \sim 100 \pi$  mm mr) fill a small fraction of the machine acceptance and thus allow the evolution of the beam profile to be observed. As beam accumulates, the increasing intensity depresses the coherent tune and pushes the beam over resonance [1]. Tunes are selected such that only one resonance is approached in the vertical plane: a harmonic driving term is applied to the  $2Q_y = 7$  line with the trim quadrupoles. Beam loss and transverse profiles are recorded as a function of key parameters such as tune, driving term strength and intensity. Transverse and longitudinal beam spectra are monitored to ensure coherent instabilities are avoided.

# FEASIBILITY STUDY OF A NOVEL, FAST READ-OUT SYSTEM FOR AN IONIZATION PROFILE MONITOR BASED ON A HYBRID PIXEL DETECTOR

O. Keller, B. Dehning, S. Levasseur, M. Sapinski, CERN, Geneva, Switzerland

## Abstract

The ability to continuously monitor the transverse beam size is one of the priorities for the upgrade and consolidation of the CERN Proton Synchrotron for the High Luminosity LHC era. As well as providing an average beam size measurement throughout the acceleration cycle, the requirements also cover bunch-by-bunch measurements of up to 72 bunches with a spacing of 25 ns within 1 ms. An ionization profile monitor with a hybrid pixel detector read-out is therefore being investigated as a possible candidate to provide such measurements. In this contribution the concept, based on a Timepix chip, is presented along with first laboratory measurements showing the imaging of low-energy electrons in vacuum.

## INTRODUCTION

Ionization Profile Monitors (IPM) are devices measuring the transverse size of a particle beam. Electrons or ions resulting from ionization of the residual gas in the beam vacuum are extracted and used to reconstruct the beam profile. Electrons are used if fast measurements are required. They are accelerated towards a detector by an electric field. In addition a parallel magnetic field provides confinement of their orbits along the electric field lines.

Two main types of electron readout systems are commonly used in the current IPMs:

- Multi-strip metal anodes, e.g. at Fermilab [1], BNL [2] and J-PARC [3].
- Optical readout, based on the conversion of electrons into light which is captured by a camera, e.g. in the LHC [4, 5] or at GSI [6].

Both of these methods require amplification of the electron signal in front of the detector which is achieved by Multi-Channel Plates (MCP). Here a novel system based on the emerging technology of hybrid pixel detector is investigated. The detector consist of two pixelated elements, a sensor slab and a readout chip. The sensor reassembles an array of diodes operating in reverse-bias mode. A charged particle traversing the sensor generates free charge carriers in the material which are converted into a voltage pulse and further analyzed by the readout chip.

The Timepix3 is currently the most versatile and one of the fastest hybrid pixel detector readout chips available. It was developed within the Medipix Collaboration hosted by CERN and the first chips have been tested in 2013 [7]. It is designed for a sensor size of  $14 \times 14 \text{ mm}^2$  and a resolution of 255 by 255 pixels. The size of one pixel is  $55 \times 55 \mu\text{m}^2$ .

When bump-bonded to a thin silicon sensor, the hybrid detector becomes sensitive to single low-energy electrons of a few keV. With the ability to set a threshold per pixel, high and homogeneous signal-to-noise ratios can be maintained. The pixels can operate in one of three measurements modes: deposited charge (TOT mode), time of arrival (TOA) and counting the number of events together with the total charge in one shutter period (PC/iTOT). The digital link transceivers of Timepix3 can send the recorded data continuously at a maximum hit rate of 85 Mhits/s/chip or  $42.5 \text{ Mhits/s/cm}^2$ .

The main advantages of the proposed technology are:

- The thickness is reduced with respect to the optical readout method, since no bulky light guides are needed; a magnet with a smaller aperture can be used.
- The fast readout speed enables to measure the beam size bunch-by-bunch with a spacing of 25 ns.
- No need for MCP amplification; MCPs exhibit complex behaviour in cases of prolonged usage with strong and highly repetitive input signals [8].
- Coupling to beam RF fields is expected to be small.
- Currently available charge integrators for strip detectors, with a comparable fast readout like the QIE10 [9], are orders of magnitude less radiation hard than the readout chips of the Medipix/Timepix family [10].

In addition to the readout system, we investigate here the geometry of the electrodes providing the extraction field.

## OPERATIONAL SPECIFICATION

The circumference of the CERN Proton Synchrotron [11] is 628.3 meters and the revolution time varies from  $\tau_{\text{rev}} = 5.63 \mu\text{s}$  for  $\text{Pb}^{54+}$  beams at injection to  $2.1 \mu\text{s}$  for proton beams. It was first put in operation in 1959. Today it is used to generate a broad variety of beams: for test beam areas, fixed target experiments and for the LHC [12]. The proton beams in PS undergo transition crossing and bunch splitting - two phenomena which severely affect the beam emittance.

Operators of any accelerator would like to measure the beam parameters in the best possible way, however the technology does not always allow to fulfill their requests. In case of transverse profile measurements the operational specification for the foreseen PS upgrade is as follows:

1. Continuous, bunch-by-bunch monitoring of the beam emittance over the machine acceleration cycle (2.1 s) with an acquisition rate of 0.1-1 kHz.

# INVESTIGATION OF THE EFFECT OF BEAM SPACE-CHARGE ON ELECTRON TRAJECTORIES IN IONIZATION PROFILE MONITORS

D. Vilsmeier, B. Dehning, M. Sapinski, CERN, Geneva, Switzerland

## Abstract

The correct measurement of beam size using an ionization profile monitor relies on the confinement of electron trajectories from their source to the electron-sensitive detector. This confinement is provided by a magnetic field aligned with electric extraction field. As the initial electron velocities are boosted by the presence of a high-charge density beam, the value of the magnetic field depends on both the beam size and on the charge density. If the magnetic field is not strong enough a deformation of the observed beam profile occurs. In this paper the results of a study of electron trajectories in the presence of high charge density beams is presented along with an estimation of the required magnetic field for various scenarios. A correction procedure for compensating any residual distortions in the measured profile is also discussed.

## INTRODUCTION

During the calibration procedure of the LHC Ionization Profile Monitor (IPM) [1] it has been found that the obtained profiles at high beam energy are broader than expected [2, 3]. Several reasons for this effect have been investigated:

- wrong correction for camera tilt with respect to the beam direction,
- optical point-spread-function (PSF),
- PSF due to multi-channel plate granularity,
- underestimation of electron gyroradius.

Finally the problem was tracked down to the beam space charge which kicks electrons before they leave the beam, significantly increasing their gyroradius. An increase of the magnetic field was suggested, however it is a costly solution. In this paper the details of the interaction of electrons with the beam field are investigated and numerical methods to correct the profiles are suggested.

In order to simulate the beam space charge impact on electron trajectories a modified version of PyECLLOUD [4] code is used. PyECLLOUD is a 2D tracking code which does not take into account the longitudinal electric field nor the magnetic field of the bunches. Both limitations are a good approximation for high-relativistic beams interacting with slowly-moving electrons. The external fields in the simulation are perfectly aligned and uniform. The beam optics functions in the monitor are assumed to be:  $\beta_x = 213$  m,  $\beta_y = 217$  m (corresponding to vertical device on beam 2) and dispersion is zero. The emittance has the same value in horizontal and vertical plane. Table 1 shows beam parameters of cases analyzed in detail.

Table 1: Simulated Cases Studied in Detail

parameter	450 GeV	4 TeV	6.5 TeV
emittance [ $\mu\text{m}$ ]	1.7	2.4	1.7
bunch			
-intensity [ $\cdot 10^{11}$ ]	1.5	1.7	1.3
-length [ns]	1.2	1.2	1.25
$\sigma_{\text{beam}}$ [ $\mu\text{m}$ ]	869	346	229

In addition three cases of beam energy ramps are considered, for beams with normalized emittance  $\epsilon_n = 1.5 \mu\text{m}$ , bunch length of 1.1 ns and bunch charge of  $N_b = 1.1 \cdot 10^{11}$ ,  $1.3 \cdot 10^{11}$  and  $1.5 \cdot 10^{11}$  protons. Fifteen beam energies between 450 GeV and 7 TeV are simulated in each case. The simulated bunches are gaussian in transverse and longitudinal directions.

In the following we describe the initial velocity distribution of electrons and effects of space charge on profile shape and the gyroradius. In the end we discuss the corrections for the observed distortions of the beam profiles.

## INITIAL VELOCITIES

In the previous work it has been estimated that the distribution of initial velocities of electrons plays an important role in the shape of the beam profile observed in IPM (see Fig. 4.5 in [5]). This distribution was obtained using Geant4 program and turned out to be significantly overestimated. Here the generation of initial velocities is based on an analytic model [6].

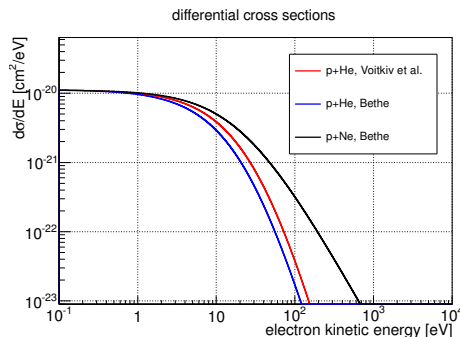


Figure 1: Example of cross-sections calculated with Bethe [7] approximation and a more accurate [6] model for 4 TeV protons.

The main contribution to the ionization process is due to electric dipole interaction between the projectile and the target electron. Most of the interactions are associated with small momentum transfer and the produced electrons are soft.

# STUDIES ON HEAVY ION LOSSES FROM COLLIMATION CLEANING AT THE LHC

P. D. Hermes\*, CERN, Geneva, Switzerland and University of Münster, Germany  
 R. Bruce, J. M. Jowett, S. Redaelli, B. M. Salvachua, G. Valentino,  
 D. Wollmann, CERN, Geneva, Switzerland

## Abstract

The LHC collimation system protects superconducting magnets from beam losses. By design, it was optimized for the high-intensity proton challenges but so far provided adequate protection also during the LHC heavy-ion runs with  $^{208}\text{Pb}^{82+}$  ions up to a beam energy of 4 Z TeV. Ion beam cleaning brings specific challenges due to different physical interactions with the collimator materials and might require further improvements for operation at 7 Z TeV. In this article, we study heavy-ion beam losses leaking out of the LHC collimation system, both in measurement and simulations. The simulations are carried out using both ICOSIM, with a simplified ion physics model implemented, and SixTrack, including more detailed starting conditions from FLUKA but without including online scattering in subsequent collimator hits. The results agree well with measurements overall, although some discrepancies are present. The reasons for the discrepancies are investigated and, on this basis, the requirements for an improved simulation tool are outlined.

## INTRODUCTION

The CERN Large Hadron Collider (LHC) [1] is equipped with a multi-stage collimation system [2] designed to intercept halo-particles at large amplitudes which could hit otherwise the superconducting magnets and potentially cause them to quench. The efficiency of the collimation system depends on the collimator and optics settings. Simulation tools have been developed to enable a thorough analysis of the cleaning efficiency before operating with specific machine configurations. At the passage through the collimator material, proton and heavy-ion beams are subject to different physics processes. Unlike protons, heavy ions can break up into lighter isotopes having a different magnetic rigidity from the reference beam. Both the tracking and scattering/fragmentation routine of a simulation code for heavy-ion collimation must be able to handle the different isotopes. LHC collimation simulations for protons are usually realized with the SixTrack code, while heavy ion loss maps have previously been simulated with the ICOSIM software [3]. The aim of this study is the comparison of the measured losses during the first LHC run with simulated loss maps using either ICOSIM or SixTrack, where for the latter we track protons of equivalent magnetic rigidity.

## SIMULATION SETUP

### ICOSIM

ICOSIM (Ion COLLIMATION SIMulation) is the present state of the art simulation code for heavy-ion loss maps [3]. Ions are tracked by means of a linear transfer matrix formalism, until all particles have hit a collimator. Chromatic effects are taken into account in linear approximation. Nuclear fragmentation and electromagnetic dissociation due to the ion-matter interaction in collimators are simulated using a built-in routine based on tabulated cross section tables generated by FLUKA [4–6]. From the particles generated by these processes, only the heaviest fragment in each interaction is kept track of and kicks in energy or angle are not taken into account. Besides, the software contains an integrated routine to calculate multiple scattering in Gaussian approximation and ionization using the Bethe-Bloch equation [7]. Information about the beam and optics properties as well as the collimator settings is given by the user via input files. Optics input is generated using MAD-X [8] which facilitates the simulation with new machine configurations. ICOSIM generates the beam halo based on different models which can be chosen by the user. For the presented simulation  $2 \cdot 10^6$  initial ions are generated as an annular halo at IP1, sufficiently large to hit the primary collimators (TCP) without including diffusion, following the methods outlined in Ref. [9, 10]. Based on the hierarchy of the LHC collimation system the TCPs in the betatron collimation region IR7 are the only collimators which should be exposed to the initial beam halo.

### SixTrack with Protons of Ion-Equivalent Rigidity

SixTrack with protons of ion-equivalent rigidity is introduced as an alternative tool for the simulation of heavy-ion loss maps. In this framework, protons of effective energies are tracked to simulate the rigidities of the different isotopes. In the presented approach, the tracking of effective protons starts from a distribution of fragments exiting the TCP in IR7. No subsequent scattering at the collimators is applied.

**Tracking tool** SixTrack [11, 12] provides an integrated environment for the magnetic tracking of protons together with a Monte-Carlo module to simulate interactions of protons with the collimator material. The software provides predictions of the performance of the LHC collimation system which have proved to be very consistent with the measured proton losses in the LHC [9]. A thin lens model of the accelerator lattice is used to calculate the particle transport. Chromatic effects are taken into account up to 20<sup>th</sup> order.

\* phermes@cern.ch

# BEAM HALO MEASUREMENT USING A COMBINATION OF A WIRE SCANNER TYPE BEAM SCRAPER AND SOME BEAM LOSS MONITORS IN J-PARC 3-GEV RCS.

M. Yoshimoto#, H. Harada, K. Okabe, M. Kinsho,  
J-PARC, JAEA, Tokai, Ibaraki, 319-1195, Japan

## Abstract

Transverse beam halo is one of the most important beam parameters because it should limit the performance of the high intensity beam accelerator. Therefore the transverse beam halo measurement is one of the important issues to achieve the design beam power of 1MW in the J-PARC 3-GeV RCS. Thus the new beam halo monitor, which is combined a wire scanner and some beam loss monitors, was developed and installed in the extraction beam transport line. By using several beam loss monitors with different sensitivities, an ultra-wide dynamic range can be achieved and beam profile including both of the beam core and halo can be obtained.

## INTRODUCTION

The 3-GeV Rapid Cycling Synchrotron (RCS) has been beam commissioned for initial beam tuning tests since October 2007 [1] and afterwards we started user operation for the Material and Life science experimental Facility (MLF) and the 50-GeV Main Ring synchrotron (MR). Since December 2009, we have started a beam tuning for high-intensity beams and 420kW beam operation could be demonstrated successfully [2]. In order to achieve the design performance of the 1MW of the RCS, the LINAC is required both of the beam energy upgrade from 181MeV to 400MeV and the beam current upgrade from 25mA to 50mA. For the beam energy upgrade, a new accelerating structure “Annular-ring Coupled Structure (ACS)” had been installed in 2013. And then, during the summer shutdown in 2014, new front-end consisted both of the ion source and the Radio Frequency Quadrupole (RFQ) are replaced for the beam current upgrade in the LINAC [3]. Then the beam energy upgrade and the beam current upgrade in the LINAC were completed. After completing these LINAC upgrades, the RCS is to start the final beam tuning toward the design output beam power of 1 MW.

To provide such a high power proton beam for the MR with small injection beam loss or for the MLF with broad range and uniformity irradiation to the target using the octupole magnet [4], it is required to improve the extraction beam quality, namely to achieve the Low-Halo and High-Intensity beam by finer beam tuning in the RCS. Therefore the measurement of the transverse beam profile including both of the beam core and the beam halo is one of the key issues for the high power beam operation in the RCS. Thus a new beam halo monitor was developed and installed at the 3GeV-RCS to Neutron source Beam Transport (3NBT) line as shown in Fig. 1. And examination of the new halo monitor with the extraction

beam was started. In this paper, we report the first trial test of the new beam halo monitor after the LINAC energy upgrade.

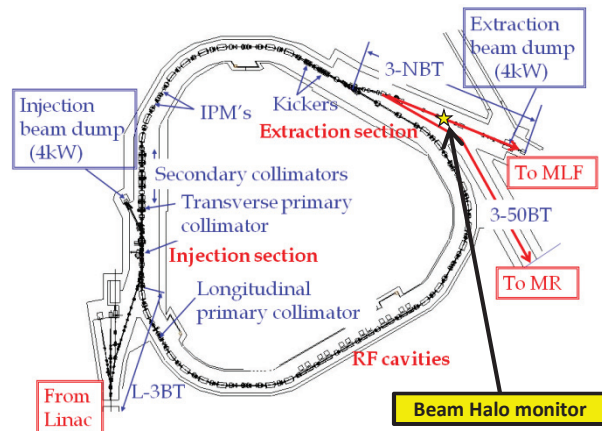


Figure 1: Top view of the RCS and location of the beam halo monitor installation.

## NEW BEAM HALO MONITOR

### Concept Design

For the halo measurement of the extraction beam from the RCS, the original beam halo monitor, which was a scraper plate type detecting the emissive secondary electron and the plate temperature during the beam irradiation into the scraper plate, had been installed at the 3NBT line [5]. The scraper plate was limited to scanning within the beam halo area, thus the beam core cannot be observed. Moreover, it is difficult to obtain the pure signal due to the secondary electron emission because there are much floating electrons in the vacuum chamber and they disturb the raw signal of the halo monitor. On the other hand, the temperature did not increase during the beam irradiation because the sensitivity is too low to detect the beam halo component.

To resolve these problems, the new halo monitor installed at the 3NBT adjoining the original halo monitor. The conception of this new halo monitor is that the beam signal disturbance by the floating electrons should be suppressed and the quick signal response should be achieved. Thus the new halo monitor is combined a wire scanner and the several kinds of beam loss monitors (BLM), and it detects the radiation due to the beam scraping by the wire scanner. Figure 2 shows the schematic diagram of the

# PROPOSED VARYING AMPLITUDE RASTER PATTERN TO UNIFORMLY COVER TARGET FOR THE ISOTOPE PRODUCTION FACILITY (IPF) AT LANSCE\*

J. Kolski<sup>†</sup>, LANL, Los Alamos, NM, 87545, USA

## Abstract

The Isotope Production Facility (IPF) at LANSCE[1] produces medical isotopes strontium-82 and germanium-68 by bombarding rubidium chloride and gallium metal targets respectively with a 100 MeV proton beam, 230  $\mu$ A average current. Rastering the proton beam is necessary to distribute heat load on the target and target window, allowing higher average beam current for isotope production. Currently, we use a simple circular raster pattern with constant amplitude and frequency. The constant amplitude raster pattern does not expose the target center to beam and few isotopes are produced there. We propose a raster pattern with varying amplitude to increase isotope production at the target center, achieve uniform beam flux over the target, and expose more of the target surface to beam heating. Using multiparticle simulations, we discuss the uniformity of target coverage using the proposed varying amplitude raster pattern, compare with the constant amplitude raster pattern currently used, and consider dependencies on transverse beam size, beam centroid offset, and macropulse length and repetition rate.

## INTRODUCTION

Beam rastering for IPF is controlled by a horizontal and a vertical steering magnet[2]. The steering magnets are modulated by the same frequency generator with maximum bandwidth 5 kHz. Steering magnet amplitude can be con-



Figure 1: Measured beam at the IPF target by foil irradiation: 300 s exposure time at 2 Hz, 7  $\mu$ A average current.

\*Work supported by in part by United States Department of Energy under contract DE-AC52-06NA25396. LA-UR 14-28471

<sup>†</sup> Electronic address: jkolski@lanl.gov

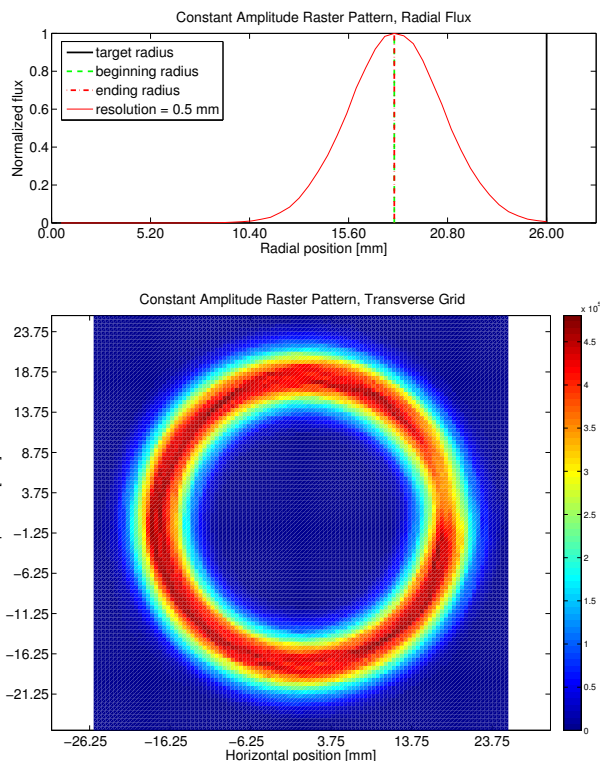


Figure 2: Simulated beam at the IPF target with constant radius 18 mm: 1 macropulse, beam  $\sigma = 2.5$  mm, grid resolutions 0.5 mm. Top: beam flux binned radially. Bottom: beam binned transversely.

trolled separately via digital controllers. During production, IPF receives 625  $\mu$ s long macropulses at an uneven 40 Hz rep rate, consisting of micropulses separated by 5 ns due to the RF acceleration at 201.25 MHz. Due to the raster frequency and pulse length, there are  $\sim 3$  raster revolutions during a macropulse.

The current raster pattern is a simple circle with 18 mm radius. The beam measured at the IPF target by foil irradiation is shown in Fig. 1, and a one macropulse simulation (described later) using the constant amplitude raster pattern is shown in Fig. 2. The beam appears wider in measurement, but the foil coloration results from heating effects which saturate. It is clear from both measurement and simulation that little beam hits the target center and few isotopes are produced there. This is an inefficient use of expensive solid targets.

The goal of this investigation is to obtain a raster pattern

# SIMULATION OF A NEW BEAM CURRENT MONITOR UNDER HEAVY HEAT LOAD\*

J. Sun, P.A. Duperrex<sup>#</sup>, Paul Scherrer Institut, Villigen PSI, Switzerland

### Abstract

At the Paul Scherrer Institute (PSI), the High Intensity Proton Accelerator (HIPA) feeds a pion and muon source target with protons. A beam current monitor, called MHC5, installed 8 meters downstream from the target is heated by the scattered particles from the target. This thermal load on the monitor causes the resonance frequency to drift much more than expected.

A novel new beam current monitor using graphite has been developed. In order to have a good understanding of its performance, the simulation software ANSYS has been used to carry out thermal and high frequency simulations. With this software, it was possible to perform a detailed design of the thermal self-compensation scheme and to check the structural stability of the whole system. In this paper, simulation results show that frequency drift can be reduced to only 8 kHz from previous 730 kHz when expected operating conditions are assumed.

### INTRODUCTION

The proton beam current monitor, MHC5, has been operated for several years in the PSI 590 MeV proton cyclotron. The scattered particles and their secondaries from the target 8 meters upstream cause the resonance frequency of the current monitor to drift due to radiation heating. The originally designed MHC5 made of aluminium showed its operational limits with the increased beam intensity of the last few years. A newer version presently in operation still has large system gain variations caused by the frequency drift even with an active cooling system [1, 2].

To have a good understanding of the MHC5 performance and its limitations, simulations for an old prototype and for the MHC5 version in operation have been carried out using ANSYS.

### FUNDAMENTAL BEHAVIOUR OF THE MONITOR

The MHC5 is a coaxial resonator tuned at 101.26 MHz, the 2<sup>nd</sup> harmonic of the proton beam pulse frequency. The size of the capacity gap, as shown the red ellipse in Figure 1, is a critical parameter influence the resonance frequency. Figure 2 shows the relationship between the size of capacity gap and the resonance frequency of MHC5. As the capacity gap increases, the resonance frequency of the monitor is increasing non-linearly.

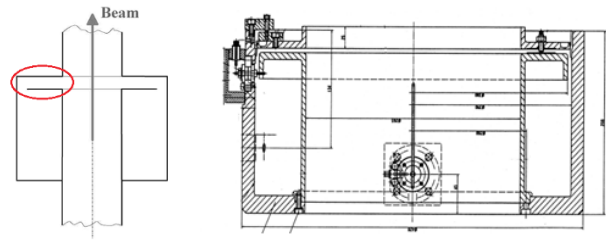


Figure 1: Schematic (left) and section view (right) of the MHC5.

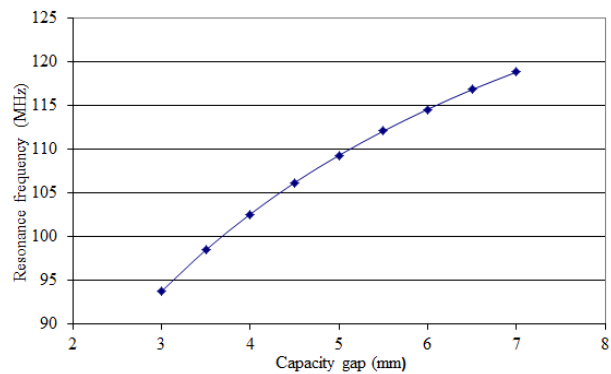


Figure 2: Resonance frequency changing with capacity gap.

Scattered particles from the target deposited on the MHC5 heat up the monitor and provoke frequency drift. Figure 3 shows the resonance frequency drift with increasing temperature on the monitor.

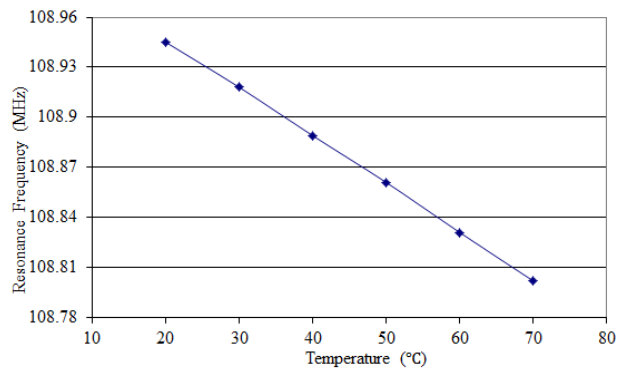


Figure 3: Resonance frequency drifting trend.

The monitor needed to be divided to 7 segments in simulation, since the distribution of the scattered particles is Gaussian in transverse plane, which means each segment has different power deposition.

### VALIDATION WITH PROTOTYPE

In order to validate the simulation results, a cross check between simulation and experiment is necessary. An old

\*The research leading to these results has received funding from the European community's seventh framework programme (FP7/2007-2013) under grant agreement n. °290605 (PSIFELLOW/COFUND)  
#pierre-andre.duperrex@psi.ch

## DESIGN OF A NEW BEAM CURRENT MONITOR UNDER HEAVY HEAT LOAD\*

J. Sun, P.A. Duperrex<sup>#</sup>, G. Kotrlé, Paul Scherrer Institut, Villigen PSI, Switzerland

### Abstract

At the Paul Scherrer Institute (PSI), a 590 MeV 50 MHz High Intensity Proton Accelerator (HIPA) has been operated for many years at 2.2 mA / 1.3 MW and it will be in future upgraded to 3 mA / 1.8 MW. Downstream from a target for pion and muon production is a beam current monitor, called MHC5. The thermal load in MHC5 induced by the scattered particles from the target causes its resonance to drift. Even with an active cooling system, the drift remains a problem.

A new beam current monitor has been designed to overcome this shortcoming. The mechanical design of the new monitor has been completed and manufactured. Different improvements have been implemented compared to the monitor in operation. For instance, graphite has been used as material for the resonator instead of aluminium to minimize the thermal expansion, a thermal self-compensation scheme has been implemented to counteract the frequency drift, its structural stability has been improved and the thermal load has been reduced. The design and the preliminary lab test results are presented in this paper.

### INTRODUCTION

A proton beam current monitor called “MHC5” has been installed in the PSI 590 MeV proton cyclotron for several years. The MHC5 is a coaxial resonator tuned at 101.26 MHz, the 2<sup>nd</sup> harmonic of the proton beam pulse frequency. The magnetic field in the resonator is directly proportional to the beam current. It is located approximately 8 m behind a 4 cm thick graphite target used for muon and pion production. As a consequence, the monitor is exposed to scattered particles and their secondaries from this target and the resulting thermal load causes the resonance frequency to drift. For the current system, the variations of the system gain caused by the frequency drift are too large (10-20%) even with an active cooling system [1]. These drifts should be minimized. A new beam current monitor should be designed and aimed to future high intensity beam operation (3 mA, 1.8 MW).

### PRELIMINARY SIMULATION

In order to have a good understanding of the performance of MHC5 in the beam tunnel, preliminary simulation about the monitor in operation was carried out by ANSYS.

The MHC5 in operation is made of aluminium (anticorodal 110), with a 10  $\mu\text{m}$  coating layer of silver to

improve the electrical conductivity. The monitor itself is in vacuum and the active water cooling keeps the resonator at an average temperature of about 50°C. Four thermocouples monitor the resonator temperature [2], as shown in Figure 1.



Figure 1: The MHC5 in operation, the pipe for water cooling at the beam entry side (left), the thermocouples installed on the beam exit side (right).

The energy deposition on MHC5 in operation under 3 mA proton beams is about 345 W, calculated by MARS [3]. The velocity and temperature of the cooling water is 1.91 m/s and 48°C, by which the convection coefficient can be calculated out, which is about 10500 W/(m<sup>2</sup>·K). The ambient temperature in the tunnel is 50°C. The thermal distribution and deformation of MHC5 in operation as shown in Figure 2. The frequency drift of this case is 730 kHz.

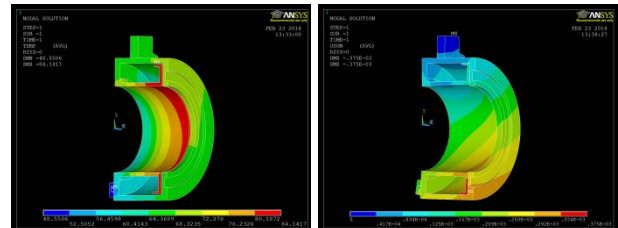


Figure 2: Thermal distribution (left) and thermal expansion (right) of MHC5 in operation with water cooling.

### Causes of the Frequency Drift

In addition to the frequency drift due to the thermal expansion of the resonator, the thermal gradient due to the active cooling is making the shift larger. From simulation calculations (Figure 2), the peak temperature and the maximum expansion part are located at the inner part of the monitor. Inner parts have larger deformations than the outer parts because of the thermal gradient, which decreases the capacity gap and lead to additional resonance frequency drifts.

To reduce the frequency drift, it is therefore essential to minimize the deformations of the monitor. Thus the

\*The research leading to these results has received funding from the European community's seventh framework programme (FP7/2007-2013) under grant agreement n.°290605 (PSIFELLOW/COFUND)  
#pierre-andre.duperrex@psi.ch

# BEAM DYNAMICS STUDY FOR J-PARC MAIN RING BY USING THE 'PENCIL' AND SPACE-CHARGE DOMINATED BEAM: MEASUREMENTS AND SIMULATIONS

A.Molodozhentsev, S.Igarashi, Y.Sato, J.Takano, KEK, Tsukuba, Oho 1-1, 305-0801, Japan

## Abstract

In frame of this report we discuss existing experimental results and compare it with simulations, performed extensively for different machine operation scenario, including the 'pencil' low intensity beam and the 'space-charge dominated' beam. The obtained results demonstrate agreement between simulations and measurements for emittance evolution and losses for different cases. The modelling of the beam dynamics has been performed by using the 'PTC-ORBIT' combined code, installed on the KEK supercomputer \* [1,2]. The developed MR computational model will be used to optimize the machine performance for the 'Mega-Watt' MR operation scenario with limited losses.

## INTRODUCTION

J-PARC Main Ring (MR) study has been performed during 2012-2014 to optimize the machine performance. As the result of this activity the '200 kW' proton beam has been delivered successfully to the 'Neutrino' beamline for the 'Super-Kamiokande' experiment. Total particle losses, localized at the MR collimation section, have been estimated as 120 W. The 'low-losses' MR operation has been achieved after optimization the injection process, stabilizing the power supply ripple, after searching the optimized setting for the MR RF system, dynamic control of the chromaticity, optimization of the 'bare' working point and compensation the linear coupling resonance.

Effects of the machine resonances, caused by imperfections of different kind of the MR magnets, have been studied experimentally by using a low intensity 'pencil' beam. The 'space-charge dominated' beam has been used to observed the effects of the machine resonances in combination with the space-charge effects, like the space charge detuning and space-charge resonances.

The appropriate scheme to compensate the 'sum' linear coupling resonance  $Q_x+Q_y=43$  has been proposed, tested and implemented successfully for J-PARC MR [3,4] for the 'basic' working point. The benchmark activity was initiated to improve the machine model, which should be used to study the Main Ring operation scenario in the case of the 'Mega-Watt' machine operation.

## 'PENCIL' BEAM

During the J-PARC Main Ring study (RUN44,

Nov.2012) the low intensity proton beam with small transverse emittance was used to study the [1,1,43] resonance and its compensation. The resonance correction approach now is based on dedicated four skew quadrupole magnets, installed in two straight sections of MR [4,5]. The single bunch injection into MR from RCS was performed to provide small beam intensity of  $4e11$  proton per bunch. The  $2\sigma$  horizontal beam emittance of the 'pencil' beam, injected into MR, was just  $3\pi$  mm.mrad. The beam profile measurements were performed by using the 'Flying Wire' monitor, installed in the dispersion-free straight section of MR

The PTC code was used to prepare the MR description taking into account measured imperfections of the machine magnets and realistic alignment of the elements. By using this machine description one can perform single or multi-particle tracking by the PTC-ORBIT code to study the beam dynamics for different scenario of the machine operation, including different time pattern for machine magnets and RF system. The ripple of the power supply can be also introduced into the machine mode. The KEK Super Computer system was used to simulate the injection and acceleration processes for J-PARC MR.

## Effect of Isolated Resonance

To model the effect of the 'isolated' [1,1,43] resonance for MR, the resonance was excited by using the negative strength of the skew quads, defined experimentally to compensate the resonance (RUN44).

The study, based on single particle tracking, shows that the periodical crossing the [1,1,43] resonance stop-band by the off-momentum particles in the case of the realistic parameters for the RF system leads to significant limitation of the maximum beam emittance, which can survive if the 'bare' working point is close to the corresponding resonance line [5].

The performed multi-particle tracking was based on the 6D particle distribution, which represented the 3GeV 'pencil' beam, injection into MR from RCS. To make the long-term multi-particle tracking during  $60\cdot000$  turns (corresponds to 320 ms at the energy of 3GeV) and to compare it with the observations we used  $20\cdot000$  macro-particles in order to represent the 6D particle distribution in the single bunch.

The benchmark between the simulations and measurements (RUN44) was performed without any resonance correction for the 'bare' working point near the resonance line ( $Q_x=22.2875$ ,  $Q_y=20.6975$ ). The particle losses during the injection and beginning of acceleration were simulated for the realistic time pattern of the MR RF

\*Work supported by the Large Scale Simulation Program (FY2012-2014) of High Energy Accelerator Research Organization (KEK)

## HIGH GRADIENT RF SYSTEM FOR UPGRADE OF J-PARC

C. Ohmori, K. Hara, K. Hasegawa, M. Toda, M. Yoshii, KEK/J-PARC, Ibaraki, Japan  
 M. Nomura, F. Tamura, M. Yamamoto, T. Shimada, JAEA/J-PARC, Ibaraki, Japan  
 A. Schnase, GSI, Darmstadt, Germany

### Abstract

Magnetic alloy cavities are successfully used for J-PARC synchrotrons. These cavities generate much higher RF voltage than ordinary ferrite-loaded cavities. The MR (Main Ring) upgrade project aims to deliver the beam power of 750 kW to the neutrino experiment. It includes replacements of all RF cavities for high repetition rate of about 1 Hz. By the replacements, the total acceleration voltage will be doubled, while power supplies and amplifiers remain the same. The key issue is the development of a high gradient RF system using high impedance magnetic alloy, FT3L. A dedicated production system for the Finemet® FT3L cores with 80 cm diameter was assembled in the J-PARC and demonstrated that we can produce material with two times higher  $\mu Qf$  product compared to the cores used for present cavities. The first 5-cell FT3L cavity was assembled and the high power test was performed. The cavity was installed in the long shut down from summer to fall. The cavity is used for the beam acceleration with two times high RF voltage.

### UPGRADE SCENARIO OF THE J-PARC

The J-PARC aims to deliver 750 kW beam to the neutrino experiment, T2K. To avoid a significant beam loss by the space charge effects and instability, the original plan was modified and a double repetition rate scenario was chosen. The scenario includes about 1 Hz operation of the MR instead of the present 2.48 sec. cycle. It requires replacements of main magnet power supplies, upgrade of injection and extraction systems and increase of the total RF voltage for the acceleration. To store new magnet power supplies, new power supply buildings will be constructed. Because the acceleration time will be 0.5 sec. instead of the present 1.4 sec, required RF voltage is 560 kV which is two times higher than the present 280 kV. To avoid the renewal of RF power supplies which is very expensive, all 9 RF cavities will be replaced by new high gradient ones which can generate two times higher voltage than the present cavities as shown in Figs. 1. The cavity becomes longer than the present one. The spaces where the present 9 cavities are sitting in will be used to install new 7 cavities. An empty drift space between the extraction kickers is used to install two cavities. To fit to these spaces, two cavities with 4 cell structure and seven cavities with 5 cell structure are prepared. In 2015, 4 FT3L cavities will be installed. And, the replacements of all cavities will be finished in 2016. To guarantee the stable operation, we plan to manage the acceleration voltage of 560 kV with 8 RF systems to reserve one system as a spare.

ISBN 978-3-95450-173-1

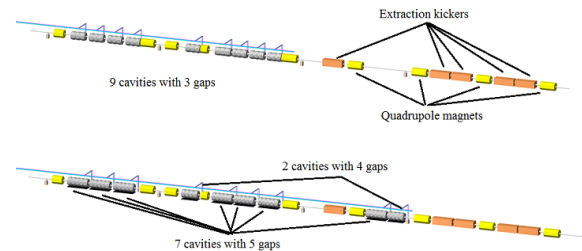


Figure 1: Upgrade scenario of the J-PARC MR cavities. The present cavities (upper) will be replaced by the FT3L cavities (lower) in 2014-2016. The total RF voltage will become more than 630 kV providing enough margin for 1 Hz operation.

### DEVELOPMENTS OF FT3L CAVITY

Magnetic alloy, FT3L, has higher shunt impedance than the FT3M, which is used in the J-PARC RCS and MR. However, there did not exist the production system which can anneal them in a magnetic field. To prove the performance of FT3L cores for the accelerator usage, we developed an annealing oven and proof-of-principle tests were carried out [1]. After the success of test production of large size FT3L, a mass production system was constructed and shipped to a company for the production of 280 FT3L cores for the MR upgrade [2].

In 2014, the first FT3L 5-cell cavity was assembled and tested at the RF test bench in summer and fall as shown in Fig. 2 [3]. After the high power test, the cavity was installed as shown in Fig. 3. The cavity was tested with 80 kV RF voltage and is used with 70 kV for beam acceleration (Fig. 4). By the replacement, the beam acceleration can be managed by 7 cavities and 2 present cavities will be used for the second harmonic RF to increase the beam power.

### DESIGN OF FT3L CAVITY

Figure 5 shows the characteristics of magnetic materials for the accelerator usage. Ferrites materials show the degradation according to increasing RF magnetic flux in the material. Magnetic alloys, FT3M and FT3L, show stable characteristics in the examined measurement ranges. The FT3L shows two times higher characteristic than the FT3M. Adopting the FT3L material, higher voltage becomes available and the length of cavity cells was reduced.

The present J-PARC MR cavity using the FT3M consists of 3 cavity cells and each cell generate 12.7 kV. To double the RF voltage of the cavity, the gap voltage increases to 15 kV and the number of cells becomes 5 instead of 3.

# UPGRADES OF THE RF SYSTEMS IN THE LHC INJECTOR COMPLEX

H. Damerau\*, M. E. Angoletta, T. Argyropoulos, P. Baudrenghien, A. Blas, T. Bohl, A. Butterworth, A. Findlay, R. Garoby, S. Gilardoni, S. Hancock, W. Höfle, J. Molendijk, E. Montesinos, M. Paoluzzi, D. Perrelet, C. Rossi, E. Shaposhnikova  
 CERN, Geneva, Switzerland

## Abstract

In the framework of the LHC Injector Upgrade (LIU) project the radio-frequency (RF) systems of the synchrotrons in the LHC injector chain will undergo significant improvements to reach the high beam intensity and quality required by the High-Luminosity (HL) LHC. Following the recent upgrade of the longitudinal beam control system in the PS Booster (PSB), tests with Finemet cavities are being performed in view of a complete replacement of the existing RF systems in the PSB by ones based on this technology. In the PS a similar wide-band Finemet cavity has been installed as a longitudinal damper. New 1-turn delay feedbacks on the main accelerating cavities to reduce their impedance have also been commissioned. Additional feedback and beam control improvements are foreseen. A major upgrade of the main RF system in the SPS by re-grouping sections of its travelling wave cavities, increasing the number of cavities from four to six, will reduce beam-loading and allow higher intensities to be accelerated. This upgrade includes the installation of two new RF power plants and new feedback systems. All upgrades will be evaluated with respect to their expected benefits for the beams to the LHC.

## INTRODUCTION

After the upgrades within the LIU project [1] the intensity of the LHC-type beams is expected to double in the injector chain. However, the longitudinal parameters, bunch length and longitudinal emittance, remain similar. This implies an important increase in longitudinal density and the need to significantly upgrade the RF systems in all accelerators of the LHC injector chain [2] to cope with an intensity of more than  $2 \cdot 10^{13}$  ppb instead of the present  $1.3 \cdot 10^{13}$  ppb with 25 ns bunch spacing [3, 4].

Although an extensive number of alternatives for the production of LHC-type beam with various RF manipulations has been studied [5, 6], the original scheme for nominal LHC beam [7] remains the baseline. In total  $4 + 2$  bunches, one per the PS Booster (PSB) ring, undergo triple splitting in the PS and batches of 72 bunches spaced by 25 ns are delivered to the SPS. Up to four of these batches are accelerated to an energy of 450 GeV in the SPS and extracted towards the LHC.

\* heiko.damerau@cern.ch

## PS BOOSTER

The PSB presently accelerates up to  $1 \cdot 10^{13}$  ppb in a single bunch eventually doubling with its connection to Linac4. It is equipped with three ferrite-loaded cavities per ring. Two of these are operated at  $0.59 - 1.75$  MHz ( $h = 1$ ) and twice that frequency for the second harmonic cavity. A further ferrite-loaded cavity at about  $6 - 16$  MHz serves for controlled longitudinal blow-up. Almost the entirety of the RF systems in the PSB is affected by the upgrades. The beam-control system has been exchanged by a fully digital low-level RF (LLRF) system [8, 9, 10] during the recent long shutdown (LS1). On the high-power side the replacement of the ferrite-loaded cavities at  $h = 1$  and  $h = 2$  by Finemet cavities covering both harmonics simultaneously is being prepared.

## Beam Controls

Each of the four PSB rings is equipped with a largely independent beam control system, implementing beam phase, radial and synchronization loops. It generates drive signals for the three ferrite-loaded cavities, as well as for present and future Finemet systems. With the start-up after LS1, fully digital beam control systems have been successfully commissioned for all beams on all rings. Figure 1 shows an overview of the new, modular digital beam control of the PSB. For each ring it consists of three digital signal processing (DSP) boards with slots for ADC, DAC or digital synthesizer mezzanine modules. The different beam

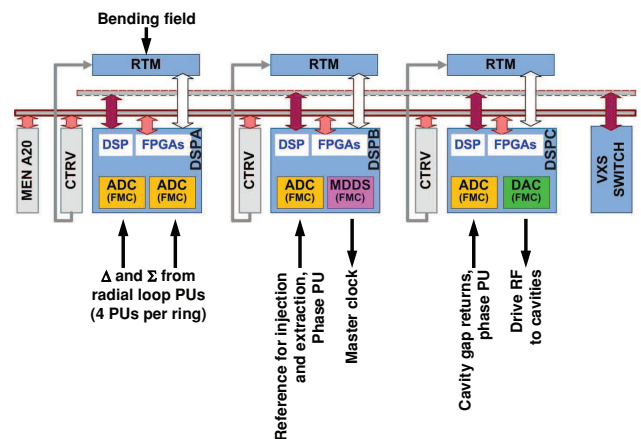


Figure 1: Digital beam control implementation in the PSB. RTM: Rear Transition Module, MDDS: Master Direct Digital Synthesizer, MEN A20: processor card, CTRV: timing card, VXS: VMEbus-switched serial standard.

# CURRENT STATUS ON ESS MEDIUM ENERGY BEAM TRANSPORT

I. Bustinduy\*, M. Magan, F. Sordo, ESS-Bilbao, Spain  
R. Miyamoto†, ESS, Sweden

## Abstract

The European Spallation Source, ESS, uses a high power linear accelerator for producing intense beams of neutrons. During last year the ESS linac cost was reevaluated, as a consequence important modifications were introduced to the linac design that affected Medium Energy Beam Transport (MEBT) section. RFQ output beam energy increased from 3 MeV to 3.62 MeV, and beam current under nominal conditions was increased from 50 to 62.5 mA. The considered MEBT is being designed primarily to match the RFQ output beam characteristics to the DTL input both transversally and longitudinally. For this purpose a set of eleven quadrupoles is used to match the beam characteristics transversally, combined with three 352.2 MHz CCL type buncher cavities, which are used to adjust the beam in order to fulfill the required longitudinal parameters. Finally, thermo-mechanical calculations for adjustable halo scraping blades, with significant impact on the HEBT, will be discussed.

## INTRODUCTION

The European Spallation Source (ESS) is a neutron source currently under construction in Lund, Sweden. The design and operation of the proton linac of ESS, which will ultimately produce a 5 MW beam power, is imposing challenges in various aspects of accelerator science and engineering. The main focus of this paper is the medium energy beam transport (MEBT), located between the RFQ and DTL.

Including all required devices in a relatively short space imposes significant challenges not only on engineering design of components but also beam physics since good beam quality and good matching to the DTL must be achieved under engineering limitations and strong space charge force. Table 1 shows selected parameters of the ESS MEBT. This paper presents status on works of beam physics and engineering component designs for the MEBT. However, due to the limitation in space, only the recent works for the scraper system are presented in detail and status on the rest of works is summarized in the next section.

## SUMMARY OF ESS MEBT STATUS

### *Lattice Design and Beam Physics*

Figure 1 shows the present MEBT layout as well as the power beam density contours. A substantial effort has been made to construct a lattice with good matching to the DTL and good beam quality, while housing the chopper and other necessary devices [1]. The impacts from various lattice element errors have been studied as a part of the campaign to find tolerances of the lattice element errors throughout

Table 1: Selected ESS MEBT Parameters

Parameter	Unit	Value
Beam energy	MeV	3.62
Peak beam current	mA	62.5
Average beam power	kW	9.05
Beam pulse length	ms	2.86
Beam pulse repetition rate	Hz	14
Duty cycle	%	4
RF frequency	MHz	352.21

the entire ESS Linac [2]. A further detailed beam dynamics calculation including effects such as multipole components of a quadrupole and the field profiles of the buncher cavity and quadrupole will be conducted in near future.

To ensure a good chopping efficiency, the optics and beam dynamics during the chopper operation must be studied in addition to the nominal case [1]. Given the rise and fall time of the chopper is presently specified as  $\sim 10$  ns, which is longer than the bunch spacing of 2.84 ns (inverse of 352.2 MHz), there are a few *partially-chopped* bunches. These bunches have large trajectory excursions but not entirely intercepted by the chopper dump, and thus raise a concern of beam losses. The dynamics and beam losses of these bunches are studied in detail and it is ensured that the losses are acceptable [3,4].

In Fig. 1, three locations at 0.85, 2.19, and 3.39 m correspond to the scrapers. The use of the scrapers for the ESS Linac has been studied in detail [1, 3–5]. The scrapers not only improve the beam quality in the nominal condition but also efficiently remove halos in the RFQ output, in case the sections upstream of the MEBT produce a bad quality beam [1] and improve the situation of the beam losses due to the partially-chopped bunches [3]. The locations of the scrapers are determined to optimize these three functions under the mechanical constraints. An analysis of the location optimization of the scrapers is presented in a following section. An ability of a scraper is estimated with a thermo-mechanical calculation and this gives an important input to the beam dynamics calculation. This is also presented in a following section.

### *Component Design and Prototyping*

In order to proceed with detailed engineering phase some constrains have to be taken into account: The elected beam pipe is the standard DN35. This beam pipe gives an upper limit of 18.4 mm radius for the beam aperture and also determines aperture for the rest of the foreseen devices (quadrupoles, bunchers, etc.). Constituting thus, the backbone of the MEBT engineering design.

\* ibon.bustinduy@essbilbao.org

† ryoichi.miyamoto@ess.se

# NEEDS AND CONSIDERATIONS FOR A CONSORTIUM OF ACCELERATOR MODELING\*

J.-L. Vay<sup>#</sup>, J. Qiang, LBNL, Berkeley, CA 94720, USA  
 C.-K. Ng, Z. Li, SLAC, Menlo Park, CA 94025, USA  
 J. Amundson, E. G. Stern, FNAL, Batavia, IL 60510, USA

## Abstract

Thanks to sustained advances in hardware and software technologies, computer modeling is playing an increasingly important role in the design of particle accelerators. This rise in importance is further fuelled by the economic pressure for reducing uncertainties and costs of development, construction and commissioning, thus pushing the field toward an increase use of “virtual prototyping”. Until now, the development of accelerator codes has been left to projects without mandate and programmatic funding for coordination, distribution and user support. While this is adequate for the development of relatively small-scale codes on targeted applications, a more coordinated approach is needed to enable general codes with user bases that extend beyond individual projects, as well as cross-cutting activities. In light of this, it is desirable to strengthen and coordinate programmatic activities of particle accelerator modeling within the accelerator community. This increased focus on computational activities is all the more timely as computer architectures are transitioning to new technologies that require the adaptation of existing - and emergence of new - algorithms and codes.

## INTRODUCTION

Particle accelerators are essential tools of science and technology, with over 30,000 accelerators in operation around the world, in support of discovery science, medicine, industry, energy, the environment and national security [1]. The size and cost of the accelerators are a limiting factor for many applications, and there is active research worldwide targeted at the development of smaller and cheaper accelerators. Computer modeling is playing a key role in the progress toward bringing the size and cost down. It is essential for the optimization of existing accelerators, cost effective design and the development of game changing technologies. Thanks to sustained advances in hardware and software technologies, computer modeling is playing an increasingly important role. This rise in importance is further fuelled by the economic pressure for reducing uncertainties and costs of development, construction and commissioning, thus pushing the field toward an increase use of “virtual prototyping”.

Until now, the development of accelerator codes has been largely left to projects without mandate and programmatic funding for coordination, distribution and

user support. While this is adequate for the development of relatively small-scale codes on targeted applications, a more coordinated approach is needed to enable general codes with user bases that extend beyond individual projects, as well as cross-cutting activities. In light of this, it is desirable to strengthen and coordinate programmatic activities of particle accelerator modeling within the accelerator community. This increased focus on computational activities is all the more timely as computer architectures are transitioning to new technologies that require the adaptation of existing - and emergence of new - algorithms and codes.

Many computer simulation codes have been developed (over 70 worldwide) for the modeling of particle accelerators and beam transport. There has been little coordination of the development of the accelerator physics codes whose aggregate involves a mix of complementarity and duplication, and they are not all actively developed and maintained. Many of the codes have been developed by a single developer (often a physicist) for a specialized purpose or accelerator. Several multi-physics frameworks were developed by small teams, some in large part with the support of SciDAC, and are capable of incorporating many physics models. A substantial fraction of the codes is serial, but a number of the codes have been ported to parallel computers and some are capable of handling massive parallelism. A small fraction of the codes were ported to GPUs. Many of the codes are written in FORTRAN, C or C++, with a growing number combining the compiled language modules (for number crunching) with a Python scripting interface.

## THE VIEW OF THE COMMUNITY

The key roles of computing, and the needs for a more cohesive approach to development, maintenance, support and training have been recognized by the community, in the 2013 DOE-HEP Snowmass report [2], the 2014 Report from the Topical Panel Meeting on Computing and Simulations in High Energy Physics [3], and the 2014 P5 report [4].

Reports [2] and [3] recommended an increased coordination of modeling effort, dedicated support of code modernization, maintenance & dissemination, increase emphasis on use & development of common tools, better user support, and more training in HEP computational physics. In addition, [3] calls for the establishment of an HEP distributed center for computational excellence (single point-of-contact, cross-cutting activities). As a result, a Forum for Computational Excellence was created [5] aiming at promoting excellence in computing,

\*Work supported by US-DOE Contracts DE-AC02-05CH11231.  
 #jlway@lbl.gov

## RECENT RESULTS FROM THE S-POD TRAP SYSTEMS ON THE STABILITY OF INTENSE HADRON BEAMS\*

H. Okamoto<sup>#</sup>, K. Ito, K. Fukushima, T. Okano,  
AdSM, Hiroshima University, Higashi-Hiroshima 739-8530, Japan

### Abstract

S-POD (Simulator of Particle Orbit Dynamics) is a tabletop experimental apparatus developed at Hiroshima University for systematic studies of various beam dynamic effects in modern particle accelerators. This novel experiment is based on an isomorphism between the basic equations governing the collective motion of a non-neutral plasma in a trap and that of a charged-particle beam in an alternating-gradient (AG) focusing channel. The system is particularly useful in exploring space-charge-induced collective phenomena whose accurate study is often troublesome in practice or quite time-consuming to simulate even with high-performance computers. This paper addresses recent experimental results on the stability of intense hadron beams traveling through long periodic AG transport channels. Emphasis is placed upon coherent resonances that occur depending on the lattice design, beam intensity, error fields, etc.

### INTRODUCTION

It is often difficult to perform systematic investigation of intense beam behavior not only in an experimental way but also in a numerical way. Experimentally, the overall lattice structure of a large machine is not changeable once it is constructed. Other fundamental parameters such as tunes, beam density, etc. are also not very flexible in general as long as we rely on real accelerators or beam transport channels. Although these parameters can be chosen freely in numerical simulations, high-precision tracking of charged particles interacting each other via the Coulomb fields is quite time-consuming even with modern parallel computers whenever the beam intensity is high. To overcome or lighten these practical difficulties that we face in fundamental beam dynamics studies, we proposed the concept “Laboratory Accelerator Physics” where the tabletop system called “S-POD” is employed instead of a large-scale machine to *experimentally* simulate the collective motion of high-intensity beams [1,2]. This accelerator-free experiment allows us to explore a wide range of parameter space simply by controlling the AC and DC voltages applied to the electrodes. Since everything is stationary in the laboratory frame, high-resolution measurements can readily be done and we do not have to worry about radio-activation due to heavy particle losses. S-POD experiment, indeed, has practical limitations [3], but it gives us useful insight into intense beam dynamics easily and quickly.

Three independent S-POD systems based on linear Paul traps (LPT) [4] were designed and constructed at Hiroshima University, which have been applied to different beam-physics purposes [2,5-7]. In this paper, we summarize recent experimental results from S-POD II and III on collective resonance instability depending on AG lattices. As mentioned above, such an experimental study cannot be conducted systematically in any real machine whose lattice structure is fixed. We here control the radio-frequency (rf) waveform of quadrupole focusing to emulate the beam behavior in several standard AG lattices involving doublet and FDDF sequence.

### S-POD

S-POD is composed mainly of a compact LPT, DC and AC power sources, a vacuum system, and a personal computer that controls a series of measurements and data saving. Figure 1 shows a side view of a typical multi-sectioned LPT employed for S-POD. Four cylindrical rods are symmetrically placed to generate the rf quadrupole potential for strong transverse focusing of ions. The transverse motion of an ion confined in a LPT is governed by the Hamiltonian [1]

$$H = \frac{p_x^2 + p_y^2}{2} + \frac{1}{2} K_{rf}(\tau)(x^2 - y^2) + I\phi, \quad (1)$$

where the independent variable is  $\tau = ct$  with  $c$  being the speed of light,  $I$  is a constant depending on the ion species, and the function  $K_{rf}(\tau)$  is proportional to the rf voltage applied to the quadrupole rods. Since the collective Coulomb potential  $\phi$  and the time-evolution of the ion distribution in phase space obey the Vlasov-Poisson equations, this many-body system is physically equivalent to a charged-particle beam traveling through an AG

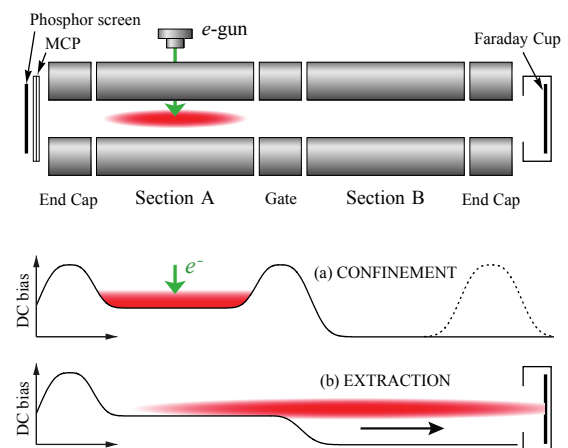


Figure 1: Typical measurement steps [8].

\*Work supported in part by a Grant-in-Aid for Scientific Research, Japan Society for Promotion of Science.  
#okamoto@sci.hiroshima-u.ac.jp

# BEAM DIAGNOSTICS FOR THE DETECTION AND UNDERSTANDING OF BEAM HALO

Kay Wittenburg, DESY, Hamburg, Germany

## Abstract

A general view that has been recently reached by different methods of halo diagnostics of high brightness hadron beams will be given. The performance (dynamic range, accuracy ...) of various monitor types will be combined with the demands from beam dynamics of different machines to discuss which methods can be envisaged for the future. The discussion will include low and high energy machines and their related halo detection schemes

## INTRODUCTION

Especially in the high power proton accelerator already a very small number of lost protons may cause serious radiation dose. In particle accelerator beam experiments, background due to beam halo can mask the rare physics processes in the experiment detectors. Both are unwanted effects of beam halo and therefore the high intensity beam quality is strongly connected to the existence of (transverse) beam halo. However, the definition of halo is still open:

In the summary of the HALO'03 workshop [1] is written: "...it became clear that even at this workshop (HALO'03) a general definition of "Beam Halo" could not be given, because of the very different requirements in different machines, and because of the differing perspectives of instrumentation specialists and accelerator physicists... ". At IPAC2014 [2] wrote: "It is very difficult to give a simple definition of the "halo". It could be a sole beam characteristic or a beam accelerator system characteristic linked to the potential losses it can produce. It could be defined by a number of particles (in the halo) or a size (of the halo). It could be described in the geometric space or in the phase-spaces... ".

This report has a look to "Halo" from the beam instrumentation point of view, that is focused more on the number of particles (in the halo) or on the size (of the halo); and on the dynamic range for halo measurements that should be of the order of  $10^5$  or better (e.g. > 12 bit).

There are numerous sources of halo formation, in linear and circular accelerators, which are not discussed here. A good summary for that topic can be found in [3].

## WHAT IS BEAM HALO

It should be stressed that there is an important difference between beam tails and beam halo: Tails are deviants from the expected beam profile in the order of percent or per mille while halo goes much beyond. As a consequence one should note that the topic "emittance" is related to the beam tails only. The emittance of the beam

is defined by the core of the beam while including more or less of the tails. The emittance can be measured with special emittance measurement devices (e.g. pepperpot) and/or by profile monitors by knowing the  $\beta$ -function, momentum spread and dispersion at the location of the measurement (see e.g. [4]). A good profile monitor can reach a dynamic range of  $\approx 10^3$  (e.g. > 8 bit), and a resolution of < 1% which is often sufficient for the emittance determination of the beam.

Unfortunately quite often the terms "tails" and "halo" are used in an undefined way. See Fig. 1 as an example of reported "halo" generation due to mismatch, while almost all effects happened in the tail regime. The reason of this uncertainty of definition might lie in the beam dynamics simulation tools which are very useful to understand the core beam behavior while computing with a limited number of particles. Therefore results in the real halo-regime have larger uncertainties or can't even be reached by these tools.

From the instrumentation point of view it is very useful to have a definition of halo in 1D spatial projection for which experimental measurements are easier to obtain by a beam profile/halo monitor. But note that the phase-space rotations of the beam might result in oscillations of the 1D projection along the accelerator. For example, at some locations the halo may project strongly along the spatial coordinate and only weakly along the momentum coordinate, while at other positions the reverse is true; with the consequence that the halo can be hidden from the 1D spatial projection [see e.g. 6]. For a complete understanding it is necessary to extend the 1D work to the whole phase space, in the measurement (resulting in many monitors at different location) as well as in the theoretical work and in the simulations [7, 8].

High power accelerators need very low losses during the beam transport to avoid serious activation and damage of components. Beam halo far beyond the beam core is one of the major reasons for these losses and therefore for activation of components. This can be illustrated by the following: Beam losses should be limited at least to a level which ensures hands-on-maintenance of accelerator components during shutdown. The hands-on limit has been found approximately between  $0.1 \text{ W/m} \leq H_L \leq 1 \text{ W/m}$  [9, 10]. Without any major beam disturbance losses are typically distributed along  $\frac{1}{2}$  of a  $\beta$ -period  $L_\beta$  (typical near the focusing quadrupole). The fraction of losses which will generate the hands on limit activation is than:

$$H_W = H_L * \frac{1}{2} * L_\beta / P_B$$

# TWO-DIMENSIONAL AND WIDE DYNAMIC RANGE PROFILE MONITOR USING OTR /FLUORESCENCE SCREENS FOR DIAGNOSING BEAM HALO OF INTENSE PROTON BEAMS

Y. Hashimoto<sup>#</sup>, T. Mitsuhashi, M. Tejima, T. Toyama, KEK/J-PARC, Tsukuba/Tokai, JAPAN  
 H. Akino, Y. Omori, S. Otsu, H. Sakai, Mitsubishi Electric System & Service Co., Ltd., JAPAN

## Abstract

The use of Optical Transition Radiation (OTR) and fluorescence screens to obtain a high dynamic range approximately six orders of magnitude in light intensity for two-dimensional beam profile measurement was demonstrated with intense 3GeV proton beams in the J-PARC in 2013[1]. A new four-section alumina screen for beam-halo measurement was installed just in front of the pre-existing titanium screen this year in order to measure the beam halo and the beam core simultaneously. Two-dimensional beam profile measurements with a high dynamic range are described in this paper.

## INTRODUCTION

The objective was to measure the two-dimensional intensity distribution from the beam core to the beam halo of the injection beam to the Main Ring (MR) of the J-PARC. The beam halo brings serious contamination by radio-activation to the accelerator by beam losses in the case of beam intensities greater than  $1.5 \times 10^{13}$ / bunch. In order to measure such a beam profile, a high dynamic range up to six orders of magnitude in light intensity was required. By using such a wide measurement range, we can

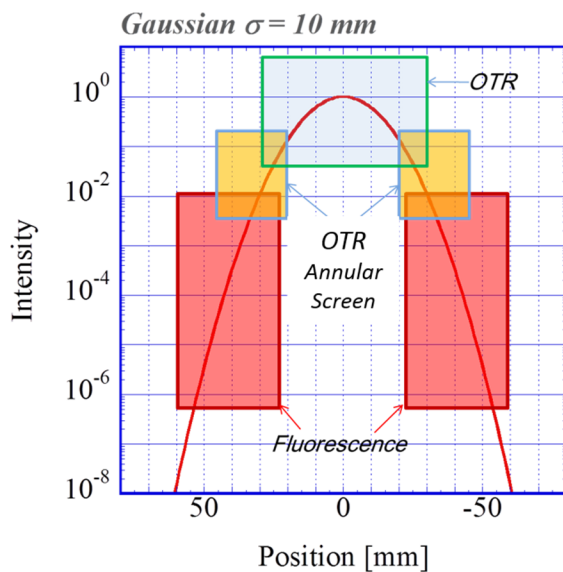


Figure 1: Six orders of magnitude measurement with three kinds of screens.

not only evaluate the beam-halo eliminations by the collimator, but also perform precise beam diagnosis for the

<sup>#</sup> yoshinori.hashimoto@kek.jp

Rapid Cycling Synchrotron (RCS) in beam extraction, which is a preceding accelerator of the MR.

## CONCEPTS

### Function of OTR and Fluorescence

We used the OTR from the titanium screen and the fluorescence from the chromium-doped alumina screen. Optical intensities of the light depend on the beam intensity at the positions of these screens. In order to detect the light, a Charge-Injection-Device (CID) camera attached to a gated Image Intensifier (II) was employed. The gain of the II was optimized for these optical intensities.

Figure 1 shows the functional range for each kind of screen. The beam intensity distribution curve shown in the figure assumes that the beam intensity is over  $10^{13}$  proton/bunch and the sigma of the Gaussian distribution is 10 mm. The measurement techniques and their ranges are as follows: the OTR from the beam core covers down to -1.5 orders of magnitude, the next OTR from the beam tail from the 50 mm diameter annular screen covers down to -2.5 orders, and finally the fluorescence from the beam halo covers down to almost -6 orders from the peak.

### Energy Losses in Screens

The screen materials for intense proton beams should be chosen carefully. Preferred materials include a 10 micron thick titanium foil for the OTR production and alumina screens of 500  $\mu\text{m}$  thickness for the fluorescence production. As for the energy loss with 3 GeV proton beam, alumina has 48 times larger loss than titanium as shown in Table 1. However, when it is only used in the halo region where the intensity is two orders of magnitude lower than the peak values, the total energy loss of alumina becomes about half of that of titanium: i.e.  $4.7\text{e-}3$  J/bunch equivalent. These energy losses are small enough to avoid damaging the screens.

Table 1: Energy losses in material [2] in the case of proton beam energy of 3 GeV, and bunch intensity of  $1 \times 10^{13}$  protons.

Material	Thickness [ $\mu\text{m}$ ]	Energy Loss [keV/proton]	Total Energy Loss [J/bunch]
Ti	10	6.79	$9.8\text{e-}3$
Cr + Al <sub>2</sub> O <sub>3</sub>	500	330	$4.7\text{e-}1$

# UNDERSTANDING BEAM LOSSES IN HIGH-INTENSITY PROTON ACCUMULATOR RINGS\*

Robert J. Macek<sup>#</sup> and Jeffrey S. Kolski, LANL, Los Alamos, NM 87545, USA

## Abstract

Beam losses and the resulting radio-activation of accelerator components are major considerations governing the operations and performance of medium-energy, high-intensity proton accumulator rings using H-charge exchange injection such as the Los Alamos Proton Storage Ring (PSR). Several beam loss mechanisms contribute including beam scattering (nuclear and large angle Coulomb scattering) in the injection foil, production of excited states of H<sup>0</sup> in the H- injection stripper foil that subsequently field strip in the magnetic fields down stream of the foil, halo growth from space charge effects, beam instabilities and losses from the fast extraction process. These are now well understood based on the progress in the diagnosis, measurement, and modeling of beam losses at PSR and related rings. The roles of the computer codes MAD8 [1], ORBIT [2], G4Beamline [3], and others used in modeling beam losses are discussed, and the modeling results are compared with relevant experimental data.

## INTRODUCTION

Minimizing uncontrolled beam losses is one of the most important objectives in the design, operations and development of high-intensity proton accumulator rings that use many hundreds to thousands of turns of H-charge exchange injection such as the Los Alamos Proton Storage Ring (PSR) or the accumulator ring for the Spallation Neutron Source (SSN) at the Oak Ridge National Laboratory. Similar concerns hold for the rapid cycling synchrotrons at the heart of the spallation neutron sources at the Rutherford Appleton Laboratory in the UK and the Japan Proton Accelerator Complex (J-PARC). To limit radio-activation of accelerator components in order to permit hands-on maintenance, it has become a rule-of-thumb to limit uncontrolled beam losses to the 1 Watt/meter level.

The Los Alamos PSR was a pioneering effort in the use of charge exchange injection for a full power, high intensity accumulator ring to drive a short pulse spallation neutron source [4]. Much has been learned about beam losses in this ring since first beam in 1985. Until 1998, PSR used a two-step injection process i.e., stripping of H- to H<sup>0</sup> in a high field dipole then stripping to H<sup>+</sup> in a stripper foil. By 1993 the beam losses for the two-step injection were reasonably well understood and had been reduced significantly by a number of improvements [5]. It should also be noted that by 1993, it was shown that the 0.2-0.3% fractional losses on the first turn were explained

by the production and stripping of H<sup>0</sup>(n=3, and 4) excited states produced in the stripper foil that subsequently Lorentz strip in the first dipole down stream of the injection foil [6].

In 1998, the upgrade of PSR to direct (one step) H- injection was completed [7] and resulted in a factor of ~3 reduction in the fractional beam losses. PSR has since then operated at 100-125  $\mu$ A with total fractional uncontrolled losses of 0.2% - 0.3%.

## PSR LAYOUT

A layout of PSR after the 1998 upgrade is shown in Figure 1. It is a small ring of 90.2 m circumference with 10 sections and FODO lattice. In normal operations, 800 MeV beam is accumulated for ~1750 turns to provide 100-120  $\mu$ A (5-6  $\mu$ C/pulse) at 20 Hz for the main user, the LANSCE spallation neutron source at the Lujan Center. The “waste” beam i.e., H- that did not strip and H<sup>0</sup> is transported via a large aperture beam line to a graphite beam dump capable of handling 10  $\mu$ A or 8 kW of beam power. Single turn extraction is accomplished with two strip line kickers and a septum magnet system. It is worth noting that in high peak intensity beam studies, as much as 10  $\mu$ C was successfully accumulated in 3400 turns.

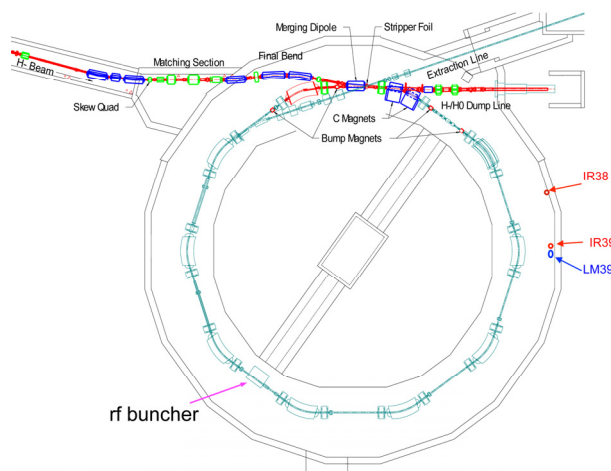


Figure 1: PSR layout since 1998.

The injection stripper foil is a ribbon 12 mm wide by 40 some mm long made up of two 200 microgram/cm<sup>2</sup> layers. Today, each layer is a hybrid composite of carbon and boron in a method developed by Professor Sugai at KEK for enhancing foil lifetime [8]. Numerous 4 micron carbon fibers are stretched across the frame to keep the foil from moving.

The stripper foil is offset from the final H<sup>+</sup> closed orbit, and the H- beam strikes the foil on a corner. A

\*Work supported by US DOE under contract DE-AC52-06NA25396.

<sup>#</sup>macek@lanl.gov

# BOOSTER UPGRADE FOR 700kW NOVA OPERATIONS \*

K. Seiya<sup>#</sup>, FNAL, Batavia, IL 60510, USA

## Abstract

The Fermilab Proton Source is in the process of an upgrade referred to as the Proton Improvement Plan (PIP) [1]. One PIP goal is to have Booster capable of delivering  $\sim 2.3E17$  protons/hour, 130% higher than the present typical flux of  $\sim 1E17$  protons/hour. The increase will be achieved mainly by increasing the Booster beam cycle rate from 9 Hz to 15 Hz. Beam loss due to the increased flux will need to be controlled, so as not to create larger integrated doses. The status of present operations and progress of beam studies will be discussed in this paper.

## 700KW OPERATION WITH RECYCLER AND MAIN INJECTOR

Fermilab is going to provide 700kW proton beam to the NOvA experiment [2]. Prior to the 2012 shutdown, Main Injector (MI) had been delivering 360 kW routinely and up to 400 kW of beam power to the NuMI target. Booster had injected 11 batches of  $4E13$  protons per pulse [ppp] to the MI. After the injection, the MI accelerated the beam from 8 GeV to 120 GeV every 2.2 sec.

For NOvA operation, 12 batches are injected into the Recycler Ring (RR) which is located on top of the MI in the same tunnel. The RR is an 8GeV fixed energy synchrotron using permanent magnets. Two 53MHz cavities were installed in the RR during 2012 shutdown for slip stacking. The harmonic number of the RR is 588 which is the same as MI. The MI power supply was upgraded and shortened the ramp from 1.6 to 1.33 sec as shown in Figure 1.

In the RR, 6 Booster batches are injected and then another 6 batches are injected and slip stacked. After the slip stacking, the beam density is doubled. This process takes 12 Booster cycles which is 0.8 sec.

In order to achieve 700 kW of beam power, the MI cycle has been shortened from 2.2 sec to 1.33 sec. This

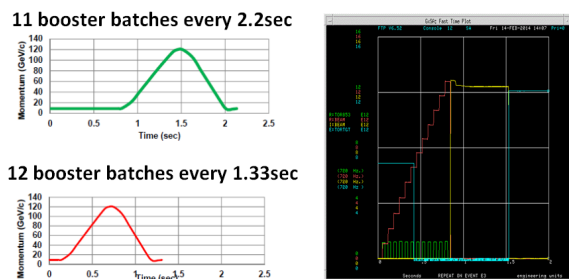


Figure 1: Left pictures; The MI ramp for 400 kW (upper) and 700 kW (lower) operations. Right picture; Intensity in the RR (red), MI (yellow) and Booster (green).

\*Work supported by Fermilab Research Alliance, LLC under Contract No. DE-AC02-07CH11359 with the United States Department of Energy.

<sup>#</sup>kiyomi@fnal.gov

was accomplished by using the RR to manage the injection and stacking of beam from the Booster while the MI is ramping.

## REQUIREMENTS FOR THE BOOSTER AND BEAM LOSS LIMIT

Booster is a 15 Hz resonant circuit synchrotron and accelerates proton beams from 400 MeV to 8 GeV. The required intensity in the Booster for NOvA is  $4.3E12$  ppp, the same as it was for 400 kW operation. However, the cycle rate will be increased from 9 Hz to 15 Hz to accommodate both NOvA and other users. The RF system and utilities are being upgraded to 15 Hz operations and are nearing completion. The plan is to start 15 Hz operations in FY15.

The beam loss limit has been set to 525W to allow workers to maintain all elements in the Booster tunnel without excessive radiation exposure. Figure 2 shows the historical beam loss in the Booster versus protons per hour. The total loss depends on the beam intensity. Given the required intensity of  $2.3E17$  protons per hour, the loss has to be reduced to half by 2016.

The present operational beam intensity at injection is about  $5E12$  ppp and extraction is  $4.5E12$  ppp. The total energy loss is 0.075 kJ in one Booster cycle and hence 1150 W when the cycle rate is 15Hz. The loss has to be reduced to half by 2016. Figure 3 shows the intensity and loss during normal operations. The points where significant beam loss occurs are when the RF feedback is turned on, when the extraction kicker gap is created and when beam acceleration passes through transition. There are slow losses from injection to 5 ms into the ramp and after transition. Beam studies and upgrades that will be done to reduce the beam losses will be discussed in this paper.

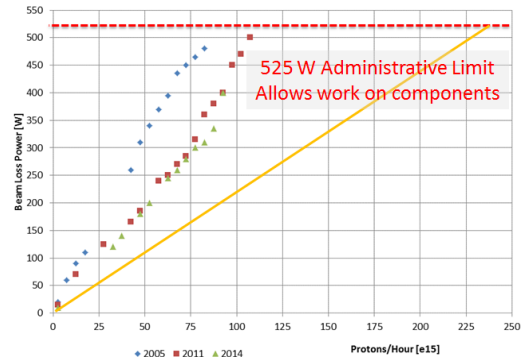


Figure 2: Beam power loss for 3 year operations (blue: 2005, red: 2011 and green: 2014)

# HIGH INTENSITY LOSS MECHANISMS ON THE ISIS RAPID CYCLING SYNCHROTRON

C.M. Warsop, D.J. Adams, B. Jones, S.J. Payne, B.G. Pine, H.V. Smith, R.E. Williamson, RAL, UK.  
V. Kornilov, GSI, Darmstadt, Germany.

## Abstract

ISIS is the spallation neutron source at the Rutherford Appleton laboratory in the UK. Operation centres on a loss limited, 800 MeV, 50 Hz proton synchrotron which delivers 0.2 MW to two targets. Understanding loss mechanisms on the ISIS ring is important for optimal operation, machine developments and upgrades, as well as improving designs for future machines. The high space charge levels, combined with the low loss achieved for high power operation, makes the ring an ideal tool for studying the physics of beam loss, particularly in a fast ramping context. The ability to reconfigure the beam in storage ring mode, and ongoing developments of diagnostics and beam measurements, are allowing detailed studies of image effects, resonances, beam stability and activation. We summarise recent work and progress on these topics, comparing with theory and simulation where appropriate.

## INTRODUCTION

The ISIS facility provides neutron and muon beams for condensed matter research. High power beams are supplied by a loss limited, 800 MeV, 50 Hz proton synchrotron. Understanding and minimising beam loss in the ring are key factors in ensuring improved machine performance, optimising future machine developments, and providing the best proposals for future upgrades.

Ongoing developments and proposed upgrades to the two ISIS neutron targets, with the accompanying requirements for low loss, reliable and consistent operations at higher powers, demand improved understanding and control of loss. Proposed upgrades to the existing ring, including the 0.5 MW design using a higher energy 180 MeV injector [1], require comprehensive beam models for their design. Similarly, upgrades and the next generation short pulse neutron sources in the 2 MW regime (and beyond) all require well benchmarked codes and theory to ensure optimal, realistic, low loss designs. A detailed, experimentally verified study of high intensity beam loss mechanisms is therefore essential to underpin these plans.

The ISIS ring is a valuable tool for studying high intensity beams. The challenging operating regime of low loss with high space charge; the fast acceleration ramp – combined with a number of key beam dynamics issues discussed below, provides important opportunities for new research. The ability to run the beam in experimental storage ring mode also opens up further areas for study.

First we review losses observed on ISIS operationally, then summarise relevant R&D topics.

## HIGH INTENSITY BEAM LOSS ON ISIS

### The ISIS RCS

The ISIS synchrotron accelerates  $3 \times 10^{13}$  protons per pulse (ppp) from 70-800 MeV on the 10 ms ramp of the sinusoidal main magnet field. At the repetition rate of 50 Hz this provides an average beam power of 0.2 MW. Charge exchange injection takes place over 130 turns, with painting in both transverse planes as the high intensity beam is accumulated and contained in the collimated acceptances of  $\sim 350 \pi$  mm mr. The ring has a circumference of 163 m. Nominal betatron tunes are  $(Q_x, Q_y) = (4.31, 3.83)$ , but these are varied using 2 families of 10 trim quadrupoles. The dual harmonic RF system captures and accelerates the initially unbunched beam, and allows enhanced bunching factors. The machine is harmonic number two, RF systems run at  $h=2$  and  $h=4$  with peak volts of 168 and 96 kV/turn respectively. Peak incoherent tune shifts of  $\Delta Q \geq 0.5$  are reached at about 80 MeV during bunching. Single turn extraction at 800 MeV uses a fast vertical kicker. Main loss mechanisms are associated with non-adiabatic trapping, transverse space charge and transverse instability.

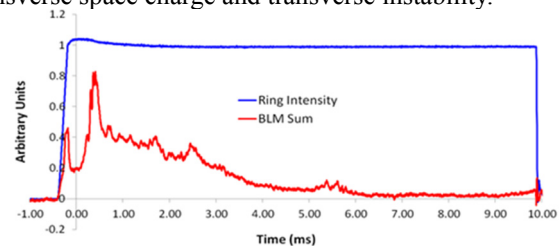


Figure 1: ISIS intensity and beam loss through the machine cycle ( $2.8 \times 10^{13}$  ppp injected).

### Summary of Losses

The average beam power delivered by the ring is typically 160-200 kW. To allow hands on maintenance, activation has to be limited; this determines tolerable loss levels and running intensity. Figure 1 shows the circulating current and beam loss signal through the 10.5 ms machine cycle. Overall losses are  $< 5\%$  and concentrated at lower energy, where activation is considerably reduced. During the injection and accumulation process (-0.5–0.0 ms) losses are about 2%. During the trapping process (0.0–2.5 ms) losses are  $< 3\%$ , and for the rest of acceleration (2.5–10.0 ms) losses reduce to 0.5% levels, finally reaching  $\sim 0.01\%$  at extraction.

Most loss ( $> \sim 98\%$ ) and activation is localised in 3 of the 10 super-periods, which include the injection,

# PRESENT STATUS OF THE HIGH CURRENT PROTON LINAC AT TSINGHUA UNIVERSITY AND ITS BEAM MEASUREMENTS AND APPLICATIONS\*

Q.Z. Xing<sup>#</sup>, C. Cheng, C.T. Du, L. Du, T.B. Du, H. Gong, X.L. Guan, C. Jiang, R. Tang, C.X. Tang, X.W. Wang, Y.S. Xiao, Y.G. Yang, H.Y. Zhang, S.X. Zheng, Key Laboratory of Particle & Radiation Imaging (Tsinghua University), Ministry of Education, Beijing 100084, China  
 W.Q. Guan, Y. He, J. Li, NUCTECH Co. Ltd., Beijing 100084, China  
 B.C. Wang, Northwest Institute of Nuclear Technology, Xian 710024, China  
 S.L. Wang, Institute of High Energy Physics, Beijing 100084, China

## Abstract

The CPHS (Compact Pulsed Hadron Source) linac at Tsinghua University, is now in operation as an achievement of its mid-term objective. The 3 MeV proton beam with the peak current of 22 mA, pulse length of 100  $\mu$ s, and repetition rate of 20 Hz has been delivered to the Beryllium target to produce the neutron beam from the year of 2013. We present in this paper the development and application of the high current linac, together with the measurement of the proton and neutron beams. The beam energy of the CPHS linac will be enhanced to 13 MeV after the DTL is ready in 2015.

## INTRODUCTION

The CPHS (Compact Pulsed Hadron Source) project, which is aimed at becoming an experimental platform for education, research, and innovative applications at Tsinghua University, was launched in the year of 2009 [1]. The facility will provide the proton beam, together with the neutron beam by delivering the proton beam to bombard the Beryllium target. The designed parameters for the proton beam is 13 MeV/50 mA with the pulse length of 500  $\mu$ s and repetition rate of 50 Hz. The ECR source produces the 50 keV proton beam followed by the LEBT which matches the beam into the downstream RFQ accelerator. The RFQ accelerates the beam to 3 MeV. The Alvarez-type DTL will accelerate the beam from 3 MeV to 13 MeV. The beam is matched to the DTL directly and there is no MEBT between the RFQ and DTL. The HEBT transports the beam from the DTL to the neutron target station. One uniform round beam spot on the Beryllium

target is expected with the diameter of 5 cm [2]. The facility has achieved its mid-term objective in 2013. In this paper, the development status of the CPHS linac is presented, including the proton/neutron beam measurement and application performed.

## OPERATION STATUS OF THE HIGH CURRENT 3MeV LINAC

On March 2013, the maximum transmission of the RFQ accelerator has reached 88% at 50  $\mu$ s (pulse duration) /50 Hz (repetition frequency) during the commissioning [3][4]. On July 2013 the CPHS facility has achieved its mid-term objective: delivering the 3 MeV proton beam to bombard the Beryllium target [5]. As shown in Fig. 1, the 3 MeV proton beam is delivered directly from the RFQ output to the neutron target station by the HEBT. Five quadrupoles have been positioned instead of the DTL. The DTL will be ready in 2015 and the beam energy of the linac will be enhanced to 13 MeV.

Though the DTL is still in development, the CPHS facility has been in operation with the 3 MeV proton beam from 2013 until now, as shown in Fig. 2 and 3. The output current of the RFQ is relatively stable (30 mA) near the end of 2013. The total operation time in 2014 is estimated to be 500 hrs. With a reduction of the RF power of the ECR source, the peak current of the proton beam before the target has decreased to 20 mA in 2014. During the experiments which need only the proton beam, the beam is not bended by 90° and does not bombard the target.



\* Work supported by National Natural Science Foundation of China (Major Research Plan Grant No. 91126003 and 11175096)  
<sup>#</sup>xqz@tsinghua.edu.cn

# INITIAL COMMISSIONING OF ION BEAMS AT SPIRAL2

Patrick Bertrand, GANIL, Caen, France

## Abstract

The official reception of the SPIRAL2 accelerator building occurred in October 2014. In parallel, the installation of the accelerator components has started in June 2013. The first part of the beam commissioning, including the ECR sources, the LEBTs and the 88 MHz RFQ should start in December, with an injection in the Linac by mid-2015. This paper describes the status of the accelerator components and installation, and the philosophy retained to commission the light and heavy ion beams at various required final energies.

## INTRODUCTION

Officially approved in May 2005, the SPIRAL2 radioactive ion beam facility at GANIL (Caen-Normandy) has been launched in July 2005, with the participation of many French laboratories (CEA, CNRS) and international partners. In 2008, the decision has been taken to build the SPIRAL2 complex in two phases: *A first one* including the accelerator, the Neutron-based research area (NFS) and the Separator Spectrometer (S3), and *a second one* including the RIB production process and building, and the low energy RIB experimental hall called DESIR [1-3]. However, in October 2013 and due to budget restrictions, the RIB production part has been postponed, and DESIR included as a continuation of the first phase.

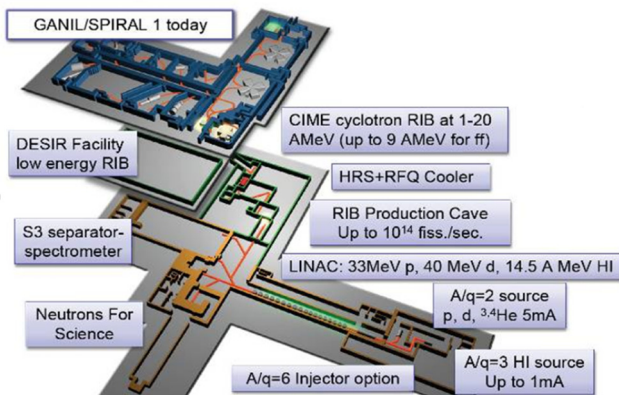


Figure 1: SPIRAL2 project layout, with experimental areas and connexion to the existing GANIL.

As recalled in Table 1, the SPIRAL2 accelerator must deal with a large variety of beams: protons, deuterons, heavy ions with  $A/q < 3$ , ( $A/q < 6$  in the future). A maximum beam power of 200kW is considered for deuterons in CW mode. We notice also that the heavy ion beam intensities can go up to 1 mA; however, some heavy ion beams like metallic ones can also have a very small intensity, which constitutes in itself a challenge, some diagnostics having to work with a huge response range!

Table 1: Beam Specifications

beam	P+	D+	ions	ions
A/Q	1	2	<3	<6 or 7
Max. I (mA)	5	5	1	1
Min. output E (MeV/A)	2	2	2	2
Max output E (MeV/A)	33	20	14.5	8
Max. beam power (kW)	165	200	44	48

In this paper, after giving updated information on the accelerator-NFS-S3 building and process installation, we will concentrate on our beam commissioning strategy.

## ACCELERATOR-NFS-S3 BUILDING

The construction permit of the accelerator-NFS-S3 building was obtained in October 2010. After a difficult excavation work and geotechnical/geologic studies, the first concrete started in September 2011. The building itself was officially received last October 2014 (Figure 2), and the utilities will be officially approved very soon.

During the construction, several inspections were made by the French Safety Authorities, in order to check the conformity of the building with respect to the requirements like confinement barriers, protection against earthquakes, etc...



Figure 2: Completion of the accelerator building (October 2014). The beam axis is 9.5 meters underground.

## STATUS OF THE ACCELERATOR

The building construction process has been organised in such a way, that it was possible to install progressively the process inside the building, starting by mid 2013 with the low energy beam lines and their power supply and utilities, all this in parallel with other parts of the building construction (HEBT for example). This strategy allowed us to gain about one year, but the coactivity between building and process teams, and the planning optimization appeared to be not so easy to manage, one difficulty being

# Chromatic and Space Charge Effects in Nonlinear Integrable Optics\*

S. D. Webb<sup>†</sup>, D. L. Bruhwiler, and R. Kishek<sup>‡</sup>, RadiaSoft, LLC., Boulder, CO  
 A. Valishev and S. Nagaitsev, FNAL, Batavia, IL  
 V. Danilov, ORNL, Oak Ridge, TN

## Abstract

The IOTA test accelerator is under construction at FNAL to study a novel method of advancing the intensity frontier in storage rings: nonlinear integrable optics. For particles at the design momentum, the lattice has two invariants and the dynamics is integrable. In the ideal single-particle two-dimensional case, this yields bounded, regular orbits with extremely large tune spreads. Off-momentum effects such as dispersion and chromaticity, and collective effects such as direct space charge, break the integrability. We discuss the origin of this broken integrability for both single- and many-particle effects, and present simulation results for the IOTA lattice used as a high intensity proton storage ring.

## INTRODUCTION

Future generations of intense, multi-megawatt accelerators have applications for discovery science as drivers for spallation sources, neutrino physics, and the next generation of high energy colliders. Such intense beams are prone to collective instabilities including, but not limited to: space charge driven beam halo, resistive wall instability, head-tail instability, and the various beam break-up instabilities. The physical origin of these instabilities is the constant transverse tunes in linear strong-focusing lattices. In the SNS accumulator ring, for example, it was found [1] that these instabilities did not appear for the natural chromaticity of the lattice, which was very large. It is then natural to conclude that the large tune spreads associated with these chromaticities are desirable for mitigating such instabilities.

The trouble with this is that the large chromaticities in the linear lattices will span an entire integer or more of tune space, which will cross many single-particle resonances. A more robust method is required to obtain large tune spreads without losing dynamic aperture due to single-particle dynamics. Enter the nonlinear integrable optics designed by Danilov and Nagaitsev [2], which introduce very large tune spreads while keeping the orbits regular. This work has already shown promise in preventing space charge driven beam halo [3] In this proceeding, we discuss how these invariants change in two real-machine situations: energy spread and space charge.

In the next section, we discuss how energy spread in coasting beams breaks the single-particle integrability, and how we may design the lattice to restore that integrability. How direct space charge changes a matched distribution of

the invariants is explored in the following section. We conclude with preliminary simulations of using the integrable optics to prevent resistive wall instability in an intense proton ring.

## OFF-MOMENTUM EFFECTS: CHROMATICITY & DISPERSION

The work in [2] considers purely two-dimensional particle dynamics – transverse oscillations with no energy spread. In real intense accelerators energy spread and the associated chromaticity, as well as the dispersion in the lattice, will modify the integrable Hamiltonian. Before asking the nonlinear integrable lattices to mitigate intensity-driven effects, it is important to restore the integrability which makes it so robust.

As we show in [4], a Lie operator treatment of a ring designed for integrable optics that includes off-momentum effects and nonlinear elements such as sextupoles and octupoles yields a correction to the Hamiltonian in [2] due to dispersion in the elliptic magnet sections and the lattice chromaticity. The integrable lattice factors into a product of maps:

$$\mathcal{M} = \mathcal{A}^{-1} e^{-t: \int ds \mathcal{U}(x - \delta \eta(s), y):} e^{-:h:} e^{-t: \int ds \mathcal{U}(x - \delta \eta(s), y):} \mathcal{A} \quad (1)$$

where  $\mathcal{A}$  is the normalizing map, and  $h$  is the Hamiltonian that generates the single turn map for the integrable optics lattice when the nonlinear elliptic potential strength is zero. Thus,  $h$  includes drifts, dipoles, and quadrupoles, as well as chromaticity-correcting families of nonlinear magnets. The details of this calculation may be found in [4] and are too lengthy to include here.

The resulting Hamiltonian for the total single turn map is given, to lowest order, by:

$$\overline{\mathcal{H}} = \frac{\mu_0}{2} \left\{ [1 - C_x(\delta)] (\overline{p}_x^2 + \overline{x}^2) + [1 - C_y(\delta)] (\overline{p}_y^2 + \overline{y}^2) + \frac{t}{1 - \delta} \int_0^{\ell_{\text{drift}}} \mathcal{U}(\overline{x} - \eta(s') \delta, \overline{y}) ds' \right\} + \dots \quad (2)$$

where  $\dots$  are higher order terms, including any nonlinear terms left over after adjusting the chromaticity. Here we have assumed a coasting beam with no synchrotron oscillations, thus  $\delta$  is a constant.  $\eta(s)$  is the dispersion function through the drift where the elliptic magnetic element will be placed, and  $\mathcal{U}$  is the nonlinear elliptic potential from [2]. This means that the vertical and horizontal chromaticities,  $C_y(\delta)$  and  $C_x(\delta)$  respectively, are general functions of  $\delta$ . We also concluded that conventional chromaticity correction schemes – using sextupoles to correct

\* This material is based upon work supported by the U.S. Department of Energy, Office of Science, Office of High Energy Physics under Award Number DE-SC0011340.

<sup>†</sup> swebb@radiasoft.net

## SPES BEAM DYNAMICS

A. Pisent, L. Bellan, M. Comunian, INFN-LNL, Legnaro, Italy

B. Chalykh, ITEP, Moscow, Russia

A. Russo, L. Calabretta, INFN-LNS, Catania, Italy

### Abstract

At LNL INFN is under construction a Rare Isotope Facility (SPES) based on a 35-70 MeV proton cyclotron, able to deliver two beams with a total current up to 0.5 mA, an ISOL fission target station and an existing ALPI superconducting accelerator as a post accelerator (up to 10 MeV/u for  $A/q=7$ ).

In this talk will be described the elements between the production target and the experiments, like the selection system, the ECR charge breeder, the second separation system and the new CW RFQ (80 MHz, 714 keV/u, internal bunching).

The problems that have been solved during the design phase are partly common to all RIB facilities, like the necessity to have an high selectivity and high transmission for a beam of a very low intensity, plus the specific challenges related to the use of ALPI (with a reduced longitudinal acceptance) and related to the specific lay out.

At present the design phase has been finalised, and the procurement procedure for the charge breeder, the transfer lines and the RFQ are in an advanced state and will start in the next months. The main beam dynamics aspects of the transfer lines (including magnetic selections) and the linac ALPI will be discussed in detail.

### INTRODUCTION

SPES, acronym of *Selective Production of Exotic Species*, is a CW radioactive ion beam facility under construction at LNL INFN in Italy. It will produce and accelerate neutron-rich radioactive ions, in order to perform nuclear physics experiments, which will require beams above Coulomb barrier.

The main functional steps of the facility are shown in Fig.1, namely the primary beam from the cyclotron, the beam from the fission target (up to  $10^{13}$  fission/second), the beam cooler, the spectrometers, the charge breeder and the accelerator, the existing ALPI with a new RFQ injector.

The use of the continuous beam from the +1 source (LIS, PIS, SIS) maximizes the RNB efficiency but needs a CW post accelerator (RFQ and ALPI); this layout also needs a charge breeder chosen to be an ECR that works in continuous.

The energy on the transfer lines are determined by the chosen RFQ input energy ( $w_{RFQ}=5.7$  keV/u); namely, all the devices where the beam is approximately stopped (production target, charge breeder and RFQ cooler) lay at a voltage:

$$eV = (A/q)w_{RFQ} \quad (1)$$

The charge state range ( $3.5 \leq A/q \leq 7$ ) is bounded by the RFQ field level for the upper limit and by the minimum voltage on  $q=1$  transport line (overall space charge from the source and contaminants separations).

The beam preparation scheme satisfies various requirements:

1. the zone with worst radiation protection issues is reduced by means of the first isobar selection (resolution  $R=1/200$ ).
2. after that with an RFQ cooler the beam energy spread and transverse emittance are reduced both for further separation and to cope with the charge breeder acceptance (about 5 eV).
3. HRMS and MRMS (high and medium resolution mass spectrometers,  $R=1/40000$  and  $R=1/1000$  respectively) are used to select the RNB (with good transmission) and to suppress the contaminants from the charge breeder source.
4. Both the HRMS and the MRMS are installed on a negative voltage platform, to decrease the beam geometrical emittance, the relative energy spread and to keep the dipole field in a manageable range ( $>0.1$  T).
5. The 7 m long RFQ has an internal bunching and relatively high output energy; this eases the setting and allows 90% transmission into ALPI longitudinal acceptance (constraint deriving from quite long ALPI period, 4 m).
6. An external 5 MHz buncher before the RFQ will be available for specific experiments.
7. The dispersion function is carefully managed in the various transport lines; where possible the transport is achromatic, otherwise the dispersion is kept low (in particular at RFQ input  $D=0$ ,  $D'$  is about 50 rad).

### Radiation Containment

RIB facilities require special radiation protection. The SPES building itself is designed in order to reduce the radiation exposure. From the beam dynamic design point of view, the separation of the nominal beam from its contaminants (nA nominal current respect to  $\mu$ A contaminants) in safety areas is mandatory. In this perspective, the low separation stage is placed inside radiation containment walls (see Fig. 2); at the same time such boundary conditions impose restrictions on the beam dynamics design.

As far as the HRMS is concerned, it is important to clean the nominal species from contaminants in order to reduce radioactive species implantation inside the CB.

## BEAM PHYSICS CHALLENGES IN RAON\*

Ji-Ho Jang, Dong-O Jeon<sup>#</sup>, Hyojae Jang, Hyung Jin Kim, Ilkyoung Shin, IBS, Daejeon, Korea  
 Ji-Gwang Hwang, Eun-San Kim, KNU, Daegu, Korea

### Abstract

Construction of the RAON heavy ion accelerator facility is under way in Korea. As high intensity 400 kW superconducting linac (SCL) is employed as a driver, beam physics aspects are carefully studied. The SCL is based on lattice consisting of cryomodules and quadrupole doublets. Beam dynamics studies for the RAON has progressed to cover start-to-end simulations and machine imperfection studies confirming beam loss less than 1 W/m. At present, prototyping of major components are proceeding including 28 GHz ECR ion source, RFQ, superconducting cavities, magnets and cryomodules. First article of prototype superconducting cavities have been delivered that were fabricated through domestic vendors. Prototype HTS quadrupole is under development. Progress report of the RAON accelerator systems is presented.

### INTRODUCTION

The RISP (Rare Isotope Science Project) is developing a heavy ion accelerator called RAON, and experimental facilities. One of the characteristics of RAON facility is that it will be able to supply RI beams with both IF (In-flight Fragmentation) and ISOL (Isotope Separator On-Line) methods [1,2]. The layout of the facility is given in Fig. 1.

The RAON consists of a driver linac and a post linear accelerator. The driver linac includes an injector of an ECR ion source, an RFQ, and a SCL (superconducting linac) called SCL1 and SCL2 which are separated by a 90° charge selection section. It can accelerate uranium beams up to 200 MeV/u and proton beams up to 600 MeV as summarized in Table 1. The stable ion beams with beam power up to 400 kW are delivered to the IF target and various experimental areas. The post linac is used to accelerate RI beams which are generated by the ISOL facility. A cyclotron delivers 1 mA 70 MeV proton beams to the ISOL target. The cyclotron has dual extraction ports with thin carbon foils for charge exchange extraction of H<sup>-</sup> beam. The rare isotope beams generated by the ISOL system is accelerated by a chain of post accelerators including RFQ and another superconducting linac, SCL3. The RI beams can be delivered into the low energy experimental hall or can be injected through P2DT to the SCL2 in order to accelerate to higher energy.

Construction of the RAON heavy ion accelerator facility started on December 2011. The design of the accelerator systems has progressed, and prototyping of critical components and systems have been materialized.

In this paper, the status of the RAON accelerator systems is presented along with beam dynamics design and prototyping progress.

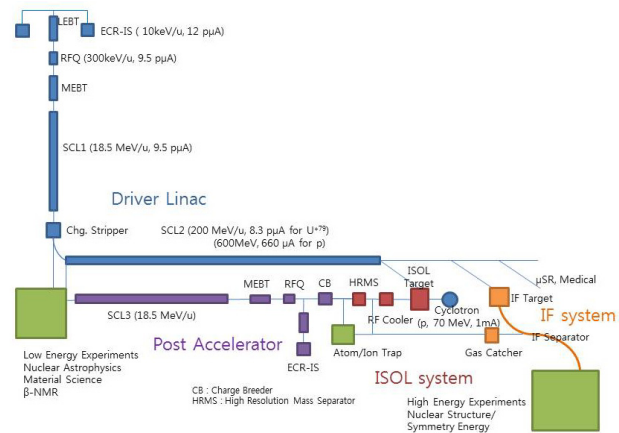


Figure 1: Layout of RAON Linac.

Table 1: Beam Specification for the Driver Linac

Parameters	H <sup>+</sup>	O <sup>8+</sup>	Xe <sup>54+</sup>	U <sup>79+</sup>
Energy [MeV/u]	600	320	251	200
Current [pμA]	660	78	11	8.3
Power on target [kW]	>400	400	400	400

### DRIVER LINAC

#### Injector

The injector of RAON driver linac consists of a 28 GHz ECR ion source, an LEBT (Low Energy Beam Transport), a 500 keV/u RFQ (Radio-Frequency Quadrupole), and a MEBT (Medium Energy Beam Transport) [1, 3].

The two-charge-state (33 and 34) uranium beams are injected into the RFQ in order to achieve the required beam power of 400 kW at the IF target. The electrostatic quadrupoles are used to focus the two charge state beams. We considered a multi-harmonic buncher and a velocity equalizer for reducing the longitudinal rms beam emittance. The beam envelope in the LEBT is shown in

\*Work supported by Ministry of Science, ICT and Future Planning

<sup>#</sup>jeond@ibs.re.kr

# BEAM DYNAMICS STUDIES FOR THE FACILITY FOR RARE ISOTOPE BEAMS DRIVER LINAC\*

M. Ikegami<sup>†</sup>, Z. He, S.M. Lidia, Z. Liu, S.M. Lund, F. Marti, E. Pozdeyev, J. Wei, Y. Yamazaki, Q. Zhao, Y. Zhang, Facility for Rare Isotope Beams, Michigan State University, MI 48824, USA

## Abstract

The Facility for Rare Isotope Beams (FRIB) is a high-power heavy ion accelerator facility presently under construction at Michigan State University to support nuclear physics. FRIB consists of a driver linac and experimental facility, and the linac accelerates all stable ions including uranium to kinetic energies of more than 200 MeV/u and continuous wave beam power up to 400 kW. This beam power is more than two orders of magnitude higher than the existing heavy ion linac facilities, resulting in various beam dynamics challenges for the driver linac. In this paper, we review these challenges for the FRIB driver linac and undergoing studies to address them.

## INTRODUCTION

The Facility for Rare Isotope Beams (FRIB) is a high-power heavy ion accelerator facility now under construction at Michigan State University under a cooperative agreement with the US DOE [1]. Its driver linac operates in CW (Continuous Wave) mode and accelerates all stable ions to kinetic energies above 200 MeV/u with the beam power on target up to 400 kW. This novel facility is designed to accelerate and control multiple ion species simultaneously to enhance beam power. The linac has a folded layout as shown in Fig. 1, which consists of a front-end, three Linac Segments (LSs) connected with two Folding Segments (FSs), and a Beam Delivery System (BDS) to deliver the accelerated beam to the production target. The front-end consists of two ECR (Electron Cyclotron Resonance) ion sources, a normal conducting CW RFQ (Radio Frequency Quadrupole), and beam transport lines to separate, collimate, and bunch the multiple ion charge states emerging from the ECR sources. Ion sources are located on the ground level (not shown in Fig. 1) and an extracted beam from one of two ion sources is delivered to the linac tunnel through a vertical beam drop. In the FRIB driver linac, superconducting RF cavities are extensively employed.

After acceleration up to 0.5 MeV/u with a normal conducting RFQ, ions are accelerated with superconducting QWRs (Quarter Wave Resonators) and HWRs (Half Wave Resonators) to above 200 MeV/u. There are two types each for QWRs ( $\beta = 0.041$  and  $0.085$ ) and HWRs ( $\beta = 0.29$  and  $0.53$ ). The frequency and aperture diameter for QWRs are 80.5 MHz and 36 mm respectively, and those for HWRs are 322 MHz and 40 mm respectively. We have three  $\beta = 0.041$  cryomodules with four cavities each and 11  $\beta = 0.085$  cryomodules with eight cavities each in LS1 (Linac Segment 1). We have 12  $\beta = 0.29$  cryomodules with four cavities each and 12  $\beta = 0.53$  cryomodules with six cavities each in LS2 (Linac Segment 2). There are 6  $\beta = 0.53$  cryomodules followed by a space to add cryomodules for future upgrade. The total number of superconducting RF cavities is 330 including those for longitudinal matching in the Folding Segments. Transverse focusing in the superconducting linac sections is provided by superconducting solenoids (8 Tesla, 20 mm bore radius). It is unique to have such large scale linac sections with low- $\beta$  superconducting RF cavities together with multi-species transport at high CW power. This poses beam dynamics challenges specific to the FRIB driver linac.

In addition to realizing high CW beam power, stringent beam-on-target requirements are imposed for the FRIB driver linac to support novel experimental program in nuclear physics. It is of essential importance at these high power levels to control and mitigate beam losses to avoid damage and excessive radio-activation of accelerator components. Detection of beam losses and halo collimation are major elements of beam loss mitigation, both of which requires careful beam dynamics considerations in their design.

In this paper, beam dynamics studies now under way in support of the FRIB driver linac are reviewed. We briefly outline five major areas and their particular challenges.

## SPACE-CHARGE EFFECTS AT LOW ENERGY FRONT-END

While the FRIB driver linac is at the frontier of CW power, its space-charge intensity is modest as high average beam power is realized by CW operation. Due to this modest intensity, space-charge effects are negligible for most of the FRIB driver linac. The exception to this is in the front-end where the beam kinetic energy is low. Space-charge effects are especially important for beam transport between the ECR ion source and the first bending magnet for charge selection. Species with unwanted charge states are transported together with the (typically) two desired species in this section. This increases space-charge intensity by a factor of 15 (typical).

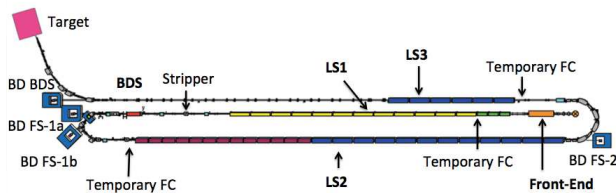


Figure 1: Schematic layout for the FRIB driver linac.

\* Work supported by the U.S. Department of Energy Office of Science under Cooperative Agreement DE-SC0000661.

<sup>†</sup> ikegami@frib.msu.edu

# INSTABILITIES AND SPACE CHARGE\*

M. Blaskiewicz<sup>†</sup>, K. Mernick  
BNL, Upton, NY 11973, USA

## Abstract

The coherent stability problem for proton and heavy ion beams is reviewed. For all but the highest energies space charge is the dominant coherent force. While space charge alone appear benign its interaction with other impedances is less clear. The main assumptions used in calculations and their justifications will be reviewed. Transverse beam transfer function data from RHIC will be used to compare theory and experiment and some pitfalls will be discussed.

## MODELING THE TRANSVERSE FORCE

The effect of space charge on longitudinal instabilities goes back to early work on the negative mass instability [1]. Early work on coasting beam transverse instabilities included the effect of space charge as well [2]. Both these treatments used a leading order approximation with a longitudinal force proportional to the derivative of the instantaneous current and a transverse force

$$F_x = \kappa I(\tau)[x - \bar{x}(\tau, t)] \quad (1)$$

where  $\tau$  is the particle arrival time with respect to the synchronous particle,  $t$  is time,  $I(\tau)$  is the instantaneous current,  $x$  is the transverse coordinate and  $\bar{x}(\tau, t)$  is the transverse centroid position as a function of longitudinal coordinate and time. The constant  $\kappa$  depends on the beam radius. There are several assumptions [3]:

1. The fields are electrostatic in the comoving frame.
2. The wavelength of perturbations in the comoving frame are long compared to the beam radius.
3. The unperturbed transverse distribution is KV, resulting in a constant density within the beam at a given  $\tau$ .
4. First order perturbation theory is used.
5. The fields due to boundary conditions are neglected.

For small perturbations the nonlinearities due to images do not depend on the beam dynamics and will be subsumed in a generic octupolar force. For direct space charge actual beams are generally not KV and the accuracy of Eq. (1) has been studied in [4–8] within the context of coasting beams. It was found that the nonlinearity due to direct space charge is relevant only when other forms of damping are present. Space charge enhances damping due to lattice nonlinearity if the betatron tune increases with betatron amplitude. Changing the sign results in less damping than without space charge. The tune shift with amplitude due to short strong quadrupoles has the right sign and works in both planes [9].

Figures 1 and 2 show threshold diagrams where  $\Delta Q_0$  is the complex tune shift an undamped beam would have.

\* Work performed under the auspices of the United States Department of Energy

<sup>†</sup> blaskiewicz@bnl.gov

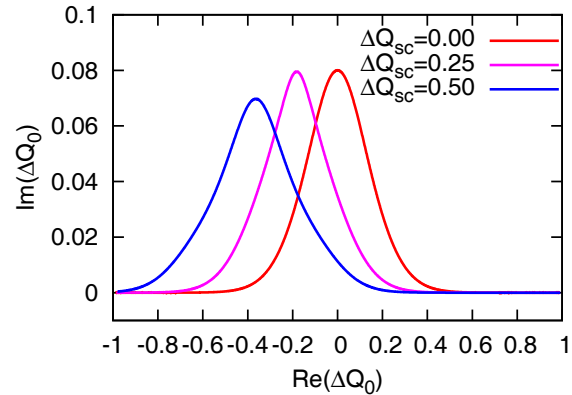


Figure 1: Threshold diagrams for tune spread due to chromatic tune spread with space charge. Average space tune shifts are quoted and the rms chromatic tune spread is 0.1.

Stable tune shifts for damped beams are below the curves. The unperturbed transverse action distribution is  $F_0(J) = (3/J_0)(1 - J/J_0)^2$  and space charge is modeled as an inter-particle force containing linear and cubic terms [3]. The ratio of the tune spread to the average tune shift matches that for a round gaussian beam. These solutions are for one dimensional motion and the expression for the threshold impedance as a function of coherent beam tune is a rational function of three different dispersion integrals [5][Eq. (31)]. As is clear from the plots these effects are important if true and we go on to test them with particle tracking.

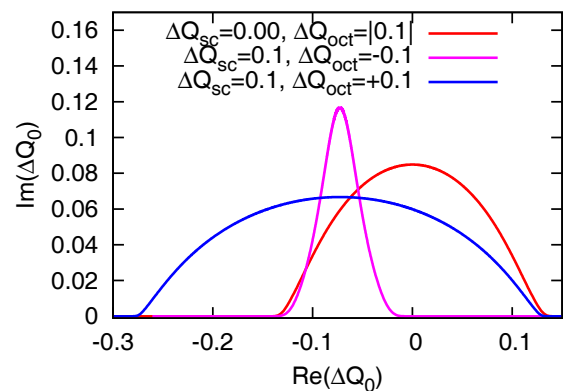


Figure 2: Threshold diagrams for tune spread due to octupoles with space charge. Average space charge and octupolar tune shifts are quoted and a chromatic tune spread of 0.01 is also included.

When both transverse dimensions are included and the space charge is modeled more accurately, certain forms of

# THRESHOLDS OF THE HEAD-TAIL INSTABILITY IN BUNCHES WITH SPACE CHARGE

V. Kornilov, O.Boine-Frankenheim, GSI Darmstadt, and TU Darmstadt, Germany  
C. Warsop, D. Adams, B. Jones, B.G. Pine, R. Williamson, STFC/RAL/ISIS, Oxfordshire, UK

## INTRODUCTION

Head-tail instabilities are expected to be one of the main limitations of the high-intensity operation in the future SIS100 synchrotron of the FAIR facility [1], especially for the heavy-ion bunches [2]. This instability is already beginning to limit the operation at the highest intensities in the ISIS spallation neutron source [3] at the Rutherford Appleton Laboratory in the UK. General ISIS bunch parameters, especially the space-charge conditions, are similar to the expected heavy-ion beams in SIS100, thus it might be possible to use the physical insight and the experience from the ISIS studies for anticipating the transverse stability in the SIS100 high-intensity bunches. Of particular interest is the dependence of unstable beam modes on the configuration of the RF system (single or dual harmonic), the influence of high space charge levels, the key role of the betatron tune and the determination of driving beam impedances.

## OBSERVATIONS IN ISIS

A dedicated experimental campaign of three shifts has been performed at the ISIS synchrotron in November 2013, with the primary goal to understand more about the fast losses and associated vertical oscillations around 2 ms of the ISIS cycle, see Fig. 1. These losses are a concern for the high-intensity operation and have been usually attributed to head-tail instabilities. In standard ISIS operation, a 2RF system is used. In order to be able to compare with classical theories, and to simplify the first comparisons with simulations, the most of the study was made with the 1RF ( $h = 2$ ) operation. Approximately one-third of the measurements were done with different types of 2RF ( $h = 2, 4$ ).

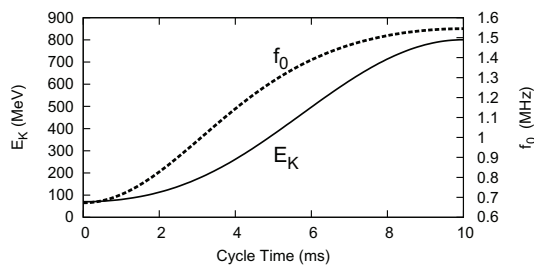


Figure 1: ISIS cycle: the proton kinetic energy (solid line) and the revolution frequency (dashed line),  $C = 163.26$  m.

According to the experience at ISIS [4–6], the instability appears if the vertical tune is set closer to integer from below. The normal tune ramp at ISIS applies  $Q_v = 3.85$  at 0 ms decreasing to  $Q_v = 3.68$  at 10 ms, with  $Q_v = 3.758$  at 2 ms. In order to focus on the operation-type instabil-

ISBN 978-3-95450-173-1

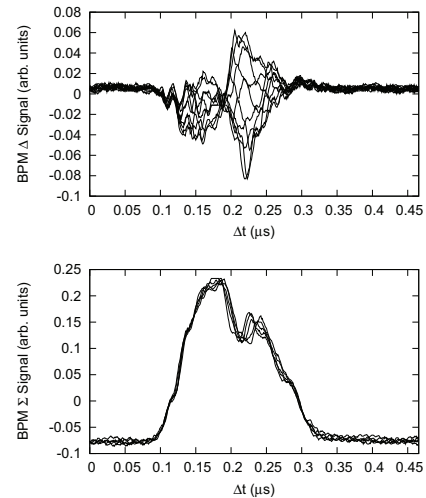


Figure 2: Consecutive bunch traces from the vertical BPM delta (top) and sum (bottom) signal of a typical instability for a 1RF bunch around Cycle Time 2 ms.

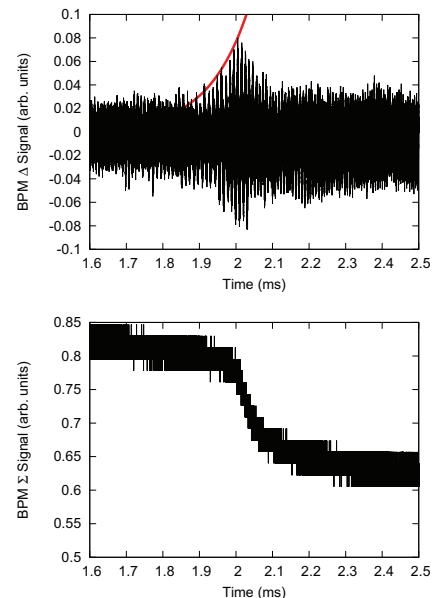


Figure 3: Time evolution of the BPM delta (top) and sum (bottom) signal for the instability from Fig. 2. The red line is an exponential with the growth time  $\tau = 0.1$  ms.

ity, we have pushed the vertical tune higher around 2 ms cycle time. Once tune reaches  $Q_v \approx 3.86$ , reproducible strong losses and vertical collective oscillations appear. Figures 2, 3 present typical BPM signals around 2 ms. The overlaid bunch traces in Fig. 2 show a standing wave pattern

## UPGRADE OF THE UNILAC FOR FAIR

L. Groening, A. Adonin, X. Du, R. Hollinger, S. Mickat, A. Orzhekhovskaya, B. Schlitt, G. Schreiber, H. Vormann, C. Xiao, GSI, D-64291 Darmstadt, Germany  
 H. Hähnel, R. Tiede, U. Ratzinger, Goethe University of Frankfurt, D-60438 Frankfurt, Germany

### Abstract

The UNiversal Linear Accelerator (UNILAC) at GSI has served as injector for all ion species from protons to uranium for the past four decades. Especially its 108 MHz Alvarez type DTL providing acceleration from 1.4 MeV/u to 11.4 MeV/u has suffered from material fatigue. The DTL will be replaced by a completely new section with almost the same design parameters, i.e. pulsed current of up to 15 mA of  $^{238}\text{U}^{28+}$  at 11.4 MeV/u. However, operation will be restricted to low beam duty cycles as 200  $\mu\text{s}$  at 10 Hz. Since preservation of beam quality is mandatory, a regular focusing lattice, as along an Alvarez section for instance, is aimed for. A new source terminal & LEBT dedicated to operation with  $^{238}\text{U}^{4+}$  is under design. The uranium sources need to be upgraded in order to provide increased beam brilliances and for operation at 2.7 Hz. Revision of the subsequent 36 MHz RFQ electrode design has started as well as the layout activities of the section providing transition from the 36 MHz section to the 108 MHz DTL.

### INTRODUCTION

GSI is currently constructing the Facility for Ion and Antiproton Research (FAIR). It aims at provision of  $4 \times 10^{11}$  uranium ions at 1.5 GeV/u [1]. As injector for FAIR serves the existing UNiversal Linear ACcelerator UNILAC (Fig. 1) together with the subsequent synchrotron SIS18. The UNI-

entrance. Transverse focusing is provided through three internal triplets per cavity. The IH-cavities operate at 36 MHz and provide acceleration to 1.4 MeV/u. Alternatively, an ECR source followed by an RFQ and one IH-cavity operated at 108 MHz can provide ions with 1.4 MeV/u as well. The 36 MHz pre-stripper DTL is followed by a stripping section, where the ion beam is intercepted by a gaseous jet of nitrogen for increase of the charge state. For instance uranium is stripped from the charge state 4+ to the charge state 28+. The subsequent post-stripper DTL comprises five Alvarez type cavities for acceleration to 11.4 MeV/u being the injection energy required by the synchrotron SIS18. The UNILAC has a high flexibility in its 50 Hz operation. Several virtual accelerators can be operated, all differing wrt to the beam they deliver, i.e. ion species, energy, pulse length, and repetition rate.

This DTL was designed in the late 1960ies and it is in operation for 40 years now. The cavities suffered from considerable material fatigue. Sparking damaged the copper surface. Especially, fast changes of the rf-duty cycles and rf-amplitudes from switching between different virtual accelerators caused rf-sparking. As a consequence, the last years saw limitations in the rf-amplitudes that could be set to the tanks. This manifested in degradation of beam quality of heaviest ions as  $^{238}\text{U}^{28+}$ . Additionally, the beam dynamics design did not foresee provision of intense beams, which are prone to space charge effects. The beam design parameters of the UNILAC are listed in Table 1. The age of the

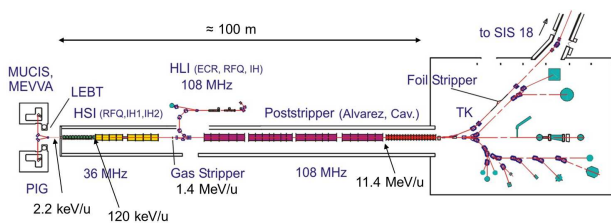


Figure 1: The UNiversal Linear ACcelerator (UNILAC) at GSI.

LAC comprises three ion source terminals. Two of them provide beams at 2.2 keV/u which are injected into an RFQ and are accelerated to 120 keV/u. It is followed by a MEPT comprising a doublet and a super lens, i.e. a 1m long RFQ that just provides longitudinal and transverse focusing without acceleration. The MEPT matches the beam into an IH-DTL. This DTL comprises 2 IH-cavities which apply the KONUS accelerating scheme [2], i.e. the design rf-phase slips from positive to negative phases. This technique allows for high effective shunt impedance and less transverse defocusing. But it provides less longitudinal focusing and requires very accurate longitudinal matching to the DTL

Table 1: Beam Design Parameters for the Upgraded UNILAC

Ion A/q	$\leq 8.5$	
Beam Current (low duty cycle)	128-q/A	emA
Beam Current	$\approx 500$ -q/A	$\mu\text{A}$
Input Beam Energy	1.4	MeV/u
Output Beam Energy	11.4	MeV/u
Output Emit. (norm., tot.) hor/ver	0.8/2.5	mm mrad
Beam Pulse Length	$\leq 5000$	$\mu\text{s}$
Beam Repetition Rate	$\leq 50$	Hz
Rf Frequency	108.408	MHz

UNILAC together with the requirement to provide reliable and intense beams for the upcoming FAIR era calls for a revision of the UNILAC, especially its post-stripper DTL. The following section will describe the envisaged upgrade measures.

# CODE REQUIREMENTS FOR LONG-TERM TRACKING WITH SPACE CHARGE

H. Bartosik, E. Benedetto, M. Bodendorfer, V. Forte, S. Gilardoni, N. Hoimyr, A. Huschauer, M.A. Kowalska, M. Martini, E. Metral, A. Oeftiger, B. Panzer-Steindel, F. Schmidt\*, E.G. Souza, M. Titze, R. Wasef, CERN, Switzerland; J. Amundson, V. Kapin, L. Michelotti, E. Stern, Fermilab, USA; S.M. Cousineau, J. Holmes, A.P. Shishlo, SNS, USA; G. Franchetti, GSI, Germany; S. Machida, RAL, UK; C. Montag, BNL, USA; J. Qiang, LBNL, USA

## Abstract

In view of the LHC Injectors Upgrade (LIU) program of the LHC pre-accelerators LEIR [1], PSB [2], PS [3] and SPS [4] we have started a new working group at CERN to deal with space charge issues of these machines. The goal is to operate with basically twice the number of particles per bunch which will further increase the space charge tune shifts which presently are already large. Besides obvious remedies like increasing the injection energy we are obliged to better understand the space charge force to optimize our machines. To this end it has become clear that we need computer models that faithfully represent the linear but also the non-linear features of our machines. We have started close collaborations with several laboratories around the world to upgrade existing self-consistent space charge Particle-In-Cell (PIC) codes for our CERN needs. In parallel we have created a frozen space charge facility in CERN's MAD-X code. Both types of codes are being used to study long-term stability and to compare it with machine experiments.

## INTRODUCTION

It has been realized in 2011 that at CERN a concerted effort was needed to study the space charge (SC) effects in the pre-accelerators of the LHC in view of achieving a two-fold increase of beam intensity needed to fulfill the goals of the LIU project. To this end a SC working group has been established to build a new team of competence in the field of space charge effects at CERN. Students and staff members have been won to study the 4 circular machines LEIR, PSB, PS and SPS both with experiments and simulations. In the meantime there is also a team to study SC effects in more general terms.

In regular meetings [5] the machine related SC issues are being discussed but also an educational series of talks has been started given by experts from inside CERN and other laboratories.

From the beginning it has been clear that one need to know well the non-linear dynamics in conjunction with SC forces to allow for a full understanding of emittance growth and losses in any of the machines. Expertise is required in both regimes and also a close collaboration with magnet experts is mandatory to get a good modeling and measurements of critical magnets in the rings.

\* Speaking as the representative of the CERN Space Charge working group

The codes would need to be adapted towards an adequate treatment of both the non-linear machine models and SC. A decision has been made to invest into existing codes and adapt them to CERN needs, unless we could modify CERN codes with moderate effort. Essential is that any code would have to pass a rigorous benchmarking test before the code results could actually be trusted. Ease of use, flexible structure and computing performance are further critical issues for the LIU studies. Last and not least a code benchmarking with machine experiments is the ultimate way to give us confidence that the whole chain from magnet modeling, the codes and the experimental data taking are all sufficiently well prepared and mastered so that the machines can be understood well enough to minimize the combined effect of machine non-linearities and SC.

Intense collaborations have been initiated around the world and we have started series of workshops [6]<sup>1</sup> and collaboration meetings [7]<sup>2</sup> to make progress on the open issues in the theoretical understanding and program development.

This report is based on the outcome of those two meetings and an outlook is given for the next steps. We concentrate here on CERN machines where presently there is a high demand for SC studies. Many of these discussed issues should be of wider interest to the SC community as a whole.

We have added an Appendix about CERN's new method to create perfectly matched 6D distribution that hasn't been discussed anywhere before.

## CODES

In the SC field there are basically two classes of codes: on the one hand there are the self-consistent PIC codes with 2D, 2.5D and 3D SC treatment. These codes are most relevant over a short period at the beginning of injection when the coherent SC are largest, the fields may be time dependent and the dynamics are most complex. Despite these advantages the codes tend to be slow and the results suffer from PIC noise. On the other hand frozen SC codes are being used over longer time ranges and when non-linear resonances play a decisive role in conjunction with SC. These second type of codes perform much better due to a much simpler 2D treatment of SC and they do not suffer from PIC noise. It remains to be fully understood when either approach is truly required and how one might combine them. To this

<sup>1</sup> sponsored by ICFA

<sup>2</sup> both co-sponsored by EuCARD-2 XBEAM

# STATUS OF PY-ORBIT: BENCHMARKING AND NOISE CONTROL IN PIC CODES \*

J.A. Holmes, S. Cousineau, A. Shishlo, Oak Ridge National Laboratory, Oak Ridge, TN, USA

## Abstract

PY-ORBIT is a broad collection of accelerator beam dynamics simulation models, written primarily in C++, but accessed by the user through Python scripts. PY-ORBIT was conceived as a modernization, standardization, and architectural improvement of ORBIT, a beam dynamics code designed primarily for rings. Although this goal has been substantially achieved, PY-ORBIT has additional capabilities. A major consideration in high intensity beam dynamics codes, such as PY-ORBIT and ORBIT, is the simulation of space charge effects. Computational space charge simulation is, of necessity, accompanied by noise due to discretization errors, which can compromise results over long time scales. Discretization errors occur due to finite step sizes between space charge kicks, due to graininess of the numerical space charge distribution, and due to the effects of spatial grids embedded in certain solvers. Most tracking codes use space charge solvers containing some or all of these effects. We consider the manifestation of discretization effects in different types of space charge solvers with the object of long time scale space charge simulation.

## PY-ORBIT

PY-ORBIT [1] is a collection of computational beam dynamics models for accelerators, designed to work together in a common framework. It was started [2] as a “friendly” version of the ORBIT Code [3], written using publicly available supported software. Users run the code using Python scripts and the higher-level routines are in Python. The computationally intensive portions are written in C++, except for the Polymorphic Tracking Code, PTC [4], which is linked to PY-ORBIT and written in Fortran. The C++ routines and PTC are wrapped to make them available at the Python level. PY-ORBIT accommodates multiprocessing through MPI. The only additional software required by PY-ORBIT is the FFTW fast Fourier transform library [5]. The code is finding an increasing number of users and the source code is publicly available via Google Codes [1]. It is not difficult for users to develop extensions to PY-ORBIT, and it is possible for users to obtain permission to add new routines to the publicly available code. Recently, researchers at CERN and at GSI have added new methods to PY-ORBIT.

At present, PY-ORBIT is capable of performing most calculations that ORBIT does for rings and transfer lines. Many of the most widely used methods in ORBIT have been ported to PY-ORBIT and benchmarked. Single

particle tracking methods include ORBIT’s native symplectic tracker, PTC tracking, and a 3D field tracker. It is planned to add the option to use linear and second order tracking by matrices from the MAD codes [6,7]. Space charge models include ORBIT’s longitudinal, 2D potential and direct force methods, a full 3D (not parallel) solver, and uniform charge density 3D ellipses. A 2.5D solver has recently been added and tested by Hannes Bartosik of CERN. ORBIT’s longitudinal impedance model has also been ported to PY-ORBIT, and we are now in the process of porting the transverse impedance model. Other methods that have been ported from ORBIT include injection, foil and painting, RF cavities, collimation, apertures, and many diagnostics.

Some capabilities have been developed in PY-ORBIT that are not included in the original ORBIT code. Routines have been developed for linac modeling, including RF cavities, magnets, and 3D full Particle-in-Cell (PIC) and elliptical space charge models. A detailed set of atomic physics routines has been developed for laser stripping applications, and special maps have been developed for nonlinear optics studies. One ORBIT code package that has not been ported to PY-ORBIT is the self-consistent electron cloud model.

Detailed documentation of PY-ORBIT is, at best, incomplete. In the downloaded source code there are many examples that demonstrate the use of models in scripts. Some of the methods are documented in Google Code wikis. When in doubt, the user is advised to contact one of the developers for detailed answers. Finally, some of the nice features of PY-ORBIT come from the flexibility of Python. For example, the bunch class is extendable. The basic bunch contains only the 6D coordinates of each macroparticle. It is easy, however, for the user to add various properties, such as a particle index, spin, species, ionization number, excited state, etc. Because of this flexibility, it is easy and convenient to work with PY-ORBIT.

## SPACE CHARGE MODELING OVER LONG TIMES

Particle-tracking simulations for accelerators involve following particle distributions over time. Space charge physics has been successfully incorporated into particle-tracking studies of linacs, transfer lines, accumulator rings, and rapid cycling synchrotrons (RCS). These space charge models have allowed the successful simulation of phenomena that would have been impossible otherwise. Even so, the evaluation of space charge effects is typically

\* ORNL/SNS is managed by UT-Battelle, LLC, for the U.S. Department of Energy under contract DE-AC05-00OR22725.

# ARTIFICIAL NOISE IN PIC CODES AND CONSEQUENCES ON LONG TERM TRACKING

Kazuhiro Ohmi, KEK

## Abstract

Emittance growth and beam loss due to nonlinear space charge force has been studied using Particle In Cell simulation. Artificial noise due to macro-particle statistics sometimes presents unphysical emittance growth. Artificial noise in Particle In Cell method disturbs the accurate prediction of the emittance growth. Using a fixed periodic space charge potential is one way to study emittance growth in a first step. Frozen potential and induced resonance are discussed in this paper. While emittance growth in a presence of real noise is a serious issue in accelerators. Emittance growth under tune fluctuation is discussed with relation to studies in beam-beam effects.

## INTRODUCTION

In Particle In Cell codes, space charge force is given by solving Poisson equation for macro-particles distribution mapped on grid space. Statistics of macro-particles, which cause a density modulation in the grid space, result in turn by turn fluctuation of the space charge force. Emittance conservation/growth in a periodic system is subject of our concern for the space charge effects. Artificial emittance growth caused by the fluctuation disturbs an accurate prediction, especially in long term simulation. Emittance growth in a fixed periodic potential can be discussed. In J-PARC, limitation of particle loss is very severe (1kW for the beam energy 1MW). Space charge potential is nearly determined by the core distribution. We can study emittance growth in the potential given by distribution which is initial or is fixed(frozen) at a time. Resonance and chaotic behavior in the fixed potential are subjects to be studied. It is important to study emittance growth dynamically changing potential for the next step.

Figure 1 shows evolution of  $x$  and  $\sigma_x$  in PIC simulation (SCTR) [1]. The space charge force is calculated turn-by-turn, where the number of macro-particle is 200,000. Fluctuations in  $x$  and  $\sigma_x$  are seen. The noise level is  $\langle x \rangle \approx \pm 0.05$  mm ( $0.5\% \sigma_{x,0}$ ) and  $\sigma_x \approx 8.5 \pm 0.02$  mm ( $0.2\% \sigma_{x,0}$ ). Higher order moments of the beam distribution must have similar fluctuation. Each particle experiences nonlinear force with the fluctuations in the simulation. Unphysical phenomena is seen in the simulation.

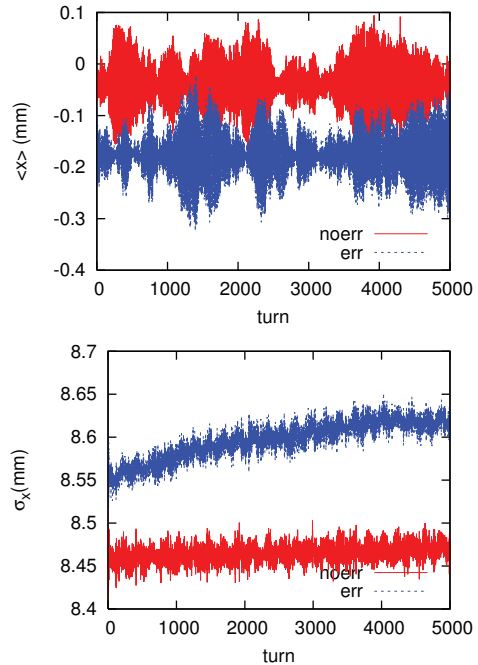


Figure 1: Evolution of  $x$  and  $\sigma_x$  in Particle-In-Cell simulation (SCTR). Red and blue lines are given for lattice without and with magnet alignment errors.

## EXPERIENCES OF BEAM-BEAM INTERACTIONS IN COLLIDERS AND APPLICATION TO SPACE CHARGE EFFECTS

### *Experiences of Beam-beam Interactions in Colliders*

Statistical noise in simulations is artifact, but noise in accelerator is sometimes a real issue. Noise of collision offset from bunch-by-bunch feedback system degraded luminosity performance in KEKB [2]. Crab cavity is planned to be used in High Luminosity LHC. Noise in crab cavity phase and in bunch-by-bunch feedback system, which causes collision offset, has been studied in LHC [1, 3]. Theory for the noise effects was developed by G. Stupakov [4] and T. Sen et al.[5].

Potential (effective Hamiltonian) of the beam-beam interaction is expressed by

$$U(x) = \frac{N_p r_p}{\gamma_p} \int_0^\infty \frac{1 - e^{-x^2/(2\sigma_r^2+q)}}{2\sigma_r^2 + q} dq \delta_P(s) \quad (1)$$

ISBN 978-3-95450-173-1

# INSTRUMENTATION DESIGN AND CHALLENGES AT FRIB\*

S. Lidia<sup>#</sup>, Facility for Rare Isotope Beams, Michigan State University, East Lansing, MI, USA

## Abstract

The Facility for Rare Isotope Beams (FRIB) will use a superconducting linear accelerator to extend the heavy ion intensity frontier for ion species from protons to uranium. The unique design of the twice-folded linac, coupled with the 5 orders of range of beam intensities present new challenges for instrumentation, and machine protection systems. Multi-charge state beams in the low energy linac and dispersive arc regions add complexity to instrumentation systems used for longitudinal tuning and transverse orbit optimization. Beam loss monitoring systems must distinguish losses from the three parallel linac segments sharing the same enclosure. Finally, quick response to abnormal conditions is required to prevent catastrophic damage to beam line components from the high power, heavy ion beams. We present an overview of beam diagnostic systems and detection networks required for the safe tuning, operation, and maintenance of FRIB.

## FRIB FACILITY OVERVIEW

Facility for Rare Isotope Beams (FRIB) is a high-power, high-brightness, heavy ion facility under construction at Michigan State University under cooperative agreement with the US DOE [1]. The linac will accelerate ions to energies above 200 MeV/u, with up to 400 kW of beam power on target. The linac facility, shown in Fig. 1, consists of a Front End, three Linac Segments (LSs) connected by two Folding Segments (FSs), and a Beam Delivery System (BDS) leading to the production target [2].

The front-end consists of two ECR (Electron Cyclotron Resonance) ion sources, a normal conducting CW (continuous wave) RFQ (Radio Frequency Quadrupole) linac, and beam transport lattices. Ion sources are located

on the ground level and beam from one of two ion sources is delivered to the linac tunnel through a vertical beam drop. An electrostatic chopper upstream of the vertical beam drop is the primary control of the time structure and duty cycle of the ion beam. A multi-harmonic buncher (MHB) precedes the RFQ and impresses the initial 80.5 MHz RF time structure on the beam. The front end is shown schematically in Fig. 2.

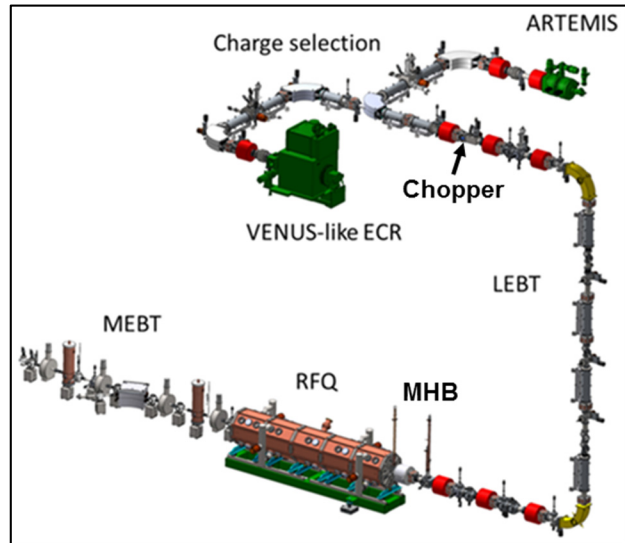


Figure 2: Front end schematic layout.

This paper will first discuss the requirements and specifications of the beam instrumentation systems necessary for FRIB commissioning and operation. Then specific challenges and issues will be presented, along with proposed solutions, which arise from the unique design and operation of this facility.

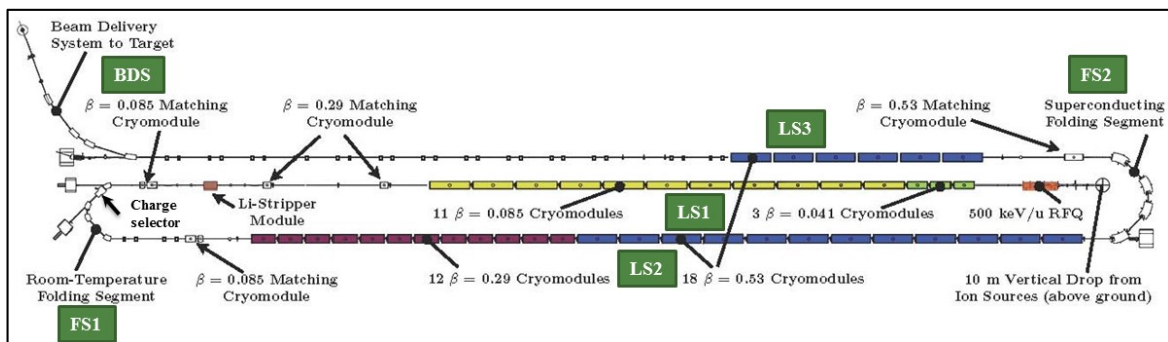


Figure 1: FRIB drive linac schematic layout.

## OVERVIEW OF BEAM DIAGNOSTIC INSTRUMENTATION

The suite of beam instrumentation systems is designed to facilitate initial commissioning and tuning activities

\*This material is based upon work supported by the U.S. Department of Energy Office of Science under Cooperative Agreement DE-SC0000661, the State of Michigan and Michigan State University.  
#lidia@frib.msu.edu

# BEAM LOSS MECHANISMS, MEASUREMENTS AND SIMULATIONS AT THE LHC (QUENCH TESTS)

M. Sapinski, CERN, Geneva, Switzerland

## Abstract

Monitoring and minimization of beam losses is increasingly important for high-intensity and superconducting machines. In the case of the LHC, the collimation system is designed to absorb the energy of lost particles and confine the main multi-turn losses to regions without sensitive equipment. However many loss mechanisms produce local loss events which can be located elsewhere in the machine. A beam loss monitoring system, covering the whole machine circumference is therefore essential, and is used for both machine protection and diagnostics. In order to fully understand the measured signals and set-up the beam abort thresholds, extensive simulation work is required, covering particle tracking in the accelerator and the generation of the particle showers created by the lost particles. In order to benchmark these simulations and verify beam-abort thresholds, special tests have been performed where beam losses are provoked in a controlled manner over a wide range of duration. This work summarizes the experience in understanding beam losses in the LHC during Run 1.

## INTRODUCTION

When the beam particles deviate from their optimal trajectory and hit the vacuum chamber or if they interact with objects inside the vacuum chamber (rest gas molecules, dust) they are usually lost from the beam. These beam losses are a natural aspect of every machine operation. Their effects are: decrease of beam intensity and lifetime, activation and radiation damage of accelerator elements. In case of catastrophic losses, when unexpectedly large fraction of the beam is lost in the area which is not designed to accept such a loss, they may lead to a damage of the vacuum chamber and other machine elements.

In case of superconducting accelerator the beam losses heat up the magnet coils and may lead to a sudden transition to normal-conducting state called a *quench*. In LHC the total energy stored in a circulated beam reaches 392 MJ while the quench level is only about a few mJ/cm<sup>3</sup>, therefore a loss of about 10<sup>-10</sup> of the total beam intensity on superconducting magnet aperture may heat up the coil above transition temperature and quench the magnet.

The most obvious way to quantify the beam losses is a decrease rate of the beam current, measured typically in loss of particles per turn, per second or per a given phase of the machine cycle. This measurement is done using beam current transformers.

Another loss quantification is the beam power lost in a given location, for instance on a collimator or along the beam chamber. In case of LHC primary collimators only a small fraction (~ 2%) of the impacting beam power is

deposited in the graphite jaw. The rest is deposited in the downstream collimators and absorbers. In order to allow hands-on intervention on beamline elements the activation must be limited and therefore the regular losses should be kept at the level below 1 W/m.<sup>1</sup>

Finally the beam losses are measured by Beam Loss Monitors (BLM) using radiation units, for instance Grays. This way of loss quantification is usually used in protection-related studies, for instance assessing the damage or quench potential of the losses. It is related to the energy density deposited inside accelerator components.

These various quantifications of beam losses are related. For instance a single proton lost in LHC generates BLM signal between 10<sup>-12</sup> and 10<sup>-10</sup> Gy.

This paper describes the beam losses in LHC and concentrates on a special case of controlled loss experiments called quench tests. They were analyzed and simulated with unprecedented precision using state-of-art techniques.

## BEAM LOSS MECHANISMS AND TIMESCALES

Beam losses are often divided into normal and abnormal. The normal losses are those which cannot be avoided, for instance losses due to luminosity debris or due to particle diffusion from beam core to the halo which are usually caught on the collimation system. The beam instabilities due to operational variations, for instance tune change during the squeeze or ramp, are also producing normal losses. In LHC the average intensity lost during a fill, between capture and start of physics is about 3.5%. Table 1 shows the distribution of losses between various phases of the machine cycle.

Table 1: Beam Losses During Various Phases of Machine Cycle During Luminosity-production Year 2012 [1]

phase	average	maximum
RF capture	0.5%	2%
ramp	1.2%	15%
squeeze+adjust	1.7%	10%

Abnormal losses happen due to malfunction of accelerator equipment, for instance spurious discharge of the kicker magnets or dust particles falling into the beam. The last ones, called colloquially Unidentified Falling Objects (UFO), are of special concern in LHC, because they can provoke magnet quenches compromising machine operation at 6.5 TeV.

It is convenient to classify beam losses according to their duration:

<sup>1</sup> This value is applicable for a beamline shielded with magnets.

# BEAM INSTRUMENTATION AT THE 1 MW PROTON BEAM OF J-PARC RCS

K. Yamamoto<sup>#</sup>, N. Hayashi, K. Okabe, H. Harada, P. K. Saha, M. Yoshimoto, S. Hatakeyama, H. Hotchi, Y. Hashimoto and T. Toyama, J-PARC Center, Tokaimura, Japan

## Abstract

Rapid Cycling Synchrotron(RCS) of Japan Proton Accelerator Complex(J-PARC) is providing more than 300 kW of proton beam to Material and Life science Facility(MLF) and Main Ring(MR). Last summer shutdown, a new ion source was installed to increase output power to 1 MW. In order to achieve reliable operation of 1 MW, we need to reduce beam loss as well. Beam quality of such higher output power is also important for users. Therefore we developed new monitors that can measure the halo with higher accuracy. We present beam monitor systems for these purposes.

## INTRODUCTION

The 3 GeV rapid cycling synchrotron (RCS) at the Japan Proton Accelerator Research Complex (J-PARC) is a high-intensity proton synchrotron. It delivers an intense proton beam to the target for neutron production in the Materials and Life Science Experimental Facility (MLF) as well as to the Main Ring (MR) synchrotron at a repetition rate of 25 Hz[1]. The RCS commissioning started since 2007, and output beam power was gradually increased. So far, RCS is providing about 300 kW of proton beam to MLF and MR[2]. Last summer shutdown, we installed a new ion source and radio frequency quadrupole linac to achieve designed output power of 1 MW[3]. In the beam commissioning of October 2014, we achieved 770 kW output with acceptable beam loss[4].

In order to achieve reliable operation of 1 MW, we need to reduce beam loss as well. Beam quality of such higher output power is also important for users. Therefore we developed new monitors that can measure the halo with higher accuracy. At first we present beam monitor systems which are used for the beam commissioning to establish higher power operation. Next we introduce some new monitors to measure the beam halo with higher accuracy and to achieve higher reliability.

## REGULAR MONITORS FOR BEAM COMMISSIONING

The monitor system is important to conduct the beam commissioning. Figure 1 shows RCS parameters and the monitor location. Some parameters of regular monitors are written in a reference[5].

### Beam Position Monitor (BPM)

We prepared 54 BPMs (Normal BPM) to measure a beam orbit in the RCS. Since the physical aperture of the RCS is too large (more than 250mm), it is difficult to

ensure the linear response. In order to clear this issue, we chose the diagonal cut electrode[6]. Figure 2 shows the 3-D model of the BPM head. Three BPMs ( $\Delta R$ -BPM), which are installed in the arc section of the large dispersion function, are used for RF radial feedback system. We also have extra two BPMs (324BPM) which can detect 324 MHz frequency signal. 324 BPM are used to obtain the information of the injection beam[7].

The normal BPM system has two operation modes. The one mode, so-called "COD mode", is to record the averaged beam position of each 1 ms by the full 25 Hz repetition. The other is to store the whole waveform data of all BPMs for further analysis, like turn-by-turn position calculation (not 25Hz but 1 shot per several seconds).

The position accuracy is estimated to be about 0.5 mm using a newly developed Beam Based Alignment method[8].

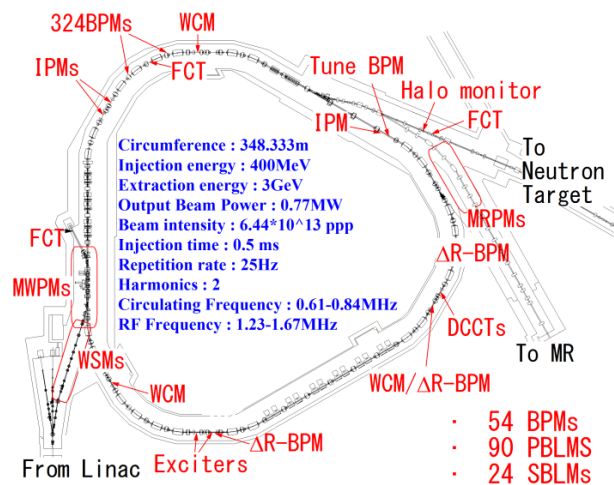


Figure 1: Monitor Layout and RCS parameters.

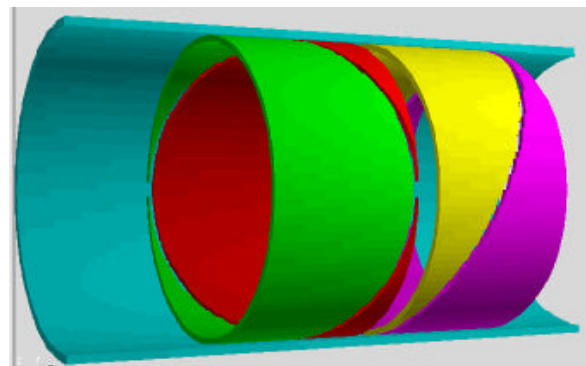


Figure 2: 3-D model of the diagonal cut electrodes.

# BEAM DIAGNOSTIC CHALLENGES FOR HIGH ENERGY HADRON COLLIDERS

E. B. Holzer\*, CERN, Geneva, Switzerland

## Abstract

Two high energy hadron colliders are currently in the operational phase of their life-cycle, RHIC and LHC. A major upgrade of the LHC, HL-LHC, planned for 2023 aims at accumulating ten times the design integrated luminosity by 2035. Still further in the future, studies in the frameworks of the Future Circulating Collider (FCC) and the Super Proton Proton Collider (SppC) are investigating machines with a center-of-mass energy of up to 100 TeV and with up to 100 km circumference. The existing machines already pose considerable diagnostic challenges, which will become even more critical with any increase in size and energy. Cryogenic environments lead to additional difficulties for diagnostics and further limit the applicability of intercepting devices, making non-invasive profile and halo measurements essential. The sheer size of these colliders requires the use of radiation tolerant read-out electronics in the tunnel and low noise, low loss signal transmission. It also implies a very large number of beam position and loss monitors, all of which have to be highly reliable. To fully understand the machine and tackle beam instabilities, bunch-by-bunch and intra-bunch measurements become increasingly important for all diagnostic systems. This contribution discusses current developments in the field.

## INTRODUCTION

The Relativistic Heavy Ion Collider (RHIC) is operating since the year 2000. It accelerates various ion species for symmetric and asymmetric collisions. Furthermore, it has the unique capability of colliding high energy polarized protons to study the spin structure of the proton. The Large Hadron Collider (LHC) is operational since 2009, mostly running p-p collisions, and for four weeks per operational year Pb-Pb or p-Pb collisions. While the maximum RHIC beam energy is 100 GeV/n for ions and 255 GeV for protons, the LHC was running at 3.5 and 4 TeV and is scheduled to run at 6.5–7 TeV beam energy in the coming years. The average beam current at RHIC is well above 100 mA for almost all ions, while at LHC it is around half an Ampere for proton, but much lower for lead ions. The peak luminosity as well as the integrated luminosity per year for heavy ion collisions at LHC is considerably lower than at RHIC. With its proton luminosities, on the other hand, LHC is unmatched with  $7.7 \times 10^{33} \text{ cm}^{-2}\text{s}^{-1}$ . Table 1 (top) gives an overview of RHIC and LHC parameters. The estimated performance is shown for the LHC Run2, which starts in 2015 after the current long shutdown 1 (LS1), and for the planned luminosity upgrade HL-LHC (High Luminosity LHC). HL-LHC is scheduled for Pb ions for 2020, at the start of Run3, and

for protons for 2025, at the start of Run4. LHC beam instrumentation experiences during Run1 and challenges for Run2 are discussed in [1] and [2] respectively.

Looking still further in the future, there are currently two studies for hadron colliders, the FCC-hh and the SppC. Both studies include as a potential intermediate step an electron-positron collider in the same tunnel, called FCC-ee and Circular Electron-Positron Collider (CEPC) respectively. The FCC-hh study considers p-p, Pb-Pb and p-Pb collisions, the SppC p-p collisions. With an envisaged circumference of 80 or 100 km the FCC is somewhat larger than the SppC with 50–70 km. Physics start date (2035–2042), beam energy (25–50) TeV/n and beam current ( $\approx 0.5 \text{ A}$ ) are rather comparable. Table 1 (bottom) summarizes parameters under consideration.

## STORED ENERGY

The energy stored in one LHC beam has reached the record level of 140 MJ during the 4 TeV run. 362 MJ are expected at 7 TeV, 694 MJ at HL-LHC and even 8 GJ for FCC-hh. 10 GJ will be contained in the LHC magnets at 7 TeV. Already one LHC pilot bunch of  $5 \times 10^9$  is close to damage limits at 7 TeV. The machine protection system is vital for the survival of these colliders, and must be integrated with the machine design. A dependability analysis comprises reliability, availability, maintainability and safety. It yields the allowed budgets for each subsystem in terms of: probability of component damage due to malfunctioning; downtime due to false alarms; and downtime due to maintenance. There is an inherent conflict between these budgets. By reducing the damage probability (increasing protection) the machine availability will go down due to increased numbers of false dumps and maintenance time. Several beam instrumentation systems are/will be part of machine protection, e. g. beam loss measurement (BLM), beam position measurement (BPM) at critical locations, and a fast measurement of the beam current change.

## Beam Cleaning and Losses

The collimation system gets increasingly complex with increasing beam energy and brightness. At the LHC there are already more than 100 collimators installed. At the same time the tolerance for collimator set-up becomes tighter. LHC has installed 18 new collimators with embedded BPM buttons at the tapered ends of both collimator jaws, retracted by 10.6 mm from jaw surface. The new design was successfully tested at the CERN SPS. The readout is via a newly designed compensated diode peak detector electronics. It achieves an excellent resolution of less than 100 nm for centered beams [3]. With this system the collimator alignment will take less than 20 s with an achieved tolerance

\* barbara.holzer@cern.ch

## EMITTANCE TRANSFER IN LINACS

L. Groening, X. Chen, M. Maier, O.K. Kester, GSI, D-64291 Darmstadt, Germany

M. Chung, Ulsan National Institute of Science and Technology, Ulsan 698-798, Republic of Korea

### Abstract

Flat beams feature unequal emittances in the horizontal and vertical phase space. Such beams were created successfully in electron machines by applying effective stand-alone solenoid fringe fields in the electron gun. This contribution is an extension of the method to ion beams and on the decoupling capabilities of such a round-to-flat adaptor. The beam line provides a single-knob tool to partition the horizontal and vertical rms emittances, while keeping the product of the two emittances constant as well as the transverse rms Twiss parameters ( $\beta_{x,y}$  and  $\alpha_{x,y}$ ) in both planes. This single knob is the solenoid field strength. The successful commissioning of the set-up with beam will be presented as well.

### INTRODUCTION

Transformation of a round beam (equal transverse emittances) to a flat beam (different transverse emittances) requires changing the beam eigen-emittances. The eigen-emittances are defined through the beam second moments as

$$\varepsilon_1 = \frac{1}{2} \sqrt{-tr[(CJ)^2] + \sqrt{tr^2[(CJ)^2] - 16det(C)}} \quad (1)$$

$$\varepsilon_2 = \frac{1}{2} \sqrt{-tr[(CJ)^2] - \sqrt{tr^2[(CJ)^2] - 16det(C)}} \quad (2)$$

where

$$C = \begin{bmatrix} \langle xx \rangle & \langle xx' \rangle & \langle xy \rangle & \langle xy' \rangle \\ \langle x'x \rangle & \langle x'x' \rangle & \langle x'y \rangle & \langle x'y' \rangle \\ \langle yx \rangle & \langle yx' \rangle & \langle yy \rangle & \langle yy' \rangle \\ \langle y'x \rangle & \langle y'x' \rangle & \langle y'y \rangle & \langle y'y' \rangle \end{bmatrix} \quad (3)$$

and

$$J = \begin{bmatrix} 0 & 1 & 0 & 0 \\ -1 & 0 & 0 & 0 \\ 0 & 0 & 0 & 1 \\ 0 & 0 & -1 & 0 \end{bmatrix}. \quad (4)$$

Linear transport elements as drifts, quadrupoles, dipoles, and rf-gaps do not change neither the beam rms emittances nor the eigen-emittances. Solenoids, skew quadrupoles, and -dipoles change the rms emittances through x-y coupling. But they do not change the eigen-emittances. This is often expressed by the symplecticity criterion for the transport matrix  $M$  representing the transport element [1]

$$M^T J M = J. \quad (5)$$

A matrix  $M$  satisfying the above criterion, is called symplectic and the eigen-emittances of a beam being transported by  $M$  remain constant. Beam particle coordinates are expressed by displacements  $x$  and  $y$  in space and by the respective

derivatives  $x'$  and  $y'$  w.r.t. the longitudinal coordinate  $s$ . The matrix of a solenoid fringe field reads as

$$M_F = \begin{bmatrix} 1 & 0 & 0 & 0 \\ 0 & 1 & k & 0 \\ 0 & 0 & 1 & 0 \\ -k & 0 & 0 & 1 \end{bmatrix} \quad (6)$$

with  $k = \frac{B}{2(B\rho)}$ .  $B$  is the solenoid on-axis magnetic field strength and  $B\rho$  is the beam rigidity.  $M_F$  does not satisfy Equ. 5 and changes the eigen-emittances. However, it leaves constant the 4d rms emittance defined as the square root of the determinant of  $C$  from Equ. 3.

Stand-alone fringe fields do not exist since magnetic field lines are closed. Effective stand-alone fringe fields act on the beam if the beam charge state is changed in between the fringes of the same solenoid. This is the case for rf-guns [2,3] (free electron creation inside solenoid), extraction from an Electron-Cyclotron-Resonance ion source [4] (ionisation inside the solenoid), and for charge state stripping inside a solenoid [5]. Further discussion of symplecticity of fringes shall be avoided here and we refer to [6] instead. We just point out that changing the ion beam charge state is equivalent to cancelling the stripped-off electrons from the system. This cancellation is a non-symplectic action and conservation of the eigen-emittances within the remaining subsystem cannot be assumed in general.

In this report we assume that an effective fringe field (Equ. 6) coupled an initially round & decoupled beam. The second moments matrix of this beam at the entrance to that fringe is given by

$$C'_1 = \begin{bmatrix} \varepsilon\beta & 0 & 0 & 0 \\ 0 & \frac{\varepsilon}{\beta} & 0 & 0 \\ 0 & 0 & \varepsilon\beta & 0 \\ 0 & 0 & 0 & \frac{\varepsilon}{\beta} \end{bmatrix}, \quad (7)$$

where  $\varepsilon$  is the rms emittance in both transverse planes and  $\beta$  is the rms beta function.

The report is organized in the following: in the first section we repeat parts of references [7] and [8], i.e. decoupling of the beam using a generic decoupling beam line. The subsequent section treats the extension of the generic case to any decoupling beam line. Finally, we report on successful experimental demonstration of one-knob emittance transfer.

### DE-COUPLING FOR THE GENERIC CASE

The beam second moment matrix after passing the fringe field of Equ. 6 is

$$C'_2 = M_F C'_1 M_F^T = \begin{bmatrix} \varepsilon_n R_n & -k\varepsilon_n \beta_n J_n \\ k\varepsilon_n \beta_n J_n & \varepsilon_n R_n \end{bmatrix}, \quad (8)$$

ISBN 978-3-95450-173-1

# MEASUREMENTS OF BEAM HALO DIFFUSION AND POPULATION DENSITY IN THE TEVATRON AND IN THE LARGE HADRON COLLIDER\*

G. Stancari<sup>†</sup>, Fermilab, Batavia, IL 60510, USA

## Abstract

Halo dynamics influences global accelerator performance: beam lifetimes, emittance growth, dynamic aperture, and collimation efficiency. Halo monitoring and control are also critical for the operation of high-power machines. For instance, in the high-luminosity upgrade of the LHC, the energy stored in the beam tails may reach several megajoules. Fast losses can result in superconducting magnet quenches, magnet damage, or even collimator deformation. The need arises to measure the beam halo and to remove it at controllable rates. In the Tevatron and in the LHC, halo population densities and diffusivities were measured with collimator scans by observing the time evolution of losses following small inward or outward collimator steps, under different experimental conditions: with single beams and in collision, and, in the case of the Tevatron, with a hollow electron lens acting on a subset of bunches. After the LHC resumes operations, it is planned to compare measured diffusivities with the known strength of transverse damper excitations. New proposals for nondestructive halo population density measurements are also briefly discussed.

## INTRODUCTION

Understanding particle losses and beam quality degradation is one of the fundamental aspects in the design and operation of accelerators. From the point of view of machine protection, losses must be absorbed by the collimation system to avoid damaging components. Beam lifetimes and emittance growth determine the luminosity of colliders. Knowledge of the machine aperture (physical and dynamical) and of the mechanisms that drive particle loss is essential.

The LHC and its planned luminosity upgrades (HL-LHC) represent huge leaps in the stored beam energy of colliders. In 2011, the Tevatron stored a beam of 2 MJ at 0.98 TeV, whereas the LHC reached 140 MJ in 2012 at 4 TeV. The nominal LHC will operate at 362 MJ at 7 TeV in 2015, and the HL-LHC project foresees that around 2023 the machine will store proton beams of 692 MJ.

No scrapers exist in the LHC for full beam at top energy. Moreover, the minimum design HL-LHC lifetimes (about 0.2 h for slow losses during squeeze and adjust) are close to the plastic deformation of primary and secondary collimators.

Halo populations in the LHC are not well known. Collimator scans [1, 2], van-der-Meer luminosity scans [3], and losses during the ramp [4] indicate that the tails above  $4\sigma$  (where  $\sigma$  is the transverse rms beam size) represent between 0.1% and 2% of the total population, which translates to megajoules of beam at 7 TeV. Quench limits, magnet damage, or even collimator deformation will be reached with fast losses [5]. In HL-LHC, these fast losses include crab-cavity failures, which generate orbit drifts of about  $2\sigma$  [6].

Hence, the need arises to measure and monitor the beam halo, and to remove it at controllable rates. For HL-LHC, beam halo monitoring and control are one of the major risk factors for operation with crab cavities. Hollow electron lenses were proposed as an established and flexible tool for controlling the halo of high-power beams [7].

The dynamics of particles in an accelerator can be quite complex. Deviation from linear dynamics can be large, especially in the beam halo. Lattice resonances and nonlinearities, coupling, intrabeam and beam-gas scattering, and the beam-beam force in colliders all contribute to the topology of the particles' phase space, which in general will include regular and chaotic regions, and resonant islands. In addition, various noise sources are present in a real machine, such as ground motion (resulting in orbit and tune jitter) and ripple in the radiofrequency and magnet power supplies. As a result, the macroscopic motion can acquire a stochastic character, which can be described in terms of particle diffusion [8–12].

Calculations of lifetimes, emittance growth rates, and dynamic aperture from various sources are routinely performed in the design stage of all major accelerators, providing the foundation for the choice of operational machine parameters. Experimentally, it was shown that beam halo diffusion can be measured by observing the time evolution of particle losses during a collimator scan [13]. These phenomena were used to estimate the diffusion rate in the beam halo in the SPS at CERN [14, 15], in HERA at DESY [13], and in RHIC at BNL [16]. An extensive experimental campaign was carried out at the Tevatron in 2011 [17–19] to characterize the beam dynamics of colliding beams and to study the effects of the novel hollow electron beam collimator concept [20]. Following the results of the Tevatron measurements, similar experiments were done in the LHC [2, 21].

In this paper, we review some of the present and future experimental methods to estimate beam halo populations, with a discussion of their systematic effects. We also survey the experimental data on the dynamics of the beam halo, with a discussion on the relationship between diffusivities and population densities.

\* Fermilab is operated by Fermi Research Alliance, LLC under Contract No. DE-AC02-07CH11359 with the United States Department of Energy. This work was partially supported by the US DOE LHC Accelerator Research Program (LARP) and by the European FP7 HiLumi LHC Design Study, Grant Agreement 284404. Report number: FERMILAB-CONF-14-450-AD-APC.

<sup>†</sup> Email: (stancari@fnal.gov).

# STATUS OF PREPARATIONS FOR A 10 MICROSECOND LASER-ASSISTED H<sup>-</sup> BEAM STRIPPING EXPERIMENT

S. Cousineau, A. Aleksandrov, V. V. Danilov, T. Gorlov, Y. Liu, A. Menshov, M. Plum, A. Rakhman, A. Shishlo, ORNL, Oak Ridge, Tennessee, TN, USA  
 N. Luttrell, F. Garcia, University of Tennessee, Knoxville, TN, USA  
 David Johnson, Fermilab, Batavia, Illinois, IL, USA  
 Y. Wang, University of Alabama, Huntsville, AL, USA  
 Y. Takeda, High Energy Accelerator Research Organization, Tsukuba, Japan

## Abstract

At the Spallation Neutron Source accelerator preparations are underway for a 10 us laser-assisted H-stripping experiment. This is a three orders of magnitude increase in pulse duration compared to the initial 2006 proof of principle experiment. The focus of the experiment is the validation of methods that reduce the average laser power requirement, including laser-ion beam temporal matching, ion beam dispersion tailoring, and specialized longitudinal and transverse optics. In this presentation we report on the status of preparations and the anticipated schedule for the experiment.

## INTRODUCTION

Many high intensity hadron synchrotrons accumulate beam through the process of charge exchange injection, whereby an H<sup>-</sup> ion is converted to a proton via passage through a thin carbon foil that strips the two electrons. This method has been demonstrated to work for beam powers up to 1.4 MW. However, the survivability of the carbon stripper foils beyond the 1.4 MW level is unknown. Evidence of foil damage including tears, curls, and bracket melts, is routinely observed at high power hadron facilities such as the Spallation Neutron Source (SNS) [1]. The damage is exponentially worse with increasing beam powers. Although there are a number of research programs dedicated to improving foil durability [2], currently there is no viable alternative technology to replace the foils once the power limit is reached.

Beyond the issue of foil survivability, there is also the problem of beam scattering in the foil. This leads to emittance dilution and more importantly, beam loss and radiation. At the SNS and similar accelerators, the injection region is the hottest area of the accelerator.

The idea of using a laser and two magnets to replace the carbon foil in the charge-exchange process was proposed almost three decades ago. In this scenario the first, loosely bound electron is Lorentz stripped from the ion using a magnetic field. Because the second, more tightly bound electron cannot be stripped with a conventional magnet, a laser is used to resonantly excite the electron to a more loosely bound state (typically n=3 or n=4), whereby it can be Lorentz stripped with a second magnet, resulting in a proton. Figure 1 illustrates the concept.

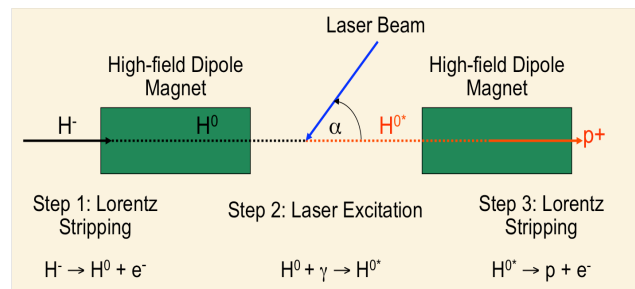


Figure 1: The laser stripping concept.

This method was successfully demonstrated in a 2006 proof of principle experiment at the SNS, where 90% stripping of a 6 ns, 900 MeV H<sup>-</sup> beam was accomplished using a 355 nm laser and two magnets. Unfortunately, a straightforward scaling of this experiment to the full SNS duty cycle would require ~600 kW of average laser power, which is not feasible. Rather, it is necessary to reduce the average laser power requirement through laser and ion beam manipulations [3,4].

At SNS, preparations are underway for the next laser stripping experiment. The goal of the experiment is to achieve 90% stripping efficiency of a 5-10 us, 1 GeV H<sup>-</sup> beam. The central theme of the experiment is the validation of methods used to reduce the required average laser power. For a future operational system that would strip millisecond-level pulses, these methods would be employed along with a power recycling optical cavity. The recycling cavity is under development in the laser lab at SNS, but is not part of the current stripping experiment.

This paper describes the configuration for the 10 us experiment, the work underway to prepare the ion and laser beam parameters, and the schedule.

## EXPERIMENTAL CONFIGURATION AND HARDWARE

Four primary goals drove the design of the experimental configuration:

- 1) Achieve high efficiency stripping.
- 2) Protect the laser.
- 3) Prevent disruptions to production beam operations.
- 4) Provide schedule flexibility for the experiment.

# THE PARTICLE-IN-CELL CODE BENDER AND ITS APPLICATION TO NON-RELATIVISTIC BEAM TRANSPORT

D. Noll\*, M. Droba, O. Meusel, U. Ratzinger, K. Schulte, C. Wiesner  
Institute of Applied Physics, Goethe University Frankfurt am Main

## Abstract

A new non-relativistic, electrostatic Particle-in-Cell code named *bender* has been implemented to facilitate the investigation of low-energy beam transport scenarios. In the case of high-intensity beams, space-charge compensation resulting from the accumulation of secondary particles – electrons for positively charged ion beams – is an important effect. It has been shown, that the distribution of compensation electrons can have a significant influence on the beam and lead to an emittance growth. To improve the understanding of the dynamics of the compensation and the resultant self-consistent steady state, ionization of residual gas as well as secondary electron production on surfaces have been implemented and used to study a number of test systems. We will present first results of these compensation studies as well as further applications of the code, among them the chopper section of the future FRANZ facility [1].

## IMPLEMENTATION

The Particle-in-Cell [2] code *bender* is written in the C++ language and uses MPI for parallelisation. It reads input files in an XML-style format. All numerical values in this file are affixed with units. The output of the code can be configured to include particle distributions and losses, field and potential distribution and single particle tracks, as required.

External fields can either be loaded from data exported from tools like the CST Suite or Opera, calculated numerically via either the solution of Laplace's equation on a lattice or from the Biot-Savart law by integrating the current flow through wires defined by analytic expressions, or calculated from several available field models, including multipole field distributions and several solenoid field models.

For use as boundaries for either particle movement or the Poisson solver, various geometric primitives like planes, tubes and plates are implemented. For more complex geometries, an import from STL files is available.

All geometric objects in the code can then be transformed by one or multiple affine transformations, which allows objects like fields, geometric objects, monitors and even poisson solvers to be placed in the simulation "space" at will.

To simulate dc beams, a fixed number of particles, spread out over  $v_{\text{beam}}\Delta t$ , are inserted in every time step, continuously building up the beam volume.

## Field Solvers

The code provides three solvers for Poisson's equation.

For problems requiring either non-equidistant grid spacing or geometrically complex boundary conditions, there is

a cartesian solver using a Shortley-Weller finite-difference stencil [3]

$$\frac{\varphi_{i-1,j,k}}{\Delta_- (\Delta_+ + \Delta_-)} - \frac{\varphi_{i,j,k}}{\Delta_+ \Delta_-} + \frac{\varphi_{i+1,j,k}}{\Delta_+ (\Delta_+ + \Delta_-)} + \text{other dir.} = -\frac{\rho_{i,j,k}}{2\epsilon_0} + \mathcal{O}(\Delta^3), \quad (1)$$

where  $\Delta_{\pm}$  are the distances to either the neighbouring grid points or a grid boundary. Dirichlet, Neumann and periodic boundary conditions on the grid boundaries can be considered. The grid can be distributed among processors in blocks in all directions, which allows bent geometries to be followed without wasting memory on inactive regions. An example is shown in Fig. 1.

On initialisation of the solver, all processors calculate the positions and the sizes of boundary surfaces with their neighbours. In a second step, intersections between the grid lines and the boundary objects given for the solver are calculated in multiple passes over each direction. In the first of the three passes, grid points not contained in any boundary object are assigned a global index. When an intersection with an object is found on the line between two grid points, its position is stored for the respective active grid point using its index. In a third step, the geometric information gathered is communicated in the bounding areas found in the first step.

After mesh generation, a sparse matrix for the potential on the grid points is constructed using Eq. (1). To solve this matrix, the PetSc library [4] is used. After the solution process, to be able to calculate the electric field in the region between the grid portions local to two processors, potential

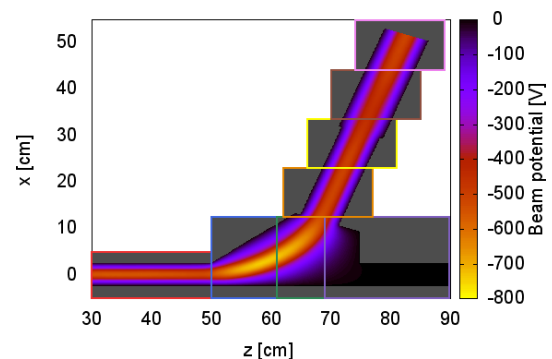


Figure 1: Example of a calculation of electric potential of a guided electron beam on 16 processors. The coloured rectangles show the grid portions on each processor. Each domain is additionally split in vertical direction. The grey portions of the grid are disabled on each processor, the white portions are not considered by any processor.

\* noll@iap.uni-frankfurt.de

# NOISE AND ENTROPY IN NON-EQUIPARTITIONED PARTICLE BEAMS

I. Hofmann and O. Boine-Frankenheim

GSI Helmholtzzentrum für Schwerionenforschung GmbH, Planckstr.1, 64291 Darmstadt, Germany  
 Technische Universität Darmstadt, Schlossgartenstr.8, 64289 Darmstadt, Germany

## Abstract

The numerical noise inherent to particle-in-cell (PIC) simulation of 3d high intensity bunched beams in periodic focusing is explored on the basis of the rms entropy model by Struckmeier and of simulations with the TRACEWIN code using linac relevant parameters. Starting from noise in a matched equilibrium beam and its dependence on grid and particle number we explore the relevance of this noise under dynamical situations. The cases under study are fast emittance exchange; an initially mismatched beam; slow crossing through space charge structure resonances. We find that an effect of the equilibrium noise can be retrieved in a dynamical case, if the process is evolving sufficiently slowly.

## INTRODUCTION

In this paper we deal with the numerical noise generated by the discreteness of the spatial grid used for the Poisson solver as well as the effect of artificial collisions due to using highly charged super-particles. In simulation of extended plasmas this type of noise received attention since the 1970's, when interest in this field was growing in parallel with the performance of numerical computation.

More recently, the interest has revived to get a quantitative understanding of this noise in the field of high intensity beam simulation, where numerical noise may play a role for long-term simulation. In this context new interest was found in the analytical modelling of noise and the associated entropy growth based on the rms entropy model by Struckmeier [1, 2]. It is based on second order moments of the Vlasov-Fokker-Planck equation and assumes that collisional behaviour and temperature anisotropy can drive rms emittance growth, which is used to define an rms entropy growth. The associated noise and entropy growth in 2d beams - the transverse 4d phase space - is studied in a recent paper by Boine-Frankenheim et al. [3]. A companion paper by Hofmann et al. [4] deals with the rms entropy model and noise in 3d short bunches - in 6d phase space - with particular emphasis on linear accelerator applications. Some results of the latter are reviewed in the following section.

## REVIEW OF ENTROPY AND NOISE THEORY

The basic equation for the rms entropy growth is based on the idea that the change of the six-dimensional rms emittance defined as product of individual plane rms emittances,  $\epsilon_{6d} \equiv \epsilon_x \epsilon_y \epsilon_z$ , is a suitable measure for rms entropy growth, hence the system noise. The resulting relative change of rms

emittance is given by:

$$\frac{1}{k} \Delta S = \frac{\Delta \epsilon_{6d}}{\epsilon_{6d}} = \Delta s \frac{k_f^*}{3} (I_A + I_{GN}) \quad (1)$$

with a term related to temperature anisotropy,

$$I_A \equiv \left( \frac{(T_x - T_y)^2}{T_{xy}} + \frac{(T_x - T_z)^2}{T_{xz}} + \frac{(T_y - T_z)^2}{T_{yz}} \right), \quad (2)$$

$k^*$  the dynamical friction coefficient and  $I_{GN}$  describing an offset explained as grid noise in connection with the periodic focusing (see Ref. [4]).

We consider a periodic FODO lattice of 1000 cells with symmetrically arranged rf kicks. The zero current phase advance per cell of this lattice is assumed to be  $k_0 = 60^\circ$  in  $x, y, z$  with equal emittances in all three directions. The beam is matched for a Gaussian distribution and the current is chosen such that the tune depression is  $k/k_0 \approx 0.55$ . The envelopes obtained with the TRACEWIN code are shown in Fig. 1:

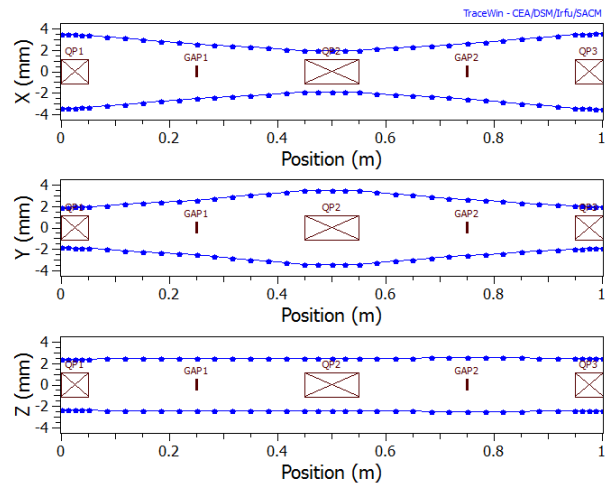


Figure 1: Basic cell of periodical FODO lattice with rf gaps.

The alternating focusing causes a strong modulation and local imbalance of "temperatures". According to Eq. 2, with more details in Ref. [1], this purely collisional effect is as source of entropy growth, which is amplified by grid heating effects Ref. [4]. Following Ref. [4], results for the relative growth of  $\epsilon_{6d}$  are shown in Fig. 2 as function of  $n_c$  and for different  $N$ . The  $n_{c,x,y,z}$  are understood as half number of cells between the maximum grid extent values of  $\pm 3.5\sigma$ . Beyond, the mesh is replaced by an analytical continuation for the space charge potential based on a Gaussian core of identical rms size. We note that the number of space charge

# RADIO FREQUENCY QUADRUPOLE FOR LANDAU DAMPING IN ACCELERATORS: ANALYTICAL AND NUMERICAL STUDIES

A. Grudiev, K. Li, CERN, Geneva, Switzerland  
 M. Schenk, University of Bern, Bern, Switzerland

## Abstract

It is proposed to use a radio frequency quadrupole (RFQ) to introduce a longitudinal spread of the betatron frequency for Landau damping of transverse beam instabilities in circular accelerators. The existing theory of stability diagrams for Landau damping is applied to the case of an RFQ. As an example, the required quadrupolar strength is calculated for stabilizing the Large Hadron Collider (LHC) beams at 7 TeV. It is shown that this strength can be provided by a superconducting RF device which is only a few meters long. Furthermore, the stabilizing effect of such a device is proven numerically by means of the PyHEADTAIL macroparticle tracking code for the case of a slow head-tail instability observed in the LHC at 3.5 TeV.

## INTRODUCTION

In accelerators, the effect of Landau damping [1] provides a natural stabilizing mechanism against collective instabilities if the particles in the beam have a small spread in their natural (betatron or synchrotron) frequencies, see for example [2] and references therein. If the spread introduced by non-linearities naturally present in an accelerator is too small, a dedicated non-linear element is added to the system. For example, in LHC [3], 84 focusing and 84 defocusing (arranged in 16 families – two per sector), 0.32 m long superconducting magnetic octupoles is used to introduce a betatron frequency spread for Landau damping of the dipole modes. The LHC octupoles have been successfully used to stabilize the beams up to the energy of 4 TeV at which LHC has been operated so far [4]. The effect of the transverse spread however, reduces as the transverse geometrical beam emittance decreases at higher energies due to adiabatic damping.

Recently [5], it has been proposed to use an RFQ to introduce a longitudinal spread of the betatron frequency for Landau damping of the transverse collective oscillations. The basic idea is to use the harmonic dependence of the quadrupolar focusing strength of the RFQ on the longitudinal position of the particles in the bunch. It has been shown that in high energy accelerators, the longitudinal spread is more effective than the transverse one due to the longitudinal emittance of the beam being much larger than the transverse one. The higher efficiency of the longitudinal spread for Landau damping allows for a compact, only a few meters long, RF device based on several 800 MHz superconducting cavities operating in a TM quadrupolar mode to provide the same functionality as the LHC octupoles whose total length is about 56 m. In this paper, the work presented

in [5] is summarized and the first results on the implementation of the RFQ in the PyHEADTAIL macroparticle tracking code and on the simulation of its stabilizing effect on a slow transverse head-tail instability observed in LHC at 3.5 TeV [4] are reported.

## RFQ FOR LANDAU DAMPING

For an ultra-relativistic particle of charge  $q$  and momentum  $p$  traversing an RFQ along the  $z$ -axis at the time moment  $t$ , the transverse kick in the thin-lens approximation is given by

$$\Delta \mathbf{p}_\perp = pk_2(-x\mathbf{u}_x + y\mathbf{u}_y) \cos \omega t, \quad (1)$$

where  $\omega$  is the RFQ frequency,  $\mathbf{u}_\alpha$  is the unit vector along the  $\alpha$  coordinate and  $k_2$  is the amplitude of the normalised integrated quadrupolar strength

$$k_2 = \frac{q}{pc} \frac{1}{\pi r} \int_0^{2\pi} \int_0^L (E_x - cB_y) e^{j\omega z/c} dz \Big| \cos \varphi d\varphi, \quad (2)$$

where  $c$  is the speed of light,  $L$  is the length of the RFQ and  $[r, \varphi, z]$  are cylindrical coordinates. Assuming that the bunch centre ( $z = 0$ ) passes the thin-lens RFQ at  $t = 0$ , the substitution  $t = z/c$  gives the dependence of the quadrupolar strength along the bunch. Substituting this dependence in the expression for the betatron frequency shift due to quadrupolar focusing yields the expression for the variation of the betatron frequency (so-called detuning) along the bunch

$$\Delta \omega_{x,y} = \pm \beta_{x,y} \frac{\omega_0}{4\pi} k_2 \cos(\omega z/c), \quad (3)$$

where  $\omega_0$  is the revolution frequency and  $\beta_{x,y}$  are the horizontal and vertical beta functions, respectively. Taking into account that  $\cos \omega z/c$  can be approximated as  $\sim 1 - (\omega z/c)^2/2$  for small arguments and  $\langle z^2 \rangle = \sigma_z^2 J_z/\varepsilon_z$  after averaging over the synchrotron period  $T_s$ , one can derive the expression for the variation of the betatron frequency in terms of the longitudinal action  $J_z$

$$\langle \Delta \omega_{x,y} \rangle_{T_s} \approx \pm \beta_{x,y} \frac{\omega_0}{4\pi} k_2 \left[ 1 - \frac{1}{2} \left( \frac{\omega \sigma_z}{c} \right)^2 \frac{J_z}{\varepsilon_z} \right], \quad (4)$$

where  $\sigma_z$  and  $\varepsilon_z$  are the RMS bunch length and the longitudinal emittance, respectively. Equation (4) is composed of two terms. The first one is a constant betatron frequency shift which, if necessary, can be compensated by a static magnetic quadrupole. The second term describes the incoherent spread required for Landau damping. It is used to estimate the integrated quadrupolar strength amplitude needed to stabilize a transverse instability with a coherent betatron frequency shift  $\Delta \Omega_{x,y}^{coh}$  according to the following condition

## NEW PSB H<sup>-</sup> INJECTION AND 2 GeV TRANSFER TO THE CERN PS

W. Bartmann, J.L. Abelleira, B. Balhan, E. Benedetto, J. Borburgh, C. Bracco, C. Carli, V. Forte, S. Gilardoni, G.P. Di Giovanni, G. Gräwer, B. Goddard, K. Hanke, M. Hourican, A. Huschauer, M. Meddahi, B. Mikulec, G. Rumolo, L. Sermeus, R. Steerenberg, G. Sterbini, Z. Szoke, R. Wasef, Y. Wei, W. Weterings, CERN, Geneva, Switzerland

### Abstract

At CERN Linac4 is being commissioned as first step in the LHC injector upgrade to provide 160 MeV H<sup>-</sup> ions. In order to fully deploy its potential, the PSB conventional multiturn injection will be replaced by a charge exchange injection. An expected brightness improvement of about a factor 2 would then be difficult to digest at PS injection due to space charge. Therefore the transfer energy between PSB and PS will be increased at the same time from 1.4 to 2 GeV. This paper describes the new PSB injection system and the status of its test stand. Modifications of the PSB extraction and recombination septa and kickers in the transfer line are shown. A new focussing structure for the transfer lines to match the horizontal dispersion at PS injection and the design of a new Eddy current septum for the PS injection are presented.

### MOTIVATION

The described CERN PS Booster (PSB) upgrades - undertaken within the LHC injector upgrade (LIU) - aim at providing brighter beams for the LHC after Long Shutdown 2 (LS2) and at preparing the beams for the High Luminosity upgrade of LHC (HL-LHC) in Long Shutdown 3 (LS3).

The upgrade of the PSB injection has two main ingredients. Linac4 will provide beams at 160 MeV instead of the present beam energy of 50 MeV from Linac2. Considering the present incoherent space charge tune shift as acceptable, the intensity which can be accumulated during the multi-turn injection process can be doubled within a given emittance [1].

The second important upgrade at injection is the change from a conventional multi-turn injection of protons from Linac2 to a charge exchange injection of H<sup>-</sup> from Linac4. The injection of H<sup>-</sup> onto an already occupied phase space area allows to better tailor the brightness of the various beams used in the CERN accelerator complex. In addition, the conventional multi-turn injection process is inherently loss dominated due to the exploitation of a septum (40% loss with respect to delivered intensity by Linac2). The septum width together with the available aperture at PSB injection also limits the number of injection turns to about 13. The new H<sup>-</sup> injection will allow to significantly reduce the losses per injection turn to the order of a few percent, dominated by the stripping efficiency of the foil.

In Figures 1 and 2 the brightness limitations before and after the upgrades are compared for the standard production of the 25 ns LHC beam in the LHC injector chain [2]. Before the upgrades of its injection system, the PSB represents the

limit in brightness of the LHC beams. After upgrading the PSB with the potential factor two gain in brightness, the injection into the PS would replace the PSB as the brightness bottleneck in the accelerator chain. Thus, an increase of the PS injection energy from 1.4 to 2.0 GeV is foreseen, which shall give the possibility to increase the brightness by about 60% at PS injection. In order to reach the HL-LHC beam requirements for after LS3, also upgrades concerning the SPS beam loading are required [2].

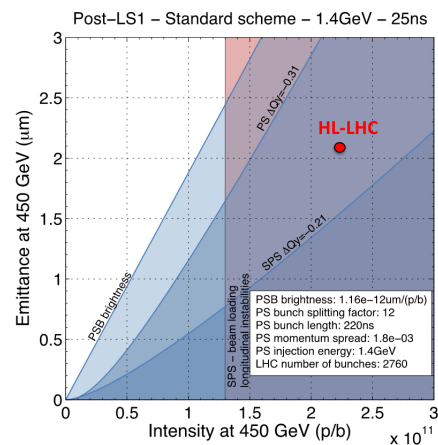


Figure 1: Emittance as a function of intensity at SPS extraction for LHC beams after LS1.

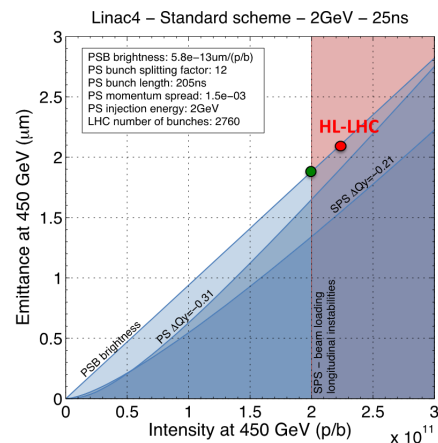


Figure 2: Emittance as a function of intensity at SPS extraction for LHC beams with the foreseen upgrades of the LHC injectors after LS2.

## LONG-TERM BEAM LOSSES IN THE CERN INJECTOR CHAIN

S. Gilardoni, G. Arduini, H. Bartosik, E. Benedetto, H. Damerau, V. Forte, M. Giovannozzi, B. Goddard, S. Hancock, K. Hanke, A. Huschauer, M. Kowalska, M. J. McAteer, M. Meddahi, E. Métral, B. Mikulec, Y. Papaphilippou, G. Rumolo, E. Shaposhnikova, G. Sterbini, R. Wasef  
CERN, Geneva, Switzerland

### Abstract

For the production of the LHC type beams, but also for the high intensity ones, the budget allocated to losses in the CERN injector chain is maintained as tight as possible, in particular to keep as low as possible the activation of the different machine elements. Various beam dynamics effects, like for example beam interaction with betatronic resonances, beam instabilities, but also reduced efficiency of the RF capture processes or RF noise, can produce losses even on a very long time scale. The main different mechanisms producing long term losses observed in the CERN injectors, and their cure or mitigation, will be revised.

### INTRODUCTION

The three synchrotrons forming the CERN LHC injector chain, namely the PSB (PS Booster), the PS (Proton Synchrotron) and the SPS (Super Proton Synchrotron), were built in laps of time of about 20 years with the goal of providing the largest variety of beams to the physics user community, thus leading to the implementation of very versatile machines. The PS was built as a sort of prototype machine in the late 50s and it is the first proton synchrotron with strong focusing ever operating [1]. The PSB was built to increase the PS injection energy from the 50 MeV of the Linac1 to 800 MeV. Then in the course of the CERN history, the extraction energy was increased first to 1 GeV, then to 1.4 GeV [2] and finally it will be upgraded to 2 GeV [3], with the goal of reducing the effect of direct space charge at PS injection. For the very same reason, the injection energy of the PSB is going to be increased from the 50 MeV of the proton Linac2 to the future 160 MeV provided by the H<sup>-</sup> Linac4. The last in the chain, the SPS, was built to produce high intensity beams for fixed target physics [4], but then was transformed first into a proton-antiproton collider, then – as the PS – into a lepton injector for LEP, and finally – as the PSB and the PS – is today operating as LHC injector.

All the three machines are producing two main families of beam types: high brightness beams for the collider, high intensity beams either for the following machine or for fixed target local users. The goal of this paper is to present a review of the loss mechanisms identified and eventually limiting the production of these two categories. Special attention will be given to the losses appearing on very long time scale, up to few hundreds ms or few thousand turns, considering that the synchrotrons magnetic cycles last few seconds. Some details are also given to the injection and extraction processes and related losses.

### LHC Beam Production Schemes

The LHC collider operates for luminosity production with two different bunch spacing, either 50 ns or 25 ns, the latter being the nominal configuration. The role of the injectors in the beam production is as follows: the PSB defines the initial transverse emittances, the PS the bunch spacing whereas in the SPS, on top of adapting the bunch length to the longitudinal acceptance of the LHC, tails in the transverse plane are scraped to avoid excessive losses during the LHC filling process.

The production of the 25 ns bunch spacing beam is realized as follows. Linac2, or Linac4 in the future, fills each of the 4 PSB rings into  $h=1+2$  bucket. Each PSB bunch is injected to the PS on  $h = 7$  and after 1.2 s, the PS receives two other PSB bunches. A first acceleration takes place up to 2.5 GeV, where the bunches triple split. Eighteen bunches are accelerated up to 26 GeV/c on  $h=21$  where two consecutive double splittings produce the final bunch spacing of 25 ns creating a batch of 72 bunches. The 50 ns spacing is realised by eliminating the last splitting. Prior to the transfer to the SPS, the bunches are rotated in the longitudinal plane to reduce the total bunch length to about 4 ns. Up to five consecutive batches of 72 bunches can be injected in the SPS at 26 GeV/c, and accelerated to 450 GeV/c to be delivered to the LHC. The longitudinal emittance is increased in the PS and SPS to reduce longitudinal instabilities, whereas transverse scraping is done in the SPS before reaching the extraction energy to eliminate tails. Besides the classical production scheme, alternative ones were proposed to overcome the current brightness limitation of the PSB. One realised during the 2012 run is BCMS (Batch Compression Merging and Splittings). It comprises the injection of  $2 \times 4$  bunches on the 9th harmonic in the PS, batch compression from  $h=9$  to  $h=14$ , bunch merging followed by a triple splitting all done at low energy instead of the triple splitting only. These evolved RF gymnastics are performed at an intermediate kinetic energy to avoid transverse emittance blow up due to space charge and to relax the requirements on the longitudinal emittance at injection. The resulting 12 bunches are accelerated to the extraction flat top where two bunch splittings occur to obtain the final 25 ns bunch spacing as for the nominal scheme. The advantage with respect to the traditional scheme results from the smaller splitting factor of the PSB bunches (6 instead of 12). Before extraction to the SPS, 25 ns spaced bunches can have the same intensity in only half of the transverse emittance. Typical beam parameters realised for the 25 ns beam and expected after the injector upgrade within the LIU (LHC Injector Upgrade)

ISBN 978-3-95450-173-1

## RECENT DEVELOPMENT IN THE MITIGATION OF LONG TERM HIGH INTENSITY BEAM LOSS

G. Franchetti, S. Aumon, F. Kesting, H. Liebermann, C. Omet, D. Ondreka, R. Singh, GSI  
S. Gilardoni, A. Huschauer, F. Schmidt, R. Wasef, CERN

Long term beam loss are due to the presence of several factors, but lattice nonlinearities and high intensity certainly rank among the main causes for long term beam loss. Experimental and numerical studies have shown that periodic resonance crossing induced by space charge in a bunched beam is a deleterious effect for beam survival [1, 2]. Given the complexity of the topic, the studies in the past have been focused to investigate one dimensional resonances, for example in Ref. [1] the resonance was  $4Q_x = 25$ , while in Ref. [2] the resonance was  $3Q_x = 13$ . The underlying mechanism leading to beam loss is explained, in this case, in terms of instantaneous stable islands in a two-dimensional phase space and their crossing the particles orbits. This mechanism was studied in details in Ref. [3].

Studies for SIS100 have shown, however, that in the injection scenario of the uranium ions, random components of magnets nonlinearities excite a significant web of resonances including coupled resonances [4]. One of the simpler of the nonlinear coupled resonances is the  $Q_x + 2Q_y = N$ . Although the mechanism of the beam loss remains the same (the periodic resonance crossing induced by space charge), the details of the mechanism have never been, in this case, studied. The reason for that is in the complexity of the 4-dimensional coupled motion, which poses an extraordinary challenge to disentangle the dynamics. While for 1-dimensional resonances the mechanism is relatively well understood, for 2-dimensional resonances it remains still unraveled.

In this context, within the collaboration between CERN and GSI, in 2012 a new experimental campaign in the CERN-PS for investigating the resonance  $Q_x + 2Q_y = 19$  has been undertaken. The results of measurements collected in a scan of beam intensity/profiles versus tunes have shown puzzling features: when the space charge tune-spread overlaps the third order resonance an asymmetric beam response is found: in one plane we find halo, whereas in the other plane a core growth takes place. In Fig. 1 we show a plot with the beam profiles resulting from the space charge tune spread overlapping with the third order resonance, the tunes of the measurement are reported on the picture, the tune-shift is  $\Delta Q_x \approx -0.046$ ,  $\Delta Q_y \approx -0.068$ . The asymmetry of the profile is quite evident and shows that a new and more complex dynamics is driving the beam halo formation. The details of these measurements will be part of a dedicated article.

The explanation of this beam profile shape have to be searched into the effects created by the 4D coupled dynamics. In this scenario the analogous of the fix points become the fix-lines [5]. These extended closed lines play a similar role as the fix points for the crossing of the 1D resonances. The description of this dynamics is beyond the purpose of this

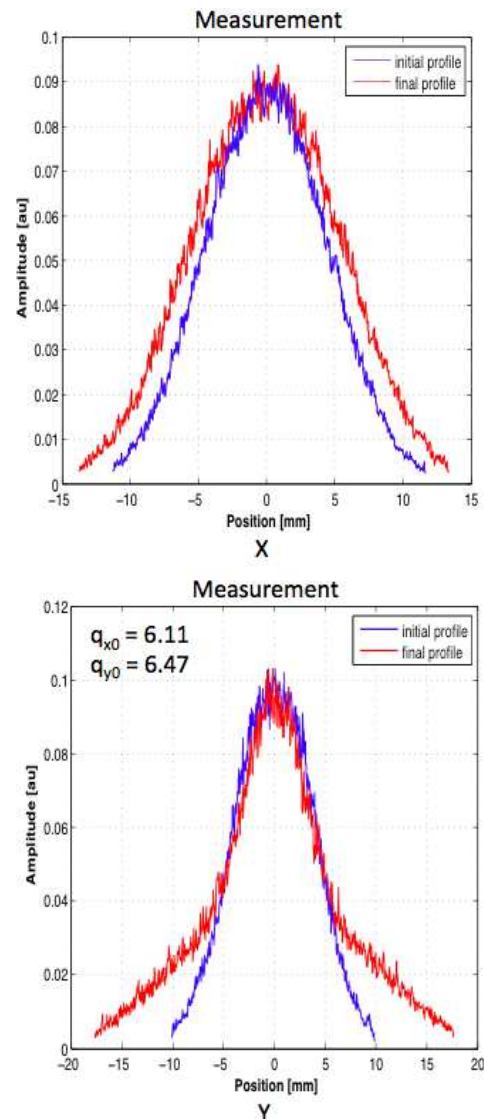


Figure 1: Beam profiles after 1 second storage of the beam in the CERN-PS. The asymmetry of the beam response is evident.

proceeding, a full study for the case of single particle is part of a future work [6].

If the halo edge is exceeding the beam pipe, long term beam loss is unavoidable. While the issue of the self-consistency during a substantial change of the space charge intensity is of relevance, practically this scenario is not really foreseen in practical operation in order to avoid significant machine or collimators damage.

The relevant issue is therefore if a strategy that allows to mitigate beam loss in a conventional operational scenario

## SIMULTANEOUS ACCELERATION OF RADIOACTIVE AND STABLE BEAMS IN THE ATLAS LINAC\*

B. Mustapha<sup>#</sup> and P.N. Ostroumov, ANL, Argonne, IL 60439, USA

A.A. Perry, ANL and IIT, Chicago, IL 60616, USA

M.A. Fraser, CERN, Geneva, Switzerland

### Abstract

ATLAS is now the only US DOE National User Facility for low-energy heavy-ion stable beams. With the recent commissioning of the Californium Rare Isotope Breeder Upgrade (CARIBU), ATLAS is now also used to accelerate radioactive beams. The demand for both stable and radioactive beam time is already exceeding two to three times the 5500 hours delivered by ATLAS every year. The time structure of the EBIS charge breeder to be installed next year for CARIBU beams is such that less than 3% of the ATLAS duty cycle will be used for radioactive beams. Being a CW machine, ~ 97% of the ATLAS cycle will be available for the injection and acceleration of stable beams without retuning. This simultaneous acceleration is possible for stable and radioactive beams with charge-to-mass ratios within 3%. We have developed a plan to upgrade ATLAS for this purpose to be implemented over the next few years, where two to three beams could be delivered simultaneously to different experimental areas. The upgrade concept will be presented along with the recent studies and developments done in this direction.

### THE ATLAS FACILITY AND RECENT UPGRADES

The Argonne Tandem Linear Accelerator System (ATLAS) was the first superconducting linac for ion beams in the world [1]. It has been operating and delivering ion beams for over thirty years at different capacities. Over the same period, ATLAS has undergone several upgrades [2]. The most recent are CARIBU [3] and the Efficiency and Intensity upgrade [4].

CARIBU uses a Californium fission source to produce radioactive daughter nuclei which are collected, separated and then cooled to form a beam. An ECR charge breeder [5] is used to increase the charge state of these beams for injection and acceleration in ATLAS.

The Efficiency and Intensity upgrade consisted of a new RFQ [6] and a new superconducting module [7]. The RFQ replaced the first three superconducting cavities of the Positive Ion Injector (PII) to avoid deterioration of the beam quality due to fast acceleration of low energy beams. The RFQ uses the existing multi-harmonic buncher (MHB) as a pre-buncher. Two notable features of the ATLAS RFQ are trapezoidal modulations in the accelerating section and

a compact output matcher to produce an axis symmetric beam for direct beam injection into PII which uses solenoidal focusing [8]. The new cryomodule replaced three old modules with split-ring resonators [9]. The splitting cavities are known to cause beam steering which results in beam loss and the subsequent quench of solenoids. The new cryomodule is made of 7 quarter-wave resonators (QWR) and 4 superconducting solenoids. The QWRs were designed and built with steering correction [10]. The new module should be able to accelerate 10 to 100 times higher intensity stable beams without significant beam loss.

Both the new RFQ and cryomodule have been recently commissioned and are now being used for routine ATLAS operations. Following this upgrade, the transmission has improved by 50 to 100% for all beams accelerated in ATLAS [11]. The overall transmission is now routinely over 80%, which is dictated by the MHB used to produce a small longitudinal emittance for more efficient beam transport and acceleration in ATLAS [12]. Figure 1 shows the current layout of ATLAS after the recent upgrades.

### THE NEED FOR MULTI-USER CAPABILITIES AT ATLAS

ATLAS is now the only US DOE National User Facility for low-energy heavy-ion stable beams delivering upward of 5500 hours of beam-on-target every year. With CARIBU online, ATLAS is also being used for the acceleration of radioactive beams, which often require longer beam time for experiments due to their lower intensity. In the past two years, the demand for ATLAS beam time has more than doubled and with longer radioactive beam run periods, less and less users will be served, especially stable beam users. Therefore the need for a multi-user capability is significant at ATLAS in order to satisfy more users and maximize the scientific output of the ATLAS facility.

\* This material is based upon work supported by the U.S. Department of Energy, Office of Science, Office of Nuclear Physics, under Contract number DE-AC02-06CH11357. This research used resources of ANL's ATLAS facility, which is a DOE Office of Science User Facility.

<sup>#</sup>brahim@anl.gov

# EXPERIENCE WITH STRIPPING HEAVY ION BEAMS

H. Okuno, RIKEN Nishina Center for Accelerator-based Science, Wako, Japan

## Abstract

Charge strippers play a critical role in many high-intensity heavy ion accelerators. Recent progress on accelerator technology make charge strippers so critical that traditional carbon foils can easily reach the limit of their application due to their short lifetime. In fact, three major heavy ion accelerator facilities (GSI, MSU/ANL, and RIKEN) have extensively studied alternatives to carbon foils to realize high-intensity acceleration of very heavy ions such as uranium. For example, the liquid lithium stripper was developed at MSU/ANL, and the helium gas stripper and rotating beryllium disk stripper were developed at the RIKEN radioactive-isotope beam factory (RIBF). The RIBF two strippers greatly contributed to the increase in the uranium beam intensity. However, we believe the Be disk stripper will reach its limit in near future due to its large deformation and requires further development for the RIKEN RIBF intensity upgrade program.

## INTRODUCTION TO CHARGE STRIPPERS

The production of high-intensity radioactive-isotope (RI) beams is one of the important applications of heavy ion accelerators. The three major heavy ion accelerator facilities (RIKEN, MSU/NSCL, and GSI) are each operating or constructing facilities (Radioactive-Isotope Beam Factory (RIBF) [1], the Facility for Rare Isotope Beams (FRIB) [2], or the Facility for Antiproton and Ion Research (FAIR) [3], respectively) to produce high-intensity RI beams using in-flight fission or projectile fragmentation of accelerated uranium ions in order to explore inaccessible regions of the nuclear chart. These facilities adopted different accelerator schemes, such as cyclotrons for RIBF, superconducting linear accelerators (linacs) for FRIB, and synchrotrons for FAIR. However, all facilities begin the acceleration with low charge state ions from the ion source and strip their charge once or twice during acceleration to increase the energy gain or decrease magnetic rigidity.

After passing through a stripper thick enough to reach a charge equilibrium, the charge state is an increasing function of projectile energy. Figure 1 shows the equilibrium charge state of uranium ions in solid as a function of projectile energy. In this study, we focus on charge strippers for uranium ion acceleration because these strippers encounter the most difficult problems due to largest heat deposits and heaviest radiation damage. The lines in Fig. 1 show the paths of the charge states at the three facilities. To increase the charge from 4+ to 28+, FAIR uses an N<sub>2</sub> gas stripper at 1.4 MeV/u because the acceleration of the low charge state to 28+ is essential for reducing space charge forces in the pulsed operation. To increase the charge from 33.5+ to 78+ on average, FRIB uses a liquid lithium stripper at 17 MeV/u. About 80% of the input ions can be gathered

using multi-charge-acceleration technique. Finally, RIBF adopted two-step charge stripping at 11 MeV/u and 51 MeV/u to increase the charge from 35+ to 86+. We identify the following requirements for charge strippers:

- High charge state,
- High stripping efficiency,
- Small energy spread,
- Long lifetime,
- Good stability.

A high charge state is required to reduce the total accelerating voltage and cost. In this sense, solid or liquid strippers are preferred because the density effect provides about 20% higher charge states compared to gas strippers. Suppression of electron capture in low-Z materials is another method for obtaining a higher charge state [4]. This suppression comes from the slow velocity of electrons in low-Z materials, and the resulting stripping efficiency should be high. The typical stripping efficiency of a charge stripper is around 10–30%. Using too many strippers decreases beam intensity to zero. In some cases, the shell effect aids the high stripping efficiency. Moreover, the energy spread after the beam passes through the stripper should be small. There are the main two causes for the energy spread: non-uniformity in the stripper thickness, and straggling charge state energy arising from the fluctuation of charge states in the material [5]. The lifetime of the charge stripper should be long. In particular, lifetime-related problems are critical to high-power beam operation. Finally, good stability contributes to the stable operation of the accelerator complex.

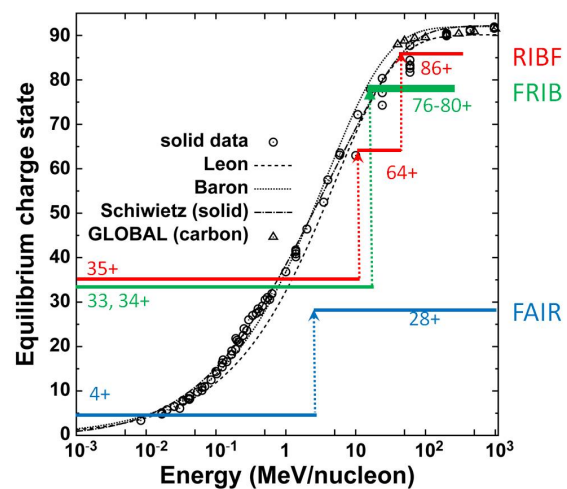


Figure 1: Charge evolutions in uranium acceleration for FAIR, FRIB, and RIBF as a function of projectile energy with an equilibrium charge state.

# PRESERVING BEAM QUALITY IN LONG RFQS ON THE RF SIDE: VOLTAGE STABILIZATION AND TUNING

Antonio Palmieri INFN-LNL, Legnaro (PD), Italy

## Abstract

RFQs are the injectors customarily used in modern linacs and the achievement of a high beam transmission for a RFQs is of paramount importance in case of both high intensity linacs and RIBs facilities. This calls for an accurate control of the longitudinal inter vane voltage along the four structure quadrants (field stabilization), in order to keep its deviation from nominal value as low as possible (a few %, typically). In particular, for long RFQs (in which the structure length can be significantly higher than the RF wavelength), this aspect is more challenging, since the effect of a perturbation (e.g. due to mechanical errors and/or misalignments) on the nominal RFQ geometry has a major impact on voltage. This paper describes and analyses these issues, as well as the methods used to tackle them.

## INTRODUCTION

In some important cases, the achievement of a high beam transmission (>95%) for a RFQ is a key issue for the proper operation of the overall facility in which the RFQ is included. This is particularly true in the cases of high intensity proton and/or deuteron RFQs (avg. beam power > 10 kW) and in the case of RIB acceleration. In the first case, the high space charge at low energy induces beam losses giving rise to the structure activation with the production of neutrons, (p-Cu and d-d reactions), and the loss control has to be compliant with a hands-on maintenance of the machine. In the second case, the RIB current loss can jeopardize the quality of the outcomes of Nuclear Physics experiments, while lost RIBs in the RFQ can give rise to high-lifetime decay products, which can undergo implantation reactions in the RFQ body.

These circumstances call for the adoptions of some adjustments in beam dynamics design and some stricter constraints on mechanical and electromagnetic parameters.

One of the adjustments is the accurate control of the longitudinal behavior of the inter-vane voltage along the four quadrants of the structure, and of voltage disuniformities among the quadrants with deviations from the nominal values that shall not exceed a few %. For instance, the following table lists these constraints for the RFQs being developed at LNL, namely the IFMIF RFQ [1], the TRASCO RFQ [2] and the SPES RFQ [3]. All of these RFQs have been designed for CW operation.

Table 1: RFQs Developed at LNL: Main Parameters

	TRASCO	IFMIF	SPES
status	Constructed	Construction in progress	Developing
f [MHz]	352.2	175	80
l [m]	7.13	9.8	7.2
R <sub>0</sub> [mm]	2.93-3.07	4.13-7.10	5.27-7.86
ρ/R <sub>0</sub>	1	0.75	0.76
I <sub>b</sub> [mA]	30	125	1e-6
V[kV]	68	79-132	64-86
W [MeV/u]	5	5	0.727
E.M. segments	3	1	1
Mech. modules	6	18	6
dV/V range	±1%	±2%	±3%
Q <sub>0</sub>	8000 (20% margin)	12000 (25% margin)	16000 (20% margin)
RF power [kW]	800 (20% margin)	1250(25% margin)	120(20% margin)

In order to understand the causes of these voltage deviations, it should be pointed out that the effect of a perturbation (e.g. due to mechanical errors and/or misalignments) on the nominal geometry in a four-vane RFQ provokes a mixing of the operating TE<sub>210</sub> mode (Quadrupole mode) with neighboring quadrupole TE<sub>21n</sub> and TE<sub>11n</sub> dipole modes. Now, if the overall RFQ length l is significantly greater than the wavelength λ, the eigenfrequencies f<sub>n</sub> of the neighbouring modes can be very close to the operational one, i.e. f<sub>0</sub>, thus enhancing the perturbation effect. The measures that are undertaken to tackle this issue consist in the “stabilization” and “tuning”. In particular, the RFQ stabilization involves actions that can be taken before knowing the actual RFQ voltage profile (i.e. in the design phase), namely: 1) The usage of coupling elements (resonant coupling) [4] this method consists in dividing the RFQ in N resonantly coupled segments and has the advantage of increasing the frequency spacing between the f<sub>0</sub> and the frequencies of the other quadrupole modes. This method is used mainly in RFQs with L/λ > 6 [5, 6, 7], 2). The usage of stabilizing devices for the dipole modes (dipole stabilizers or DSRs) [8]: this method consists in inserting longitudinal bars in the RFQ volume in correspondence of the end-cells and coupling cells, which do not perturbate

# H<sup>-</sup> BEAM OPTICS FOR THE LASER STRIPPING PROJECT

T. Gorlov, A. Aleksandrov, S. Cousineau, V. Danilov, M. Plum, ORNL, Oak Ridge, TN, USA

## Abstract

Successful realization of the laser stripping experiment depends on the correct tailoring of the H<sup>-</sup> bunch and the laser beam. H<sup>-</sup> beam preparation is a challenging task, with the requirement to tune up about 10 parameters simultaneously in situ, taking into account the live state of the accelerator. This makes a huge technological difference compared to the foil stripping method. In this paper, we present our experience and our methods of tuning the H<sup>-</sup> beam.

## INTRODUCTION

We prepared an experiment to demonstrate laser assisted stripping of a 10 microsecond H<sup>-</sup> beam at the Spallation Neutron Source (SNS) accelerator. The general up-to-date information about the status of the project can be found in [1, 2]. More information about the history and background can be found in [3, 4]. The new experiment expects to achieve more than 90% stripping efficiency. This requires an experimental station including routine hardware, magnets [5], and beam instrumentation. The most important scientific aspect for successful realization of the experiment is the tuning of the laser beam and the H<sup>-</sup> beam at the interaction point. The recent work about the laser system can be found in [6]. In this present paper, we present a theory and experimental methods of tuning the H<sup>-</sup> beam.

The first big challenge of beam tuning is that all of the H<sup>-</sup> beam parameters, such as Twiss parameters and the dispersion functions, must be tuned simultaneously for high efficiency stripping. Laser tuning is a large, separate work and is based on the H<sup>-</sup> beam parameters. This factor makes the method of laser stripping injection much more difficult compared to the foil stripping injection. Another particular difficulty is that the SNS accelerator has not been developed for this sort of experiment, and beam tuning and manipulation is limited and not optimized. The location of the experiment has been chosen taking into account maximum beam flexibility at the interaction point (Figure 1).

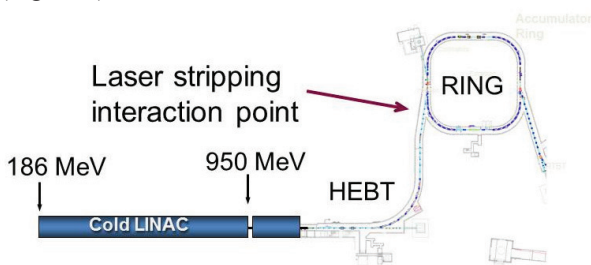


Figure 1. Location of the laser stripping experiment at SNS.

In this paper we will discuss various methods of H<sup>-</sup> beam parameter tuning for the laser stripping experiment.

ISBN 978-3-95450-173-1

## INTERACTION BETWEEN H<sup>0</sup> AND LASER BEAM

After H<sup>-</sup> → H<sup>0</sup> + e<sup>-</sup> stripping by the first stripping magnet, the H<sup>0</sup> bunch interacts with the laser beam at the interaction point (Figure 2), which provides excitation of

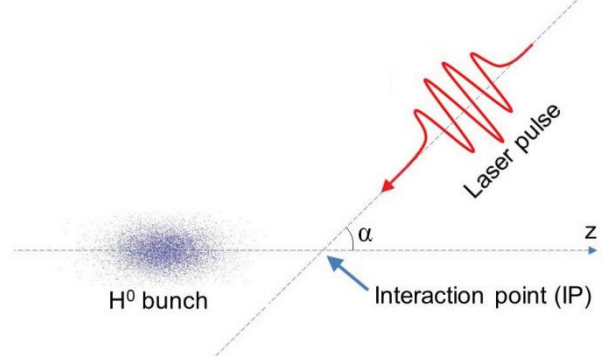


Figure 2. Interaction of H<sup>0</sup> beam with the laser beam.

H<sup>0</sup> from the first ground state to the third excited state. The beam energy is supposed to be 1 GeV in the experiment and incidence angle  $\alpha$  between laser and H<sup>0</sup> beam, which can be calculated from Equation (1) [3]:

$$\lambda_0 = \frac{\lambda}{\gamma(1 + \beta \cos \alpha)} \tag{1}$$

where  $\gamma$  and  $\beta$  are relativistic factors of a bunch. This formula gives most optimal resonant conditions for H<sup>0</sup> beam excitation. This formula gives  $\alpha = 39.33^\circ$  for  $T_{H^0} = 1$  GeV. The theory of laser stripping excitation [3] shows that each particle of the H<sup>0</sup> beam should interact with the laser beam in a proper way (it must have proper energy, angle, and position). In this way, Twiss parameters of the H<sup>0</sup> bunch must be properly tuned for high efficiency excitation.

## TRANSVERSE BEAM OPTICS

Transverse beam parameters can be defined at least by three vertical  $\{\alpha_y, \beta_y, \epsilon_y\}$ , and three horizontal  $\{\alpha_x, \beta_x, \epsilon_x\}$  Twiss parameters plus dispersion and its derivative. The laser stripping location point (see Figure 1) has a large number of "knobs" to control these parameters.

### Transverse Emittances

Equation (1) can be considered as a perfect resonant condition for particle excitation, although the whole bunch has some angular spread depending on emittances  $\epsilon_x, \epsilon_y$ . The default non-normalized emittances during SNS production is about  $0.3 \pi \text{ mm} \times \text{mrad}$  for the vertical and the horizontal plane. This number can be reduced to  $0.1 \pi \text{ mm} \times \text{mrad}$  and smaller with the help of LINAC apertures. In addition to the angular spread, small

## BEAM DYNAMICS AND EXPERIMENT OF CPHS LINAC \*

L. Du<sup>#</sup>, C.T. Du, X.L. Guan, C.X. Tang, R. Tang, X.W. Wang, Q.Z. Xing, S.X. Zheng, Key Laboratory of Particle & Radiation Imaging (Tsinghua University), Ministry of Education, Beijing 100084, China

M.W. Wang, Northwest Institute of Nuclear Technology, Xian, China

### Abstract

We present, in this paper, the present beam dynamics simulation results and experiments of the 3 MeV high current proton linac for the Compact Pulsed Hadron Source (CPHS) at Tsinghua University. The beam dynamics simulations of the recent status of the linac have been done, which helps the operation. Facility used for 2D beam profile measurement which is based on the CT algorithm with rotatable multi-wires, is under development. Some other experiments such as beam position measurement will also be introduced below.

### INTRODUCTION

The Compact Pulsed Hadron Source (CPHS) project at Tsinghua University was launched in the year of 2009 [1], whose layout is shown in Figure 1. The final expected parameters of the CPHS linac are: beam energy to be 13 MeV, beam current to be 50 mA, repetition rate to be 50 Hz and pulse length to be 500  $\mu$ s.

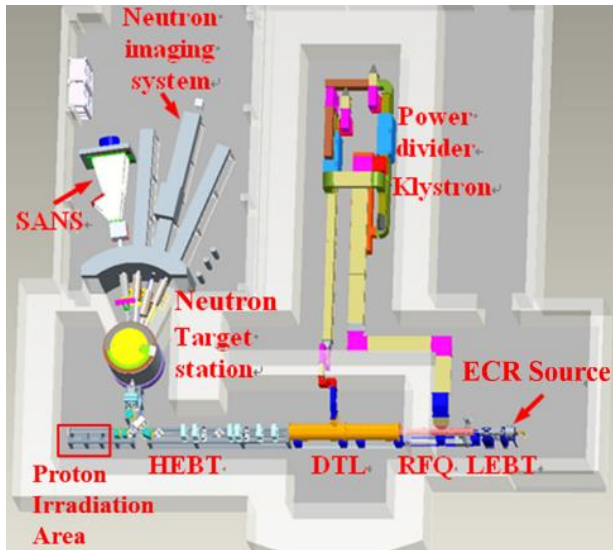


Figure 1: Layout of CPHS project.

So far, CPHS has achieved its mid-term objective: delivering the 3 MeV proton beam to bombard the Beryllium target [2]. Figure 2 shows the status of CPHS linac facility at Tsinghua University recently, which contains one ECR Ion Source (IS), one Low Energy Beam Transport line (LEBT), one 4-vane Radio Frequency Quadrupole (RFQ) accelerator, and one High Energy Beam Transport line (HEBT) [3].

\*Work supported by National Natural Science Foundation of China (Major Research Plan Grant No. 91126003 and 11175096) #807749514@qq.com

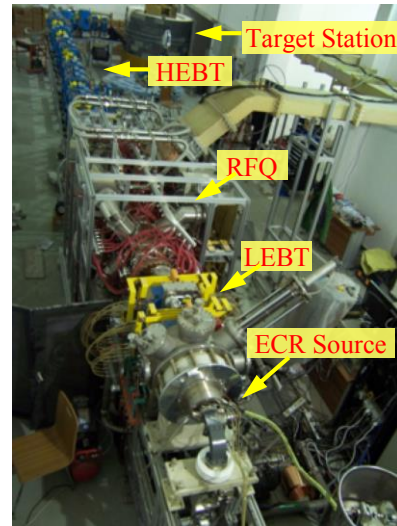


Figure 2: CPHS linac facility and the target station.

Figure 3 shows the operation status of the CPHS linac in 2014. The transmission rate of the RFQ is 70% recently, which is lower than the designed value of 97% and primary experimental value of 88% (with input peak current of 50mA at 50  $\mu$ s/50 Hz). The reason may come from the unmatched beam from the LEBT, or the deformation of the RFQ cavity. Therefore, the linac will be inspected separately to solve the problem in the next stage.

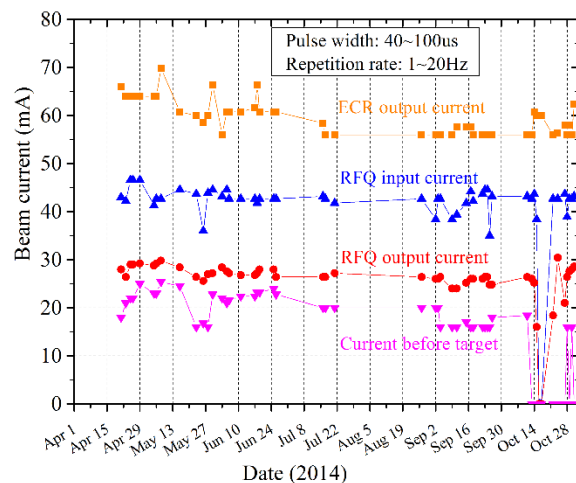


Figure 3: Operation history of the 3 MeV linac in 2014.

In this paper, the beam dynamics simulation results of the recent status of the CPHS linac are presented. Experiments such as beam profile measurement and beam position measurement are introduced.

# CATALOGUE OF LOSSES FOR THE LINEAR IFMIF PROTOTYPE ACCELERATOR

N. Chauvin\*, P.A.P. Nghiem, D. Uriot, CEA, IRFU, F-91191 Gif-sur-Yvette, France  
 M. Comunian, INFN/LNL, Legnaro, Padova, Italy  
 C. Oliver Amoros, CIEMAT, Madrid, Spain

## Abstract

One of the activities of the EVEDA (Engineering Validation and Engineering Design Activities) phase of the IFMIF (International Fusion Materials Irradiation Facility) project consists in building, testing and operating, in Japan, a 125 mA/9 MeV deuteron accelerator, called LIPAc, which has been developed in Europe.

For the accelerator safety aspects, a precise knowledge of beam loss location and power deposition is crucial, especially for a high intensity, high power accelerator like LIPAc. This paper presents the beam dynamics simulations allowing to estimate beam losses in different situations of the accelerator lifetime: starting from scratch, beam commissioning, tuning or exploration, routine operation, sudden failure. Some results of these studies are given and commented. Recommendations for hot point protection, beam stop velocity, beam power limitation are given accordingly.

## INTRODUCTION

For a high power megawatt class accelerator, any loss, even a tiny proportion of the beam, can be harmful. A careful and detailed loss study is thus necessary for various loss scenarios. That should be analysed for all the different stages of the accelerator lifetime, from its starting up, beam commissioning through routine operation, as well as for the various accidental breakdowns. Such a catalogue will be useful, or even necessary in the definition of safety procedure, limitations and recommendations, aiming at protecting personnel or facilities.

The linear IFMIF prototype accelerator (LIPAc) is being constructed in Europe and will be assembled in Japan [1]. This machine aims at accelerating a 125 mA  $D^+$  continuous beam at 9 MeV. The general layout of LIPAc is recalled in Fig. 1, where beam energy and power for each subsystem are also given (for more details see Ref. [2]).

The LIPAc very high continuous beam intensity implies that almost the whole accelerator is concerned by a high power beam which ranges from 0.012 to 1.125 MW. It is common to consider that it is safe enough to use the lowest duty cycle and the lowest beam intensity during beam commissioning or during accelerator tests and exploration. But in the present case, as the ion source is optimised to provide a 140 mA continuous beam, the lowest duty cycle for which the beam is still stable is a few  $10^{-3}$ . Indeed, 1 ms is a typical time scale for the ECR source plasma to be established and for the extracted beam to reach a steady state. Furthermore,

the nominal beam intensity implies a very high space charge regime. So, any beam tuning with too low intensity will not be representative of the nominal conditions because of much lower space charge effects. Thus, the ability to lower the beam power is considerably limited. In the same way, a beam stop system is foreseen in the LEBT to shut off the beam in an accidental case in less than 10  $\mu$ s. It is not sure that such a machine protection system is fast enough for a MW beam power.

This paper will mainly focus on the protocol and methodology that has been employed to simulate different loss situations; then, some results are presented and discussed in a few loss scenarios and finally, consequences on safety measures are drawn.

## LOSS STUDY PROTOCOL

In the following, the losses are given in power deposition (Watt). They are obtained with the nominal (maximum) current of 125 mA, continuous wave. From that, losses can be reduced if needed, by reducing consequently the duty cycle and even the current if necessary. Theoretically, because space charge effects decrease with intensity, losses at lower current are less than what can be inferred by a linear relation. But as a precaution, it is wise to deduce losses at lower current with a simple linear transformation.

The double issue is to define as exhaustively as possible all the typical loss situations in the accelerator lifetime and to define the procedure to simulate and estimate them. The following stages have been identified: (A) Ideal machine; (B) Starting from scratch; (C) Beam commissioning, tuning, exploration; (E) Routine operation; (E) Sudden failure.

### *Situation A: Ideal Machine*

“Ideal” means here nominal machine parameters and tunings, without any error. That should correspond, on the real machine, to a completely satisfying situation, if all the accelerator components would be perfectly fabricated and aligned, or else corrected at the source, and the beam would have been tuned. Losses in such conditions should be minimum; we cannot hope to have less. These are minimum and permanent losses that have to be withstood. It is very unlikely, (although highly desirable!) that this situation will occur on the real machine. At least, this situation is an optimal reference case that can be used as a comparison to the other scenarios described in the following subsections. The losses are obtained by a start-to-end simulation without any error for the nominal tuning [3].

\* Nicolas.Chauvin@cea.fr

# ECRIS DEVELOPMENTS TOWARDS INTENSE HIGH BRIGHTNESS HIGHLY-CHARGED ION BEAMS \*

L. Sun<sup>#</sup>, W. Lu, Y. Yang, X. Fang, Y. C. Feng, W. H. Zhang, J. W. Guo, X. Z. Zhang, C. Qian,  
H. W. Zhao  
IMP/CAS, Lanzhou, 730000, China

## Abstract

To meet the increasing needs of modern heavy ion accelerators, ECR ion source must be developed to deliver high intensity high brightness high charge state ion beams, in terms of accelerator output power and beam transmission efficiency. With the success in several laboratories on fully superconducting ECR ion source development, the performance of highly charged heavy ion beams have been greatly enhanced. For instance,  $U^{33+}$  intensity had been doubled in 2011 by VENUS source at LBNL. This paper will present the development work at IMP towards high performance ECR ion source. Recent high intensity bismuth results will be given, such as 710  $\mu\text{A}$   $Bi^{30+}$  with SECRAL source. The first room temperature ECR ion source using evaporative cooling technique will also be reviewed. And the discussion of ECRIS beam extraction and the transmission beam line elements on ion beam quality will also be presented in this paper.

## INTRODUCTION

Since been used as preinjectors for heavy ion accelerators about 30 years ago, Electron Cyclotron Resonance (ECR) ion source has been an indispensable machine to provide intense CW or long pulse ( $\sim\text{ms}$ ) highly charged ion beams. The development of nuclear research strongly demands the modern heavy ion accelerators to be constructed or under construction to be capable of delivering high power heavy ion beams on the targets. To make the accelerators cost efficient, and achieve the design goal, intense highly charged heavy ion beams must be provided in the front end section. The FRIB project under construction at MSU campus needs 13  $\mu\text{A}$   $U^{33+}$  &  $34+$  beam from the ion source and a dedicated achromatic transmission line and the successive matching beam line for downstream RFQ [1]. The SPIRAL 2 project going on at GANIL laboratory, eventually 1  $\text{emA}$   $Ar^{12+}$  is expected to be delivered from the ion source to reach the goal of 1  $\text{emA}$  heavy ion beam with the  $M/Q = 3$  for  $M \leq 36$  [2]. And the RIKEN RIBF project also demands 15  $\mu\text{A}$   $U^{35+}$  eventually [3]. For the upgrade programme at IMP, the HIRFL facility needs the ion source being capable of producing very high charge state heavy ion beams with sufficient beam intensities, such as 100  $\mu\text{A}$   $Xe^{31+}$  and  $U^{41+}$ . All these facilities have made ECR ion sources in the baseline design to reach the desired parameters, due to the features of its high capacity

of intense high charge state heavy ion beam production. Fundamentally, the front end beam properties are determined by the ion source performance and the successive low energy beam transmission (LEBT) line design. The intrinsic properties have big impact on its output beam quality, which should be taken care of during the ion source and its LEBT design. A high performance ECR ion source injector front end should be an optimum design of both the ion source and the matching LEBT line, which enables the front end section to be capable of providing high brightness ion beam with sufficient beam intensity. In the following contents, the production of intense heavy ion beams with an ECR ion source will be generally reviewed, and the features of the ECR ion source LEBT line will also be discussed in terms of beam quality.

## INTENSE BEAM PRODUCTION WITH MODERN ECR ION SOURCES

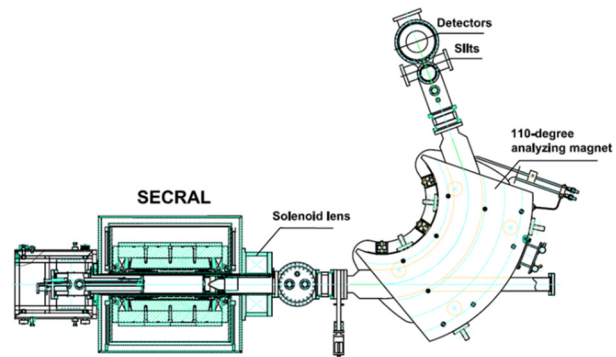


Figure 1: SECRAL ion source and LEBT layout.

ECR ion source is a kind of magnetic confined plasma machine, which was actually developed based on plasma fusion device [4]. Plasma electrons are heated through ECR heating to high energy by coupled microwave power with the frequency in the range of 2.45 GHz to 28 GHz. The plasma is confined by a strong nested so-called mini-B magnetic field configuration, which is the superposition of an axial mirror field and a radial multiple field (normally a hexapole field). Hot electrons are confined at the centre of the nested field and the HCIs, which are produced by stepwise ionization while they are confined in the plasma, are trapped by the space charge established by the electrons inside the plasma. The lost ions that enter the extraction region will be accelerated by the applied HV potential to form intense mixed ion beams. HCI beams in the extracted mixing beam can be separated with an analyser dipole magnet. Normally, a solenoid is used to focus the extracted intense beams to match the downstream elements. Fig. 1

\*Work supported by the 100 Talents Program of the CAS (No. Y214160BR0), NSF (contract No. 11221064) and MOST (contract No. 2014CB845500).

#sunlt@impcas.ac.cn

# THE KICKER IMPEDANCE AND ITS EFFECT ON THE RCS IN J-PARC

Y. Shobuda, P. K. Saha, T. Toyama, M. Yamamoto, J-PARC Center, Ibaraki, JAPAN  
 Y. H. Chin and Y. Irie, KEK, Ibaraki, JAPAN

## Abstract

Measurements demonstrate that the kicker impedance dominates along the RCS. Based on a newly developed theory, the impedance is measured by observing the beam-induced voltages at the ends of power cable of the kicker. Toward one mega-watt goal, it is essential to take advantage of tune manipulations and the space charge damping effect. A reduction scheme of the kicker impedance is proposed to pursue the ultimate goal at the RCS.

## INTRODUCTION

There are the accelerators aiming at producing mega-watt class beams in the world [1, 2]. One of such facilities is the 3GeV rapid cycling synchrotron (RCS) in Japan Proton Accelerator Research Complex (J-PARC) [1]. In order to extract the high intensity beams from the RCS, eight distributed type kicker magnets are installed in the RCS [3].

On the other hand, in order to steadily circulate the high intensity beams in the RCS, it is important to precisely estimate the coupling impedances along the ring. In the RCS, the coupling impedance has been lowered except the kicker impedance [4]. When we apply Sacherer's formula [5], the beam should become unstable around 100 kW, where the chromaticity  $\xi$  is fully corrected in the entire energy. Accordingly, it has been concerned that the kicker impedance disturbs realizing the high intensity beam in the RCS.

Contrary to our expectation, the beam at last becomes unstable beyond about 300 kW with the fully chromaticity correction. This means that a significant gap exists between the theoretical prediction and the measurement results.

The situation has goaded us to review the estimation of the kicker impedance from theoretical and experimental points of view. In the process, the authors have found that the causality condition is not satisfied in Nassibian's formula [6, 7] describing the impedance of the kicker where all terminals are connected to the matched resistors.

Accordingly, a theory has been developed to estimate the kicker impedance. The theory describes the impedance, where the terminals of the kicker magnet are connected to the power cables [8] as well as to the matched resistors [9]. The theoretical results well reproduce the measurement results by using the standard wire-measurement scheme [10]. Moreover, the theory successfully relates the beam-induced voltages at the ends of the cables to the kicker impedance. One advantage of developing the theory is to enable to find the kicker impedance by letting a beam pass through the kicker and by measuring the beam-induced voltages at the ends of the cables.

At the same time, simulation studies have been progressing. The beam simulation code ORBIT, which is originally developed in SNS [2] for storage rings, has been upgraded by

J. Holmes in order to incorporate the Lorentz- $\beta$  dependence of the kicker impedance into the code. The precise estimation of the impedance brings the code into action, especially in the serious condition as in the RCS.

Before we discuss a strategy to accomplish one mega-watt beam, let us review how to produce the kicker impedance from the beam-induced voltage.

## KICKER IMPEDANCE

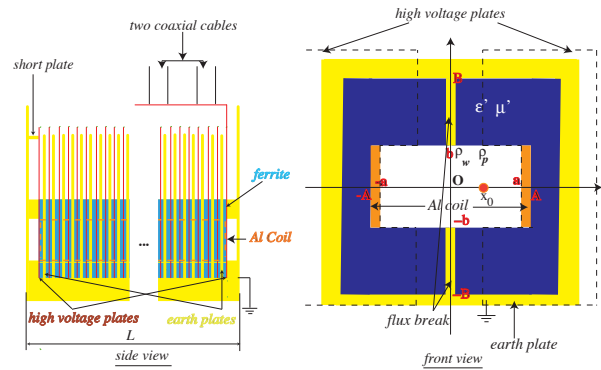


Figure 1: A schematic picture of the kicker magnet.

A schematic picture of the kicker magnet is shown in Fig. 1. The kicker magnet has four terminals at the corners. The right front and the left back terminals of the kicker are terminated by the short plates, respectively. The short plates double the excitation current by superposing the forward and backward currents, when a beam is extracted from the RCS. The right back and the left front terminals are connected to two-parallel coaxial cables, respectively.

The formulae of the kicker impedances are described as follows,

$$Z_L = Z_L^{(0)}(x_0 = x = 0) + Z_L^{(1)}(x_0 = x = 0) + Z_L^{(crr)}(x_0 = x = y = 0) \approx Z_L^{(0)}(x_0 = x = 0) + Z_L^{(crr)}(x_0 = x = y = 0), \quad (1)$$

$$Z_x = \frac{\partial^2 Z_L(x_0, x, y = 0)}{k \partial x_0 \partial x} \Big|_{x_0=x=0} \approx \frac{\partial^2 Z_L^{(1)}(x_0, x, y = 0)}{k \partial x_0 \partial x} + \frac{\partial^2 Z_L^{(crr)}(x_0, x, y = 0)}{k \partial x_0 \partial x} \Big|_{x_0=x=0}, \quad (2)$$

where  $Z_L$  and  $Z_x$  are the longitudinal and the horizontal impedances, respectively,  $x_0$  and  $x$  are the horizontal positions of the source and the witness particles, respectively,

# RING SIMULATION AND BEAM DYNAMICS STUDIES FOR ISIS UPGRADES 0.5 TO 10 MW

D.J. Adams, B. Jones, B.G. Pine, C.R. Prior\*, G.H. Rees\*, H.V. Smith, C.M. Warsop, R.E. Williamson, ISIS and \*ASTeC, Rutherford Appleton Laboratory, STFC, UK

## Abstract

Various upgrade routes are under study for the ISIS spallation neutron source at RAL in the UK. Recent work has concentrated on upgrading the injector, increasing injection energy from 70 to 180 MeV, and studying the challenging possibility of reaching powers up to 0.5 MW in the existing 800 MeV RCS. Studies for the longer term are exploring the possibilities of a 5 MW, 3.2 GeV RCS that could form part of a new stand-alone 10 MW next generation “ISIS II” facility. A central part of these ring studies is the use of computer simulations to guide designs, for example optimising the injection painting configuration and providing an indication of expected loss levels. Here we summarise the computer models used, indicate where benchmarking has been possible, describe optimisations and results from studies, and outline the main uncertainties. Understanding the limitations in high power RCS accelerators is an important part of determining optimal facility designs for the future.

## INTRODUCTION

A range of ISIS upgrade routes is now under study, a lower beam power regime of 0.5 MW, and a higher power regime from 1 MW upwards. A key factor determining the optimal beam power for future short pulse spallation sources will be the results of ongoing target and moderator studies, which are working to optimise the brightness of neutron beams for the user.

In the lower power regime, an upgrade replacing the existing 70 MeV ISIS linac with a new 180 MeV injector is the favoured route. This could potentially boost powers to 0.5 MW and also address obsolescence issues with the present linac. This paper summarises the design of the beam dynamics for the existing ISIS RCS with the new 180 MeV injector.

For the higher power routes, a new stand alone option (“ISIS II”) is the favoured route, with an initial beam power of 1 - 2 MW, capacity for multiple targets and further upgrade routes to 5 or even 10 MW. Studies are presently concentrating on a “base-line” option, consisting of an 800 MeV H<sup>-</sup> linac and a 3.2 GeV RCS, which has been studied in some detail [1]. Such a design would have the potential for 2 – 5 MW with a single ring, and 10 MW with two stacked rings. Understanding the limitations and optimising parameters for this 3.2 GeV RCS are thus an important step in identifying the best designs. Other options, (e.g. FFAGs), will have to compare favourably with this base-line. Initial results from 1D and 3D simulations of the 2 - 5 MW, 3.2 GeV RCS are also presented below.

## 180 MEV INJECTION UPGRADE

The main potential benefits to the synchrotron of a new higher energy linac, chopper and energy ramping injection line are reduced transverse space charge and more flexible, optimised transverse and longitudinal injection systems.

Currently a 70 MeV, 25 mA H<sup>-</sup> linac provides a pulse length of 200  $\mu$ s for injection into the RCS. Beam is accumulated via charge exchange through a foil centred in a 4-magnet, symmetric, horizontal bump, with 45 mr deflections. Beam is painted dispersively in the horizontal plane, exploiting orbit motion due to the falling main magnet field. Vertically a sweeper magnet paints the position at the foil. About  $3 \times 10^{13}$  protons per pulse (ppp) are accumulated over 130 turns. Transverse acceptances are collimated at  $\sim 350 \pi$  mm mr using an adjustable collector system.

The DC accumulated beam is non-adiabatically trapped into two bunches by the ring dual harmonic RF (DHRF) system. The RF system consists of 10 ferrite tuned cavities, with peak design voltages of 168 and 96 kV/turn for the  $h=2$  and 4 harmonics respectively. Nominal betatron tunes are  $(Q_x, Q_y)=(4.31, 3.83)$ , with peak incoherent tune shifts of  $\sim 0.5$ . Intensity is loss limited: the main mechanisms are longitudinal trapping, transverse space charge and stability. Single turn extraction uses a fast vertical kicker and septum.

Most of the existing ring would remain unchanged for the upgrade. However, a new injection straight with higher field bump magnets and new injection beam dumps would be required. Also the ring collimation system would need modifications to intercept beam losses at higher energies. To facilitate hands on maintenance machine activation levels would be kept at existing levels.

## Transverse Space Charge and Stability

Reduction of transverse space charge with increasing injection energy is expected to scale as  $\beta^2 \gamma^3$  allowing the existing injection intensity of  $3 \times 10^{13}$  ppp at 70 MeV (0.2 MW) to be raised to  $8 \times 10^{13}$  ppp (0.5 MW). This simple scaling law gives basic guidance, but detailed assessment and simulations with the in-house code Set [2] confirm that these intensities are the upper limit, which depend on achieving optimal bunching factors, emittances and working points. The smaller energy ramp, 180 - 800 MeV, also reduces emittance damping, which will require a small increase in the extraction system acceptance [2]. Instabilities are one of the major concerns with the most obvious problem being resistive-wall head-tail already observed on ISIS [3]. This is presently avoided by lowering  $Q_y$ . The growth rate can be expected

# RECENT RESULTS ON BEAM-BEAM EFFECTS IN SPACE CHARGE DOMINATED COLLIDING ION BEAMS AT RHIC\*

C. Montag, BNL, Upton, NY 11973, USA

## Abstract

To search for the critical point in the QCD phase diagram, RHIC has been colliding gold ions at a variety of beam energies ranging from 2.5 GeV/n to 9.8 GeV/n. During these low energy operations below the regular injection energy, significant lifetime reductions due to the beam-beam interaction in conjunction with large space charge tune shifts have been observed. Extensive simulation studies as well as beam experiments have been performed to understand this phenomenon, leading to improved performance during the 7.3 GeV run in FY2014.

## INTRODUCTION

The Relativistic Heavy Ion Collider RHIC was designed to collide beams of fully stripped Au ions at a top energy of 100 GeV/nucleon. To search for the critical point in the QCD phase diagram, center-of-mass energies in the range from 5 to 20 GeV per nucleon pair are required, which extends far below the nominal RHIC injection energy of 9.8 GeV/nucleon. At such low energies, the space charge tune shift becomes significant, and typically exceeds the beam-beam tuneshift by an order of magnitude [1].

When RHIC operated at beam energies of 3.85 and 5.75 GeV/nucleon in 2010, a significant reduction in beam lifetime due to the beam-beam interaction was observed, as illustrated in Figure 1. During that entire physics run, the working point was set at  $(Q_x, Q_y) = (28.13, 29.12)$  as the result of a brief tune scan.

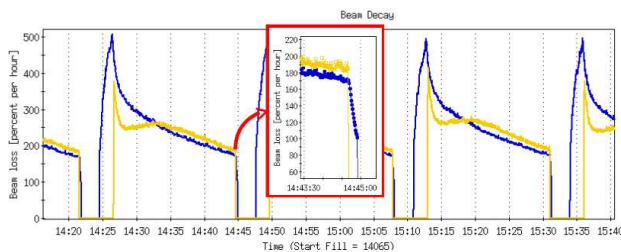


Figure 1: Beam decay rates during several Au beam stores at 5.75 GeV/nucleon beam energy. The Blue beam decay rate improves dramatically as soon as the Yellow beam is dumped at the end of each store (see insert). Note that the algorithm to calculate the beam decay rate from the measured beam intensity has a time constant of 20 sec. Hence, the actual drop in instantaneous beam decay is even more dramatic than suggested by the picture.

To gain a better understanding of beam-beam effects in space charge dominated colliding ion beams, extensive sim-

ulations have been performed. In the following sections, we describe the simulation methods and present results on emittance growth as well as frequency map analysis and diffusion studies.

## TRACKING MODELS

Space charge simulations tend to be very CPU-time consuming due to the frequent recalculations of the particle distributions and associated electro-magnetic fields. However, in the particular problem under study here, we can take advantage of the fact that the evolution of the particle distribution is comparatively slow, as indicated by the experimentally observed beam decay of several hundred percent per hour, which is equivalent to a beam lifetime of tens of minutes. Since typical simulations track particles only over a number of turns that corresponds to seconds in real beamtime, we can therefore assume that the particle distribution remains constant in amplitude space over the course of the simulation. This approach, which is similar to the weak-strong method of beam-beam simulations, significantly speeds up the simulation. In addition, since re-calculating the electro-magnetic fields from the actual particle distribution is avoided, no artificial noise due to the limited number of particles is introduced into the simulation. Furthermore, since the space charge kicks do not depend on the actual distribution of test particles, we can apply methods such as frequency map analysis or action diffusion that require special, non-realistic distributions.

Two different accelerator models are used for tracking, a simplified “toy model”, and the realistic RHIC lattice. The simplified model consists of 11 FODO cells. The quadrupoles are modeled as thin lenses, while the dipoles in this “ring” are just drifts, i.e. their bending radius is infinite. 10 of these FODO cells are identical, while in the 11th cell the quadrupole strengths are increased by 3 percent to break the periodicity of the lattice. The phase advance per FODO cell is approximately 108 degrees, depending on the exact working point. In the center of one of the drifts of the 11th cell a beam-beam kick is applied. The drift spaces (“dipoles”) are subdivided into 32 slices of equal length each; at the end of each slice a space charge kick is applied according to the local  $\beta$ -functions and the beam emittance, which is assumed to be constant. The tune is adjusted using all quadrupoles simultaneously. The space charge tune shift in this model is set to  $\xi_{sc} = -0.05$ , while the beam-beam tune shift is set to  $\xi_{bb} = -0.003$ . In cases without beam-beam interaction, the space charge tune shift is set to  $\xi_{sc} = -0.053$ ; this ensures that the total tune shift is identical in both cases.

\* Work supported by Brookhaven Science Associates, LLC under Contract No. DE-AC02-98CH10886 with the U.S. Department of Energy.

# PERFORMANCE OF TRANSVERSE INTRA-BUNCH FEEDBACK SYSTEM AT J-PARC MR

Y. H. Chin, T. Obina, M. Okada, M. Tobiyama, T. Toyama, KEK, Ibaraki, Japan  
 K. Nakamura, Kyoto University, Kyoto, Japan  
 Y. Shobuda, JAEA, Ibaraki, Japan

## Abstract

A new broadband ( $\sim 100$  MHz) feedback system has been developed for suppression of intra-bunch oscillations and reduction of particle losses at the J-PARC Main Ring (MR). A new BPM has been designed and fabricated, based on Linnecar's exponential coupler stripline type, for a flatter and wider frequency response. The design and performance of the new BPM as well as preparation of a newly installed exciter and power amplifier is presented. We also report beam test results of suppression of horizontal intra-bunch oscillations at 3 GeV with the bunch length of 150-200 ns. Simple simulation results without wake fields and the space-charge effects qualitatively reproduce the experimental results of the intra-bunch FB system.

## INTRODUCTION

The J-PARC is composed of three proton accelerators: the 400 MeV linear accelerator (LINAC), the 3 GeV Rapid Cycling Synchrotron (RCS), and the Main Ring (MR) Synchrotron. The main parameters are listed in Table 1. At the J-PARC MR, transverse instabilities have been observed during the injection and at the onset of the acceleration. The present narrowband bunch-by-bunch feedback system (BxB FB) is effectively suppressing these transverse dipole oscillations, allowing to attaining the 230 kW beam power [1]. But the BxB feedback system can damp only the center of mass motions of the whole bunches. Even with the BxB feedback system on, internal bunch oscillations have been still observed, which is causing additional particle losses [2]. To suppress intra-bunch oscillations, a more wideband and elaborate feedback system (named the intra-bunch feedback system) has been developed [3].

## INTRA-BUNCH FEEDBACK SYSTEM

Figure 1 shows the schematic of the new intra-bunch feedback system. It is composed mainly of three components: a BPM, a signal processing circuit (iGp12) and kickers. It divides each bucket to 64 slices and acts on each slice as if it is a small bunch (bunch-let) in a narrow band feedback system. The signal processing circuit detects betatron oscillation of each bunch slice using signals from the BPM and calculates feedback signals. These feedback signals are sent to the kickers through the power amplifiers. The new system and its set-up are similar to those of the current BxB feedback system. The main improvement is that each component now has a (64 times) wider frequency sensitivity than the one for the

BxB feedback system. The intra-bunch feedback system has been installed at the D3 building, while the current BxB feedback system is still operational at the D1 building.

Table 1: Main Parameters of J-PARC Main

Circumference	1568m
Injection Energy	3GeV
Extraction Energy	30GeV
Repetition Period	2.48s
RF Frequency	1.67-1.72 MHz
Number of Bunches	8
Synchrotron Tune	0.002-0.0001
Betatron Tune (Hor./Ver.)	22.41/20.75

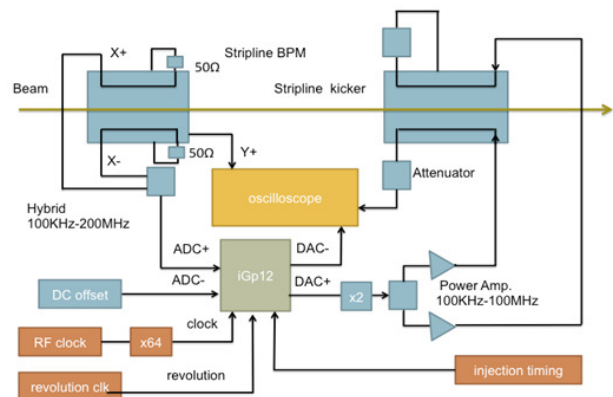


Figure 1: Schematic of the intra-bunch feedback system.

## BPM

The new stripline BPM has been designed and fabricated based on Linnecar's electrode design [4] (see Fig. 2). It is equipped with the exponentially tapered electrodes which, in principle, allow a flatter and wider frequency response (the green line in Fig.3) than the conventional rectangular ones (the blue line in Fig.3). The diameter of the beam pipe is 147mm, and the length of the electrodes is 300mm. The electrodes are placed 67mm from the center of the beam pipe. The height of the electrodes from the chamber surface needs to be gradually reduced (proportional to its width) toward their tips for the impedance matching. The BPM characteristics were measured by the stretched wire method. The measured frequency response is shown by the red line in Fig. 3. It can be seen that the new BPM has a good frequency response up to 1GHz. The position sensitivity is also measured and it is found to be fluctuating around 0.027 by 0.002.

# DYNAMIC CORRECTION OF EXTRACTION BEAM DISPLACEMENT BY FIELD RINGING OF EXTRACTION PULSED KICKER MAGNETS IN THE J-PARC 3-GEV RCS

H. Harada<sup>#</sup>, P.K. Saha, F. Tamura, S. Meigo and H. Hotchi  
J-PARC Center, KEK & JAEA, Tokai-mura, Naka-gun, Ibaraki-ken, Japan

## Abstract

The 3-GeV rapid cycling synchrotron (RCS) of J-PARC is designed for a high-intensity output beam power of 1MW. The RCS is extracted two bunches by using eight pulsed kicker and three DC septum magnets with 25Hz repetition. The extracted beam is simultaneously delivered to the material and life science experimental facility (MLF) as well as the 50-GeV main ring synchrotron (MR). The kicker magnets have the ringing of flat-top field and the ringing causes the position displacement. The displacement is big issue because it causes an emittance growth of the extracted beam directly. In the beam tuning, we performed a timing scan of each kicker magnet by using a shorter pulse beam in order to understand the characteristics of ringing field. We then carefully optimized the trigger timings of each kicker for the ringing compensation. We have successfully compensated the extracted beam displacements to (min., max.) = (-1.1 mm, +0.6 mm) as compared to (-14 mm, +10 mm) with no ringing compensation. The procedure for ringing compensation and experimental results are reported in this paper.

## INTRODUCTION

The Japan Proton Accelerator Research Complex (J-PARC) is a multipurpose proton accelerator facility [1,2], comprising three accelerator facilities that are a 400-MeV LINAC, a 3-GeV rapid cycling synchrotron (RCS), and a 50-GeV main ring synchrotron (MR), and three experimental facilities that are a materials and life science experimental facility (MLF), a hadron experimental hall, and a neutrino beam line to Kamioka. In this chain of accelerators, the RCS has two functions as a proton driver to produce pulsed muons and neutrons at the MLF and as an injector to the MR, aiming at 1-MW output beam power. The RCS was beam-commissioned in October 2007 and the output beam power has been steadily increasing following progressions in the beam tuning, hardware improvements and the realistic numerical simulations [3,4,5]. After the LINAC had been upgraded output energy from 181 to 400-MeV by installation of ACS linac section in 2013 summer-autumn maintenance period, the RCS has successfully achieved output beam power of 300-kW for user operation and demonstrated 550-kW equivalent intensity with beam loss mitigation in our beam study [6]. In 2014 summer maintenance period, the Ion Source (IS)

and RFQ in LINAC were replaced in order to upgrade a peak current from 30 to 50 mA. After upgrading the peak current from LINAC, the RCS started a beam tuning of the designed 1-MW intensity in October 2014. In first trial of the designed 1-MW intensity, we achieved 770-kW equivalent intensity [7]. In higher intensity beams, the trip of RF power supplies was happened. In December 2014 and January 2015, we will retry a beam tuning of 1-MW intensity after the treatment for the RF issue.

As shown in Fig. 1, the RCS extraction system consists of eight pulsed kicker magnets and three DC septum magnets. The extracted beam of two bunches is simultaneously delivered to MLF and MR with a repetition rate of 25 Hz. The pulsed kicker magnet has a ringing of flat-top field and the ringing causes position displacements to the extracted beam for horizontal plane. In this paper, the configuration and field ringing of kicker magnet are introduced and the effect on extracted beam is mentioned. The measured beam displacements by kicker timing scan and the procedure for kicker ringing compensation are reported. Finally, the results of the compensation are described.

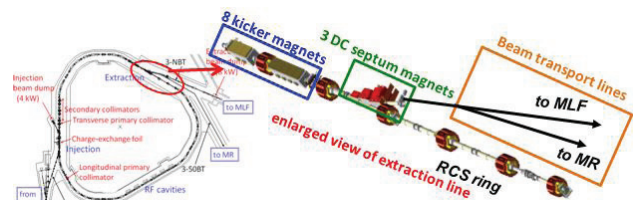


Figure 1: RCS and extraction line

## EXTRACTION KICKER MAGNET

The detail configuration and field measurement of extraction kicker magnet and power supply have already been described in reference [8]. In this section, the configuration and measured magnetic field are briefly introduced.

### Configuration

Kicker magnet consists of twin-C distributed Ferrite core with twenty units and two conductors in vacuum and the power source consists of two Thyratrons, PFN & loading cables and matching registers. Schematic diagram of kicker magnet system is shown in Fig. 2. Kicker magnet as shown in Fig. 2 is driven by two Thyratrons via two conductors. Operation charging voltage of Thyatron is 60 kV and exciting current of magnet by two Thyratrons is 6

<sup>#</sup>hharada@post.j-parc.jp

# PULSE-TO-PULSE TRANSVERSE BEAM EMITTANCE CONTROLLING FOR MLF AND MR IN THE 3-GeV RCS OF J-PARC

P.K. Saha\*, H. Harada, H. Hotchi and T. Takayanagi  
J-PARC Center, KEK & JAEA, Tokai-mura, Naka-gun, Ibaraki-ken, Japan

## Abstract

The 3-GeV RCS (Rapid Cycling Synchrotron) of J-PARC (Japan Proton Accelerator Research Complex) is a MW-class proton beam source for the muon and neutron production targets in the MLF (Material and Life Science Experimental Facility) as well as an injector for the 50-GeV MR (Main Ring). The RCS has to meet not only the beam power but also to ensure two different transverse sizes of the extracted beam for the MLF and MR, especially at high intensity operation. Namely, a wider one for the MLF in order to reduce damage on the neutron production target, while a narrower one for the MR in order to ensure a permissible beam loss in the beam transport line of 3-GeV to the MR and also in the MR. We proposed a pulse-to-pulse direct control of the transverse injection painting area so as to ensure a desired extracted beam emittance. For that purpose, RCS injection system was carefully designed for changing painting area between MLF and MR very accurately. The extracted beam profiles for the MR are measured to be sufficiently narrower than those for the MLF and also shown to be consistent with numerical beam simulation results. The system is already in service and plays an important role even at the present 300 kW beam operation. It is thus one remarkable progress on the RCS design goal to confirm that the beam parameters can be dynamically controlled and delivered as requested by the users even in simultaneous operation. A detail of the design strategy, painting process as well as experimental results are presented.

## INTRODUCTION

The 3-GeV Rapid Cycling Synchrotron (RCS) of Japan Proton Accelerator Research Complex (J-PARC) is designed for a beam power of 1 MW [1]. A total of  $8.33 \times 10^{13}$  protons in two bunches is accelerated to 3 GeV at a repetition rate of 25 Hz and simultaneously delivered to the neutron and muon production targets in the MLF (Material and Life Science Experimental Facility) as well as to the MR (50-GeV Main Ring synchrotron). Figure 1 shows a schematic view of the RCS, which is a three-fold symmetric lattice having a circumference of 348.333 m. The injected beam energy is recently upgraded to the designed 400 MeV from the 181 MeV so far. The RCS beam power at present for the operation is 300 kW, while a beam power of nearly 800 kW with sufficiently low loss has already been demonstrated in a recent beam study [2]. A pattern dipole magnet named Pulse Bending magnet (PB) located downstream of the RCS extraction beam transport (BT) line is used to switch the beam destination to the MR

\* E-mail address: saha.pranab@j-parc.jp

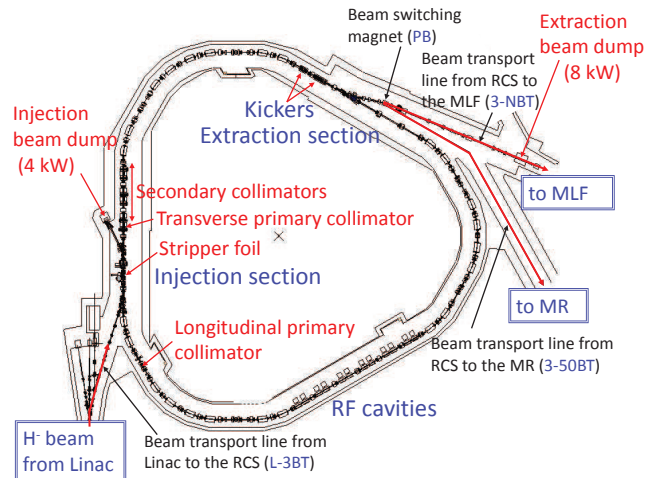


Figure 1: Schematic view of the 3-GeV RCS of J-PARC. Extracted beam is simultaneously delivered to the MLF and MR at a repetition rate of 25 Hz. A pattern dipole magnet named Pulse Bending magnet (PB) located downstream of the RCS extraction line acts as a switching magnet for changing beam destination MLF to MR.

according to the operation strategy. At present for the MR with fast extraction operation, RCS beam delivery ratio to the MLF and MR is typically 9:1.

However, RCS design goal is not only to achieve the beam power but also to ensure specific requirements of each downstream facility. One such an issue, especially at high intensity operation is to control transverse emittance of the extracted beam pulse-to-pulse between MLF and MR even in simultaneous operation. Namely, a wider transverse beam distribution for the MLF in order to reduce damage on the neutron production target, while a narrower one for the MR in order to ensure a permissible beam loss in the BT of 3-GeV RCS to the MR (3-50BT) as well as in the MR. The BT of RCS to the MLF targets named 3-NBT has the aperture of  $324\pi$  mm mrad, same as the RCS primary collimator but 3-50BT and MR designed apertures are much smaller,  $120\pi$  mm mrad and  $81\pi$  mm mrad, respectively. In order to realize such a requirement, we proposed pulse-to-pulse direct control of the transverse painting area during multi-turn  $H^-$  charge-exchange injection process in the RCS so as to ensure a desired transverse beam profile or in other words, a desired transverse emittance of the extracted beam. The designed injection painting area in the RCS for the MLF and MR are  $216$  and  $144\pi$  mm mrad, respectively. The RCS injection system was carefully designed for varying both hor-

# MODELING AND FEEDBACK DESIGN TECHNIQUES FOR CONTROLLING INTRA-BUNCH INSTABILITIES AT CERN SPS RING \*

C. Rivetta<sup>†</sup>, J. Fox, O. Turgut, SLAC, Menlo Park, California, USA  
W. Hofle, K. S. B. Li, CERN, Geneva

## Abstract

The feedback control of intra-bunch instabilities driven by electron-clouds or strong head-tail coupling (transverse mode coupled instabilities MCI) requires bandwidth sufficient to sense the vertical position and apply multiple corrections within a nanosecond-scale bunch. These requirements impose challenges and limits in the design and implementation of the feedback system. This paper presents model-based design techniques for feedback systems to address the stabilization of the transverse bunch dynamics. These techniques include in the design the effect of noise and signals perturbing the bunch motion. They also include realistic limitations such as bandwidth, nonlinearities in the hardware and maximum power deliverable. Robustness of the system is evaluated as a function of parameter variations of the bunch.

## INTRODUCTION

The feedback control of intra-bunch instabilities induced by electron-cloud (ECI) or strong head-tail interaction (transverse mode coupled instabilities - TMCI) requires enough bandwidth to sense the vertical position motion and apply correction fields to multiple sections of a nanosecond-scale bunch. Through the US LARP-CERN collaboration a wide-band feedback system is under research and development to control these intra-bunch instabilities. The effort is motivated by the plans to increase the beam current in the Super Proton Synchrotron (SPS) as part of the HL-LHC upgrade.

The feedback controller is implemented based on a digital reprogrammable processing channel, sampling the transverse bunch motion at a rate of 4 GS/s. The approach followed to design the controller is to consider the bunch dynamics as a multi-input multi-output system (MIMO). This conception arise because the multiple samples (multi-input) measuring the transverse motion across the bunch are used input to generate the multiple output samples that defines the control signal driving the kicker device.

During the first part of this development, the feedback control system is using a bank of finite-impulse response (FIR) filters to conduct MDs at CERN SPS ring during January 2013. In this bank, a filters are used to process individually each sample of the input signal. This planning was followed, in part, because of the simplicity of the filter implementation and the definition of its parameters and the limitations imposed by the hardware installed in the machine. The band-

width of the existent kicker is about 160 MHz, limiting the effective feedback control on a 3.2ns bunch length to the first side-band around the betatron tune. Additionally, the setting of the Q26 lattice in the machine defined the fractional betatron frequency  $\omega_\beta = 0.185$  and the fractional synchrotron frequency  $\omega_s = 0.0059$  and the phase lag of the FIR filter was not a limitation to damp the transverse bunch dynamics corresponding to the barycentric and head-tail motions [1].

In the second stage of this development, new strip-line kickers with wider bandwidth were installed in the SPS ring and a slotted-coaxial kicker is under development [2,3]. That potentially will define a true wide-band feedback channel able to drive multiple intra-bunch modes. A new challenge in the design of the feedback controller exists due to the re-definition of the SPS lattice from the Q26 to the Q20 optics [4,5]. The new optics in the machine sets a fractional synchrotron frequency  $\omega_s = 0.0170$ , spreading out the frequency of the satellite bands around the betatron frequency  $\omega_\beta = 0.185$ . In [6], the design of a controller based on a bank of infinite-impulse response (IIR) filters is analyzed to stabilize the intra-bunch dynamics corresponding to the new Q20 optics. In that pre-design, the phase of the filters is kept almost constant in the frequency range corresponding to the fractional betatron tune and its dominant side-bands ( $f_\beta \pm n f_s$ ). That design uses the bunch dynamics model to define the fundamental parameters of the controller and test the stability and performance robustness of the controller. It does not incorporate specifically the model into the design of the controller.

This paper addresses another methodology for the controller design to stabilize the intra-bunch dynamics of the beam at SPS with Q20 optics. The model of the intra-bunch dynamics is included intrinsically in the controller design providing the maximum information of the bunch modes to be stabilized. This realization gives higher order controllers respect to the FIR/IIR filter banks. In this paper we design a full model-based controller to stabilize the dominant bunch modes, analyze different controller options comparing the stability and performance robustness of the system when the betatron and synchrotron frequency are changed and the initial modal instability (growth rates) are varied. Based on this full controller, simplified versions or reduced order controllers has to be evaluated. The study of these reduced controllers is attractive to simplify the firmware implementation and the setting of the controller parameters in real-time operation.

\* Work supported by the U.S. Department of Energy under contract DE-AC02-76SF00515 and the US LHC Accelerator Research Program (LARP).

<sup>†</sup> rivetta@slac.stanford.edu

# LONGITUDINAL MICROWAVE INSTABILITY IN A MULTI-RF SYSTEM

T. Argyropoulos, CERN, Geneva, Switzerland

## Abstract

The longitudinal microwave instability is observed as a fast increase of the bunch length above some threshold intensity. Recently, this type of instability was seen for a single proton bunch at high energies in the CERN SPS and is proven to be one of the limitations for an intensity increase required by the HL-LHC project. In this paper a theoretical approach to the analysis of the microwave instability is verified by particle simulations. The study is applied to the SPS and is based on the current SPS impedance model. Finally, the effect of the 4th harmonic RF system on the microwave instability threshold is investigated as well.

## INTRODUCTION

There is a very wide range of phenomena in high-intensity circular accelerators that is called by the same name “microwave ( $\mu w$ ) instability”. Usually, but not always, an instability is called  $\mu w$  if

$$f_r \tau \gg 1, \quad (1)$$

where  $\tau$  is the bunch length and  $f_r = \omega_r / (2\pi)$  is the resonant impedance frequency. In proton accelerators  $\mu w$  instability is observed as a fast increase of the bunch length and thus of the longitudinal emittance  $\varepsilon_l$ . This bunch lengthening can be distinguished from the bunch lengthening due to potential well distortion by a change in the slope of bunch length versus intensity. The break point where the slope changes is considered as the instability threshold.

The operation of the CERN SPS in the past was limited by  $\mu w$  instability. At that time, measurements with long bunches and RF off had allowed the dominant resonant impedances with high  $R_{sh}/Q$  to be seen as peaks in the unstable beam spectrum [1], where  $R_{sh}$  is the shunt impedance and  $Q$  the quality factor. Most of the impedance sources were identified and it was proved, both by measurements and simulations, that the pumping port impedance was the main source of instability. Consequently, shielding these devices led to a significant improvement of the beam stability [2].

Today, the SPS is used as the LHC injector where particles are accelerated by the main 200 MHz RF system. In addition to that, for proton beams, a 4<sup>th</sup> harmonic RF system (800 MHz) operated in bunch shortening mode (BSM) is used for beam stability (Landau damping). During measurements in 2012, before long shutdown 1 (LS1), a stable LHC proton beam (4 batches of 72 bunches each) with a bunch spacing of 25 ns and a bunch intensity of  $N_b = 1.35 \times 10^{11}$  p/b was accelerated to the SPS top energy (450 GeV/c) [3]. Nevertheless, according to the HL-LHC project [4], beams with an intensity of up to  $2.5 \times 10^{11}$  p/b

will be requested from the SPS. This means that one needs to almost double  $N_b$ , while maintaining the same bunch length at SPS extraction ( $\tau_{4\sigma} \leq 1.7$  ns), restricted by the LHC 400 MHz RF system. The maximum bunch length allowed by the Beam Quality Monitor (BQM) for injection into the LHC is  $\tau = 1.9$  ns.

Recent measurements for single high-intensity bunches ( $N_b > 2.0 \times 10^{11}$  p/b) showed that longitudinal emittance increases during the cycle, pointing out that a  $\mu w$  instability could be responsible for this effect.

## UNCONTROLLED EMITTANCE BLOW-UP

Longitudinal emittance blow-up is observed in the SPS for both single and multi-bunch beams. An example of bunch lengths measured in 2012 for single high-intensity bunches at the SPS flat top is presented in Fig. 1. The measurements were performed in a double RF system in BSM with RF voltages  $V_{200} = 2$  MV and  $V_{800} = 200$  kV in the 200 MHz and 800 MHz RF systems, respectively [5]. Note that  $V_{200} = 2$  MV is much lower than the  $V_{200} = 7$  MV that is used in normal operation in order to compress the bunch before extraction to the LHC.

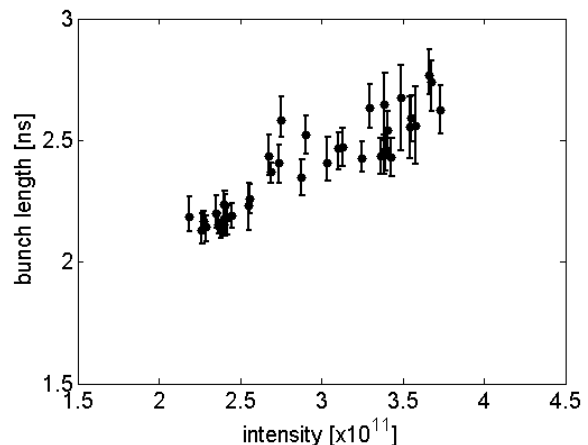


Figure 1: Measured bunch length as a function of intensity for a single bunch at the SPS flat top in a double RF system (BSM). The voltages  $V_{200} = 2$  MV and  $V_{800} = 200$  kV [5].

A strong increase of the bunch length with intensity is shown in Fig. 1 which can not be attributed to the potential well distortion with the SPS longitudinal impedance model [6]. In particular, in the current model, which includes the RF cavities, resistive wall, injection and extraction kickers, the low frequency reactive part of the SPS impedance is  $\text{Im}Z/n \approx 3.5 \Omega$ , while much higher

# SYNCHROTRON FREQUENCY SHIFT AS A PROBE OF THE CERN SPS REACTIVE IMPEDANCE

A. Lasheen\*, T. Argyropoulos, J. F. Esteban Müller, D. Quartullo, E. Shaposhnikova, H. Timko, J. Varela Campelo, CERN, Geneva, Switzerland

## Abstract

Longitudinal instability in the CERN SPS is a serious limitation for the future increase of bunch intensity required by the HiLumi LHC project. The impedance driving this instability is not known precisely and a lot of effort goes into creating an accurate impedance model. The reactive impedance of the machine can be probed by measuring the bunch length oscillations of a mismatched bunch at injection. The frequency of these oscillations as a function of intensity has a slope that depends on the reactive impedance and the emittance. Measurements were done for three values of longitudinal emittance and then compared with particle simulations based on the impedance model using particle distribution close to the measured one. Comparison of measured and calculated frequency shifts gives an estimation of the missing impedance in the model. In addition, scanning of initial emittance for diverse particle distributions in simulations shows that the frequency shift greatly depends on emittance and initial distribution. Small variations of these parameters can lead to very different results and explain partially the discrepancy between measured and calculated values of frequency shifts.

## INTRODUCTION

Reference measurements were done in the past in the SPS to monitor the evolution of the impedance from 1999 and successively after the 2001 impedance reduction program. Main changes were due to the installation of extraction kickers MKE in 2003 - 2006, and their shielding later [1]. New measurements were done in 2013 [2] and 2014, not only in order to continue the reference measurements, but mainly to test the SPS impedance model needed to simulate different intensity effects observed in the SPS. Below, simulations using this model are compared to measurements in order to test the model accuracy. This will allow to have a better understanding of SPS instabilities, as well as the synchrotron frequency distribution dependence on bunch intensity and bunch length.

Voltage induced due to the reactive impedance leads to the synchrotron frequency shift. This voltage can be found as the convolution of the reactive impedance with the beam spectrum (effective impedance), and is proportional to the bunch intensity  $N_b$ . The shift consists of two parts: the incoherent shift  $\Delta f_{inc}$ , corresponding to the convolution of the stationary bunch spectrum, and the coherent shift  $\Delta f_{coh}$ , corresponding to the convolution of the perturbation spectrum with the impedance. This perturbation can be due to a shift in the bunch position ( $m = 1$ , dipole) or a mismatch

of the bunch length ( $m = 2$ , quadrupole). The frequency of these oscillations can be written in the form [3]:

$$f_{s,m}(N_b) \approx m f_s^{(0)} + m \Delta f_{inc}(N_b) + \Delta f_{coh}(m, N_b), \quad (1)$$

with  $f_s^{(0)}$  being the synchrotron frequency without intensity effects (first term of Eq. 3). One can then measure the oscillations of a mismatched bunch for several intensities in order to probe the effective reactive impedance. For a bunch with a parabolic line density, the dipolar incoherent and coherent frequency shifts are exactly canceling [3], making it difficult to measure intensity effects with dipole oscillations. Thus it is more practical to measure the quadrupole frequency shift.

Above transition, inductive effective impedance will produce  $\Delta f_{inc} < 0$  and  $\Delta f_{coh} > 0$ , and vice-versa for capacitive impedance.

Below, measurements are compared to simulations and analytical calculations in order to study the effect of the different SPS impedance sources on the synchrotron frequency shift, as a function of the bunch distribution.

## MEASUREMENTS

The measurements of bunch length oscillations are done in the SPS just after injection ( $P = 25.92$  GeV/c, above transition). The RF voltage is set to a value for which the injected bunch is mismatched, allowing the bunch length to oscillate for several periods (the emittance being small enough so that the oscillations are not damped too fast because of filamentation). These measurements were done for several emittances ( $\epsilon_1 \in [0.1, 0.20]$  eVs), and several intensities ( $N \in [1, 10] \times 10^{10}$  ppb). Dipole oscillations were damped using a phase loop in order to measure only the quadrupole oscillations (referred to as oscillations for the rest of the paper). Two optics are available in the SPS (named Q26 and Q20) with transition gamma factors  $\gamma_t = 22.8$  for Q26 and  $\gamma_t = 18$  for Q20, which affect the synchrotron frequency. A single RF system (200 MHz) was used in measurements, with respective voltages of  $V_{Q26} = 0.9$  MV for Q26 and  $V_{Q20} = 2.5$  MV or  $V_{Q20} = 4.5$  MV for Q20.

For each measurement set, bunch profiles were acquired every revolution turn for 1000 turns after injection and analyzed. From the oscillations of the bunch length (defined as  $\tau = 4\sigma_{RMS}$ ), we extract the average bunch length, the peak-to-peak amplitude and the frequency of the oscillations (via FFT). Like this we get a scatter plot of the quadrupole frequencies as a function of intensity and average bunch length  $f_2(\tau, N_b)$ . For a narrow frame of bunch length  $\tau = \tau_0 + \Delta\tau$ , we plot the quadrupole frequency as a function of intensity as in Fig. 1(bottom). The top plot corresponds to a single point of the bottom one with

\* alexandre.lasheen@cern.ch

# STUDIES ON CONTROLLED RF NOISE FOR THE LHC

H. Timko\*, P. Baudrenghien, E. Shaposhnikova, CERN, Geneva, Switzerland  
T. Mastoridis, California Polytechnic State University, San Luis Obispo, USA

## Abstract

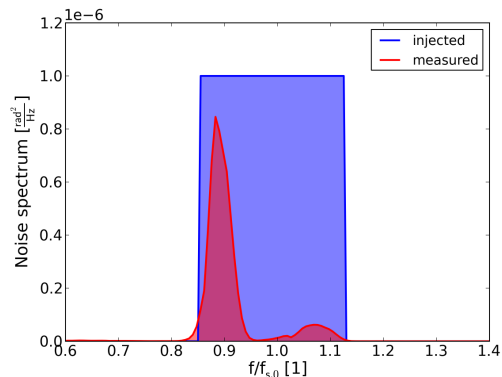
RF phase noise is purposely injected into the LHC 400 MHz RF system during the acceleration ramp for controlled longitudinal emittance blow-up, in order to maintain longitudinal beam stability. Although the operational blow-up works reliably, studies of the injected RF noise are desirable not only to allow for a better-controlled, more flexible blow-up, but also for other applications such as the mitigation of machine-component heating through appropriate bunch shaping. Concerning the noise injection, an alternative algorithm was developed and implemented in the hardware, but first tests revealed unexpected modulation of the achieved bunch length along the ring, and subsequently, theoretical studies have been launched. In this paper, we present a summary of ongoing measurement analysis and simulation studies that shall explain previous observations, predict what can be expected in different cases, and thus help to optimise the RF noise in general.

## INTRODUCTION

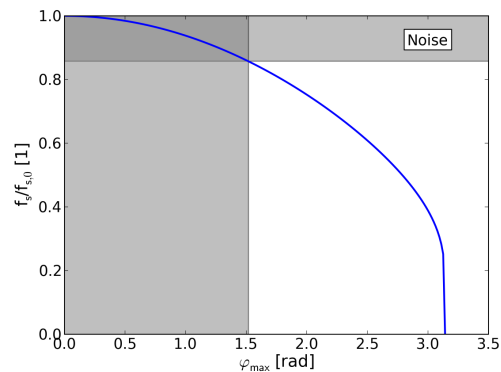
Controlled longitudinal emittance blow-up is necessary in the LHC to maintain longitudinal beam stability during the acceleration ramp. For a constant stability margin, the emittance  $\varepsilon$  should be increased with energy as  $\varepsilon \propto \sqrt{E}$  [1], resulting in a roughly constant bucket filling factor and relative synchrotron frequency spread. In practice, a good blow-up was achieved by a feedback that scales the RF phase noise  $\varphi_N(t)$  to keep the bunch length constant [2, 3]. At flat top, also bunch shaping through noise injection can be desirable, for instance to mitigate machine-component heating.

The noise spectrum  $S_\varphi(f)$  applied determines in what frequency range diffusion is triggered in the bunch, and hence, determines also the resulting bunch shape. Diffusion under external noise [4–6] and bunch shaping with band-limited white noise [7] has been studied in the past. Controlled emittance blow-up for the SPS and LHC was designed and implemented [2, 8] subsequently. In the LHC, a band-limited white noise spectrum is applied, however, feedback loops complicate the analysis. A constant relative noise band is chosen with the range  $(0.86–1.1)f_{s0}$  (Fig. 1a), where  $f_{s0}$  is the synchrotron frequency of the synchronous particle. In a single-RF system this will affect the core of the bunch that has a maximum phase amplitude of synchrotron oscillations in the range of  $\varphi_{\max} = (0–1.52)$  rad (Fig. 1b).

Operationally,  $\varphi_N(t)$  is applied through the phase loop (PL), as an additional phase shift to the phase correction between bunch and RF phase [2]. This works reliably, and even for a full machine the beam can be brought stably through the acceleration ramp, with a typical target bunch length of 1.2 ns



(a) Injected (blue) and measured (red) noise power spectral density. The measured noise is applied through the PL.



(b) Synchrotron frequency distribution in a single-RF system as a function of maximum phase coordinate. The dashed region marks the range affected by the injected noise.

Figure 1: LHC controlled longitudinal emittance blow-up.

achieved homogeneously ( $\pm 30$  ps) for all bunches [2]. However, since the phase loop corrects the centre-of-mass motion, the effective noise spectrum is reduced greatly around  $f_{s0}$ , see Fig. 1a. This modification of the spectrum makes it difficult to shape bunches in a well-determined way.

Alternatively,  $\varphi_N(t)$  can be applied through the cavity controller (CC). The PL is still required for the ramp, but an interaction between the noise and the PL can be avoided: using a symmetric filling pattern, and injecting the noise on a revolution frequency side-band, the noise is practically invisible to the PL. This scheme was tested in early 2012, and indeed,  $S_\varphi(f)$  in the cavity field reproduced the desired spectrum exactly [9]. At the time, however, this noise injection scheme could not be made operational, because tests with few bunches led to a bifurcation of the final bunch length: although on average the target bunch length was obtained, the bunches were either too short or too long. Further studies are planned after the start-up of the LHC early 2015.

\* helga.timko@cern.ch

# FAST TRANSVERSE INSTABILITY AND ELECTRON CLOUD MEASUREMENTS IN FERMILAB RECYCLER

J. Eldred, Department of Physics, Indiana University, Bloomington, IN 47405, USA  
 P. Adamson, D. Capista, N. Eddy, I. Kourbanis, D.K. Morris, J. Thangaraj, M.J. Yang,  
 R. Zwaska, FNAL, Batavia, IL 60510, USA  
 Y. Ji, Department of Physics, Illinois Institute of Technology, Chicago, IL 60616, USA

## Abstract

A new transverse instability is observed that may limit the proton intensity in the Fermilab Recycler. The instability is fast, leading to a beam-abort loss within two hundred turns. The instability primarily affects the first high-intensity batch from the Fermilab Booster in each Recycler cycle. This paper analyzes the dynamical features of the destabilized beam. The instability excites a horizontal betatron oscillation which couples into the vertical motion and also causes transverse emittance growth. This paper describes the feasibility of electron cloud as the mechanism for this instability and presents the first measurements of the electron cloud in the Fermilab Recycler. Direct measurements of the electron cloud are made using a retarding field analyzer (RFA) newly installed in the Fermilab Recycler. Indirect measurements of the electron cloud are made by propagating a microwave carrier signal through the beampipe and analyzing the phase modulation of the signal. The maximum betatron amplitude growth and the maximum electron cloud signal occur during minimums of the bunch length oscillation.

## INTRODUCTION

Beginning in July 2014, a fast intensity-induced transverse instability was observed in the proton beam of the Fermilab Recycler. This instability is currently a limiting factor on the stable proton intensity in the Recycler. The Recycler is currently being commissioned from slip-stacking [1, 2]. The instability has the unusual feature of selectively impacting the first high-intensity batch. Our studies focus on electron cloud because it is the most probable mechanism for the Recycler instability.

A qualitatively similar phenomenon, referred to as a “first pulse” electron cloud instability, has been observed at Los Alamos National Laboratory (LANL) [3, 4]. It should be noted, however, that the LANL macropulse timing structure is a very different timescale from the Fermilab batch timing structure [5].

The azimuthal space in the Fermilab Booster is divided into 84 buckets with typically 82 of those buckets are filled during operation. The Booster extracts to the Recycler (or the Main Injector) at a rate of 15 Hz and each Booster pulse is known as a batch. Six 84-bucket Booster batches and a 84-bucket kicker gap fill the 588-bucket azimuthal space of the Booster Recycler. During slip-stacking operation another six Booster batches can be injected.

When the first batch exceeds a certain intensity threshold (originally  $3e12$ ), the Recycler instability causes the horizon-

tal betatron dipole oscillation to grow dramatically and can lead to  $\sim 25\%$  loss within the first 150 turns. At this point, the beam is aborted to minimize loss activation as described in [1]. The rapid amplitude growth of the instability is only consistent with electron cloud [6, 7, 8]. Below the intensity threshold, the increased betatron oscillation amplitude is only apparent in the first batch.

If the first batch is just below threshold, the subsequent batches can have intensities above the single-batch intensity threshold without significant beam loss. When the Recycler beam is running in this configuration the most significant betatron excitation appears in the second batch, followed by the first batch. This configuration, with the first batch at  $\sim 80\%$  intensity of subsequent batches, enables the greatest total beam intensity at normal loss rates. On July 24th the Recycler titanium sublimation pumps were fired [9] and on August 1st the Recycler switched to running with the first batch at lower intensity than subsequent batches. The maximum beam intensity was  $22e12$  protons on August 1st 2014 but gradually increased to  $26e12$  protons by August 10th 2014. The change in the instability threshold is consistent with beampipe conditioning effects which increase the threshold associated with electron cloud [10, 11].

The Recycler is outfitted with a digital damper system designed to mitigate transverse instabilities during antiproton accumulation (see [12]). The damper system is at least an order of magnitude too weak to prevent losses from this new instability in the Recycler. This Recycler instability also occurs when the damper system is turned off.

The shorter bunch lengths appear to lower the intensity threshold of the Recycler instability. In one illuminating study (July 16th 2014), six batches each with  $3.3e12$  protons were injected into the Recycler with a deliberate RF phase mismatch to induce a bunch length oscillation. Figure 1 shows that the instability immediately overpowers the damper when the bunch length is short but the betatron motion damps and decoheres when the bunch length is long. This figure also demonstrates that the instability begins in the horizontal plane but the betatron motion spreads to the vertical plane via the linear coupling of the lattice [13]. It appears in this case that the instability begins the middle of the batch and migrates to the tail of the batch. If the instability has increased the emittance in the center of the batch than this would delay the onset of the electron cloud and could account for the movement of the instability towards the tail of the batch.

# TRANSVERSE EMITTANCE PRESERVATION STUDIES FOR THE CERN PS BOOSTER UPGRADE

E. Benedetto, C. Bracco, B. Mikulec, V. Ragine1, G. Rumolo, CERN, Geneva, Switzerland, V. Forte, CERN, Geneva, Switzerland, and Université Blaise Pascal, Clermont-Ferrand, France

## Abstract

As part of the LHC Injectors Upgrade Project (LIU), the CERN PS Booster (PSB) will undergo an ambitious upgrade program, which includes the increase of injection energy from 50 MeV to 160 MeV and the implementation of an H<sup>-</sup> charge-exchange injection from the new Linac4. Compared to rings characterized by similar space-charge tune spreads (about 0.5 at low energy), the peculiarity of the PSB is the small transverse emittance that needs to be preserved in order to provide high brightness beams to the LHC. We here try to identify what is the minimum emittance that can be achieved for a given intensity, via measurements, scaling estimates and simulation studies. The latest are based on our best knowledge of the optics model and take into account known perturbations such as the one induced by the short and fast ramping chicane injection magnets.

## INTRODUCTION

CERN PS Booster is the first circular accelerator in the LHC proton injector chain and it is where the transverse emittance is defined.

It is made of four superposed rings and accelerates protons up to 1.4 GeV (it will be upgraded to 2 GeV) for the downstream machine, the Proton Synchrotron (PS).

Currently it has a conventional multi-turn injection of 50 MeV protons from Linac2 and the plan is to replace it with a H<sup>-</sup> charge-exchange injection from Linac4 at 160 MeV [1]. These upgrades will allow increasing the beam brightness, i.e. the intensity in a given emittance, for the same space-charge tune spread, to reduce the injection losses, which in the present machine are dominated by the interaction with the injection septum, and to better control the filling of the transverse phase-space.

Particles are injected at a given working point (Q<sub>x</sub>, Q<sub>y</sub>) around (4.3, 4.5), to optimize multi-turn injection and allocate the maximum possible space-charge tune spread, which in the PSB is around 0.5. The tunes are then reduced during acceleration, as soon as the necktie gets smaller, down to about (4.2, 4.2) at extraction. Figure 1 shows the working point variation during the ramp for the LHC-type beam discussed in the following section, which is injected at a slightly larger horizontal tune, as a result of beam optimization in operation.

With respect to the production of the high intensity beams, in which the goal is to minimize the injection losses [2], for the LHC beams the challenges are to assure a good quality beam in the three planes and to minimize the transverse emittance blow-up.

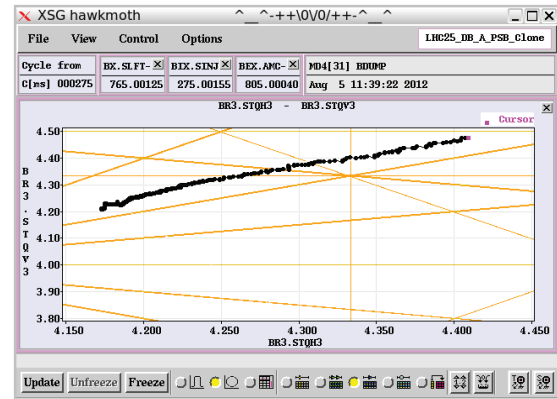


Figure 1: The working point during acceleration of the LHC-type beams goes from around (4.4,4.47) down to (4.18,4.20).

## MEASUREMENTS

In 2012 a measurement campaign has been done for the LHC operational beams, with the aim to quantify and define a budget for the emittance blow-up in the entire injection chain.

Figure 2 summarizes the major results for the PSB, i.e. the curve of the average normalized transverse emittance as a function of the beam intensity, at constant longitudinal emittance. The horizontal and vertical emittances have been measured at the extraction flat-top in Ring 3, which featured the best performances, as the result of a careful optimization [3].

Different beam intensities have been produced by increasing the number of injected turns from 1 to 4 and the only other parameter which was slightly changed and optimized for each measurement point was the tune at injection. Two sets of measurements appear in the plot, for different longitudinal emittances, that are 1.20 eVs and 0.86 eVs (matched area), corresponding to the two main LHC beams produced in 2012, i.e. respectively the standard LHC25ns and the BCMS [4].

The first consideration is that the points lie on a straight line on the emittance versus intensity plot; the second is that the slope increases for a smaller longitudinal emittance.

Additional measurements [3] show that, provided that the working point is optimized all along the cycle, the transverse normalized emittance is constant during acceleration (however measurements at injection are difficult to read due to scattering at the wires, which induces 10% blow-up during the measurement itself). This indicates that the final values of the transverse emittance

# DPA AND GAS PRODUCTION IN INTERMEDIATE AND HIGH ENERGY PARTICLE INTERACTIONS WITH ACCELERATOR COMPONENTS

A.Yu. Konobeyev<sup>#</sup>, U. Fischer, KIT, Karlsruhe, Germany

## Abstract

A brief overview of methods for the calculation of the number of stable defects in irradiated materials is presented. Special attention is given to the evaluation of gas production cross-sections performed using nuclear models, experimental data, and systematics. The perspective of the use of evaluated data files for dpa and gas production calculations is discussed.

## INTRODUCTION

A calculation of radiation damage and gas production rates in materials is a challenging task combining the modelling of nuclear interactions, the simulation of the material behaviour, and taking into account, as far as possible, experimental data.

The calculation of atomic displacement cross-section consists of two independent parts: the calculation of recoil energy distributions for involved nuclear reactions and the evaluation of the number of stable displacements in materials. The report presents a brief overview of methods of calculation and main important results obtained for the number of defects produced in materials under irradiation. Special attention is given to the evaluation of gas production cross-sections using results of nuclear model calculations, experimental data, and systematics predictions.

## DPA PRODUCTION

The dpa production (radiation damage) rate is calculated by summing of integrals of particle- and energy-dependent displacement cross-section  $\sigma_d$  and particle flux over all particle types. The displacement cross-section for incident particle with the kinetic energy  $E_p$  is calculated as follows:

$$\sigma_d(E_p) = \sum_i \int_{E_d}^{T_i^{\max}} (d\sigma_i(E_p, T_i) / dT_i) N_D(T_i) dT_i \quad (1)$$

where  $d\sigma_i/dT_i$  is the recoil atom energy distribution for  $i$ -th reaction;  $N_D(T_i)$  is the number of Frenkel pairs produced by the primary knock-on atom (PKA) with the kinetic energy  $T_i$ ,  $T_i^{\max}$  is the maximal kinetic energy of the PKA in  $i$ -th reaction;  $E_d$  is the effective threshold displacement energy of material.

### Estimating the Number of Stable Defects

The number of stable displacements  $N_D$  can be calculated using different approaches with varying degrees of complexity of code implementation and accuracy of predictions.

<sup>#</sup>alexander.konobeev@kit.edu

The NRT displacement model [1] remains popular in spite of well known shortcomings such as neglecting of an athermal recombination and the use of isotropic displacement energy [2]. The model in more general form [3] is implemented in NJOY [4], LAHET [5], MCNP [6] and other codes, which maintains its popularity for applications. According to the model the number of stable defects produced by the ion with the kinetic energy  $T_{PKA}$  is equal to

$$N_{NRT}(T_{PKA}) = (0.8/2E_d) T_{dam}(T_{PKA}), \quad (2)$$

where  $T_{dam}$  is the energy transferred to lattice atoms reduced by the losses for electronic stopping of atoms in displacement cascade.

The measure of deviations of the  $N_D$  number obtained experimentally or theoretically from one predicted by NRT is quantified as “defect production efficiency”

$$\xi = N_D(T_{PKA}) / N_{NRT}(T_{PKA}), \quad (3)$$

The NRT model has “internal” limitations like for the maximal kinetic energy of PKA [1,7]. Predicted  $N_{NRT}$  numbers differs with some exceptions from the measured values for neutron irradiation in reactors [8,9] as for high energy protons [8], and results of molecular dynamics (MD) simulations. For example, the typical  $\xi$  value obtained using MD for iron and nickel at  $T_{dam}$  below 100 eV exceeds one, and is about 0.3 at 10 -100 keV [2].

The binary collision approximation model (BCA) is a popular method for the simulation of ion interactions with materials, which should be used with care for the estimation of realistic number of stable defects produced under irradiation.

An attempt to reproduce results of MD simulations by a proper choice of BCA parameters leads in many cases to an uncertainty of predictions at ion energies outside MD modelling [8,9]. The recent evaluation of popular BCA code SRIM [10] stated the problem of the calculation of correct number of stable displacements “in any absolute sense” [11].

One of advantages of BCA is the relative simplicity of the direct implementation in codes for the simulation of the particle transport using the Monte Carlo method.

The molecular dynamics simulation is the most adequate method to get realistic number of stable defects produced in irradiated materials.

The electronic losses and interatomic potential are still crucial points concerning the reliability of simulations. At least for iron and copper the total number of stable displacements calculated using MD with modern interatomic potentials are in agreement with experimental

## NOVEL MATERIALS FOR COLLIMATORS AT LHC AND ITS UPGRADES\*

A. Bertarelli<sup>#</sup>, A. Dallochio, M. Garlasché, L. Gentini, P. Gradassi, M. Guinchard, S. Redaelli, A. Rossi, O. Sacristan de Frutos, CERN, Geneva, Switzerland  
 F. Carra, CERN, Geneva, Switzerland; Politecnico di Torino, Turin, Italy  
 E. Quaranta, CERN, Geneva, Switzerland; Politecnico di Milano, Milan, Italy

### Abstract

Collimators for last-generation particle accelerators like the LHC, must be designed to withstand the close interaction with intense and energetic particle beams, safely operating over an extended range of temperatures in harsh environments, while minimizing the perturbing effects, such as instabilities induced by RF impedance, on the circulating beam. The choice of materials for collimator active components is of paramount importance to meet these requirements, which are to become even more demanding with the increase of machine performances expected in future upgrades, such as the High Luminosity LHC (HL-LHC). Consequently, a far-reaching R&D program has been launched to develop novel materials with excellent thermal shock resistance and high thermal and electrical conductivity, replacing or complementing materials used for present collimators. Molybdenum Carbide - Graphite and Copper-Diamond composites have been so far identified as the most promising materials. The manufacturing methods, properties and application potential of these composites will be reviewed along with the experimental program which is to test their viability when exposed to high intensity particle beams.

### INTRODUCTION

The introduction in recent years of new, extremely energetic particle accelerators such as the Large Hadron Collider (LHC) [1] brought about the need for advanced cleaning and protection systems, such as collimators, in order to safely increase the energy and intensity of particle beams to unprecedented levels. LHC collimators must adopt materials able to withstand the extreme conditions (temperatures, pressures and densities) induced by the accidental impact of particle beam pulses; on top of outstanding thermal shock resistance, these materials are typically required a number of additional relevant properties, such as high electrical conductivity, geometrical stability and resistance to radiation damage. These requirements are set to become even more compelling in consideration of the High-Luminosity upgrade of the LHC (HL-LHC) [2], expected to increase by a factor of two beam intensity and energy: Carbon-

Carbon (C-C) composites used for primary and secondary collimators may limit the accelerator performance as a result of the high impedance induced by C-C low electrical conductivity, while the Tungsten alloy (Inermet180) used in tertiary collimators has very low robustness in case of beam impacts.

To face these challenges, an intense R&D program has been launched at CERN in recent years to explore or develop a palette of novel materials which are to combine the excellent properties of graphite or diamond, specifically their low density, high thermal conductivity, low thermal expansion, with those of metals and transition metal-based ceramics possessing high mechanical strength and good electrical conductivity. This article presents the most promising materials identified so far, namely Molybdenum Carbide - Graphite (MoGr) and Copper-Diamond (CuCD).

### MOLYBDENUM CARBIDE - GRAPHITE

Pure molybdenum possesses very high melting point, low Coefficient of Thermal Expansion (CTE) and excellent mechanical strength and electrical conductivity, while graphitic materials feature low density, extremely high service temperature, large damping properties (particularly useful in attenuating shock waves) and, if graphite crystallite ordering is sufficiently extended (high graphitization degree), excellent thermal conductivity and very low CTE, at least in the direction aligned with graphite basal plane. At high temperatures, molybdenum rapidly reacts with carbon, forming stable carbides ( $\text{MoC}_{1-x}$ ) which, in spite of their ceramic nature, retain a good electrical conductivity; in this respect, MoGr is therefore a ceramic-matrix composite. Several MoGr grades, in the frame of a collaboration between CERN and Italian SME BrevettiBizz, were investigated, with processing temperatures ranging from 1700° C to 2600° C [3].

A broad range of compositions, powder types and dimensions were tested: the best results so far were obtained for a sintering temperature of 2600° C. The C-phase can be composed of natural graphite flakes or by a mixture of natural graphite and mesophase pitch-based carbon fibres (Fig. 1).

\* The research leading to these results has received funding from the European Commission under the FP7 Research Infrastructures project EuCARD-2, grant agreement no.312453  
 #alessandro.bertarelli@cern.ch

## WG-A SUMMARY

J. Holmes, SNS, U.S.A.  
Y-H. Chin, KEK, Tsukuba, Japan  
S. Machida, STFC RAL, Didcot, U.K.

### Abstract

WG-A took three main themes this year, short term beam loss, instability and space charge and long term beam loss. In the following, three conveners will summarise each theme.

### BACKGROUND

At this workshop, working groups were asked to consider the following general questions:

- Is it possible to understand the beam losses in detail and to predict them?
- What really has to be provided by simulation and diagnostics to make this possible?
- What seems actually feasible/has been delivered?
- If a detailed understanding of losses would be possible, how would it affect operation/tuning/hardware improvements?
- How important is a detailed understanding for decreasing/limiting the beam losses?

Working Group A was tasked with the topics of Beam Dynamics in Rings. We broke the discussion for rings down into three specific areas:

- Short-term beam loss – Beam loss in short cycling rings.
- Instability and space charge.
- Long-term beam loss – Beam loss in long cycling rings.

Our consideration of the general questions led us to pose specific questions for each of the three areas:

#### *Beam loss in fast cycling rings*

- Are single particle resonances important? If so, to what order do these need to be taken into account?
- Is the beam loss due to coherent (excluding instability) or incoherent phenomena?
- What techniques can be used to mitigate beam loss mechanisms that are independent of intensity? How will such losses be detected?

#### *Instability and space charge*

- Do we have a reasonable model of instability including space charge effects? What are the concerns – Emittance growth? Beam loss? Other?
- Can we separate pure space charge problems from impedance related instabilities (incl. electron clouds) in observation?
- How important is it to include space charge effects when we design mitigation methods?

#### *Beam loss in long cycling rings*

- Can we define dynamic aperture concept with space charge? Is it a right way to understand long-term beam loss?
- Is it possible to identify the source of beam loss; instability with slow growth rate or resonance coupled with space charge?
- To what energy range must we consider direct space charge effects?

### BEAM LOSS IN SHORT CYCLING RINGS BY J. HOLMES

Presentations included:

- R. Macek, LANL, “Understanding Beam Losses in High Intensity Proton Accumulator Rings”.
- K. Seiya, FNAL, “The Status of the Proton Improvement Plan (PIP) at Fermilab Booster”.
- C. Warsop, RAL, “High Intensity Loss Mechanisms on the ISI Rapid Cycling Synchrotron”.

Presentations included from other sessions that had a direct bearing on this topic included:

- H. Hotchi, JAEA/J-PARC, “Lessons from 1 MW Proton RCS Beam Tuning”, Plenary session.
- I. Hofmann, GSI, “Grid Noise and Entropy Growth in PIC Codes”, WG-B with A/C.
- M. Blaskiewicz, BNL, “Instabilities and Space Charge”, WG-A – instabilities.
- V. Kornilov, GSI, “Instability Thresholds of the Head-Tail Modes in Bunches with Space Charge”, WG-A–instabilities.
- S. Cousineau, ORNL, “Status of Preparations for a 10 us H-Laser-Assisted Stripping Experiment”, WG-D.

#### *Response to questions*

Question 1: Are single particle resonances important? If so, to what order do these need to be taken into account?

Even in fast cycling rings, low order single particle resonances must be avoided. In addition to integer and half-integer resonances, low (certainly second, third, and fourth) order coupling resonances, and especially sum resonances, should be avoided in choosing operating scenarios. It is important to include the effect of space charge on the tune distribution in choice of operating point. In addition to avoiding low order resonances, correction of the driving terms may be important in certain situations.

Question 2:

# WG B- Beam Dynamics In High Intensity Linacs

D. Raparia, BNL, Upton, USA

I. Hofmann, GSI Helmholtzzentrum für Schwerionenforschung GmbH, Germany

Y. He, Chinese Academy of Sciences Institute of Modern Physics, China

## Abstract

Grid noise and entropy growth, equi-partitioning, equi tune depression, halo, and losses were a few topics, which were discussed thoroughly during parallel session for beam dynamics in high intensity linacs (group B). Linac designs for the future, under construction, upgrade and the existing linacs from around the world were presented in three working sessions.

A total of 17 talks were presented. Three presentations are general beam dynamics in nature and twelve talks were project specific. One talk was new experimental work on the Gabor lens to neutralize space charge. The detail of each contribution can be found in these proceedings. Here we report the summary of the discussions and some concluding remarks of general interest to all the projects presented in the working group.

## INTRODUCTION

Beam Dynamics of High Intensity Linacs (working group B) had 17 invited/contributed talks and two poster presentations. Unfortunately five participants could not attend due to visa problems. Two talks were upgraded from the poster session.

Three talks were presented on tele-conference. The first time it took unusually long time to set up, and one of the discussion sessions was cancelled. These presentations included two on linac beam dynamics, nine on design of linacs for specific projects. Out of them two talks were designed to generate discussion and had one two hours long discussion session.

## GENERAL BEAM DYNAMICS FOR LINACS

Noll presented his new code BENDER, which allows fully self-consistent inclusion of space charge compensating electrons.

Hofmann discussed grid noise and entropy growth in PIC code, in particular with TraceWin examples. He found in his studies there exists an optimum number of grid cells below which grid heating dominates and above collision heating. Secondly, anisotropy effects are in good agreement with theory.

Nghiem proposed new concepts and methods for beam analysis, beam loss prediction, beam optimization, beam measurement and beam characterization in case of “very high intensity beams”.

Eshraqi proposed a linac design based on equi-tune-depression instead of equi-partition lattice design for

linacs. He showed that since linac beams are usually pretty spherical choosing an equi-partitioned point in the linac is very close to having an equi-tune-depressed lattice.

Other noteworthy results were reported by Yong Liu. For J-PARC linac simulations he showed that his non equi-partitioned lattice is an order of magnitude more sensitive to errors than an equi-partitioned lattice.

For the Gabor lens study partial agreement with modelling was achieved, but more work is needed to better understand the limitations.

Groenings work on emittance transfer between horizontal/vertical is of interest for linacs as injectors into rings with horizontal multi-turn injection. The transfer requires stripping and matches with low charge state ion linacs as for the FAIR synchrotron.

In HB2012, Lagniel raised the question about validity of equi-partition theory and lattices in his talk entitled, “Equipartition Reality or Swindle”[1], Discussions in HB2012 hinted there is more work (simulations) needed to reach consensus [2]. Since then further simulations were published by Hofmann in response to Lagniel’s arguments [3].

## BEAM DYNAMICS DESIGN OF LINACS

Table 1 gives a brief description of the linacs discussed in the WG-B at HB2014. Two high power linacs, ESS and ADS, were optimized for different parameters. The ESS linac is optimized for cost by reducing the number of cavities and increasing the peak current by 25% and the cavity gradient by 11.25% keeping the beam power at 5 MW. The ADS lattice is optimized for losses by increasing the longitudinal acceptance and avoiding the longitudinal parametric and transverse structure resonances and longitudinal –transverse coupling.

The J-PARC linac was upgraded to 400 MeV from 181 MeV, ion source and RFQ were also changed with better performing units. They were expecting a signature of intra-beam-stripping but did not find any indication of intra-beam stripping. The SNS linac production tune still does not match with modelling in spite of better calibration of the measurement devices and modified methods. The linac was able to achieve the design goal of 1.4 MW beam power.

## DISCUSSIONS SESSION

In the discussion session following topics were discussed:

- Equi-partition versus equi-tune-depressed lattice were discussed:

# WORKING GROUP C SUMMARY: COMPUTATIONAL CHALLENGES, NEW CONCEPTS, AND NEW PROJECTS

Steven M Lund\*, Facility for Rare Isotope Beams, Michigan State University, USA  
 Giuliano Franchetti, GSI, Germany  
 Hiromi Okamoto, Hiroshima University, Japan

## Abstract

We summarize workshop discussions held in Working Group C at the 54th ICFA Advanced Beam Dynamics Workshop on High-Intensity, High-Brightness, and High Power Hadron Beams (HB2014; East Lansing, Michigan) taking place 10–14, November, 2014. The charge of Working Group C was to formulate a workshop-oriented agenda on *Computational Challenges, New Concepts, and New Projects*. In this summary, we list topics selected and linked presentations that were delivered, and summarize discussions held. Only limited attempts are given to summarize details of individual presentations. Focus is primarily on recommendations based on material presented both in the topically grouped talks and in linked workshop discussion sections immediately following each group of talks.

## INTRODUCTION

The charge of Working Group C (WGC) to address *Computational Challenges, New Concepts, and New Projects* is very broad to cover adequately in 14 invited presentations of 25 minutes duration (20 minutes + 5 minutes discussion) each and approximately 100 minutes of workshop discussion time. Moreover, the potential for the WGC charge to overlap and conflict with Working Groups A (*Beam Dynamics in Rings*; WGA) and B (*Beam Dynamics in LINACS*; WGB) was significant. In an attempt to focus to a reasonably limited agenda to be productive, the conveners tried to pick workshop-oriented topics to group into four sessions with 25 minute joint discussion periods held after the topically grouped talks. Care was taken to minimally overlap with topics taken up in WGA and WGB. Topics likely of interest in WGA and WGB were organized in the overall workshop agenda (two parallel sessions) to allow joint sessions. Topical groupings in WGC were as follows:

- First Session, Tuesday morning, Nov. 11th.  
**Computational: Simulation Infrastructure**  
**New Concepts: Scaled Experiments**
- Second Session, Tuesday afternoon, Nov. 11th.  
 (Combined with WGA, WGB)  
**New Concepts: Nonlinear Integrable Optics**
- Third Session, Wednesday morning, Nov. 12th.  
**Computational Challenges: Long Path Length Simulations / Benchmarking**

- Fourth Session, Thursday afternoon, Nov. 13th.  
 (Combined with WGA, WGB)  
**New Projects: New Projects: ISIS Upgrade, FFAG, Beam-Beam, Electron Lenses**

In the four WGC topical summary sections that follow, we give titles and speakers of invited presentations delivered and primarily summarize highlights of 25 minute discussions held (following each session listed). Discussions were largely, but not exclusively, stimulated by the talks within the immediately preceding sessions. Individual talks can be obtained (provided speakers did not opt out) on the HB2014 web site [1]. Recommendations given reflect perceptions of the conveners based on discussions held. Efforts were made to be balanced in summary, but limitations on the conveners backgrounds may result in some of these being of limited value.

## SIMULATION INFRASTRUCTURE AND SCALED EXPERIMENTS

Framing invited presentations delivered under simulation infrastructure were [1]:

- Jean-Luc Vay (LBNL), *Needs and considerations for a consortium of accelerator modeling*;
- Ji Qiang (LBNL), *Development of integrated workflow for end-to-end modeling of accelerators*;

and a single presentation for scaled experiments was [1]:

- Hiromi Okamoto (Hiroshima University), *Recent results from the S-POD trap systems on the stability of intense Hadron beams*.

The talks by J.-L. Vay and J. Qiang were invited to cover code collaborations and infrastructure issues which could benefit from community discussion in the workshop. The talk by H. Okamoto was grouped since it overviews an experimental alternative to simulation to efficiently model aspects of beam physics with a trap experiment.

Consensus appeared strong that the code consortium initiative (Consortium for Advanced Modeling for Particle Accelerators; CAMPA) reported by J.-L. Vay is a good cause for community support. If successful, many will benefit in the long term and duplicative efforts will be minimized, allowing resources to be more productively employed to extend and improve the simulation tools. The goal is to provide reliable tools for accelerator modeling

\* lund@frib.msu.edu

## SUMMARY FROM WORKING GROUP F: INSTRUMENTATION AND BEAM MATERIAL INTERACTIONS

R. Dölling, Paul Scherrer Institute, Villigen, Switzerland

M. Minty<sup>#1</sup>, Brookhaven National Laboratory, Upton, NY 11973, U.S.A.

N.V. Mokhov<sup>#2</sup>, Fermilab, Batavia, IL 60510, U.S.A.

T. Toyama, High Energy Research Organization (KEK), Tsukuba, Japan

### *Abstract*

This workshop on High-Intensity, High Brightness and High Power Hadron Beams, held in East Lansing, MI and hosted by Facility for Rare Isotope Beams (FRIB), included a Working Group which combined the topics of Instrumentation and Beam Material Interactions. Continuing with the HB Workshop series tradition, progress, status and future developments of hadron accelerators in these subfields were presented and discussed. Leveraging off of experiences from existing accelerators including FNAL, IFMIF, JPARC, the LHC, RHIC and the SNS, this workshop provided occasion to discuss new technical challenges for beam instrumentation and beam material interactions as relevant for future high power hadron beam facilities both approved (e.g. FRIB, ESS) and in planning (e.g. CADS). Discussions between this and the other working groups during this workshop were quite lively as necessitated by the need to seriously address strong interdependencies (between beam dynamics, technologies, instrumentation and interaction of the beams with materials such as targets, beam dumps and collimators) in the regime of megawatt beam powers as anticipated in approved and future accelerators.

### WG-F ORGANIZATION

At this HB workshop, the topics of Instrumentation and Beam Material Interactions (BMI) were combined into a single working group. Working group F consisted of (1) two sessions with nine talks on Instrumentation, (2) one joint discussion session with working group A (beam dynamics in circular accelerators), (3) one joint discussion session with working groups B (beam dynamics in linear accelerators), (4) one session including discussion with three talks on Beam Material interactions and (5) seven posters contributed to the general poster session.

Since the HB workshop series places strong focus on beam dynamics, the selection of talks for WG-F aimed to reflect this. The instrumentation sessions therefore included topics such as beam profile and halo measurements and

their relevance to beam dynamics analyses and simulations as well as comparisons of beam measurements with predictions.

The Beam Material Interactions session included presentations on activation and radiation damage / material response to high-power beams, thermo-mechanical simulations including design tools for targets, collimators and beam dumps, irradiation facilities capable of supporting future desired measurements, and novel materials for interception of high power beams. The orientation of this working group was therefore quite distinct from the IBIC, Linac, Cyclotron or IPAC conferences. Selected highlights from the presentations in WG-F are summarized below.

### INSTRUMENTATION

Challenges in existing and future accelerators [1-3]: Experiences at the LHC were presented [1] providing vital input for the design of instrumentation for future high power accelerators (either high in beam current or in beam energy, or both). This includes all aspects related to avoiding uncontrolled beam losses such as measurements of beam loss and halo, sophisticated collimation schemes and machine protection systems. An outstanding challenge at the LHC pertains to precise measurement of the transverse beam emittances of the high brightness beams. Wire scanners are used for profile measurements at low beam intensities and for cross-calibration of other beam size measurements. These include necessarily non-invasive measurement devices including ionization profile monitors, synchrotron light monitors and transverse Schottky measurements. Under development are synchrotron light-based interferometric measurement and, as shown in Fig. 1, a novel non-invasive beam-gas vertex monitor. Based on concepts used by the LHCb vertex detector, this detector will allow measurement of the absolute transverse profiles using reconstruction of the location of inelastic beam-gas interactions based on particle tracking with coincidence detectors [1].

Multi megawatt accelerators of the future require fast beam loss detection (for damage protection) and high dynamic range (to avoid activation) which demands the use

<sup>#1</sup> Author on Instrumentation: [minty@bnl.gov](mailto:minty@bnl.gov)

<sup>#2</sup> Author on Beam Material Interactions: [mokhov@fnal.gov](mailto:mokhov@fnal.gov)